Memory of Initial Conditions in Quantum Many Body Dynamics: A Non-Equilibrium Field Theoretic Approach

A Thesis

Submitted to the

Tata Institute of Fundamental Research, Mumbai

for the degree of **Doctor of Philosophy**

in

Physics

by

Ahana Chakraborty

Department of Theoretical Physics,

Tata Institute of Fundamental Research,

Mumbai 400005,India

August, 2019

Final version submitted in December, 2019

DECLARATION

This thesis is a presentation of my original research work. Wherever contributions of others are involved, every effort is made to indicate this clearly, with due reference to the literature, and acknowledgement of collaborative research and discussions. The work was done under the guidance of Professor Rajdeep Sensarma, at the Tata Institute of Fundamental Research, Mumbai.

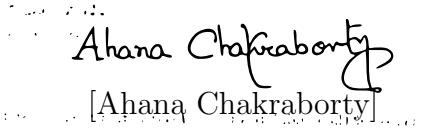

[Ahana Chakraborty]

In my capacity as supervisor of the candidate's thesis, I certify that the above statements are true to the best of my knowledge.

[Prof. Rajdeep Sensarma]

Date: 06/12/2019

Acknowledgements

First, I would like to express my gratitude and regards to my PhD advisor, Prof. Rajdeep Sensarma for mentoring me over the last five years. Staring from the courses he offered to our long Physics discussions during my doctoral research, he has been playing a crucial role in shaping my ideas on how to think about a physics problem, even without going into the details of the calculations. His broad research interests helped me a lot in extending the horizon of my physics knowledge. He has been a constant source of encouragement and motivation over the last few years, even through failures and tough phases of my PhD life.

I would also like to thank Prof. Kedar Damle and Prof. Gautam Mandal for offering us very good courses and being part of my thesis monitoring committee. Their physics intuitions have enlightened me a lot in thinking about various aspects of my research projects.

I am extremely thankful to my friends Angana, Pallabi, Disha and Suman for being my very good friends. Our friendship and all the things we enjoyed together made my PhD life a memorable experience. I am hopeful that we will continue these and meet very soon at some different part of the world. I would really like to thank my colleagues Sounak, Sarath, Sarbajaya, Manibrata, Biswajit, Abhisek, Santanu and Krishnendu who made my stay at TIFR more enjoyable.

I would like to convey my heartfelt regards to my grandfather, late Prof. Santi Kumar Chatterjea and my grandmother, Momota Chatterjea who always encouraged me in all phases of my life. Finally, words seem to be insufficient to express my gratitude to my parents, Samir Chakraborty and Dipa Chakraborty and my sister, Angana Chakraborty,

for being my constant support system in ups and downs of my life. I am extremely delighted to dedicate this thesis to my family without whom this journey would not have been possible.

To my respected parents and beloved sister...

Abstract

Schwinger Keldysh field theory is a widely used paradigm to study non-equilibrium dynamics of quantum many-body systems starting from a thermal state. In this thesis, we have developed a new extension of this formalism to describe non-equilibrium dynamics starting from arbitrary initial many-body density matrices. In this action based formalism, the information of the initial conditions of the system is incorporated by, (i) using additional sources coupled to bilinears of the fields at the initial time, (ii) calculating Green's functions in a theory with these sources, and (iii) then taking appropriate set of derivatives of these Green's functions with respect to initial sources to obtain physical observables. This formalism is applicable for both bosons and fermions, and for both closed and open quantum systems. The physical correlators in a dynamics with arbitrary initial conditions do not satisfy Wick's theorem, even for non-interacting systems. Within the scope of the new formalism, we provide exact analytical solutions for physical correlation functions and obtain an estimate of the violation of Wick's theorem in terms of connected multi-particle initial correlations in non-interacting systems. We then apply this formalism to solve imbalance dynamics in strongly disordered (quasi-periodic) quantum systems starting from Fock states which have recently been realized in experiments. We provide analytical relation between experimentally measurable non-equilibrium observables and traditional ways of characterizing disordered systems in terms of localization length. Our analysis reveals that the microscopic mechanism responsible for retaining initial memory in the long time dynamics is very different for a non-interacting disordered system than that of a many body localized system. Another interesting platform to study role of initial conditions is the dissipative stochastic dynamics of an open quantum system, where a system can exchange energy/ particles with a large external bath. In this thesis, using Schwinger-Keldysh field theoretic technique, we study the evolution of a many body open quantum system whose dynamics is non-Markovian, i.e it exhibits pronounced feedback effect from the external bath and retains long-range memory kernel in its dynamics. We have shown that if the bath spectral function has non-analyticities as a function of frequency, the dissipative and noise kernels governing the dynamics have distinct power-law tails in time, rendering the

reduced dynamics of the system non-Markovian. The Green's functions show a short-time "quasi"- Markovian exponential decay before crossing over to a power-law tail. Using a canonical model of open quantum system, we have explicitly shown the exponent of the power law decay is solely determined by the nature of the non-analyticity, whereas the crossover time scale depends on the strength of the system-bath coupling and the location of the non-analyticity in the bath spectrum. While the dynamics of a quantum many body system is traditionally probed by calculating a few body correlation functions, an alternative description of the dynamics can be formed in terms of non-local information theoretic measures, like Wigner functions and entanglement entropy. In this thesis, we propose a new method of calculating entanglement entropy of a many-body (interacting) Bosonic system (open or closed) from a non-equilibrium field theoretic approach. This completely bypasses complications of the replica method commonly used in equilibrium field theory. The Wigner function and Renyi entropy of a Bosonic system undergoing arbitrary non-equilibrium dynamics can be obtained from Wigner characteristic function, which we identify with the Schwinger Keldysh partition function in presence of quantum sources turned on at the time of measurement. For non-interacting many body systems, starting from arbitrary density matrices, we provide exact analytic formulae for Wigner function and entanglement entropy in terms of the single particle Green's functions. For interacting systems, we relate the Wigner characteristic to the connected multi-particle Green's function of the system. We use this formalism to study the evolution of Wigner distribution and Renyi entropy in an open quantum system starting from a Fock state with negative Wigner function and zero entropy, to a thermal state with positive Wigner function and finite entropy.

Contents

Publications Relevant for This Thesis

Most parts of this thesis have appeared as published works or pre-prints previously. A chapter wise summary is given here.

- Chapter 3 :"Nonequilibrium field theory for dynamics starting from arbitrary athermal initial conditions"
  Authors: Ahana Chakraborty, Pranay Gorantla, Rajdeep Sensarma
  Journal ref: PHYSICAL REVIEW B 99, 054306 (2019)

- Chapter 4 :"Memories of initial states and density imbalance in dynamics of interacting disordered systems"
  Authors: Ahana Chakraborty, Pranay Gorantla, Rajdeep Sensarma
  Journal ref: arXiv:1906.02205 (2019) [Under review process of Physical Review Letters]

- Chapter 5 :"Power law tails and non Markovian dynamics in open quantum systems: An exact solution from Keldysh field theory"
  Authors: Ahana Chakraborty, Rajdeep Sensarma
  Journal ref: PHYSICAL REVIEW B 97, 104306 (2018)

  Partially based on, "Nonequilibrium field theory for dynamics starting from arbitrary athermal initial conditions"
  Authors: Ahana Chakraborty, Pranay Gorantla, Rajdeep Sensarma
  Journal ref: PHYSICAL REVIEW B 99, 054306 (2019)

- Chapter 6 : "Wigner Function and Entanglement Entropy for Bosons from Non-Equilibrium Field Theory"
  Authors: Ahana Chakraborty, Rajdeep Sensarma
  Journal ref: arXiv: 1810.10545 (2018) [Under review process of Physical Review Letters]

List of Tables

List of Figures

Chapter 1

Introduction

1.1 Importance of Initial Conditions in Quantum Dynamics

Evolution of quantum many body systems driven out of equilibrium is crucial to a wide spectrum of physics problems, from evolution of the early universe [1] to quantum switches[2] to dynamics of chemical reaction [3]. A deep understanding of dynamics of quantum many body systems is required in diverse platforms for quantum manipulations and quantum computing [4] like quantum optics [5], hybrid atom-optomechanical systems [6], superconduting qbits, trapped ions [7] etc. Experimental realization of highly tunable quantum many body Hamiltonians in ultracold atomic systems [8] and pump-probe experiments with ultrafast probes in traditional material based systems [9] have opened up a new window to observe the non-equilibrium dynamics of interacting many body quantum systems in a controlled manner. The cold-atomic systems are characterized by almost perfect isolation from external baths [10] and the long timescales ($\sim$ milliseconds), compared to material based systems, provide easy access to the dynamics without requiring ultra-fast probes.

Dynamics of quantum systems driven out of equilibrium is in general governed by two key ingredients: (a) equation of motion of the system (eg Schrodinger equation in closed systems, various master equations in open quantum systems etc.) and (b) the initial density matrix in which the system is prepared. It is obvious that the initial density matrix plays a crucial role in the transient dynamics of quantum systems. Interesting examples of transient dynamics, where it is important to keep track of initial conditions explicitly, include (i) quantum computation, which works on the principle that different initial conditions (inputs) will generically lead to different measurements (outputs) in the

system [11, 4]. It is obvious that ignoring initial conditions in problems related to the implementation of quantum gates would lead to trivial results. (ii) transient quantum transport[12, 13, 14, 15, 16, 17, 18, 19] studied in ultra-fast spectroscopy on condensed matter systems, where the system is initialized to a highly excited state and the change in its transport properties are measured during evolution. The full counting statistics of charge and spin in these systems [20, 21, 22] measure highly non-linear response in these time-evolving systems.

On the other hand, the importance of initial conditions in the long-time behaviour of an out-of-equilibrium quantum system is a much more challenging and highly debated question. Equilibrium quantum statistical mechanics assumes that in the longtime, quantum systems relax to a state independent of initial conditions. The static and dynamic correlations in this state can be descried in terms of an ensemble, with a probability measure governed solely by the Hamiltonian of the system. However, recent success in experimental design and control of out-of-equilibrium systems has resurrected old conceptual questions about the validity of the above description. The discussion on thermalization of quantum systems can be broadly categorized in two classes: (a) open quantum systems (OQS)[23], where a quantum system can exchange energy/particles with a large external reservoir/bath and eventually lead to a thermal state or a non-equilibrium steady state in the long time limit. In the open quantum system set-up, it is interesting to study how the memory of the initial state of the system is being retained in its subsequent dynamics while the external dissipative effect from the baths tries to erase it, as it approaches towards the long-time limit. Interplay of multiple time scales, governing the inherent dynamics of the system and the relaxation coming from the external bath, make this problem particularly interesting. (b) the dynamics of isolated quantum systems. In this case, Eigenstate Thermalization Hypothesis (ETH) [24, 25, 26] states that a generic isolated quantum many body system, starting from a typical initial state, thermalizes in the long time and justifies the applicability of quantum statistical mechanics in this system. The expectation values of the observables averaged over long time can be correctly reproduced by micro-canonical or Gibbs ensemble average of the observables by quantum statistical mechanics.

In contrast to systems which thermalize, there is a large class of quantum many body systems driven out of equilibrium, where their initial conditions crucially govern their long

time dynamics. Here, we would like to point out some important questions/problems in non-equilibrium many body dynamics, where it is important to keep track of the initial conditions explicitly in the long time limit. (i) Integrable systems [27, 28] and many body localized systems [29] retain memory of the initial state for long times and hence they do not thermalize. It is important to note that the only experimental evidence [30, 31] for MBL is to measure the residual memory of the initial state in the long-time dynamics. The fact that the MBL systems do not thermalize and retain memory of the initial state in the long time dynamics, is robust to the choice of the initial conditions of the system. In contrast to this, the quantum scars [32] that appear in a many body system, shows slow thermalization and retention of the initial memory when the system is designed to start from special initial states in an otherwise thermalizing many body spectrum. This phenomenon has been recently observed in ultracold atom experiments [33] in the form of periodic revival of crystalline order in an array of Rydberg atoms. To capture these aspects of absence of thermalization in a quantum many body system, it is important to construct a description which explicitly takes the initial condition into account. (ii) There are quantum systems whose long-time behaviour changes qualitatively depending on the initial condition, e.g. systems with mobility edges [34, 29] may or may not thermalize depending on the state in which they are prepared. Driven dissipative superfluids realized in cold atom systems with strong local dissipation [35] have also been found to reach qualitatively different steady states at the lossy site depending on initial preparation. (iii) Problems related to aging in quantum glasses [36, 37, 38] also require a description of dynamics starting from non-equilibrium initial conditions. This is not an exhaustive list, but provides some context as to why it is important to study the role of initial conditions in the dynamics of a quantum many body systems.

Let us briefly discuss various commonly used theoretical tools to study the dynamics of quantum systems and the scope of keeping track of initial conditions of the systems explicitly within these formulations. A widely used approach to study non-equilibrium dynamics of quantum systems is to solve the equation of motion (EOM) of the density matrix, $\hat{\rho}(t)$, given by the Heisenberg equation,

$$\mathbf{i}\frac{\partial\hat{\rho}(t)}{\partial t} = \left[\hat{H}(t), \hat{\rho}(t)\right]. \tag{1.1}$$

For a closed system, $\hat{H}(t)$ denotes the Hamiltonian governing the dynamics of the system. In case of an open quantum system, $\hat{H}(t)$ represents the total Hamiltonian of the combined system, including the system, the bath as well as their interaction. The time-evolving density matrix, $\hat{\rho}(t)$ can then be used to calculate few body local correlation functions of the system by, $\langle \hat{A}(t) \rangle = Tr[\hat{A}\hat{\rho}(t)]$. This is the traditional approach to describe quantum many body systems as these quantities are easily measured in experiments. For a thermal density matrix, there are a lot of standard techniques devised to compute them routinely in quantum many body systems [39]. Different properties of the expectation values of the local observables [40] in the many body eigenstates have been extensively used as important probes to check validity of ETH and hence the possibility of thermalization in quantum systems. A relatively new approach to study these systems involve non-local information theoretic measures like Wigner functions [41] and entanglement entropy of the reduced density matrix of a subsystem [42] with the rest of the degrees of freedom. In the context of thermalization of a quantum system, various properties of entanglement entropy, such as its scaling with sub-system size [40], growth of entanglement in a sub-system with time [43], have been recently used to detect quantum phase transition between ergodic to non-thermal phases.

Solving the equation of motion for the dynamics of a generic quantum many body system is a challenging and cumbersome task. To avoid the complexity of solving Eq. 1.1 in an OQS, various quantum master equations have been formulated governing the evolution of $\hat{\rho}(t)$ for Markovian dynamics [23, 44] and more complicated equations with non-local memory kernels for non-Markovian dynamics [45, 46, 47, 48, 49]. While a lot of progress has been made within this direct approach of solving the equation of motion of $\hat{\rho}(t)$, the method runs into the difficulty of dealing with a Hilbert space growing exponentially with the size of the system. Several techniques [50, 51, 52] have been proposed in recent years to reduce the size of the Hilbert space to be considered in the dynamics, with varying amount of success beyond one dimensional systems [53, 54, 52]. Moreover, in presence of long range memory kernel in the dynamics [23, 44] solving the EOM of $\hat{\rho}(t)$ becomes extremely challenging, even for a few body system.

The problem of exponentially growing Hilbert space can be avoided by using field theoretic methods which allow us to obtain useful approximate answers for few body correlation

functions for large systems [39]. A field theory for the ground state of a many body systems can be obtained by considering the adiabatic evolution of a single state and expanding the matrix element of the time-evolution operator in a path/functional integral. For systems in thermal equilibrium at finite temperature [39], the partition function, $Z = Tr[exp(-\beta H)]$, can be written as a path integral in imaginary time. For non-equilibrium dynamics, the density matrix evolves as $\hat{\rho}(t) = U(t,0)\hat{\rho}_0 U^\dagger(t,0)$. The expansion of U and $U^\dagger$ in path/functional integrals leads to the Schwinger-Keldysh (SK) field theory with two copies of fields at each space-time point [55]. The SK path integral formalism provides a modern and very powerful platform to study the non-equilibrium dynamics of quantum many body systems, even those evolving with non-local memory kernels. It also provides a systematic approach to include the effect of inter-particle interaction in an out of equilibrium system via perturbative/non-perturbative diagrammatic expansion.

1.2 Schwinger-Keldysh Field Theory for Arbitrary Initial Condition

However, the current formulation of SK field theory has a major drawback: it works efficiently under two conditions, (a) description of steady states of quantum systems where the memory of the initial condition is assumed to be erased [56, 49] and (b) transient dynamics where the initial density matrix is thermal. Hence, several interesting questions in non-equilibrium dynamics, where dependence on athermal initial conditions need to be tracked explicitly, cannot even be posed within this formalism. This severely restricts the applicability of SK field theory.

The central objective of this thesis is to develop an extension SK field theoretic formalism [57] to describe non-equilibrium dynamics of quantum systems starting from arbitrary athermal initial many-body density matrices. It extends the domain of applicability of SK field theory to a large class of problems which were previously inaccessible to field theoretic treatment. In chapter 3,

- we develop an action based formalism [57] which can include arbitrary athermal initial many body density matrix in the dynamics. We show how this can be done for both bosons and fermions, using additional sources coupled to bilinears of the fields at the initial time in the Keldysh action, calculating Green's functions in a

theory with these sources, and then taking appropriate set of derivatives of these Green's functions with respect to initial sources to obtain physical observables. The set of derivatives depends on the initial density matrix.

- The physical correlators in a dynamics with arbitrary initial conditions do not satisfy Wick's theorem, even for non-interacting systems. However, our formalism constructs intermediate "n-particle Green's functions" that obey Wick's theorem. In this case, our formalism provides exact analytical solutions for all multi-particle correlation functions for non-interacting systems initialized to an arbitrary density matrix and also a starting point for making approximations in the interacting case.

- We use these exact expressions to obtain an estimate of the violation of Wick's theorem and relate it to the presence of connected multi-particle initial correlations in the system.

In this thesis, we then use this formalism to tackle several interesting problems in the dynamics of disordered and open quantum systems to understand role of initial conditions in their dynamics.

1.3 Role of Initial Condition in Dynamics of Disordered System

A generic quantum many body system, initialized to a typical state, forgets the memory of the initial state [24, 25]. In the long time limit, local observables in the system can be described by an ensemble of states with a probability measure determined by its Hamiltonian. This basic tenet of equilibrium statistical mechanics has been challenged in recent years in strongly disordered interacting quantum systems, a phenomenon called many body localization(MBL) [58, 59, 40, 60, 61, 62]. These systems fail to thermalize and retain memory of initial conditions in their long time dynamics.

So far, the theoretical studies of many body localization (MBL) have mainly focused on the properties of many body eigenstates of the system in the middle of the spectrum in equilibrium [29]. However, it is impossible to experimentally access a single many body eigenstate in the middle of the spectrum.

Recent success in observing MBL in ultra-cold atomic experiments [30, 31, 63, 64, 65] in the long time dynamics of interacting Bosons and Fermions, both in one and two

dimensional disordered (quasi-periodic) optical lattices, has drawn a huge attention in this direction. In these experiments on disordered systems, the system is initialized in a state with a known pattern of density modulation and the residual memory of this pattern is measured during the time evolution. A finite long time memory of the initial density-imbalance imprinted on the system indicates lack of thermalization due to MBL. The state-of-art numerical techniques, like exact diagonalisation of the many-body Hamiltonian and density-matrix renormalization group (DMRG) [66], which have been extensively used to study MBL, are highly restricted by the size of the Hilbert space and the dimensionality of the system. Moreover, these numerical methods fail to render insights in understanding the microscopic mechanism leading to long time memory retention in MBL systems. Hence, non-equilibrium field theoretic approach, more importantly our newly developed formalism [57] to include arbitrary athermal initial condition in many body dynamics (chapter 3), is a new promising direction to study long-time dynamics of the MBL systems.

In chapter 4, we use this new formulation to work out a theory of imbalance dynamics [67] in disordered (quasi-periodic) systems, both in presence and absence of inter-particle interaction. For localized non-interacting system, our work establishes an explicit connection between long time memory retention and the absence of transport in the system. For interacting systems, this work provides a new insight into the microscopic mechanism responsible for retaining initial memory in the long time dynamics in presence of many body localization.

We consider one and two dimensional disordered (quasi-periodic) lattice bosons/fermions initialized to a Fock state with a pattern of 1 and 0 particles on A and $\bar{A}$ sites respectively, similar to the experimental set-up used in Ref. [30, 63, 68].

- For non-interacting systems we establish a universal relation between the long time density imbalance between A and $\bar{A}$ site, $I(\infty)$, the localization length ξ_l, and the geometry of the initial pattern. For alternating initial pattern of 1 and 0 particles in 1 dimension, $I(\infty) = \tanh[a/\xi_l]$, where a is the lattice spacing. This is the key result of this work which provides a new method for extracting the localization length, ξ_l, which is a traditional way of characterising disordered system in terms of an experimentally measurable non-equilibrium quantity, $I(\infty)$.

- We have extended this result for systems with mobility edge, where we find analytic

relations between $I(\infty)$, the effective localization length $\tilde{\xi}_l$ and the fraction of localized states f_l. The imbalance as a function of disorder shows non-analytic behaviour when the mobility edge passes through a band edge.

- Finally we consider an interacting system of Bosons in an incommensurate potential and calculate the imbalance in different diagrammatic approximations. We provide a new understanding of the mechanism for maintaining a finite imbalance in an interacting system at long times. For interacting bosonic systems, we show that dissipative processes lead to a decay of the memory of initial conditions. However, the excitations created in the process act as a bath, whose noise correlators retain information of the initial pattern. This sustains a finite imbalance at long times in strongly disordered interacting systems. This work, to the best of our knowledge, is the first one in the literature which provides a comprehensive non-equilibrium field theoretical study of the imbalance dynamics of a disordered interacting Bosonic system, which includes the effects of both the dissipation and noise fluctuations coming from inter-particle interaction. This is the minimal approximation needed to account for possible thermalisation of the system in the long time limit.

In this section, we have discussed how strongly disordered isolated quantum systems fail to thermalize and retain memory of initial condition in long time dynamics. In the next section, we will now switch our focus to an alternate description of thermalization of a quantum system coupled to an external bath, i.e an open quantum system.

1.4 Non-Markovian Dynamics of Open Quantum Systems

The dynamics of open quantum systems (OQS) [23] is the key to some fundamental questions in statistical physics, including issues of emergence of irreversibility, generation of entropy [69, 70], generation of quantum entanglement [71] and approach to thermal equilibrium [72]. A widely used paradigm to analyze the dynamics of OQS is the Born-Markov approximation, which assumes that (i) coupling of the quantum system to the bath does not change the dynamics of the bath and (ii) the effective reduced dynamics of the system is local in time. In systems with short range memory kernels, the Markovian approximation emerges as a coarse-grained description of OQS dynamics over a scale τ_{course} in the limit $\tau_s \gg \tau_{course} \gg \tau_b$. Here τ_b and τ_s are the autocorrelation times in the bath and the system.

However, a broad class of systems, like BEC in trapped ultracold atoms [73, 74], quantum dots coupled to superfluid reservoirs [75, 76], nanomechanical oscillators coupled to BEC [77, 78], atoms/impurities coupled to radiation field in photonic crystals [79, 80] have displayed signatures of non-Markovianness in their dynamics in various forms. Hence, the study of non-Markovian dynamics in OQS has been gaining a lot of prominence in recent years [81, 82].

In the dynamics of OQS, if the bath spectral function has non-analyticites (sharp features) as a function of frequency, the reduced dynamics of the system becomes non-Markovian [48]. These non-analyticites arise from a variety of sources like band edges, Van-Hove singularities, Kohn anomalies [83] in phonon spectrum, etc. In chapter 5, we will provide a detailed analysis of this phenomenon in presence of a vast set of non-analyticites in a generic OQS using SK field theory and its new extension developed by us. We will study both the transient and steady state dynamics of the non-Markovian OQS, arising from the bath induced singularities. Our analysis yields,

- exact analytic solution for the reduced dynamics of the system at arbitrary strength of system-bath coupling for a large class of experimentally relevant non-analyticites in the bath spectrum. The reduced dynamics inherits the non-Markovianess in the form of power-law tail in dissipative and noise kernel in effective equation of motion.

- We have shown that the Green's functions and hence the unequal time observables (c.f current-current correlation function) in the steady state of the OQS, show a short time "quasi"-Markovian exponential decay before crossing over to a power law tail. The exponent of the power law decay is solely determined by the nature of the non-analyticity, whereas the crossover time scale does depend on the strength of the system-bath coupling and the location of the non-analyticity in the spectrum.

- We show that the power law decays survive in presence of inter-particle interaction in the system, but the cross-over time scale is shifted to larger values with increasing interaction strength.

Using the newly developed SK field theory formalism, which can include arbitrary athermal initial conditions in the dynamics, we also study quantum transport in the transient dynamics of the non-Markovian OQS, initialized to non-trivial density matrices.

In the first five chapters of the thesis, we have focused on calculating few body correlation functions in non-equilibrium dynamics of quantum many body systems starting from arbitrary initial states. However, recent developments, with their roots in quantum information theory, have led to descriptions of quantum many body systems in terms of non-local measures like Wigner functions, entanglement entropy, quantum discord etc. These have often provided complementary understanding [84, 85, 43, 86] of questions regarding thermalization of quantum systems. In the last chapter of the thesis (chapter 6), we take a step towards understanding the dynamics of these non-local measures using SK field theoretic approach.

1.5 Dynamics of Wigner Functions and Entanglement Entropy for Bosons

We know that, in classical statistical mechanics, given the distribution function, $f(x,p)$ in phase space, the average value of any observable can be calculated as a phase space integral, $\langle A\rangle = \int dx\ dp A(x,p)f(x,p)$. But because of quantum mechanical uncertainty, a joint probability distribution function for all the phase space variables can not be measured simultaneously in a quantum system. In this case, the Wigner quasi-probability distribution function (WQD) [87] of a many body density matrix is a crucial construction in understanding the quantum system, as it provides a detailed tomography of the density matrix and is the closest approximation to a"phase-space distribution function" for quantum systems [41, 88]. The crucial distinction between the classical phase space description and the WQD is that the later can take negative values in parts of the phase space. Negativity of the Wigner function indicates the presence of non-classical correlations in the system which can not be sampled by Monte Carlo techniques [89] in a classical computer and serves as an important resource of quantum computation [90]. It also provides a promising direction to understand fundamental questions like thermalization and generation of quantum entanglement, through entanglement entropy of a reduced density matrix, in the context of an interacting many body quantum system driven in/out of equilibrium. Recent success in measuring Wigner function [91] and entanglement entropy in experiments [92] has prompted a lot of interest in this field. In a seminal work by K. E. Cahill and R. J. Glauber [41] in 1969, it has been shown that both Wigner function and

Renyi entanglement entropy (of order 2), $S^{(2)}$, can be calculated from a quantity, "Wigner characteristics function" (WCF), defined as the trace of the displacement operator defined in coherent state basis.

In chapter 6 [93], we have derived a Keldysh field theoretic way of calculating WCF and hence WQD and $S^{(2)}$ in a generic (interacting) many body set up, applicable to both open or closed Bosonic system. The key result of this work is to

- identify the WCF as the Keldysh partition function with a quantum source turned on only at the time of measurement.

- Using this, we provide exact analytical solutions for WQD and $S^{(2)}$ in terms of single-particle Green's function for non-interacting system and connected multi-particle Green's functions for interacting system. A major advantage in this field theoretic technique to calculate entanglement entropy is to bypass the complicated boundary conditions among different copies of the fields earlier used in replica method [94].

- We apply this technique to study the evolution of WQD and $S^{(2)}$ in transient dynamics of an interacting open quantum system. The system starts from a many body Fock state, a non-classical state having negativity in Wigner function and zero entropy. We probe how the non-classical correlations decay and the entanglement entropy grows in presence of the external dissipation, as the system evolves towards thermal state using the new extension of the SK field theory developed by us in chapter 3. We show interesting anti-correlated connection between the negativity of the Wigner function and the Renyi entropy in the dynamics of the OQS.

1.6 Organization of the Thesis

We plan to present the main results of the thesis in the following way: In chapter 2, we will introduce the structure of the standard Schwinger-Keldysh field theory for both Bosonic and Fermionic systems. In chapter 3, we will derive the new extension of the SK field theory to treat quantum dynamics starting from arbitrary athermal initial conditions. In chapter 4, we will apply this formalism to the dynamics of a disordered (quasi-periodic) Bosonic (Fermionic) many body system starting from a Fock state, as realized in the ultra-cold atomic experiments on many body localized systems and provide physical insights

into how the memory of the initial conditions are retained in the long time dynamics. In chapter 5, we will study the role of initial conditions in the dynamics of a non-Markovian many body OQS whose correlation functions show distinct power-law decay in the long-time limit, governed by bath non-analyticites. In chapter 6, we will propose a new SK field theoretic technique, of calculating Wigner function and Renyi entanglement entropy in a Bosonic many body system, which does not require solving the field theory on complicated manifolds. Finally, in chapter 7, we will briefly conclude with the main finding of the thesis and future directions.

Chapter 2

Review of Standard Schwinger-Keldysh Field Theory

The most general problem in non-equilibrium dynamics of quantum many body systems can be stated in the following way: given a many body Hamiltonian $H(t)$, and an initial many body density matrix $\hat{\rho}_0$ at $t = 0$, one needs to find the evolution of the density matrix $\hat{\rho}(t)$. This can then be used to calculate equal and unequal time correlation functions in the system. The information of the full many body density matrix can also be used to construct the reduced density matrix of a subsystem by tracing out remaining degrees of freedom. This leads to calculation of non-local information theoretic measures like entanglement entropy of the subsystem [42] with the rest of the degrees of freedom.

2.1 Two Contour Evolution

The time evolution of a many body density matrix is given by $\hat{\rho}(t) = U(t,0)\hat{\rho}_0 U^\dagger(t,0)$, where, for Hamiltonian dynamics of a closed quantum system, the time evolution operator is $U(t,0) = \mathcal{T}[e^{-i\int_0^t dt' H(t')}]$. For an open quantum system, U is not a unitary operator in general. From standard path integral formulation, we know that the time evolution operator $U(t,t')$ can be expressed as a path integral over many body coherent states (eigenstate of the annihilation operator). Since the evolution of $\hat{\rho}(t)$ involves two time evolution operator $U(t,0)$ and $U^\dagger(t,0)$, its path integral representation requires two copies of this fields, corresponding to forward and backward direction of time evolution. This results in standard Schwinger-Keldysh field theory [55, 39], where the Keldysh partition function is

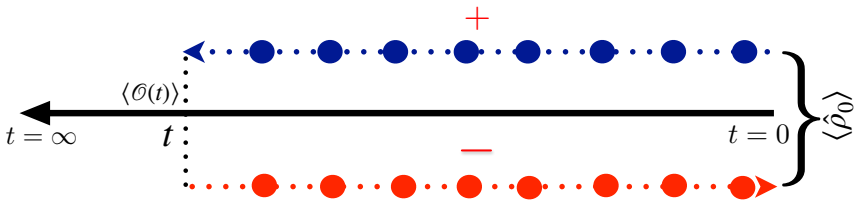

Figure 2.1: Two contour evolution of $\hat{\rho}(t)$ in standard Schwinger Keldysh (SK) field theory showing forward and backward propagation in time. At initial time $t = 0$, the system is completely specified by the many body density matrix, $\hat{\rho}_0$. Expectation value of the physical observable, $\mathcal{O}(t)$, is calculated by inserting the operator at time t on any one (or place it symmetrically) of the two branches.

defined as,

$$Z = Tr[U(\infty, 0)\hat{\rho}_0 U^{\dagger}(\infty, 0)] \tag{2.1}$$

The quantities that are of physical interest are the expectation value of observables $\mathcal{O}(t)$ at time t, given by

$$\langle \mathcal{O}(t) \rangle = Tr[\mathcal{O}\hat{\rho}(t)] = Tr[\mathcal{U}(0, t)\ \mathcal{O}\ \mathcal{U}(t, 0)\hat{\rho}_0] \tag{2.2}$$

where trace is taken over the many body Hilbert space. This suggests an evolution of the non-equilibrium system over a closed contour along the real time axis which is illustrated by Fig. 2.1. Starting from $t = 0$, where the system is completely specified by the initial density matrix $\hat{\rho}_0$, it evolves forward to t along $(+)$ branch of the contour, the observable is measured at t and then it evolves back along backward contour$(-)$ to $t = 0$ again. The trace operation connects the evolution along the two branches of the contour at the initial and end point i.e $t = 0$ giving rise to closed Keldysh contour[95].

To calculate these observables in non-equilibrium dynamics of quantum many body systems, the standard trick is to add a source term to the Hamiltonian , which couples to the observable in question as, $H_{\mathcal{O}}(t) = H(t) \pm \mathcal{O}\ \frac{\eta(t)}{2}$. The source term explicitly breaks the symmetry between the forward and backward branch of the Keldysh contour. In this case the closed contour evolution operator, $\mathcal{U}_C = \mathcal{U}(0, \infty)\mathcal{U}(\infty, 0)$ with the full Hamiltonian $H_{\mathcal{O}}(t)$ is not equal to identity. The Keldysh partition function (generating functional) is then calculated in presence of the source, η, as, $Z[\eta] = Tr[\mathcal{U}_C\ \hat{\rho}_0]$. From this, the physical observables are calculated by $\langle \mathcal{O}(t) \rangle = \delta Z[\eta]/\delta\eta|_{\eta=0}$.

Now we will briefly illustrate how one can recover the thermal limit, i.e the standard one contour evolution in real time formalism of quantum field theory from the SK field theory. In the special case of a system in thermal equilibrium, the theory can be formulated in terms of an adiabatic switching on and off of time dependent interaction in distant past, $t = -\infty$, and distant future, $t = \infty$, respectively. In this case, the evolution along the forward and backward path of a closed keldysh contour can be avoided by the following argument. For a system at temperature, $T = 0$, the trace operation essentially reduces to taking the expectation value in ground state, $|0\rangle$, of the non-interacting Hamiltonian, governing the system at $t = -\infty$. By the virtue of adiabaticity, the state of the system at $t = \infty$ is the same as that of the non-interacting Hamiltonian at $t = -\infty$ modulo a phase factor e^{iL}. Hence, we can write, $\langle 0|\mathcal{U}(\infty, -\infty) = \langle 0|e^{iL}$. Inserting $\mathcal{U}(\infty, -\infty)$ at the left most position of the trace operation in Eq. 2.2, we get, $\langle \mathcal{O}(t)\rangle = \langle 0|\mathcal{U}(\infty, -\infty)\mathcal{U}(-\infty, t)\ \mathcal{O}\ \mathcal{U}(t, -\infty)\hat{\rho}_0|0\rangle / \langle 0|\mathcal{U}(\infty, -\infty)|0\rangle$. This immediately implies that the evolution of a thermal system can be described by the forward branch only. In contrast, for systems out-of-equilibrium we need to carry out the evolution along the two-branch contour.

In this chapter, we will briefly review of the structure of the standard SK field theory [55] for out-of-equilibrium closed systems, starting from thermal $\hat{\rho}_0$, both to set up notations and to provide context for our extension of the formalism for non-thermal $\hat{\rho}_0$ in the next chapter. We will work out the structure of the theory for non-interacting Bosonic and Fermionic many body systems in sections section 2.2 and section 2.4 which will be extended to interacting systems in section section 2.3. The contents of this chapter are adopted from standard textbooks [55, 39] on non-equilibrium field theoretic techniques for quantum many body system.

2.2 Bosonic Systems Starting from Thermal $\hat{\rho}_0$

In this section, we will illustrate the basic structures of the SK path integral formalism with an example of a simple many body quantum system consisting of a bunch of non-interacting

Bosons, governed by the Hamiltonian,

$$H = \sum_k \omega_k \; a_k^\dagger a_k. \tag{2.3}$$

Here, $a_k^\dagger$ is the Bosonic creation operator of the k-th mode of energy ω_k and $[a_k, a_k^\dagger] = 1$. In this case, the Keldysh partition function, defined in Eq. 2.1, can be written as a path integral in terms of the many body Bosonic coherent state, $|\phi\rangle$, of the form,

$$Z = \int D[\phi_+, \phi_-] e^{\mathbf{i}(S[\phi_+] - S[\phi_-])} \langle \phi_+(0)|\hat{\rho}_0|\phi_-(0)\rangle \tag{2.4}$$

where, $\phi_+(t)$ and $\phi_-(t)$ represent the field configurations of the Bosonic field $\phi(t)$ along the forward and backward path respectively. We note that the two copies of the fields, $\phi_+(t)$ and $\phi_-(t)$, are not independent, but they are correlated by the matrix element of the initial density matrix, as shown in Eq. 2.4. For a system starting from thermal density matrix, $\hat{\rho}_0 = exp[-\beta \hat{H}]$, the matrix element, $\langle \phi_+(0)|\hat{\rho}_0|\phi_-(0)\rangle$ can easily be exponentiated to obtain the Keldysh partition function of the form,

$$Z = \int D[\phi_+, \phi_-] e^{\mathbf{i}[\int_0^\infty dt \int_0^\infty dt' \sum\limits_{k,k'} \phi^\dagger(k,t) \hat{G}^{-1}(k,t;k',t') \phi(k',t')]} \tag{2.5}$$

where $\phi^\dagger(k,t) = [\phi_+^*(k,t), \phi_-^*(k,t)]$, and

$$\begin{aligned} G_{++}^{-1}(k,t;k',t') &= -G_{--}^{-1}(k,t;k',t') = \delta(t-t')\delta_{k,k'}[i\partial_t - \omega_k], \\ G_{+-}^{-1}(k,t;k',t') &= -\mathbf{i}\; \rho_{0k}\; \delta(t)\delta(t')\delta_{k,k'},\; G_{-+}^{-1}(k,t;k',t') = 0, \end{aligned}$$

with $\rho_{0k} = exp[-\beta\omega_k]$. Here it is worthwhile to mention that the information about initial distribution, $\hat{\rho}_0$, is included as a boundary term in the continuum SK field theory. Inverting the kernel in Eq. 2.5, we can define four kinds of two point correlators involving $\phi_+(t)$ and $\phi_-(t)$, namely,

$$\begin{aligned} \langle \phi_+(k,t)\phi_-^*(k',t')\rangle &= iG_{+-}(k,t;k',t')\;,\; \langle \phi_-(k,t)\phi_+^*(k',t')\rangle = iG_{-+}(k,t;k',t') \\ \langle \phi_+(k,t)\phi_+^*(k',t')\rangle &= iG_{++}(k,t;k',t')\;,\; \langle \phi_-(k,t)\phi_-^*(k',t')\rangle = iG_{--}(k,t;k',t') \end{aligned}$$

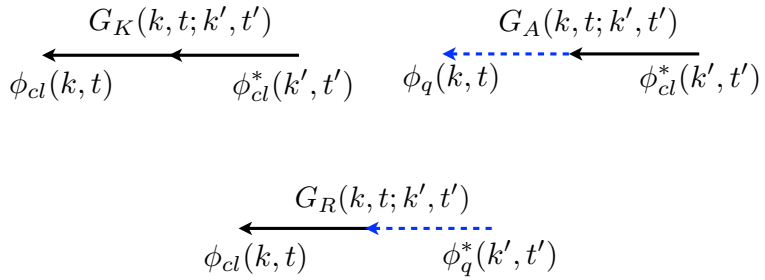

Figure 2.2: Graphical representation of three single particle Green's functions of Bosonic Keldysh field theory: retarded $G_R(k,t;k',t')$, advanced $G_A(k,t;k',t')$ and Keldysh $G_K(k,t;k',t')$ Green's functions consisting of *classical* and *quantum fields* respectively. ϕ_{cl} and ϕ_q are represented by solid and dashed lines respectively.

These four correlation functions are not independent [95] and are related by,

$$G_{++}(k,t;k',t') + G_{--}(k,t;k',t') - G_{+-}(k,t;k',t') - G_{-+}(k,t;k',t') = 0 \tag{2.6}$$

To get rid of this redundancy, we perform the Keldysh rotation, which is a linear transform among the $\phi_\pm$ fields and work with the *classical* and *quantum* fields defined as,

$$\phi_{cl}(k,t) = \frac{\phi_+(k,t) + \phi_-(k,t)}{\sqrt{2}} \ , \ \phi_q(k,t) = \frac{\phi_+(k,t) - \phi_-(k,t)}{\sqrt{2}}. \tag{2.7}$$

In the rotated basis, we obtain the two fundamental one particle Green's function of the Keldysh formalism, namely, retarded $G_R(k,t;k',t')$ and Keldysh $G_K(k,t;k',t')$ Green's function involving the new fields ϕ_{cl} and ϕ_q. In the proper continuum limit, the structure of these Green's functions in the Keldysh formalism are given by,

$$-i\langle\phi_\alpha(k,t)\phi^*_\beta(k',t')\rangle = G_{\alpha\beta}(k,t;k',t') = \begin{pmatrix} G_K(k,t;k',t') & G_R(k,t;k',t') \\ G_A(k,t;k',t') & 0 \end{pmatrix}, \tag{2.8}$$

where $\alpha,\beta = cl,q$ and $G_A = G_R^\dagger$. Here it is important to note that, the $q-q$ component of the Green's function is zero and it con continues to be valid even in presence of interaction. Graphical representations of these two point correlation functions are shown in Fig. 2.2, where ϕ_{cl} and ϕ_q fields are represented by solid and dashed lines respectively. In case of the specific example of the Bosonic Hamiltonian given in Eq. 2.3 whose initial distribution

is the equilibrium Bose distribution, $n_B(\omega_k) = \rho_{0k}/(1-\rho_{0k})$, the one particle Green's functions have the form,

$$G_R(k,t;k',t') = -\mathbf{i}\delta_{k,k'}\theta(t-t')e^{-\mathbf{i}\omega_k(t-t')}, G^K(k,t;k',t') = -\mathbf{i}[2n_B(\omega_k)+1)]\delta_{k,k'}e^{-\mathbf{i}\omega_k(t-t')}. \quad (2.9)$$

The one particle Green's functions of the Keldysh field theory, defined in Eq.2.8, possess some important universal properties, built in the structure of the formalism, which are stated below,

- The retarded and advanced Green's functions are lower and upper triangular matrix in the time domain respectively. The retarded Green's function, $G_R(k,t;k',t')$, can be physically interpreted as the conditional probability amplitude of finding the particle in mode k at time t given that it was in the mode k' at some previous time t'. Hence, it does not depend on the initial condition of the system and only contains information about spectrum of the system.

- The retarded and the advanced Green's function satisfy the product rule,

$$G^1_{R/A} \circ G^2_{R/A} \circ G^3_{R/A} \circ ... \circ G^l_{R/A} = G^{R/A}$$

  where $\circ$ implies convolution in time domain and the superscript indices denote some single-particle index .

- Keldysh Green's function is an anti-Hermitian matrix $G^K = -[G^K]^\dagger$. It explicitly depends on the initial distribution function of the system.

- Equal time correlators satisfy an important property,

$$G^R(k,t;k',t) + G^A(k,t;k',t) = 0. \quad (2.10)$$

The two point correlation functions involving ϕ_{cl} and ϕ_q can be formally constructed from a continuum Keldysh action, S, in the rotated basis. In the proper continuum limit,

S takes the following form,

$$S = \int dt \int dt' \sum_{k,k'} [\phi^*_{cl}(k,t), \phi^*_q(k,t)] \begin{bmatrix} 0 & G_A^{-1} \\ G_R^{-1} & G_K^{-1} \end{bmatrix} \begin{bmatrix} \phi_{cl}(k',t') \\ \phi_q(k',t') \end{bmatrix} \tag{2.11}$$

where $G_K^{-1} = -\mathbf{i}\coth[\omega_k/2T]\delta(t)\delta(t')$ and

$$G^{-1}_{R/A}(k,t;k',t') = \delta(t-t')\delta_{k,k'}(i\partial_t - \omega_k \pm i\eta) \text{ and } G_K^{-1} = -G_R^{-1} \circ G_K \circ G_A^{-1}. \tag{2.12}$$

with $\eta = 0^+$. This action, S maintains the following important causality structures the Keldysh of field theory:

- $S[\phi_{cl}, 0] = 0$, which implies that for a pure classical field configuration i.e $\phi_+ = \phi_-$, the dynamic phase, S_+ accumulated along forward path of the evolution is exactly canceled by that, S_-, along the backward path.
- G_A^{-1} and G_R^{-1} are upper and lower triangular matrices respectively.
- The Keldysh component, G_K^{-1} is an anti-Hermitian matrix and stores the information about the initial distribution.

It is worthwhile to note that these properties are robust and continue to hold for interacting systems as well as for systems coupled to external baths (OQS).

If we are interested in studying the steady state dynamics , we can push the initial time to $t_0 = -\infty$ and work in frequency space, ω. The initial condition can then be expressed as a Keldysh self-energy of the form $G_K^{-1}(\omega) = -2i\eta F(\omega)$, where for thermal distribution function, $F(\omega) = \coth[\omega/2T]$ for Bosons. Inverting the matrix in the action, it can be easily seen that $G_K(\omega) = [G_R(\omega) - G_A(\omega)]F(\omega)$, which is restatement of fluctuation-dissipation theorem for thermal systems.

In the next section, we will introduce the additional structures required in the non-equilibrium field theory to deal with inter-particle interaction in Bosonic systems.

2.3 Inter-particle Interaction for Bosons

In this section, we will generalize the standard SK field theoretic technique, described in the previous section, to the case of an interacting Bosonic systems. We consider a system

of Bosons interacting via spatially short-ranged, time-local pairwise potential given by the Hamiltonian,

$$H_{int} = U \sum_{q,k,k'} a_k^\dagger a_{k'}^\dagger a_{k'+q} a_{k-q} \tag{2.13}$$

where the coupling constant U is related to the scattering length. To include the effect of interaction, we add a corresponding term, S_{int} to the Keldysh action, which takes the following form in the $\pm$ basis,

$$\begin{aligned} S_{int} = U \sum_{q,k,k'} \int_{-\infty}^{\infty} dt \quad [\quad & \phi_+^*(k,t)\phi_+^*(k',t)\phi_+(k'+q,t)\phi_+(k-q,t) \\ - \quad & \phi_-^*(k,t)\phi_-^*(k',t)\phi_-(k'+q,t)\phi_-(k-q,t)] \end{aligned} \tag{2.14}$$

In the rotated basis, this term can be written in terms of the four bare interaction vertices as,

$$\begin{aligned} S_{int} = U \sum_{q,k,k'} \int_{-\infty}^{\infty} dt \quad [\quad & \phi_{cl}^*(k,t)\phi_{cl}^*(k',t)\phi_{cl}(k'+q,t)\phi_q(k-q,t) \\ + \quad & \phi_q^*(k,t)\phi_q^*(k',t)\phi_q(k'+q,t)\phi_{cl}(k-q,t) + \ c.c.] \end{aligned} \tag{2.15}$$

These four vertices are graphically shown in Fig. 2.3. The two point correlation functions can be evaluated in the full interacting action as,

$$G_{\alpha\beta}(k,t;k',t') = -i\langle \phi_\alpha(k,t)\phi_\beta^*(k',t')\rangle = \int \mathcal{D}[\phi\phi^*]\phi_\alpha(k,t)\phi_\beta^*(k',t')e^{\ iS_0+iS_{int}} \tag{2.16}$$

For a generic interaction, this problem cannot be solved exactly, but a diagrammatic perturbation theory can be constructed with the matrix of propagators and the four interaction vertices having cl/q indices. With these changes, standard field theoretic calculations, including non-perturbative resummation of the series can be undertaken in the usual way. The SK field theory then operationally becomes equivalent to the standard field theories with this added $2-$component structure. The structure of the diagrams in Eq. 2.16 admit an expansion in terms of an irreducible one particle self energy, $\hat{\Sigma}$ as in standard quantum field theory. The self energy, $\hat{\Sigma}$ also possesses the 2×2 matrix structure of the SK field theory and the effect of inter-particle interaction is included in the action by dressing the

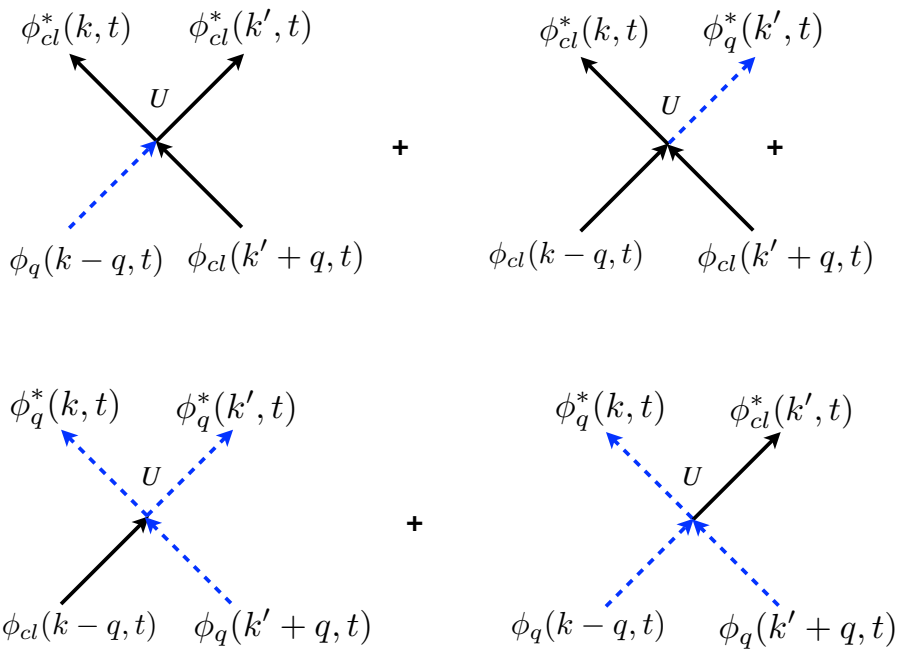

Figure 2.3: Graphical representation of interaction vertices: In the SK field theory, the effect of interaction in incorporated by the four bare interaction vertices involving ϕ_{cl} and ϕ_q fields. There is no vertex generated by interaction that contains only *classical* fields. Hence, the causality structure of the Keldysh action is maintained in presence inter-particle interaction.

inverse propagator as,

$$\hat{G}^{-1} = \hat{G}_0^{-1} - \hat{\Sigma} \tag{2.17}$$

This yields the Dyson equations relating the dressed single particle Green's functions to the non-interacting Green's functions and the irreducible one-particle self-energies, $\hat{\Sigma}$, as,

$$\begin{aligned} G_R(k,t;k',t') &= G_{R0}(k,t;k',t') + \\ &\int_{t'}^{t} dt_1 \int_{t'}^{t_1} dt_2 \sum_{l,m} G_{R0}(k,t;l,t_1)\Sigma_R(l,t_1;m,t_2)G_R(m,t_2,k',t') \\ G_K(k,t;k',t') &= G_{K0}(k,t;k',t') \\ &+ \int_{0}^{t} dt_1 \int_{0}^{t'} dt_2 \sum_{l,m} G_R(k,t;l,t_1)\Sigma_K(l,t_1;m,t_2)G^*_R(k',t';m,t_2) \end{aligned} \tag{2.18}$$

where the non-interacting one particle Green's function, $\hat{G}_0$ is calculated from the corresponding non-interacting action, S_0. We note here that one of the conditions for maintaining causality structure, namely, $(S_0 + S_{int})[\phi_{cl}, \phi_q = 0] = 0$ is automatically set by construction. The other criterion, i.e $G_R^\dagger = G_A$ and $G_{K\dagger} = -G_K$ will also be satisfied if

Σ follows the same causality structure as G_0^{-1} , i.e $\Sigma_R = \Sigma_A^\dagger$, they are lower and upper triangular matrix in time domain respectively and Σ_K is anti Hermitian. It can be shown that $\hat{\Sigma}$ maintains this causality structures order by order in perturbation theory [55].

The physical meaning of the self energies become apparent from the classical saddle point equation of motion of the classical Bosonic fields, obtained from $\partial S[\phi_{cl}, \phi_q]/\partial \phi_{cl}|_{\phi_q=0} = 0$, as,

$$[\mathbf{i}\partial_t - \omega_k]\phi_{cl}(k,t) - \sum_{k'} \int dt' \Sigma_R(k,t;k',t')\phi_j(k',t') = \eta_k(t) \tag{2.19}$$

where the random noise η has correlators, $\langle \eta_k(t)\eta_l(t')\rangle = -\mathbf{i}\Sigma_K(k,t;l,t')$. The real part of Σ_R modifies the dispersion of the Hamiltonian and the imaginary part gives rise to dissipation in the system. The Keldysh self-energy, Σ_K, is related to the correlation between the stochastic fluctuations induced by the inter-particle interaction.

We will conclude this section with this general structure of the interacting Bosonic theory within the framework of the SK path integral formulation. Here, we will not discuss various perturbative and non-perturbative methods that are widely used to solve the Dyson equation for an interacting system and leave this as topic of discussion in the coming chapters where we will apply an extension of SK field theory to study dynamics of an interacting system. In the next section, we will extend this non-equilibrium field theoretic technique to the case of a Fermionic many body system, pointing out the main differences from the Bosonic case.

2.4 Fermionic Systems Starting from Thermal $\hat{\rho}_0$

In this section, we will work out the structure of the standard SK field theory to treat the dynamics of a Fermionic system, focusing on the major changes needed to be included from the Bosonic theory. For a Fermionic system governed by the non-interacting Hamiltonian given in Eq. 2.3, the partition function can be expanded as a path integral over Grassmann coherent states as,

$$Z = \int D[\psi_+, \psi_-] e^{\mathbf{i}(S[\psi_+] - S[\psi_-])} \langle \psi_+(0)|\hat{\rho}_0|-\psi_-(0)\rangle \tag{2.20}$$

where $\psi_\pm$ are the Grassmann fields. Note the additional minus sign in the matrix element comes from writing a trace in the Fermionic Fock space as integrals over Grassmann

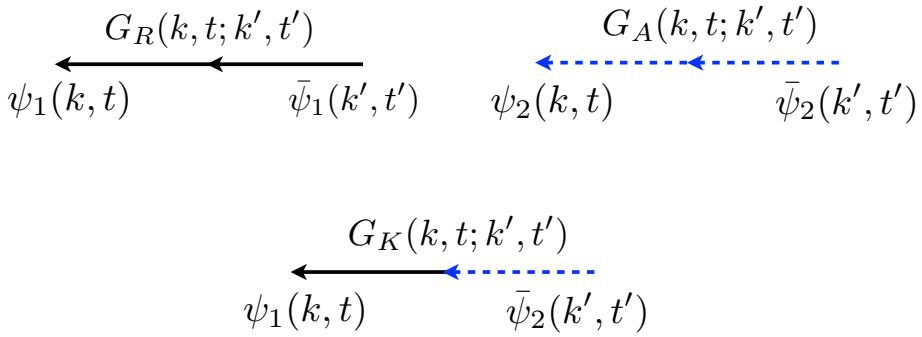

Figure 2.4: Graphical representation of three single particle Fermionic Green's functions of Keldysh field theory: retarded $G_R(k,t;k',t')$, advanced $G_A(k,t;k',t')$ and Keldysh $G_K(k,t;k',t')$ Green's functions consisting of ψ_1 and ψ_2 fields. ψ_1 and ψ_2 are represented by solid and dashed lines respectively.

fields [96]. For a Fermionic system starting from thermal density matrix, $\hat{\rho}_0 = exp[-\beta\hat{H}]$, the matrix element, $\langle\psi_+(0)|\hat{\rho}_0|-\psi_-(0)\rangle$ can easily be exponentiated to obtain the Keldysh partition function of the form,

$$Z = \int D[\psi_+,\psi_-]e^{\mathbf{i}[\int_0^\infty dt\int_0^\infty dt'\sum\limits_{k,k'}\psi^\dagger(k,t)\hat{G}^{-1}(k,t;k',t')\psi(k',t')]} \tag{2.21}$$

where $\psi^\dagger(k,t) = [\bar{\psi}_+(k,t),\bar{\psi}_-(k,t)]$. The inverse Green's function in the Fermionic action is the same as that in the Bosonic action (3.6), except for the $+-$ component which is modified to $G^{-1}_{+-}(k,t;k',t') = \mathbf{i}\ \rho_{0k}\ \delta(t)\delta(t')\delta_{k,k'}$. Similar to the case of Bosons, four kinds of one particle Green's functions can be defined by inverting the kernel in Eq. 2.21, which are not independent and related by Eq. 2.6. To get rid of this redundancy, for Fermions, we follow Larkin-Ovchinikov transformation [1], $\psi_1 = (\psi_+ + \psi_-)/\sqrt{2}$, $\bar{\psi}_1 = (\bar{\psi}_+ - \bar{\psi}_-)/\sqrt{2}$, $\psi_2 = (\psi_+ - \psi_-)/\sqrt{2}$, and $\bar{\psi}_2 = (\bar{\psi}_+ + \bar{\psi}_-)/\sqrt{2}$ and obtain the one particle Green's functions of the Fermionic field theory as,

$$-i\langle\psi_\alpha(k,t)\psi^*_\beta(k',t')\rangle = G_{\alpha\beta}(k,t;k',t') = \begin{pmatrix} G_R(k,t;k',t') & G_K(k,t;k',t') \\ 0 & G_A(k,t;k',t') \end{pmatrix}, \tag{2.22}$$

where $\alpha,\beta = 1,2$, $G_A = G_R^\dagger$ and G_K is anti-Hermitian. The retarded, advanced and Keldysh component of the Green's functions of the Fermionic theory, shown in Fig.2.4,

[1] We note that in Grassmann algebra, the choice of ψ and $\bar{\psi}$ fields are arbitrary and they are not related by conjugation as for complex Bosonic fields.

posses additional causality structures listed for the Bosonic case in section 2.2. Their exact expressions for the thermal $\hat{\rho}_0$ can be found from,

$$G_R(k,t;k',t') = -\mathbf{i}\delta_{k,k'}\theta(t-t')e^{-\mathbf{i}\omega_k(t-t')}, G^K(k,t;k',t') = -\mathbf{i}[1-2n_F(\omega_k))]\delta_{k,k'}e^{-\mathbf{i}\omega_k(t-t')}, \quad (2.23)$$

where the equilibrium Fermi distribution function, $n_F(\omega_k) = \rho_{0k}/(1+\rho_{0k})$. In this case, the fluctuation dissipation theorem relates the three Green's function by, $G_K(\omega) = [G_R(\omega) - G_A(\omega)]\tanh(\omega/2T)$. These Green's functions can be correctly reproduced by the continuum Keldysh action, S, given by,

$$S = \int dt \int dt' \sum_{k,k'} [\bar{\psi}_1(k,t), \bar{\psi}_2(k,t)] \begin{bmatrix} G_R^{-1} & G_K^{-1} \\ 0 & G_A^{-1} \end{bmatrix} \begin{bmatrix} \psi_1(k',t') \\ \psi_2(k',t') \end{bmatrix} \quad (2.24)$$

In this case, $S[\bar{\psi}_1 = 0, \psi_2 = 0] = 0$, (b) $G_{2,1} = 0$ and the retarded and advanced components of the inverse Green's functions will follow the same properties as stated for Bosons. Here, it is worthwhile to note that, in Larkin-Ovchinikov convention for Fermions, the 2×2 matrix structure of the Green's function, $\hat{G}$, is same as that of the inverse Green's function, $\hat{G}^{-1}$, which gives certain technical advantages in the Fermionic theory.

Similar to the Bosonic case, the effect of short-ranged inter-particle scattering between Fermions can be included in the Keldysh action via four bare interaction vertices involving ψ_1 and ψ_2 fields. The standard perturbative and non-perturbative diagrammatic approximations available in quantum field theory for Fermions can also be applied in this out-of-equilibrium situation by suitably incorporating the 2×2 matrix structures of the Green's functions of the Keldysh field theory.

2.5 Discussion

In this chapter, we have reviewed the non-equilibrium field theoretic formalism for the dynamics of a quantum Bosonic/Fermionic many body system. The SK field theory is written in terms of doubled fields in a real time formalism, with a path/functional integral extended over a closed contour shown in Fig. 2.1. It is clear that if the matrix element of $\hat{\rho}_0$ in Eq. 2.4 or Eq.2.20 can be written as an exponential of a low order polynomial of the fields, one can obtain a standard action based formalism for the dynamics. This

can be easily achieved if $\hat{\rho}_0$ is a thermal density matrix corresponding to a Hamiltonian $\hat{H}$ containing only a few body operators, i.e. $\hat{\rho}_0 = exp[-\beta\hat{H}]$. In this case the matrix element can be written as an Euclidean path integral, and the full Z is a path integral over the Kadanoff Baym contour, which extends into the imaginary axis from $t = 0$ to $t = -\mathbf{i}\beta$. However, for a large class of $\hat{\rho}_0$, the above prescription does not work and clearly a new formalism is required to treat the vast set of initial conditions, which do not lend themselves to a simple $\hat{H}$. In the next chapter, we will develop a new extension of the Keldysh field theory which can deal include arbitrary initial density matrix in the dynamics of a quantum many body system. This formalism will serve as an important tool to study the effect of initial conditions during the evolution of quantum systems starting from non-trivial density matrices.

Chapter 3

Non-equilibrium Field Theory for Arbitrary Initial Conditions

3.1 Introduction

The standard techniques of the Schwinger-Keldysh field theory, developed in the previous chapter, have been used extensively to study dynamics of various quantum many body systems, driven out-of-equilibrium. However, the current formulation of SK field theory has a major shortcoming: it can only efficiently deal with initial density matrices, $\hat{\rho}_0$, which are thermal (this includes ground states). As we discussed in the previous chapter, if $\hat{\rho}_0$ is a thermal density matrix corresponding to a non-interacting Hamiltonian, $\hat{H}_0$, i.e. $\hat{\rho}_0 = exp[-\beta \hat{H}_0]$, the matrix element of $\hat{\rho}_0$ in Eq.2.4 and Eq.2.20 can be written as a quadratic term in the Keldysh component, G_K^{-1} of the action. If $\hat{\rho}_0$ is a thermal density matrix corresponding to a interacting Hamiltonian containing only a few body operators, the matrix element of $\hat{\rho}_0$ is written as an imaginary time field theory and the real time path integral is extended into the Kadanoff-Baym contour [97, 98] along the imaginary time axis (see Fig. 3.1 (b)). The SK field theory is also widely used in describing steady states of quantum systems where the memory of the initial condition is assumed to be erased [56, 49]. But several interesting questions in non-equilibrium dynamics of many body systems, where dependence on initial conditions need to be tracked explicitly, cannot even be tackled within current formulation of this formalism.

In this chapter, we will develop a comprehensive action based SK field theoretic formalism [57] which can explicitly keep track of arbitrary initial conditions and their effect on the

quantum dynamics of Bosons and Fermions. To incorporate arbitrary initial conditions, we will consider a SK field theory in presence of a source, $\hat{u}$ which couples to bilinears of the initial fields in the action. This source is turned on only at the initial time, i.e. it acts like an impulse. Different n-particle Green's functions, $\hat{G}^{(n)}(u)$ are then calculated in this theory in presence of the source $\hat{u}$. The physical correlators, corresponding to dynamics starting from a particular $\hat{\rho}_0$, can then be obtained by taking a set of derivatives of the Green's functions with respect to $\hat{u}$ and then setting $\hat{u}$ to zero. The particular set of derivatives to be taken depends on $\hat{\rho}_0$. We note that, in this formulation the calculation of the Green's functions are universal, i.e. they do not depend on particular $\hat{\rho}_0$. The information of specific $\hat{\rho}_0$ is required solely to determine the set of derivatives (w.r.t $\hat{u}$) to be taken to obtain the physical correlators.

In this formalism, we are able to construct a set of intermediate quantities, $\hat{G}^{(n)}(u)$, which have the structure of "n-particle Green's functions" and are derived from the action (with the source $\hat{u}$) in the usual field theoretic way; i.e. Wick's theorem holds for these quantities. One can, for example, construct a diagrammatic perturbation theory for $\hat{G}^{(n)}(u)$ using standard rules of SK field theory. The usual paradigms of obtaining interacting Green's functions in terms of self-energies and higher order vertex functions are valid for these quantities. These are however *not* the physical n-particle correlators; we provide a prescription to compute the physical correlators for different initial density matrices from these intermediate quantities. The key theoretical advance in this formalism is to prescribe a two step process: (i) construction of intermediate quantities where we can apply the well studied structures and standard approximations of SK quantum field theory, and (ii) a prescription to obtain physical correlation functions from them. We would like to emphasize that the above statements are exact even for interacting open quantum systems and do not involve any ad-hoc approximation regarding the initial correlations.

There are some other key advantages of having an action based formalism: (i) *all* correlation functions can be derived from a unified description by adding linear source fields J to the action and then taking appropriate derivatives w.r.t J. Hence they are all on the same theoretical footing, as opposed to a focus on one particle correlators (ii) The general formalism keeps track of *all* "n-particle initial correlations". For non-interacting theories it leads to exact answers for physical correlation functions, even for open quantum systems.

This is in itself non-trivial since there is no Wick's theorem for physical correlators. This is an advantage of the new formalism over the earlier attempt in this direction, namely, Konstantinov Perel (KP) formalism [99], where it is hard to get exact answers even for non-interacting theories starting from arbitrary initial condition. (iii) For interacting theories, it leads to exact expressions on which approximations have to be made for practical calculations. In this case, this formalism provides the most transparent way to understand and make useful approximations. (iv) The action principle provides a way to integrate out degrees of freedom and construct effective theories. Effective theories of dynamics starting from arbitrary initial conditions is a completely unexplored area where there may be new surprises. This may lead to a renormalization group analysis [100, 101] of non-equilibrium dynamics starting from non-trivial initial conditions.

In this chapter, we will set up the general formalism, but focus mainly on non-interacting systems where we can make exact statements. Potential applications of this new formalism to study role of initial conditions in the dynamics of disordered systems and open quantum systems will be discussed in chapter 4, chapter 5 and chapter 6 respectively. We will now provide a guide map to explore this chapter. In section 3.2, we will briefly review some of the previous attempts to include information of arbitrary initial conditions within a non-equilibrium field theoretic framework. We will also illustrate the context of why a new action based formalism is needed to study dynamics of quantum many body systems starting from arbitrary initial conditions. In the next section 3.3, we will explain the main idea behind the extension of the SK formalism to include arbitrary initial condition and introduce the new ingredients of the field theory. In section 3.4, we will explicitly work them out for a system of Bosons starting from generic density matrix in Fock space. We first consider the pedagogical case of a single Bosonic mode starting from a density matrix diagonal in the number basis and derived the corresponding formalism. We then extend this to a multi-mode system starting with density matrix diagonal in the Fock basis. Finally, we consider the extension to arbitrary initial density matrices with off-diagonal elements in the Fock basis. In section 3.5, we consider a Fermionic theory. A large part of the derivations of the Fermionic theory follows along lines similar to that of Bosonic theory. In this section, we will mainly focus on the modifications required to convert the Bosonic theory to the Fermionic theory. In section 3.6, we will focus on calculating multi-particle

physical correlators for a system of non-interacting Bosons and Fermions starting from arbitrary initial condition. We will show how the Wick's theorem is violated by explicitly computing the corrections to the Wick reconstruction of the two particle physical correlators in terms of one particle physical correlators. Finally, in section 3.7 we will sketch the general structure of the interacting theory. We will construct the intermediate quantities for which a diagrammatic perturbation theory can be worked out in case of an interacting system, and sketch how that can be done, but we will leave the question of the different approximations and their validity in interacting systems for forthcoming chapters.

3.2 Previous Attempts to Include Non-Thermal Initial Condition

There have been two major streams of attempts in the past to include arbitrary initial conditions within a field theoretic approach. The first one starts from the Martin-Schwinger hierarchical equation [102] for the one-particle Green's function and then tries to include initial correlations in different ways. In this case one assumes a Dyson equation with a self energy structure, and then modifies the self energy to satisfy initial boundary conditions [103, 104]. There are two main problems with this approach: (i) It assumes that a Dyson equation for one-particle Green's function can be written in terms of an irreducible self energy, which is itself a function of one particle Green's functions, or with additive corrections representing initial correlations. Since Wick's theorem is not valid in a theory with arbitrary initial condition (as we will show from exact expressions in our formalism), it is not clear under what condition this can be done. (ii) Singling out the one particle correlation function does not automatically provide a way to write down equations for higher order correlation functions even in a non-interacting theory [105, 106, 107] which will be evident from our formalism. The second approach, due to Konstantinov and Perel [99], essentially states that since the density matrix is a Hermitian operator with non-negative eigenvalues, it can always be written as an exponential of *some* many body Hamiltonian, $\hat{H}_0$, i.e. $\hat{\rho}_0 = exp[-\beta \hat{H}_0]$. This imaginary time Hamiltonian, $\hat{H}_0$ can be quite different from the Hamiltonian which generates dynamics of the system [108, 109, 98]. One can then use the old Kadanoff-Baym contour, shown in Fig. 3.1(b), with the dynamics along the imaginary time contour governed by this new "Hamiltonian". However, (i) for a given generic

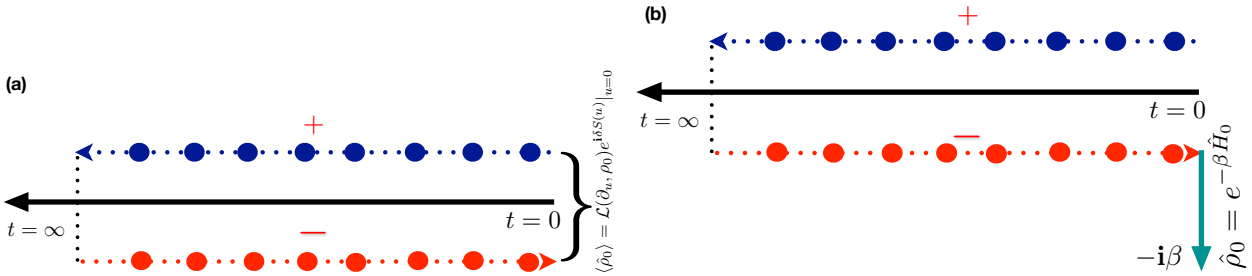

Figure 3.1: (a) Keldysh contours showing forward and backward propagation in time. In our formalism, the matrix element of the initial density matrix, $\hat{\rho}_0$ is written as the derivative of $exp[\mathbf{i}\delta S(u)]$, where $\delta S(u)$ is an added quadratic term in the action which couples to the initial bilinear source $\hat{u}$. The set of derivatives, $\mathcal{L}(\partial_u, \rho_0)$, to be taken, is completely dictated by initial $\hat{\rho}_0$. (b) The Kadanoff Baym contour with an extension along the imaginary time axis, from $t = 0$ to $t = -\mathbf{i}\beta$. For thermal $\hat{\rho}_0 = exp(-\beta\hat{H}_0)$, $\langle\hat{\rho}_0\rangle$ is written as a path integral along the imaginary axis. In KP formalism, any $\hat{\rho}_0$ is cast in the form, $\hat{\rho}_0 = exp[-\beta\hat{H}_0]$, with some imaginary time Hamiltonian, $\hat{H}_0$. For arbitrary $\hat{\rho}_0$, $\hat{H}_0$ does not necessarily contain only a few body local operator

density matrix, finding the "imaginary time Hamiltonian" requires a diagonalization in an exponentially large Hilbert space and (ii) there is no guarantee that the resulting "Hamiltonian" will be local or will only have few-body operators. Then the field theory along the imaginary time contour becomes very hard to implement. Even for systems evolving in real time with a non-interacting Hamiltonian, the arbitrary non- thermal initial state maps the problem into a non-Gaussian field theory along the imaginary time axis of the Kadanoff-Baym contour and hence cannot be solved exactly.

In the next section, we will introduce the structure of the new action based formalism, based on SK field theory, which can treat arbitrary initial density matrix of the quantum many body systems. We will illustrate how the new formalism provides a comprehensive method to calculate physical correlators in the dynamics, which can avoid the above mentioned shortcomings of the earlier attempts in this direction.

3.3 Structure of the New Formalism for Arbitrary Initial Conditions

In this section, we will describe the general structure of the formalism which allows us to treat dynamics of a system of Bosons/Fermions starting from an arbitrary initial density matrix. We will focus on the key modifications of the SK field theory required to achieve this, leaving the detailed derivation for later sections. We intend to highlight the fact that

several properties, which are taken for granted in standard field theories, do not hold in this case. We will discuss the ways to get around these difficulties.

We will develop our formalism for a system with large but finite number of degrees of freedom. We will consider the question of taking the continuum limit for the physical correlation functions at the very end. In the new formalism, the matrix element of $\hat{\rho}_0$ between coherent states in Eq. 2.4 and Eq. 2.20 is written as a polynomial of the bi-linears of the initial fields. This can be exponentiated by adding to the standard Keldysh action, a term δS, where functions of a source field $\hat{u}$, couple to *bilinears of the fields only at* $t = 0$. The polynomial can then be retrieved by taking appropriate derivatives of $exp[\mathbf{i}\ \delta S(u)]$ w.r.t $\hat{u}$ and setting $\hat{u}$ to zero [Fig. 3.1 (a)]. The detailed derivation of the source function which achieves this will be slightly different for Bosons and Fermions and depends on the structure of the initial density matrix. These details will be filled in the next sections, and are cataloged in Table 3.1. For both Bosons and Fermions, the new term can be seen as an addition to the term Σ^K in eq. 2.11 and eq. 2.24 and maintains the anti-hermiticity property of Σ^K. This term can be thought of as a generalized impulse potential felt by the system at the initial time.

The functional integral over the fields can be done first to obtain the partition function $Z(u)$ and the derivative w.r.t $\hat{u}$ can then be taken on this quantity to get the physical partition function corresponding to $\hat{\rho}_0$. On top of this, sources J which couple linearly to the fields at all times $t > 0$ can be added to this action, and the functional integrals over the fields performed to yield the partition function, $Z(J, u)$. Note that u and J couple differently to the fields: $\hat{u}$ couples to bilinears only at $t = 0$, while J couples linearly at all times. This implies that no cross derivative of any quantity w.r.t $\hat{u}$ and J survives when all the source fields are set to zero. Then the Green's function in presence of $\hat{u}$ can be calculated by taking appropriate derivatives of $Z(J, u)$ with respect to J, and setting $J = 0$. For a quadratic theory with action

$$S(u) = \int dt \int dt' \Psi^\dagger(t) \hat{G}^{-1}(t, t', u) \Psi(t'), \tag{3.1}$$

where $\Psi^\dagger(t) = [\phi^*_{cl}(t), \phi^*_q(t)]$ for Bosons and $\Psi^\dagger(t) = [\psi^*_1(t), \psi^*_2(t)]$ for Fermions, the physical one particle correlation function can be obtained by taking proper derivative of $\mathcal{N}(u)\hat{G}(u)$, where the normalization $\mathcal{N}(u) = [\text{Det}\ \{-\mathbf{i}\hat{G}^{-1}(u)\}]^{-\zeta}$ comes from performing the Gaussian

integral, with $\zeta = \pm 1$ for Bosons (Fermions), and $\hat{G}(u)$ is the inverse of the matrix in equation 3.1. While $\hat{G}(u)$ is not the physical one-particle correlation function, we will see that it is an important intermediate construction, which has very useful properties and will be used many times in developing the theory. We will call this object the "Green's function in presence of initial source $\hat{u}$", since it is indeed the Green's function for the saddle point equations of the action with the initial bilinear source term. We stress once again that this is not the physical one particle correlator of the system.

The physical one-particle correlator is now given by,

$$\hat{\mathcal{G}}_{\rho_0} = \mathcal{L}(\partial_u, \rho_0)[\mathcal{N}(u)\hat{G}(u)]|_{u=0} \tag{3.2}$$

where $\mathcal{L}$ is a differential operator which depends on $\hat{\rho}_0$ and encodes initial correlations. The different forms of δS, $\mathcal{N}(u)$ and $\mathcal{L}(\partial_u, \rho_0)$ for a large class of initial conditions for both Bosons and Fermions are tabulated in Table 3.1. The detailed derivations are given in later sections of this chapter. We can generalize the above procedure to the computation of a physical "n-particle correlator", i.e

$$\hat{\mathcal{G}^{(n)}}_{\rho_0} = \mathcal{L}(\partial_u, \rho_0)[\mathcal{N}(u)\hat{G}^{(n)}(u)]\Big|_{u=0} \tag{3.3}$$

Note that the differential operator $\mathcal{L}$ and the normalization $\mathcal{N}(u)$ is the same for all order correlation functions. $\hat{G}(u)$ and $\hat{G}^{(n)}(u)$ are derived from the action $S(u)$ using standard SK field theoretic ways, i.e. initial conditions do not play a role in the derivation. Thus, $\hat{G}^{(n)}(u)$ can be easily written as a sum of products of $\hat{G}(u)$ using Wick's theorem. This relationship is violated by the application of the differential operator $\mathcal{L}(\partial_u, \rho_0)$, i.e. $\mathcal{G}^{(n)}_{\rho_0}$ can not be written as a sum of products of $\mathcal{G}_{\rho_0}$ even for a non-interacting theory. The absence of a Wick's theorem for physical correlators in a non-interacting theory is at the heart of all the complications in constructing physical correlators in interacting theory in terms of non-interacting correlators.

Our formalism bypasses this difficulty by constructing $\hat{G}_{int}(u)$ and $\hat{G}^{(n)}_{int}(u)$ for an interacting theory. These quantities are obtained by standard SK field theoretic techniques from an action $S(u) + S_{int}$ where S_{int} represents the inter-particle interactions. The diagrammatic expansion of $\hat{G}_{int}(u)$, in terms of $\hat{G}(u)$ and the interaction vertices, follow the

System	Initial Density Matrix	$\delta S(u)$	$\mathcal{N}(u)$	$\mathcal{L}(\partial_u, \rho_0)$
Boson	Single mode :Diagonal $\hat{\rho}_0 = \sum_n c_n \lvert n\rangle\langle n\rvert$	$\mathbf{i}\phi_q^*(0)\phi_q(0)\frac{1+u}{1-u}$	$\frac{1}{1-u}$	$\sum_n \frac{1}{n!} c_n \partial_u^n$
	Multi-mode :Diagonal $\hat{\rho}_0 = \sum_{\{n\}} c_{\{n\}} \lvert\{n\}\rangle\langle\{n\}\rvert$	$\mathbf{i}\sum_\alpha \phi_q^*(\alpha,0)\phi_q(\alpha,0)\frac{1+u_\alpha}{1-u_\alpha}$	$\frac{1}{\prod_\alpha (1-u_\alpha)}$	$\sum_{\{n\}} c_{\{n\}} \prod_\gamma \frac{\partial_{u_\gamma}^{n_\gamma}}{n_\gamma!}$
	Multi-mode :Generic $\hat{\rho}_0 = \sum_{nm} c_{nm} \lvert\{n\}\rangle\langle\{m\}\rvert$	$\mathbf{i}\sum_{\alpha\beta} \phi_q^*(\alpha,0)\phi_q(\beta,0)[2\,(1-\hat{u})^{-1} - 1]_{\alpha\beta}$	$\mathrm{Det}(1-\hat{u})^{-1}$	$\sum_{nm} c_{nm} \prod_\alpha \frac{1}{\sqrt{n_\alpha! m_\alpha!}} \prod_j \partial_{\alpha_j\beta_j}$
Fermion	Single mode :Diagonal $\hat{\rho}_0 = \sum_{n=0,1} c_n \lvert n\rangle\langle n\rvert$	$\mathbf{i}\psi_1^*(0)\psi_2(0)\frac{1-u}{1+u}$	$1+u$	$c_0 + c_1 \frac{\partial}{\partial u}$
	Multi-mode :Diagonal $\hat{\rho}_0 = \sum_{\{n\}} c_{\{n\}} \lvert\{n\}\rangle\langle\{n\}\rvert$	$\mathbf{i}\sum_\alpha \psi_1^*(\alpha,0)\psi_2(\alpha,0)\frac{1-u_\alpha}{1+u_\alpha}$	$\prod_\alpha (1+u_\alpha)$	$\sum_{\{n\}} c_{\{n\}} \prod_{\gamma\in\mathcal{A}} \partial_{u_\gamma}$
	Multi-mode :Generic $\hat{\rho}_0 = \sum_{nm} c_{nm} \lvert\{n\}\rangle\langle\{m\}\rvert$	$\mathbf{i}\sum_{\alpha\beta} \psi_1^*(\alpha,0)\psi_2(\beta,0)[2\,(1+\hat{u})^{-1} - 1]_{\alpha\beta}$	$\mathrm{Det}(1+\hat{u})$	$\sum_{nm} c_{nm} \prod_j \partial_{\alpha_j\beta_j}$

Table 3.1: Modification in the structure of the Keldysh field theory to incorporate arbitrary initial density matrix, $\hat{\rho}_0$ for Bosonic and Fermionic systems: the matrix element of $\hat{\rho}_0$ is added as a quadratic term, $\delta S(u)$ in the action, where a function of the initial source $\hat{u}$ couples to the bilinears of the initial quantum fields, $\phi_q^*\phi_q$ for Bosons and $\psi_1^*\psi_2$ for Fermions. $\mathcal{N}(u)$ is the normalization of the partition function obtained from the modified action, $S + \delta S(u)$ and physical correlation functions are obtained by taking the set of derivatives, $\mathcal{L}(\partial_u, \rho_0)$, completely dictated by $\hat{\rho}_0$, of $\mathcal{N}(u)\hat{G}^{(n)}(u)$, where $\hat{G}^{(n)}(u)$ is the "n-particle Green's function" in presence of the initial source $\hat{u}$. For the generic density matrix of a multi-mode system, $\hat{\rho}_0 = \sum_{nm} c_{nm} \lvert\{n\}\rangle\langle\{m\}\rvert$ with $N = \sum_\gamma n_\gamma = \sum_\gamma m_\gamma$, $\partial_{\alpha_j\beta_j}$ denotes partial derivative with respect to $u_{\alpha_j\beta_j}$ which couples to the j^{th} pair of the fields with indices (α_j, β_j). In case of Fermions, the set $\mathcal{A}$ denotes the set of occupied modes in the initial $\hat{\rho}_0$.

Feynman rules of the standard SK theory. The series can be resumed in terms of a self-energy $\Sigma[\hat{G}(u)]$ (for a perturbative expansion of Σ) or $\Sigma[\hat{G}_{int}(u)]$ (for a skeleton diagram expansion). Similarly, one can can construct $\hat{G}_{int}^{(n)}(u)$ in terms of $\hat{G}(u)$ and higher order vertex functions. All the knowledge from the standard SK field theory and different perturbative or non-perturbative approximations can be used to compute $\hat{G}_{int}(u)$ and $\hat{G}_{int}^{(n)}(u)$. We finally need to compute physical correlators, $\mathcal{G}_{\rho_0,int}^{(n)}$ from $\hat{G}_{int}^{(n)}(u)$, which are once again related by eqn. 3.3, with $\hat{G}^{(n)}(u)$ replaced by $\hat{G}_{int}^{(n)}(u)$ and $\hat{\mathcal{G}}_{\rho_0}^{(n)}$ replaced by $\mathcal{G}_{\rho_0,int}^{(n)}$.

Our formalism thus breaks up the calculation of "n-particle correlators" in an interacting theory starting from arbitrary initial conditions into 2 parts: (i) a universal calculation of $\hat{G}_{int}(u)$ and $\hat{G}_{int}^{(n)}(u)$ which does not depend on particular choice of $\hat{\rho}_0$ and uses standard

SK field theoretic techniques with a $\hat{u}$ dependent bare Green's functions and (ii) obtaining $\mathcal{G}^{(n)}_{\rho_0,int}$ by applying $\mathcal{L}(\partial_u, \rho_0)$ on $\mathcal{N}(u)\hat{G}^{(n)}_{int}(u)$. All the dependence on $\hat{\rho}_0$ enters in the theory through the last step. We note that there is no approximation made in the construction of the theory, i.e. all statements made above are exact. In the next sections, we provide a derivation of the theory outlined above, pointing out the details of how δS, $\mathcal{N}$ and $\mathcal{L}$ depend on the statistics of the particles and the initial density matrix $\hat{\rho}_0$.

3.4 Bosonic Field theory for Arbitrary Initial Conditions

For pedagogical reasons, we will first derive the new formalism for a closed system of a single non-interacting Bosonic mode (i.e. a harmonic oscillator) starting from a density matrix diagonal in number basis. While dynamics of this system may seem trivial, we will see the general structure mentioned in the previous section emerge in this simple setting. Further, the derivation and the algebra in more complicated scenario, discussed in later subsections, follow along similar lines, and can be thought of as the extension of this basic theory.

3.4.1 Single Mode System

We consider the dynamics of a single mode system described by the Hamiltonian $H = \omega_0 a^\dagger a$, where ω_0 is the energy of the harmonic oscillator mode, starting from an initial density matrix diagonal in the number basis of $a^\dagger$, i.e.

$$\hat{\rho}_0 = \sum_n c_n |n\rangle\langle n| \tag{3.4}$$

where $|n\rangle$ are number states, and $\sum_n c_n = 1$.

The identity which enables us to exponentiate the matrix element of $\hat{\rho}_0$ is

$$\begin{aligned} \langle\phi|n\rangle\langle n|\phi'\rangle &= \frac{(\phi^*\phi')^n}{n!} = \frac{1}{n!}\left[\frac{\partial}{\partial u}\right]^n e^{u\phi^*\phi'}\Big|_{u=0} \\ \langle\phi_+(0)|\hat{\rho}_0|\phi_-(0)\rangle &= \sum_n \frac{c_n}{n!}\left[\frac{\partial}{\partial u}\right]^n e^{u\phi^*_+(0)\phi_-(0)}\Big|_{u=0}. \end{aligned} \tag{3.5}$$

where $|\phi\rangle$ are the harmonic oscillator coherent states. One can thus exponentiate the initial matrix element in terms of a source field u coupling to the bilinear of the fields $\phi^*_+\phi_-$ only

at $t = 0$, at the cost of taking multiple derivatives with respect to this initial source. In the notation of the previous section we have $\delta S(u) = -\mathbf{i}u\phi_+^*(0)\phi_-(0)$. The set of u derivatives depend on $\hat{\rho}_0$ and in this particular case, we have $\mathcal{L}(\partial_u, \rho_0) = \sum_n (c_n/n!)\partial_u^n$. Incorporating this in equation 2.4, we get the source dependent partition function,

$$Z(J,u) = \int D[\phi_+]D[\phi_-]e^{\mathbf{i}[\int_0^\infty dt \int_0^\infty dt' \phi^\dagger(t)\hat{G}^{-1}(t,t',u)\phi(t') + \int dt J^\dagger(t)\phi(t) + h.c.]} \tag{3.6}$$

where $\phi^\dagger(t) = [\phi_+^*(t), \phi_-^*(t)]$, $J^\dagger(t) = [J_+^*(t), J_-^*(t)]$, and

$$\begin{aligned} G_{++}^{-1}(t,t') &= -G_{--}^{-1}(t,t') = \delta(t-t')[i\partial_t - \omega_0] \\ G_{+-}^{-1}(t,t',u) &= -\mathbf{i}u\delta(t)\delta(t'), \quad G_{-+}^{-1}(t,t') = 0 \end{aligned}$$

Since we are working with a non-interacting system, one can easily show by working with the time discretized version of the matrix $\hat{G}(u)$, that $Det(-\mathbf{i}\hat{G}^{-1}) = (1-u)$ [95]. The gaussian integrals over the fields then give

$$Z(J,u) = \frac{1}{1-u} e^{-\mathbf{i}\int_0^\infty dt \int_0^\infty dt' J^\dagger(t)\hat{G}(t,t',u)J(t')} \tag{3.7}$$

where the normalization factor $\mathcal{N}(u) = (1-u)^{-1}$ and $\hat{G}(u)$ is given by

$$\begin{aligned} G_{+-}(t,t',u) &= \frac{-\mathbf{i}u}{1-u} e^{-i\omega_0(t-t')} \\ G_{-+}(t,t',u) &= \frac{-\mathbf{i}}{1-u} e^{-i\omega_0(t-t')} \\ G_{++}(t,t',u) &= \Theta(t-t')G_{-+}(t,t',u) + \Theta(t'-t)G_{+-}(t,t',u) \\ G_{--}(t,t',u) &= \Theta(t'-t)G_{-+}(t,t',u) + \Theta(t-t')G_{+-}(t,t',u) \end{aligned} \tag{3.8}$$

We note that setting $u = 0$ recovers the usual vacuum Green's functions for the theory. Further, the physical partition function corresponding to $\hat{\rho}_0$ reduces to, $Z_\rho = \sum_n c_n(1/n!)(\partial/\partial_u)^n Z(0,u)|_{u=0} = \sum_n c_n = Tr\hat{\rho}_0$, where we have used $(\partial/\partial u)^n(1/1-u)|_{u=0} = n!$. These act as consistency checks for the Keldysh partition function of a closed quantum system.

We take the derivatives of $Z(J,u)$ w.r.t the linear sources J and set $J = 0$, to define

an n-particle Green's function in presence of the source u

$$\frac{\mathbf{i}^n\ \partial^{2n} Z(J,u)}{\partial_{J(t_1)}..\partial_{J(t_n)}\partial_{J^*(t_{n+1})}...\partial_{J^*(t_{2n})}}\bigg|_{J=0} \quad = \quad \frac{1}{1-u}G^{(n)}(t_1,...t_{2n},u)$$

Note that other than the normalization $(1-u)^{-1}$, which is kept explicitly for its u dependence, $G^n(u)$ is a standard "n-particle Green's function" obtained from a field theory described by an action $S+\delta S(u)$. We then take appropriate derivatives of $G^{(n)}(u)/(1-u)$ with respect to u to obtain the physical correlation function for the particular initial density matrix $\hat{\rho}_0$ as

$$\mathcal{G}^{(n)}_\rho(t_1,...t_{2n}) = \sum_n \frac{c_n}{n!}\left[\frac{\partial}{\partial_u}\right]^n \frac{G^{(n)}(t_1,...t_{2n},u)}{1-u}|_{u=0}$$

Focusing on the one particle Green's functions, we get $i\mathcal{G}_{+-}(t,t') = \sum_n nc_n e^{-i\omega_0(t-t')}$ and $\mathbf{i}\mathcal{G}_{-+}(t,t') = \sum_n (n+1)c_n e^{-\mathbf{i}\omega_0(t-t')}$. At this point, it is useful to work in a rotated basis with the "classical" and "quantum" fields, $\phi_{cl} = (\phi_+ + \phi_-)/\sqrt{2}$ and $\phi_q = (\phi_+ - \phi_-)/\sqrt{2}$. In this new basis, $G_{qq}(t,t',u) = 0$ and

$$\begin{aligned} G_R(t,t') &= -\mathbf{i}\Theta(t-t')e^{-i\omega_0(t-t')} \\ G_K(t,t',u) &= -\mathbf{i}G^R(t,0)\frac{1+u}{1-u}G^A(0,t') = -\mathbf{i}\frac{1+u}{1-u}e^{-\mathbf{i}\omega_0(t-t')} \end{aligned} \tag{3.9}$$

where G_R is independent of the initial source u. It is easy to see that the physical retarded one-particle correlator, $\mathcal{G}_{R\rho_0}(t,t') = G^R(t,t')$ is independent of the initial density matrix (i.e. does not depend on c_n), while the Keldysh propagator

$$\begin{aligned} \mathcal{G}_{K\rho_0}(t,t') &= -i\sum_n c_n(2n+1)G_R(t,0)G_A(0,t') \\ &= -\mathbf{i}(2\langle a^\dagger a\rangle_0 + 1)G_R(t,0)G_A(0,t') \\ &= -\mathbf{i}(2\langle a^\dagger a\rangle_0 + 1)e^{-\mathbf{i}\omega_0(t-t')} \end{aligned} \tag{3.10}$$

carries the information of the initial distribution $\langle a^\dagger a\rangle_0$.

We now construct a continuum action in Keldysh field theory, in the cl/q basis of the form

$$S = \int_0^\infty dt \int_0^\infty dt' \bar{\phi}(t) \begin{bmatrix} 0 & G_A^{-1}(t,t') \\ G_R^{-1}(t,t') & -\Sigma_K(t,t',u) \end{bmatrix} \phi(t') \tag{3.11}$$

with $\bar{\phi}(t) = \left[\phi^*_{cl}(t), \phi^*_q(t)\right]$ and $G_R^{-1}(t,t') = \delta(t-t')[\mathbf{i}\partial_t - \omega_0]$, $\Sigma_K(t,t',u) = -\mathbf{i}(1+u)/(1-u)\delta(t)\delta(t')$. This action $S(u)$ with the u dependent part, $\delta S(u) = \mathbf{i}\phi^*_q(0)\phi_q(0)(1+u)/(1-u)$, correctly reproduces the Green's function in presence of the source u, i.e. $G_R(t,t')$ and $G_K(t,t',u)$. From now on, this is the action we will start with and then add couplings to baths or interparticle interactions, as the case may require, and work out the dynamics of the system. We will finally take necessary u derivatives to get the physical correlators with the correct initial conditions.

To summarize, we have obtained a formalism similar to the one described in the previous section for the dynamics of a single Bosonic mode starting from a $\hat{\rho}_0 = \sum_n c_n |n\rangle\langle n|$. As shown in Table 3.1,

$$\begin{aligned} \delta S(u) &= \mathbf{i}\phi^*_q(0)\phi_q(0)\frac{1+u}{1-u} \\ \mathcal{N}(u) &= (1-u)^{-1} \quad \textit{and} \\ \mathcal{L}(\partial_u, \rho_0) &= \sum_n \frac{c_n}{n!}\partial_u^n \end{aligned} \tag{3.12}$$

A special simplification takes place when the initial density matrix has the form $\hat{\rho}_0 = \rho^{\hat{n}}$; i.e. $c_n = \rho^n$ for a real ρ. In this case $\mathcal{L}$ leads to a Taylor series expansion, and as a result one can simply calculate the physical correlators by setting $u = \rho$, rather than calculating the derivatives. We note that the thermal density matrix is of this form with $\rho = e^{-\omega_0/T}$, and hence the case of an initial thermal distribution can be obtained by setting $u = e^{-\omega_0/T}$ rather than by taking derivatives with respect to u. For a time independent Hamiltonian, this gives the same result which is obtained for thermal states using usual infinitesimal regularization [55].

3.4.2 Multi-mode systems with diagonal $\hat{\rho}_0$

We now extend this formalism to a multi-mode Bosonic system starting from $\hat{\rho}_0$ which is diagonal in the occupation number basis in the Fock space. We will focus on a system with large but finite number of countable modes and develop this theory. We will comment on the continuum limit at the end of this section. Most of the algebra will be similar to the single mode case, so we will point out the main differences in this case. We consider a closed non-interacting system with $H = \sum_{\alpha,\beta} H_{\alpha\beta} a^\dagger_\alpha a_\beta$, where α, β denote one particle

basis states. We consider an initial density matrix diagonal in the Fock basis,

$$\hat{\rho}_0 = \sum_{\{n\}} c_{\{n\}} |\{n\}\rangle\langle\{n\}|, \tag{3.13}$$

where $|\{n\}\rangle = \prod_\alpha |n_\alpha\rangle$ is a configuration in the Fock space with basis α; e.g. if α indicates lattice sites, then the initial density matrix is diagonal in the basis of local particle numbers. Note that we will *not* assume that the Hamiltonian is diagonal in the basis α and hence our formalism can track non-trivial dynamics of even in a closed non-interacting system.

The first task is to find a way to exponentiate the matrix elements of $\hat{\rho}_0$. Using the many body coherent states $|\phi\rangle$ we have

$$\begin{aligned}
\langle\phi|\{n\}\rangle\langle\{n\}|\phi'\rangle &= \prod_\alpha \frac{(\phi^*_\alpha \phi'_\alpha)^{n_\alpha}}{n_\alpha!} = \prod_\alpha \frac{1}{n_\alpha!}\left[\frac{\partial}{\partial u_\alpha}\right]^{n_\alpha} e^{\sum_\beta u_\beta \phi^*_\beta \phi'_\beta}\Big|_{\vec{u}=0} \\
\langle\phi_+(0)|\hat{\rho}_0|\phi_-(0)\rangle &= \sum_{\{n\}} c_{\{n\}} \prod_\alpha \frac{1}{n_\alpha!}\left[\frac{\partial}{\partial u_\alpha}\right]^{n_\alpha} e^{\sum_\beta u_\beta \phi^*_{+\beta}(0)\phi_{-\beta}(0)}\Big|_{\vec{u}=0}
\end{aligned} \tag{3.14}$$

An analysis similar to the single mode can now be carried out, with the single source now extended to a vector $\vec{u}$. Working in the $\pm$ basis, the partition function can be written in a form similar to eqn. 3.6 with the matrix structure in the space of quantum number α. Here, $G^{-1}_{++}(\alpha,t;\beta,t') = \delta(t-t')[\mathbf{i}\partial_t\delta_{\alpha\beta} - H_{\alpha\beta}]$, $G^{-1}_{--}(\alpha,t;\beta,t') = -G^{-1}_{++}(\alpha,t;\beta,t')$, and $G^{-1}_{-+}(\alpha,t;\beta,t') = 0$. In equation 3.14, we see that the additional $\vec{u}$ dependent action is given by $\delta S(u) = -\mathbf{i}\sum_\alpha u_\alpha \phi^*_+(\alpha,0)\phi_-(\alpha,0)$, while the differential operator used to obtain physical correlation functions $\mathcal{L}(\partial_u,\rho_0) = \sum_{\{n\}} c_{\{n\}} \prod_\gamma \partial^{n_\gamma}_{u_\gamma}/n_\gamma!$

To continue the analysis similar to the single mode case, we need to find expressions for $Det(-\mathbf{i}\hat{G}^{-1})$, which gives the normalization factor $\mathcal{N}(u)$, and the Green's functions $\hat{G}(u)$. The detailed algebra for analytic expressions of $Det(-\mathbf{i}\hat{G}^{-1})$ and $\hat{G}(u)$ are provided in Appendix A.1. Here we quote the final answers for both of them. The determinant is given by

$$Det[-\mathbf{i}\hat{G}^{-1}] = Det[-\mathbf{i}\hat{G}^{-1}(0)] \prod_\alpha 1 - u_\alpha \tag{3.15}$$

where $Det[-\mathbf{i}G^{-1}(0)]$ is an $\vec{u}$ independent prefactor and can be ignored as in usual field theory, while the $\vec{u}$ dependent normalization $\mathcal{N}(u) = \prod_\alpha (1-u_\alpha)^{-1}$ has to be kept in the

calculations explicitly.

Similarly, one can invert the matrix $\hat{G}^{-1}(u)$ to obtain (see Appendix A.1 for details) the $\vec{u}$ dependent Green's functions,

$$G_{\mu\nu}(\alpha,t;\beta,t';\vec{u}) = G^v_{\mu\nu}(\alpha,t;\beta,t') + \sum_\gamma G^v_{\mu+}(\alpha,t;\gamma,0)\frac{\mathbf{i}\,u_\gamma}{1-u_\gamma}G^v_{-\nu}(\gamma,0;\beta,t')$$

where $\mu,\nu = \pm$. Here $\hat{G}^v$ are the Green's functions for the dynamics of a system starting from a vacuum state, and is obtained by setting $\vec{u}=0$ in $\hat{G}(u)$. Explicit expressions for $\hat{G}^v$ can be written in terms of the eigenvalues E_a and the corresponding eigenvectors $\psi_a(\alpha)$ of the Hamiltonian: $G^v_{-+}(\alpha,t;\beta,t') = -\mathbf{i}\sum_a \psi^*_a(\beta)\psi_a(\alpha)e^{-iE_a(t-t')}$, $G^v_{+-}(\alpha,t;\beta,t') = 0$, $G^v_{++}(\alpha,t;\beta,t') = \Theta(t-t')G^v_{-+}(\alpha,t;\beta,t')$ and $G^v_{--}(\alpha,t;\beta,t') = \Theta(t'-t)G^v_{-+}(\alpha,t;\beta,t')$. The physical one-particle correlator is then given by

$$\mathcal{G}_{\mu\nu\rho_0}(\alpha,t;\beta,t') = G^v_{\mu\nu}(\alpha,t;\beta,t') + \mathbf{i}\sum_{\{n\}} c_{\{n\}}\sum_\gamma n_\gamma G^v_{\mu+}(\alpha,t;\gamma,0)G^v_{-\nu}(\gamma,0;\beta,t')$$

Working in the *classical-quantum* basis, we find that $G_R(\vec{u}) = G^v_R = \mathcal{G}_{R\rho_0}$, i.e. the retarded Green's function is independent of $\vec{u}$ and hence the physical retarded correlator is independent of the initial condition. Similarly we find [1]

$$G_K(\alpha,t;\beta,t',\vec{u}) = -\mathbf{i}\sum_\gamma \frac{1+u_\gamma}{1-u_\gamma}G_R(\alpha,t;\gamma,0)G_A(\gamma,0;\beta,t') \tag{3.16}$$

and the physical Keldysh correlator

$$\begin{aligned}\mathcal{G}_{K\rho_0}(\alpha,t;\beta,t') &= -\mathbf{i}\sum_{\{n\}} c_{\{n\}}\sum_\gamma (2n_\gamma+1)G_R(\alpha,t;\gamma,0)G_A(\gamma,0;\beta,t') \\ &= -\mathbf{i}\sum_\gamma (2\langle a^\dagger_\gamma a_\gamma\rangle_0+1)G_R(\alpha,t;\gamma,0)G_A(\gamma,0;\beta,t') \end{aligned}\tag{3.17}$$

where $\langle a^\dagger_\gamma a_\gamma\rangle_0$ is the occupancy of the mode γ in the initial density matrix.

In this case all the correlation functions in the classical-quantum basis can be obtained from a continuum Keldysh action of the same form as in Eq. 3.11, with $G^{-1}_R(\alpha,t,\beta,t') =$

[1] The superscript v in the retarded Green's functions is redundant since the retarded Green's functions do not depend on the initial conditions. The superscript v will be omitted in future notations.

$\delta(t-t')[\mathbf{i}\partial_t\delta_{\alpha\beta} - H_{\alpha\beta}], \Sigma_K(\alpha,t,\beta,t',\vec{u}) = -\mathbf{i}\delta_{\alpha\beta}(1+u_\alpha)/(1-u_\alpha)\delta(t)\delta(t')$. One can now start with this action, add a bath or inter-particle interactions, work out the correlators and take appropriate derivatives to construct correlation functions in the physical non-equilibrium system.

To summarize, for a many body bosonic system with an initial density matrix diagonal in the Fock basis, $\hat{\rho}_0 = \sum_{\{n\}} c_{\{n\}}|\{n\}\rangle\langle\{n\}|$, we have

$$\begin{aligned} \delta S(u) &= \mathbf{i}\sum_\alpha \phi_q^*(\alpha,0)\phi_q(\alpha,0)\frac{1+u_\alpha}{1-u_\alpha}, \\ \mathcal{N}(u) &= \prod_\alpha (1-u_\alpha)^{-1} \quad and \\ \mathcal{L} &= \sum_{\{n\}} c_{\{n\}} \prod_\gamma \frac{\partial_{u_\gamma}^{n_\gamma}}{n_\gamma!} \end{aligned} \tag{3.18}$$

We note that it is not easy to obtain the continuum limit of the normalization $\mathcal{N}$ or the operator $\mathcal{L}$ which is defined w.r.t finite but large number of discrete modes. This stems from the problem of defining a continuum limit of a many body density matrix. However, it is clear from equation 3.17 that it is straightforward to take the continuum limit of the physical correlators obtained within this formalism by replacing the sum over the modes by corresponding integrals.

We note once again that the case of a thermal initial density matrix can be handled by getting rid of the derivatives and setting $u_a = e^{-E_a/T}$ and matches with the answers from usual infinitesimal regularization.

3.4.3 Generic initial density matrix for multimode systems

We now want to extend our formalism to the case of density matrices which have off-diagonal matrix elements between occupation number states [2]. We will put the following restriction on the class of initial density matrices: if the occupation number state $|\{n\}\rangle$ and $|\{m\}\rangle$ are connected by the initial density matrix, then $\sum_\alpha n_\alpha = \sum_\alpha m_\alpha$, i.e. total particle number in $|\{n\}\rangle$ and $|\{m\}\rangle$ are equal. The density matrix is thus block diagonal in the fixed total particle number sectors of the Fock space. In this case, we can again

[2]The extension of the formalism to the case of a $\hat{\rho}_0$ having off-diagonal elements in Fock space was proposed and carried out by Pranay Gorantla. This has been presented in his master's thesis. This is again presented here for the sake of completeness.

formulate the field theory in terms of an initial source coupled to bilinears of the fields. We note that this covers almost all density matrices where one can reasonably expect to prepare the many body system.

Let us consider an initial density matrix of the form

$$\hat{\rho}_0 = \sum_{nm} c_{nm} |\{n\}\rangle\langle\{m\}| \tag{3.19}$$

where $c_{nm} = c^*_{mn}$ to maintain hermiticity of the density matrix and $\sum_n c_{nn} = 1$ for conservation of probabilities. The matrix element of $\hat{\rho}_0$ between initial coherent states is given by

$$\langle\phi|\hat{\rho}_0|\phi'\rangle = \sum_{nm} c_{nm} \prod_\alpha \frac{[\phi^*_\alpha]^{n_\alpha}[\phi'_\alpha]^{m_\alpha}}{\sqrt{n_\alpha! m_\alpha!}}$$

Now, if $\sum_\alpha n_\alpha = \sum_\alpha m_\alpha$, then one can always pair up each ϕ^*_α with a ϕ'_β in the above product. While this choice is not unique, we will proceed with a particular pairing and show that our final answers for physical correlators are invariant with respect to permutations leading to different pairings.

In this case the exponentiation of the matrix element of $\hat{\rho}_0$ is achieved by

$$\begin{aligned}
\prod_\alpha [\phi^*_\alpha]^{n_\alpha}[\phi'_\alpha]^{m_\alpha} &= \prod_{j=1}^N \phi^*_{\alpha_j}\phi'_{\beta_j} = \prod_{j=1}^N \left[\frac{\partial}{\partial u_{\alpha_j\beta_j}}\right] e^{\sum_{\gamma\delta} u_{\gamma\delta}\phi^*_\gamma\phi'_\delta}\Big|_{\hat{u}=0}, \\
\langle\phi_+(0)|\hat{\rho}_0|\phi_-(0)\rangle &= \sum_{nm} \frac{c_{nm}}{\prod_\alpha \sqrt{n_\alpha! m_\alpha!}} \prod_j [\partial_{\alpha_j\beta_j}] e^{\sum_{\gamma\delta} u_{\gamma\delta}\phi^*_{+\gamma}(0)\phi_{-\delta}(0)}\Big|_{\hat{u}=0},
\end{aligned} \tag{3.20}$$

where, (α_j, β_j) are the mode indices of the fields forming the j^{th} pair out of total $N = \sum_\alpha n_\alpha = \sum_\alpha m_\alpha$ pairs. The vector source for the diagonal density matrix is now replaced by a matrix source $\hat{u}$ with elements $u_{\alpha\beta}$ and $\partial_{\alpha_j\beta_j}$ indicate derivative with respect to $u_{\alpha_j\beta_j}$. Following algebra similar to the earlier two cases, we find that we need to add a term to the Keldysh action $\delta S = -\mathbf{i}\sum_{\alpha\beta} u_{\alpha\beta}\phi^*_+(\alpha,0)\phi_-(\beta,0)$, and the differential operator used to obtain physical correlators is given by $\mathcal{L}(\partial_u, \rho_0) = \sum_{nm} c_{nm} \prod (n_\alpha! m_\alpha!)^{-1/2} \prod_j \partial_{\alpha_j\beta_j}$.

As before, we are interested in analytical expressions for $\mathrm{Det}[-\mathbf{i}G^{-1}(\hat{u})]$ and the Green's functions $G(\hat{u})$, which are given by

$$\mathrm{Det}[-\mathbf{i}G^{-1}(\hat{u})] = \mathrm{Det}[-\mathbf{i}G^{-1}(0)]\mathrm{Det}(1-\hat{u})$$

$$G_{\mu\nu}(\alpha,t;\beta,t';\hat{u}) = G^{v}_{\mu\nu}(\alpha,t;\beta,t') + \mathbf{i}\sum_{\gamma\delta} G^{v}_{\mu+}(\alpha,t;\gamma,0)[(1-\hat{u})^{-1}-1]_{\gamma\delta}G^{v}_{-\nu}(\delta,0;\beta,t') \tag{3.21}$$

Note that the derivation of these identities [See Ref. [57] for derivation] follow a different route than those for the case of diagonal initial density matrices. We can now compute the physical Green's functions, $\mathcal{G}_{\rho_0}$, by taking appropriate functional derivatives with respect to $u_{\alpha\beta}$. We find that

$$\mathcal{G}_{\mu\nu\rho_0}(\alpha,t;\beta,t') = G^{v}_{\mu\nu}(\alpha,t;\beta,t') + \mathbf{i}\sum_{\gamma\delta} G_{\mu+}(\alpha,t;\gamma,0)\langle\hat{a}^{\dagger}_{\delta}\hat{a}_{\gamma}\rangle_0 G_{-\nu}(\delta,0;\beta,t')$$

where $\langle\hat{a}^{\dagger}_{\delta}\hat{a}_{\gamma}\rangle_0$ gives the initial one-particle correlations.

After a Keldysh rotation to cl/q basis, we find that $\hat{G}_R(\hat{u}) = \hat{G}_R((\hat{u})=0) = \mathcal{G}_R$. The Keldysh Green's function, on the other hand, is given by

$$G_K(\alpha,t;\beta,t',\hat{u}) \;=\; G^{v}_{K}(\alpha,t;\beta,t') - \mathbf{i}\sum_{\gamma\delta} G_R(\alpha,t;\gamma,0)[2\,(1-\hat{u})^{-1}-1]_{\gamma\delta}G_A(\delta,0;\beta,t'), \tag{3.22}$$

where, $G^{v}_{K}(\alpha,t;\beta,t') = G_K(\alpha,t;\beta,t',\hat{u}=0)$. The physical Green's functions are then given by,

$$\begin{aligned}
\mathcal{G}_{R\rho_0}(\alpha,t;\beta,t') &= G_R(\alpha,t;\beta,t'),\\
\mathcal{G}_{K\rho_0}(\alpha,t;\beta,t') &= -\mathbf{i}\sum_{\gamma\delta} G_R(\alpha,t;\gamma,0)[2\langle\hat{a}^{\dagger}_{\delta}\hat{a}_{\gamma}\rangle_0 + \delta_{\gamma\delta}]G_A(\delta,0;\beta,t').
\end{aligned} \tag{3.23}$$

Once again, all the correlation functions in the classical-quantum basis can be obtained from a continuum Keldysh action of the same form as in Eq. 3.11, with $G^{-1}_R(\alpha,t,\beta,t') = \delta(t-t')[\mathbf{i}\partial_t\delta_{\alpha\beta} - H_{\alpha\beta}], \Sigma_K(\alpha,t,\beta,t',u) = \mathbf{i}[2\,(1-\hat{u})^{-1}-1]_{\alpha\beta}\delta(t)\delta(t')$. To summarize, for a many body Bosonic system with an initial , $\hat{\rho}_0 = \sum_{nm} c_{nm}|\{n\}\rangle\langle\{m\}|$, we have

$$\begin{aligned}
\delta S(u) &= -\mathbf{i}\sum_{\alpha\beta}\phi^{*}_{q}(\alpha,0)\phi_q(\beta,0)[2\,(1-\hat{u})^{-1}-1]_{\alpha\beta},\\
\mathcal{N}(u) &= \mathrm{Det}(1-\hat{u})^{-1} \quad \textit{and}
\end{aligned} \tag{3.24}$$

$$\mathcal{L}(\partial_u, \rho_0) = \sum_{nm} c_{nm} \prod (n_\alpha! m_\alpha!)^{-1/2} \prod_j \partial_{\alpha_j \beta_j}$$

This concludes the derivation of our new formalism which can treat the quantum dynamics of a Bosonic system starting from an arbitrary initial density matrix.

3.5 Fermionic Field Theory for Arbitrary Initial Conditions

In the previous sections, we have developed the Schwinger Keldysh path integral based formalism to study the dynamics of a many body Bosonic system starting from an arbitrary initial density matrix. In this section, we will extend this newly developed formalism to a Fermionic many body system. The basic structure of the theory follows along a line similar to that proposed for Bosons, i.e. corresponding to the matrix element $\langle \psi_+(0)|\hat{\rho}_0|-\psi_-(0)\rangle$ in Eq. 2.20, we have to add a term $\delta S(u)$ to the standard Keldysh action, where $\hat{u}$ is a source which couples to bilinears of the Grassmann fields only at initial time. One can then calculate the Green's functions, $\hat{G}(u)$ from the action $S + \delta S(u)$ and the $\hat{u}$ dependent normalization $\mathcal{N}(u)$ by Gaussian integrals of the Grassmann fields. The physical correlation functions are then obtained by applying appropriate set of derivatives $\mathcal{L}(\partial_u, \rho_0)$, determined by the initial density matrix $\hat{\rho}_0$. The derivation of $\delta S(u)$, $\mathcal{N}(u)$ and $\mathcal{L}(\partial_u, \rho_0)$ for a Fermionic theory for different initial conditions is very similar to that of Bosons, with some important changes. We will focus on the distinctions between Bosonic and Fermionic theory, instead of repeating the algebra similar to that in the previous sections.

To extend the new formalism for Fermions, we need to keep track of two major differences between Bosonic theories with complex fields and Fermionic theories with Grassmann fields. The first one is that, in a Fermionic theory, the trace of an operator, written as a functional integral over Grassmann fields, has an additional minus sign from that in the Bosonic expression [96], as seen in Eq. 2.20. This is a characteristic of all Fermionic theories. For example, for a diagonal density matrix in a single mode system, $\hat{\rho}_0 = \sum_n c_n |n\rangle\langle n|$, where $n = 0, 1$ for Fermionic systems, the matrix element

$$\langle \psi_+(0)|\hat{\rho}_0|-\psi_-(0)\rangle = \sum_n c_n [-\psi_+^*(0)\psi_-(0)]^n = \sum_n c_n [\partial_u]^n e^{-u\psi_+^*(0)\psi_-(0)}|_{u=0}$$

Thus one can exponentiate the matrix element of the initial density matrix in a way similar to that for Bosons, with the additional minus sign absorbed by the transformation

$u \to -u$. The second difference is that the Gaussian integration over Grassmann fields in the Fermionic partition function gives $Det[-\mathbf{i}\hat{G}^{-1}(u)]$ in the numerator as opposed to $1/Det[-\mathbf{i}\hat{G}^{-1}(u)]$ in the case of Bosons (eqn 3.7).

We will consider a many body Fermionic system with Hamiltonian $H = \sum_{\alpha,\beta} H_{\alpha\beta} a^\dagger_\alpha a_\beta$ where $a^\dagger_\alpha$ creates a Fermion in mode α and an initial density matrix which is diagonal in Fock basis, given in equation 3.13, where the occupation numbers of the mode α, n_α, are restricted to be only 1 or 0 due to Pauli exclusion principle. In this case the matrix element of $\hat{\rho}_0$ is given by,

$$\langle \psi_+(0)|\hat{\rho}_0|-\psi_-(0)\rangle = \sum_{\{n\}} c_{\{n\}} \prod_\alpha \left[\frac{\partial}{\partial_{u_\alpha}}\right]^{n_\alpha} e^{-\sum_\beta u_\beta \psi^*_{+\beta}(0)\psi_{-\beta}(0)}\Big|_{\vec{u}=0} \tag{3.25}$$

where ψ^* is the conjugate to the Grassmann field ψ. Using this, we obtain the Fermionic partition function $Z[J,u]$ in presence of both the sources: Grassmann source $J_\pm$ coupled linearly to $\psi^*_\pm$ and the real quadratic source $\vec{u}$ turned on at $t = 0$ as,

$$Z(J,u) = \int D[\psi_+]D[\psi_-] e^{\mathbf{i}[\int_0^\infty dt \int_0^\infty dt' \psi^\dagger(t)\hat{G}^{-1}(t,t',u)\psi(t') + \int dt J^\dagger(t)\psi(t) + h.c.]} \tag{3.26}$$

The inverse Green's function in the Fermionic action is the same as that in the Bosonic action (3.6), except for the $+-$ component which is modified to $G^{-1}_{+-}(\alpha,t;\beta,t',\vec{u}) = \mathbf{i}u_\alpha\delta_{\alpha\beta}\delta(t)\delta(t')$, i.e. $\delta S(u) = \mathbf{i}\sum_\beta u_\beta \psi^*_{+\beta}(0)\psi_{-\beta}(0)$. We perform the Gaussian integration over the Grassmann fields to obtain,

$$Z[J,u] = \prod_\alpha (1+u_\alpha) e^{-\mathbf{i}\int_0^\infty dt \int_0^\infty dt' J^\dagger(\gamma,t)G(\gamma,t;\beta,t',\vec{u})J(\beta,t')} \tag{3.27}$$

A notable difference between the Fermionic partition function and the Bosonic one is that the determinant $Det[-\mathbf{i}G^{-1}] = \prod_\alpha(1+u_\alpha)$ appears in the numerator, leading to the normalization, $\mathcal{N}(u) = \prod_\alpha(1+u_\alpha)$. It is evident from equation 3.25, that $\mathcal{L}(\partial_u,\rho_0) = \sum_{\{n\}} c_{\{n\}} \prod_\alpha [\partial/\partial_{u_\alpha}]^{n_\alpha} = \sum_{\{n\}} c_{\{n\}} \prod_{\alpha\in\mathcal{A}} \partial/\partial_{u_\alpha}$ where $\mathcal{A}$ denotes the set of modes occupied in the Fock state $|\{n\}\rangle$. We find that in the $+,-$ basis, the Fermionic Green's function $\hat{G}(u)$ can be obtained from the Bosonic ones by taking $\vec{u} \to -\vec{u}$. Working in the rotated basis $\psi_{1(2)}$, we obtain that the retarded Green's function, $G_R(\alpha,t,\beta,t')$ is again independent of

$\vec{u}$, and the Keldysh Green's function,

$$G_K(\alpha,t;\beta,t',\vec{u}) = -\mathbf{i}\sum_\gamma \frac{1-u_\gamma}{1+u_\gamma} G_R(\alpha,t;\gamma,0)G_A(\gamma,0;\beta,t')$$

The physical observables are obtained by applying $\mathcal{L}(\partial_u,\rho_0)$ on $\mathcal{N}(u)\hat{G}(u)$ and setting $\vec{u}=0$, i.e.

$$\begin{aligned}
\mathcal{G}_{R\rho}(\alpha,t;\beta,t') &= G_R(\alpha,t;\beta,t') && (3.28)\\
\mathcal{G}_{K\rho}(\alpha,t;\beta,t') &= -\mathbf{i}\sum_{\{n\}} c_{\{n\}} \sum_\gamma (1-2n_\gamma) G_R(\alpha,t;\gamma,0)G_A(\gamma,0;\beta,t') \\
&= -\mathbf{i}\sum_\gamma (1-2\langle a_\gamma^\dagger a_\gamma\rangle_0) G_R(\alpha,t;\gamma,0)G_A(\gamma,0;\beta,t') && (3.29)
\end{aligned}$$

To continue working in the rotated 1(2) basis for Fermionic fields, we construct the Keldysh action in continuum in presence of the initial source $\vec{u}$. The retarded, advanced and Keldysh Fermionic propagators, $\hat{G}(\vec{u})$ can be obtained by inverting the kernels in the action 3.30.

$$S = \int_0^\infty dt \int_0^\infty dt' \sum_{\alpha\beta} \psi^*(\alpha,t)\hat{G}^{-1}(\alpha,t;\beta,t',u)\psi(\beta,t') \tag{3.30}$$

$$\bar{G}^{-1}(\alpha,t,\beta,t') = \begin{bmatrix} G_R^{-1}(\alpha,t,\beta,t') & -\Sigma_K(\alpha,t,\beta,t',u) \\ 0 & G_A^{-1}(\alpha,t,\beta,t') \end{bmatrix} \tag{3.31}$$

with $G_R^{-1}(\alpha,t,\beta,t') = \delta(t-t')[\mathbf{i}\partial_t\delta_{\alpha\beta} - H_{\alpha\beta}]$ and $\Sigma_K(\alpha,t,\beta,t',\vec{u}) = -\mathbf{i}\delta_{\alpha\beta}\frac{1-u_\alpha}{1+u_\alpha}\delta(t)\delta(t')$. To summarize, for a many body Fermionic system with an initial density matrix diagonal in the Fock basis, $\hat{\rho}_0 = \sum_{\{n\}} c_{\{n\}}|\{n\}\rangle\langle\{n\}|$, we have

$$\begin{aligned}
\delta S(u) &= \mathbf{i}\sum_\alpha \psi_1^*(\alpha,0)\psi_2(\alpha,0)\frac{1-u_\alpha}{1+u_\alpha}, \\
\mathcal{N}(u) &= \prod_\alpha (1+u_\alpha) \quad \textit{and} && (3.32)\\
\mathcal{L} &= \sum_{\{n\}} c_{\{n\}} \prod_{\gamma\in\mathcal{A}} \partial_{u_\gamma}
\end{aligned}$$

The Fermionic Green's functions satisfy a large number of constraints reflecting the fact that initial occupation numbers can not be greater than 1. This leads to $(\partial/\partial u_\gamma)^n \mathcal{N}(u)\hat{G}(u) = 0\ |_{\vec{u}=0}$ for any γ and $n \geq 2$. The non-interacting Green's functions derived above explic-

itly satisfy these conditions. We note that these relations are manifestations of Fermi statistics and should continue to hold for interacting systems as well as open quantum systems. The simplicity of the normalization factor $\mathcal{N}(u)$ allows us to write $\mathcal{G}_{\rho_0} = \sum_{\{n\}} c_{\{n\}} \prod_{\gamma\in\mathcal{A}}(1+\partial_{u_\gamma})\hat{G}(u)|_{\vec{u}=0}$. This compact relation is useful for practical computation of physical correlators for Fermionic systems.

This formalism can be generalized to the case of generic initial density matrix with off-diagonal elements in the Fock basis, given by eqn. 3.19 in a way similar to that of Bosons with the modifications mentioned above. We will not go into the details, but provide the answers for the physical one particle correlators here,

$$\begin{aligned}
\mathcal{G}_{R\rho_0}(\alpha,t;\beta,t') &= G_R(\alpha,t;\beta,t'),\\
\mathcal{G}_{K\rho_0}(\alpha,t;\beta,t') &= -\mathbf{i}\sum_{\gamma\delta} G_R(\alpha,t;\gamma,0)[\delta_{\gamma\delta} - 2\langle\hat{a}^\dagger_\delta\hat{a}_\gamma\rangle_0]G_A(\delta,0;\beta,t').
\end{aligned} \tag{3.33}$$

Thus the initial off-diagonal density matrix for a system of Fermions leads to,

$$\begin{aligned}
\delta S(u) &= \mathbf{i}\sum_{\alpha}\psi_1^*(\alpha,0)\psi_2(\beta,0)[2\,(1+\hat{u})^{-1}-1]_{\alpha\beta},\\
\mathcal{N}(u) &= \mathrm{Det}(1+\hat{u}) \quad \textit{and}\\
\mathcal{L}(\partial_u,\rho_0) &= \sum_{nm} c_{nm}\prod_j \partial_{\alpha_j\beta_j}.
\end{aligned} \tag{3.34}$$

3.6 Two-particle Correlators and Violation of Wick's Theorem

In standard field theories, Wick's theorem states that the expectation of a multi-particle operator (i.e. a multi-particle correlation function) in a non-interacting theory (gaussian action) can be calculated as a product of single particle Green's functions, summed over all possible pairings of the operators into bilinear forms. For an interacting theory, this is the backbone of constructing a diagrammatic perturbation theory in terms of single particle Green's functions and interaction vertices, and various non-perturbative resummations that result from this. Throughout this chapter we have emphasized that the physical correlators in a dynamics with arbitrary initial conditions are not related by Wick's theorem, even for a non-interacting Hamiltonian. We will illustrate this point in details in this section by considering physical two-particle correlators in non-interacting Bosonic/Fermionic theories.

In fact, a major accomplishment of this formalism is to construct Green's functions which satisfy Wick's theorem, and for which standard approximations of field theories can be used.

Our goal is not simply to establish a violation of Wick's theorem, but to characterize and quantify the violation. To this end, we will work in the Keldysh rotated basis ((cl, q) for Bosons and $(1, 2)$ for Fermions), where the initial condition dependence of the one particle correlators is more streamlined. Any physical two particle correlator $\hat{\mathcal{G}}^{(2)}_{\rho_0}$ can be written in terms of the corresponding "two-particle Green's function in presence of source", $\hat{G}^{(2)}(u)$ through Eq. 3.3. To illustrate the violation, we will focus on a multi-mode system starting from a density matrix diagonal in the Fock basis $\hat{\rho}_0 = \sum_{\{n\}} c_{\{n\}} |\{n\}\rangle\langle\{n\}|$; in this case, $\hat{\mathcal{G}}^{(2)}_{\rho_0} = \mathcal{L}(\partial_u, \rho_0)\mathcal{N}(u)\hat{G}^{(2)}(u)|_{u=0}$ with $\mathcal{L} = \sum_{\{n\}} c_{\{n\}} \prod_\gamma [\partial^{n_\gamma}_{u_\gamma}/n_\gamma!]$ and $\mathcal{N}(u) = \prod_\mu (1 - \zeta u_\mu)^{-\zeta}$ where $\zeta = \pm 1$ for Bosons(Fermions).

As we have emphasized before, $\hat{G}^{(2)}(u)$ is related to the one particle Green's functions $\hat{G}(u)$ through Wick's theorem, i.e. $\hat{G}^{(2)}(u) = \sum_{(ab)} G_a(u)G_b(u)$, where $a, b = R/A/K$, and $\sum_{(ab)}$ indicates sum over all allowed pairings. We will now consider the action of $\mathcal{L}$ on $\mathcal{N}(u)G_a(u)G_b(u)$ for different combinations of a, b; the required sum over pairings can always be performed at the end. Let us consider the action of $\mathcal{L}$ when both a and b are either R or A; i.e. we are considering a pair of retarded or advanced Green's functions. In this case, $G_{R(A)}(u)$ is independent of u, and $\mathcal{L}\mathcal{N}(u)|_{u=0} = 1$ by normalization of the density matrix; so this part of $\mathcal{G}^{(2)}_{\rho_0} = \mathcal{G}_{a,\rho_0}\mathcal{G}_{b,\rho_0}$, i.e. this part of the physical 2-particle correlator can be written as a Wick contraction over the physical retarded or advanced one-particle correlators. We now consider the case where one, but not both of a, b is the Keldysh Green's function. In this case, $G_{R(A)}$ is independent of u, $\mathcal{L}$ acts on $\mathcal{N}(u)G_K(u)$ to give $\mathcal{G}_{K,\rho_0}$, and once again Wick contraction in terms of physical correlators work, i.e. for this part we also get $\mathcal{G}^{(2)}_{\rho_0} = \mathcal{G}_{R(A),\rho_0}\mathcal{G}_{K,\rho_0}$.

The violation of Wick's theorem comes from the pairing where both single particle Green's function are Keldysh propagators. For a non-interacting system,

$$G_K(\alpha, t, \beta, t', \vec{u}) = -\mathbf{i}\sum_\gamma G_R(\alpha, t, \gamma, 0)G^*_R(\beta, t', \gamma, 0)\frac{1 + \zeta u_\gamma}{1 - \zeta u_\gamma}. \tag{3.35}$$

To show the structure of the violation, we consider the correlator,

$\langle \phi^*_{cl}(\alpha,t)\phi^*_{cl}(\beta,t')\phi_{cl}(\gamma,t')\phi_{cl}(\delta,t)\rangle = \mathbf{i}^2\mathcal{G}^{(2)}_{\rho_0}(\alpha,t,\beta,t',\gamma,t'\delta,t)$ for Bosons,

$$\begin{aligned}\mathcal{G}^{(2)}_{\rho_0}(\alpha,t,\beta,t',\gamma,t'\delta,t) &= \sum_{\{n\}} c_{\{n\}} \sum_{x,y} [G^*_R(\alpha,t,x,0)G_R(\gamma,t',x,0)G^*_R(\beta,t',y,0)G_R(\delta,t,y,0) \\ &+ G^*_R(\alpha,t,x,0)G_R(\delta,t,x,0)G^*_R(\beta,t',y,0)G_R(\gamma,t',y,0)] \\ &\times[(2n_x+1)(2n_y+1) - 2\delta_{x,y}n_x(n_x+1)] \end{aligned} \tag{3.36}$$

Similarly, for Fermions we get,

$$\begin{aligned}\mathcal{G}^{(2)}_{\rho_0}(\alpha,t,\beta,t',\gamma,t'\delta,t) &= \sum_{\{n\}} c_{\{n\}} \sum_{x,y} [G^*_R(\alpha,t,x,0)G_R(\gamma,t',x,0)G^*_R(\beta,t',y,0)G_R(\delta,t,y,0) \\ &+ \zeta\, G^*_R(\alpha,t,x,0)G_R(\delta,t,x,0)G^*_R(\beta,t',y,0)G_R(\gamma,t',y,0)] \\ &\times[(1-2n_x)(1-2n_y) - 4\delta_{x,y}n_x] \end{aligned} \tag{3.37}$$

For a single Fock state, where the $\sum_{\{n\}}$ is redundant, we note that the first term with $(1+\zeta 2n_x)(1+\zeta 2n_y)$ can be written as $\mathcal{G}_{K\rho_0}\mathcal{G}_{K\rho_0}$, i.e. this part corresponds to a Wick contraction with physical $\mathcal{G}_{K\rho_0}$. In this case the term with $\delta_{x,y}$ contains the connected density correlations in the initial state and leads to a violation of Wick's theorem. For a generic diagonal density matrix, both terms lead to violation of Wick's theorem, since even for $x \neq y$, the connected density correlations in the initial state is non-zero. The expressions for Bosons and Fermions can be written in a compact notation in terms of initial correlations in the system,

$$\begin{aligned}\mathcal{G}^{(2)}_{\rho_0}(\alpha,t,\beta,t',\gamma,t',\delta,t) &= \sum_{x,y} [G_R(\alpha,t,x,0)G^*_R(\gamma,t',x,0)G_R(\beta,t',y,0)G^*_R(\delta,t,y,0) \\ &+ \zeta\, G_R(\alpha,t,x,0)G^*_R(\delta,t,x,0)G_R(\beta,t',y,0)G^*_R(\gamma,t',y,0)] \\ &\times[\langle(1+\zeta 2\hat{n}_x)(1+\zeta 2\hat{n}_y)\rangle_0 - 2\delta_{x,y}\langle\hat{n}_x(\hat{n}_x+1)\rangle_0] \end{aligned} \tag{3.38}$$

where $\hat{n}_x$ is the number operator in mode x, and $\langle\rangle_0$ indicates expectation with the initial density matrix. Writing the above expression in terms of a Wick' theorem and a correction term, we have

$$\mathcal{G}^{(2)}_{\rho_0}(\alpha,t,\beta,t',\gamma,t'\delta,t) = \mathcal{G}_{K\rho_0}(\alpha,t,\gamma,t')\mathcal{G}_{K\rho_0}(\beta,t',\delta,t) + \zeta\mathcal{G}_{K\rho_0}(\alpha,t,\delta,t)\mathcal{G}_{K\rho_0}(\beta,t',\gamma,t') + \delta\mathcal{G}^{(2)} \tag{3.39}$$

where

$$\delta\mathcal{G}^{(2)} = \sum_{x,y} [G_R(\alpha,t,x,0)G_R^*(\gamma,t',x,0)G_R(\beta,t',y,0)G_R^*(\delta,t,y,0) \\ +\zeta\, G_R(\alpha,t,x,0)G_R^*(\delta,t,x,0)G_R(\beta,t',y,0)G_R^*(\gamma,t',y,0)]\, 2[\langle a_x^\dagger a_y^\dagger a_y a_x\rangle_{0c}(2-\delta_{x,y})] \tag{3.40}$$

$\langle\rangle_{0c}$ indicates connected expectation value in the initial density matrix. We thus see that the violation of the Wick's theorem can be directly tied to the presence of two particle connected correlations in the initial state of the system.

The above calculation can easily be generalized to multi-particle correlators. The Wick's theorem violating terms would come from having multiple G_K in the product decomposition and are proportional to connected multi-particle correlations in the initial state.

3.7 Interacting Systems with Arbitrary Initial Condition

In the previous sections, we have built up a field theoretic formalism to describe the dynamics of quantum many body systems starting from arbitrary initial conditions. However, till now, we have only looked at non-interacting systems (quadratic or gaussian field theories), where we can solve the problem exactly and the question of calculating a correlator is reduced to evaluating one or a few integrals. In this section we finally tackle the question of applying our formalism to the dynamics of interacting quantum many body systems starting from an arbitrary initial condition.

In this case, we start by adding to the quadratic Keldysh action with the initial bilinear source, $S(u)$, a term S_{int}, representing the interaction between particles. We then consider the field theory controlled by the action $S = S(u) + S_{int}$, and calculate Green's functions $\hat{G}^{(n)}_{int}(u)$ in this theory. $\hat{G}^{(n)}_{int}(u)$ has a diagrammatic expansion in terms of the non-interacting Green's functions $\hat{G}(u)$ and the interaction vertices of a standard SK field theory. The details of this construction depend on the form of S_{int}, but the Feynman rules for computing the diagrams are exactly similar to that of a SK field theory, with u dependent propagators $\hat{G}(u)$.

The diagrammatic perturbation theory for the Green's functions work well at short times, but one needs to resum the series or part of it to all orders to obtain an accurate description of the long time behaviour. This is a general characteristic of perturbation theories

and has nothing to do with arbitrary initial conditions. This is where our formalism has an advantage: the standard resummation techniques known in field theories apply to $G^{(n)}_{int}(u)$, while they do not apply to the physical correlators $\mathcal{G}^{(n)}_{int,\rho_0} = \mathcal{L}(\partial_u, \rho_0)\mathcal{N}(u)G^{(n)}_{int}(u)|_{u=0}$. Focusing on the one-particle Green's function, one can now write a Dyson equation $\hat{G}_{int}(u) = [G^{-1}(u) - \Sigma(G(u))]^{-1}$, where the irreducible self energy can be constructed diagrammatically in perturbation theory. One can also use a skeleton expansion in terms of $\Sigma(G_{int}(u))$, or resum a class of diagrams as in a RPA expansion; in other words one can bring the full force of accumulated knowledge of such approximation schemes to bear down on the problem of calculating $\hat{G}_{int}(u)$. Similar constructions are possible for higher order correlation functions in terms of higher order vertex functions.

3.8 Discussions

In this chapter, we have formulated a field theoretic description of dynamics of a quantum many body system (Bosons and Fermions) starting from an arbitrary initial density matrix. We have shown that the matrix element of the density matrix can be incorporated using a source which couples to the bilinears of the fields only at initial time, i.e by adding an impulse term to the original SK action. The Green's functions can be evaluated in this theory as a function of the addition source $\hat{u}$. The physical correlation functions can then be obtained by taking an appropriate set of derivatives of the Green's functions w.r.t the initial source and setting the sources to zero. The initial density matrix only governs the particular set of derivatives to be taken. Our formalism thus breaks up into two parts: (i) calculation of Green's functions in presence of a bilinear source, where the hierarchy of Green's functions satisfy Wick's theorem and the standard SK field theoretic techniques can be applied to compute them, (ii) taking a particular set of derivatives, which depend on the initial conditions. We calculate the exact expressions for physical one-particle and two-particle correlators in a non-interacting system and characterize the violation of Wick's theorem, relating it to the connected to particle correlations in the initial state. We have briefly sketched how our formalism can be extended to interacting systems. The biggest challenge that we have not addressed here are strategies to obtain reasonable approximation schemes which are controlled in particular limits. The issue of making conserving approximations which are valid at long times (i.e. no perturbation

theory for physical correlators) is one of great importance which we will address in later chapters.

We will apply this new formalism to probe interesting problems in dynamics of many body disordered systems in chapter 4 and in open quantum system in chapter 5 and chapter 6. In the next chapter, we will study how the memory of initial conditions is being retained in the long time dynamics of a disordered system initialized in a Fock state with a pattern of density imbalance imprinted on it. Using this new extension of SK field theory, we, for the first time, provide an exact connection between the traditional ways of characterizing disordered systems in terms of localization length and experimentally measurable non-equilibrium observables, like long time imbalance retained by the system.

Chapter 4

Dynamics of Disordered Many Body Systems

4.1 Introduction

Isolated quantum systems, driven out-of-equilibrium, are the ideal test-bed of studying thermalization and applicability of quantum statistical mechanics in many body systems. Thermalization of an isolated quantum system is understood in the form of Eigenstate Thermalization Hypothesis (ETH) [24, 25, 26, 110]. ETH states that in a generic quantum many body system, starting from a *typical* initial state, $|\psi(0)\rangle$, of given total energy E, the quantum mechanical expectation value of any local observable, $\hat{A}$, averaged over long time, T, becomes identical to micro-canonical average of the observable, $\langle\hat{A}\rangle_{mc}$ at the energy E in the thermodynamic limit. Consequently, we have

$$\langle\hat{A}\rangle_{\infty} = \lim_{T\to\infty}\frac{1}{T}\int_{0}^{T} dt\ \langle\psi(t)|\hat{A}|\psi(t)\rangle = \langle\hat{A}\rangle_{mc}. \tag{4.1}$$

Hence, the longtime behaviour of a generic isolated quantum many body system, starting from a typical initial state, becomes independent of the choice of the initial state and can be correctly reproduced by the quantum statistical mechanical description of the system. However, in contrast to this, there are quantum many body systems that exhibit breakdown of ETH and fail to thermalize even in longtime.

A quantum system with strong disorder is one such interesting platform, both for theoretical and experimental studies, as it provides a robust mechanism of ergodicity breaking and absence of thermalization. In 1958, P.W. Anderson showed [111] that single particle wave-functions in a strongly disordered non-interacting system become localized in real

Thermal Phase	Single-particle Localized	Many-body Localized
Memory of initial conditions "hidden" in global operators at long times	Some memory of local initial conditions preserved in local observables at long times	Some memory of local initial conditions preserved in local observables at long times
ETH true	ETH false	ETH false
May have nonzero DC conductivity	Zero DC conductivity	Zero DC conductivity
Continuous local spectrum	Discrete local spectrum	Discrete local spectrum
Eigenstates with volume-law entanglement	Eigenstates with area-law entanglement	Eigenstates with area-law entanglement
Power-law spreading of entanglement from non-entangled initial condition	No spreading of entanglement	Logarithmic spreading of entanglement from non-entangled initial condition
Dephasing and dissipation	No dephasing, no dissipation	Dephasing but no dissipation

Table 4.1: Comparison of properties of many body eigenstates in thermal phase, single particle localized phase and MBL phase. The contents of the table are taken from Ref. [29] with due permission.

space which is manifested in the form of absence of transport in the system. Subsequently, this phenomenon was put in firmer footing by scaling theory of localization [112, 113, 114] which predicts a quantum phase transition between the delocalized and localized phases depending on the dimensionality of the system. Since the discovery of Anderson localization, the study of interplay of disorder and inter-particle interaction in localizing the system has become a highly debated topic of interest. More recently, the absence of transport in many body interacting disordered systems, even at non-zero temperature has been predicted in theoretical studies by Basko et al [34]. This phenomenon is called many body localization. Later, several numerical studies [40, 115, 116] also observed signatures of many body localization phase transitions in disordered quantum spin chains by exact diagonalization of the many body Hamiltonian for small systems.

So far the theoretical studies on MBL have mainly focused on the properties of many body eigenstates in the middle of the spectrum [60, 61, 62, 40] in equilibrium. These states show Poissonian gap statistics, area law growth of entanglement entropy and violation of ETH hypothesis, leading to sharp distinctions between MBL and thermalizing phases, summarized in Table 4.1. However, it is impossible to experimentally access these states individually.

Recently, evidences of many body localization have been detected in ultra-cold atomic experiments, by studying the longtime dynamics of the disordered (quasi-periodic) system. The principle behind these experimental studies [30, 31, 117] can be stated in the following

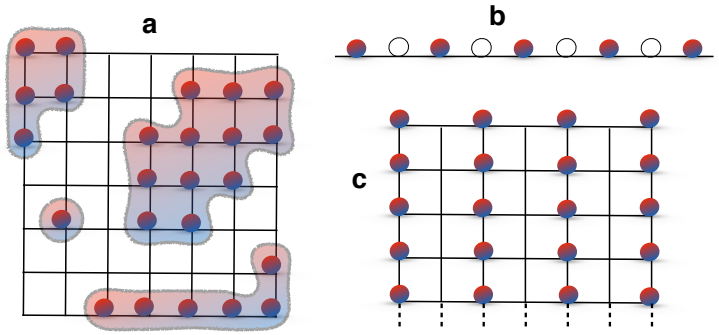

Figure 4.1: Initial density pattern of disordered (quasi-periodic) system: (a) A lattice with occupied sites forming the set A (marked with shaded regions) and empty sites forming the set $\bar{A}$. (b) A one-dimensional lattice with alternating pattern of 1 and 0 particles. (c) A square lattice with alternating chains (in vertical direction) of 1 and 0 particles. These geometry of initial patterns have been used to detect MBL in cold-atom experiments [118, 63, 68].

way: the system is initialized in a Fock state, which has 1 particle on a set of lattice sites (say A) and 0 particles on the rest of the sites (say $\bar{A}$), as shown in Fig. 4.1(a). The system is then allowed to evolve (either under Hamiltonian or under open quantum system dynamics) and the density imbalance between A and $\bar{A}$ sites, normalized by average density, is measured with time. The Hamiltonian of the system (averaged over disorder) does not distinguish between A and $\bar{A}$ sites; hence in a thermal system, the longtime imbalance should be 0. A finite imbalance in the long time limit implies that the system remembers the initial condition and indicates absence of thermalization in the system. Fig. 4.1(b) and 4.1(c) show specific examples of the geometry of the initial density implemented on 1d and 2d optical lattices in cold-atom experiments to detect MBL.

Imbalance dynamics in MBL systems has been treated theoretically using numerical techniques like exact diagonalization (ED), DMRG [118, 119, 120, 121, 122], and field theoretic approaches like Hartree-Fock approximation [123] for 1d Fermions and Gutzwiller mean-field theory[124] for 2d Bosonic system. While these methods provide varying levels of quantitative match with experiments, they do not provide insights into microscopic processes leading to long time memory retention. In this chapter, we use the new extension of Keldysh field theory [57], developed in chapter 3 to understand imbalance dynamics in systems with random or incommensurate potentials [67], both in presence and absence of inter-particle interaction.

For localized non-interacting systems, we establish an explicit connection between the

experimentally measurable non-equilibrium observable [118, 63, 68] and the traditional understanding of disordered systems in terms of localization length [111, 112], through a universal relation between the long time density imbalance, the localization length and the geometry of the initial density pattern. Inverting our results, one can extract the localization length of the system from the experimental data on the longtime density imbalance. For the initial patterns, shown in Fig. 4.1 (b) and (c) which have been used in 1-d and 2-d experiments [118, 63, 68], we derive analytic relations between localization length and long time imbalance. We show that near a localization-delocalization transition, the imbalance scales as the inverse localization length. This establishes an explicit connection between longtime memory retention and presence of localization in the system. We test our theory using the random potential Anderson model [111] on 1 and 2-dimensional lattices and the Aubry Andre model [125] in 1 dimension. In systems with mobility edge in the spectrum [126, 127, 128], only the localized states contribute to long time imbalance. The one particle Green's functions, projected on these states, decay exponentially with distance. This defines an "effective" localization length, $\bar{\xi}_l$. The imbalance, divided by the fraction of localized states in the system, is given by the same analytic relations with this effective localization length. Our analysis shows how this leads to non-analyticites in the imbalance as a function of disorder strength, when the mobility edge passes through a band edge.

Finally, we consider imbalance dynamics in an interacting Bosonic/Fermionic system with an incommensurate potential. We use a conserving approximation [129], keeping the lowest order processes leading to dissipative and stochastic dynamics. Naively one would expect the memory of the initial state to decay, as the Green's functions which propagate this memory decay in time. However, as the quasiparticles decay, they create excitations which act as a bath for the rest of the quasiparticles. The noise fluctuations of this bath remember the initial conditions at strong disorder and sustain the finite long time imbalance. Both non-interacting and interacting systems retain memory of initial states at large disorder. However, our analysis reveals that the microscopic mechanism responsible for this is very different in the two cases. This leads to widely divergent description of the longtime imbalance dynamics in Anderson localized and many body localized systems.

Now for the convenience of the readers, we will provide a road-map through this chapter: in section 4.2 we will derive a universal relation between the density imbalance retained

in the longtime and the localization length, for any geometry of initial density pattern imprinted on a generic non-interacting localized system. In section 4.3, we will use this result to obtain an analytical closed form answer for longtime imbalance in terms of the localization length in a one-dimensional system initialized to alternating pattern of filled and empty sites. We will verify this result for systems with onsite disordered (Anderson model) potential as well as quasi-periodic potential (Aubry-Andre model). In section 4.4, we will modify this result for a 1d system having mobility edge in the spectrum, which show interesting features in the long time imbalance when the mobility edge passes through the band edges. In section 4.5, we will extend this result for a square lattice with disorder potential. Finally, in section 4.6, we consider effect of inter-particle interaction in the imbalance dynamics of a many body Bosonic system. Section 4.7 renders important insights into the very different microscopic mechanisms that sustain the longtime imbalance in a non-interacting vs an interacting system. In section 4.8, we extend this analysis to the case of an interacting spinless Fermionic system.

4.2 Imbalance and Localization Length in Non-interacting Systems

We first consider non-interacting particles whose dynamics is governed by the Hamiltonian,

$$H = -J \sum_{\langle ij \rangle} a_i^\dagger a_j + \sum_i v(i) a_i^\dagger a_i, \tag{4.2}$$

where $a_i^\dagger$ is the particle creation operator on lattice site i, J is the nearest neighbour hopping and $v(i)$ is a local potential, which is quasi-periodic in the Aubry-Andre model and truly disordered in Anderson model.

We will study dynamics of this system within the Schwinger Keldysh field theory [55], which has two independent one particle physical correlators: (a) the retarded propagator, $G_R(i,t;j,t')$, which is the amplitude of propagating a particle to site i at time t provided the particle was at site j at time t', without creating additional excitations, and (b) the Keldysh propagator $\mathcal{G}_K(i,t;j,t')$, which represents the actual amplitude of exchanging a particle between site i at time t and site j at time t'. $\mathcal{G}_K(i,t;j,t)$ is related to densities

and currents in the system; e.g. for bosons (fermions), the local density is given by,

$$n_i(t) = \pm\frac{1}{2}[\mathbf{i}\mathcal{G}_K(i,t;i,t) - 1]. \tag{4.3}$$

The system is initialized to a Fock state, where $n_i(0) = 1/2(1+\sigma_i)$, with $\sigma_i = \pm 1$ if $i \in A(\bar{A})$. We use the extension of Keldysh field theory, developed in chapter 3, which can explicitly keep track of arbitrary initial conditions in quantum dynamics [57]. Here, $G_R(i,t;j,t') = \sum_n \phi_n^*(i)\phi_n(j)e^{-iE_n(t-t')}$, where E_n and $\phi_n(i)$ are the energy levels and corresponding wavefunctions of the Hamiltonian, given in Eq. 4.2. The Keldysh Green's functions $\mathcal{G}_K$ carry the information of the initial density matrix through Eq.3.17 for Bosons and Eq.3.33 for Fermions in the extended SK field theory and are given by

$$\begin{aligned} \mathbf{i}\mathcal{G}_K(i,t;j,t') &= \sum_k G_R(i,t;k,0)G_R^*(j,t';k,0)[1 \pm 2n_k(0)], \text{hence} \\ n_i(t) &= \sum_k |G_R(i,t;k,0)|^2 n_k(0). \end{aligned} \tag{4.4}$$

Note that the expression for local density is same for bosons and fermions. Hence, all the statements about imbalance dynamics in non-interacting systems are independent of statistics of particles. Starting from the Fock state, during the evolution of the system, the imbalance between the filled and the empty subsystem is calculated from,

$$I(t) = \frac{\sum\limits_{i\in A} n_i - \sum\limits_{i\in \bar{A}} n_i}{\sum\limits_{i\in A} n_i + \sum\limits_{i\in \bar{A}} n_i} \tag{4.5}$$

For a closed system having $L/2$ number of particles distributed over L sites, i.e with equal number of A and $\bar{A}$ sites, the density imbalance, averaged over disorder, is given by,

$$\langle I(t)\rangle = \frac{2}{L}\sum_{k\in A,i} \sigma_i \langle |G_R(i,t;k,0)|^2\rangle. \tag{4.6}$$

The disorder averaged retarded Green's functions, $\langle |G_R|^2\rangle$, can be calculated from the knowledge of the energy spectra and the eigenfunctions in each disorder configuration, yielding a "numerical" estimate of imbalance.

Now, to gain analytical insights into the mechanism of memory retention in the long

time dynamics, we realize that $G_R(i,t;k,0)$ is the solution to Anderson's original problem [111]: it is the wavefunction at site i and time t of a particle initially localized at k. In chapter 3, we have shown that $G_R(i,t;j,t')$ does not depend on the initial condition of the system [57] and it is insensitive to the initial density imbalance imprinted between A and $\bar{A}$ sub-lattices. Hence, the system recovers translation invariance when one looks at disorder averaged correlation functions, i.e. the disorder averaged $\langle|G_R(i,t;j,t')|^2\rangle$ becomes only a function of the spatial separation, $|\vec{r}_i - \vec{r}_j|$. In the localized system, $\langle|G_R(i,t;k,0)|^2\rangle$ which the probability of finding a particle at a site i at a long time t, given that the particle was initially at the site k, decays exponentially with the spatial distance, $|\vec{r}_i - \vec{r}_k|$. As $t \to \infty$, in the localized phase,

$$\langle|G_R^{\infty}(i,k)|^2\rangle = \langle\sum_n |\phi_n(i)\phi_n^*(k)|^2\rangle \sim e^{-2|\vec{r}_i-\vec{r}_k|/\xi_l}. \tag{4.7}$$

This decay defines the localization length ξ_l. The long time imbalance then reduces to,

$$\langle I(\infty)\rangle = \frac{2}{L}\sum_i \sum_{k\in A} \sigma_i e^{-\frac{2|\vec{r}_i-\vec{r}_k|}{\xi_l}}. \tag{4.8}$$

This is the universal relation between the long time imbalance, the localization length and the geometry of the initial pattern. In the next sections, we will use this result to derive closed form answer for $\langle I(\infty)\rangle$ considering some specific initial patterns that have been used in the cold atom experiments to detect MBL [118, 68].

4.3 Linear Chain with Alternating Density Pattern

In this section, we will concentrate on a particular geometry of the initial distribution of particles to derive a closed form analytical answer for the long time density imbalance in terms of the localization length of the system. This initial density pattern has been extensively used in cold-atomic experiments in 1d optical lattice.

We consider a linear chain initialized in the Fock state, $|1,0,1,0,...\rangle$, having one particle placed on the alternating lattice sites, as shown in Fig. 4.1(b). Hence, the density imbalance between A and $\bar{A}$ sub-lattices is maximum at $t = 0$, $\langle I(0)\rangle = 1$. Now to calculate the long time imbalance, $\langle I(\infty)\rangle$ for this pattern of initial density modulation, the series in Eq. 4.8 can be grouped in the following way: for each site $k \in A$, the exponential is added with

positive sign for all $i \in A$ where $|\vec{r}_i - \vec{r}_k| = 0, \pm 2a, \pm 4a, ...$ and with negative sign for all $i \in \bar{A}$ where $|\vec{r}_i - \vec{r}_k| = a, \pm 3a, \pm 5a, ...$ Here a denotes the lattice spacing of the linear chain. We note that the summation over $L/2$ possible values of $\vec{r}_k$ on the filled sub-lattice A, cancels the factor $2/L$, coming from the normalization with the total number of particles in the system. Assuming a large chain where boundary effects can be neglected, we extend the summation in Eq. 4.8 to infinite distance and obtain,

$$\begin{aligned} \langle I(\infty) \rangle &= 2 \sum_{r=0}^{\infty} [e^{-4ra/\xi_l} - e^{-(4r+2)a/\xi_l}] - 1 \\ &= \tanh\left(\frac{a}{\xi_l}\right). \end{aligned} \tag{4.9}$$

This is the key result of this section. From this "analytic" estimate, we see that as $\xi_l/a \to \infty$, $\langle I(\infty) \rangle \sim \frac{a}{\xi_l} \to 0$; i.e. the long time imbalance vanishes and the system forgets its initial memory when the localization length diverges. This suggests: (i) the memory retention is directly related to localization and (ii) close to a localization-delocalization transition, the scaling of the Lyapunov exponent [130] $\gamma = a/\xi_l$ governs the behaviour of the long time density imbalance.

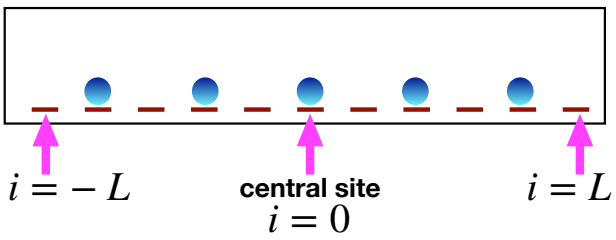

Figure 4.2: Linear chain consisting of odd number of sites, $2L+1$ with alternating density pattern. The central site is chosen to belong to filled sub-lattice A.

Now, we will address the question on how the analytical formula for the long time imbalance, $\langle I(\infty) \rangle = \tanh(a/\xi_l)$ is modified in case of a finite size linear chain initialized to the alternating density pattern shown in Fig.4.2. We will show that the finite size correction to $\langle I(\infty) \rangle$ is exponentially small in the system size. To show this, we consider a linear chain having $2L+1$ number of sites. We choose L to be an odd number and the origin, situated at the central site of the chain, belong to the filled sub-lattice A. We note that the final conclusion about exponentially small finite size correction to $\langle I(\infty) \rangle$ does not depend on this particular choice of the geometry. Using equation Eq. 4.8, we write

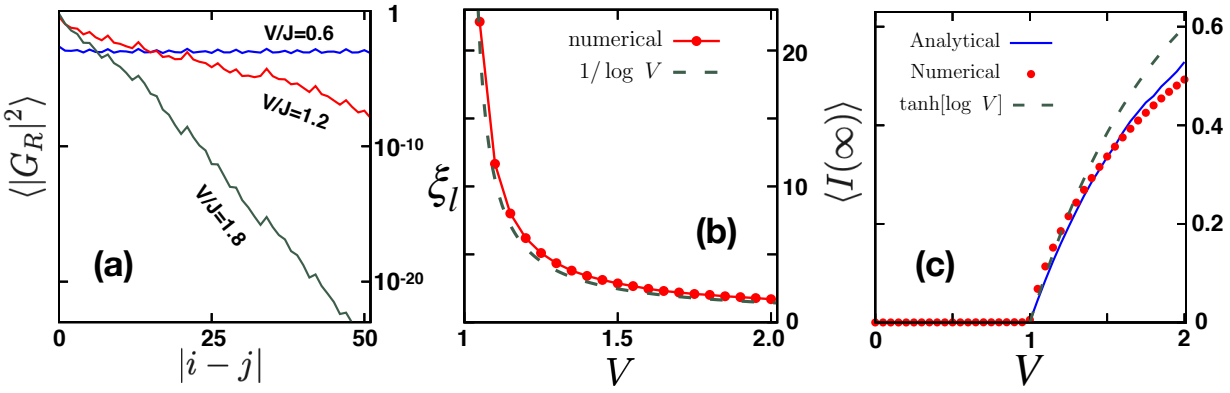

Figure 4.3: 1d Aubry Andre model: (a) The infinite time "disorder averaged" $\langle |G_R^{\infty}(i,j)|^2 \rangle$ for Aubry Andre model as a function of distance, $|i-j|$. In the delocalized phase at $V = 0.6$, the Green's function decays to a finite constant at large distances. In the localized phase ($V = 1.2,\ 1.8$), it decays exponentially and the scale of the exponential decay defines the localization length. (b) The localization length, ξ_l (solid line) extracted from the decay of $\langle |G_R^{\infty}(i,j)|^2 \rangle$ as a function of the potential strength V. The dashed line shows, $\xi_l = 1/\log[V]$ obtained from the duality relation [131]. (c) The infinite time density imbalance, $\langle I(\infty) \rangle$, starting from an alternating pattern of 1 and 0 particles, is plotted as a function of V. The red dots are numerical results. The solid and the dashed lines show the analytical result, i.e $\langle I(\infty) \rangle = \tanh[1/\xi_l]$, where the solid line uses ξ_l determined from $\langle |G_R^{\infty}(i,j)|^2 \rangle$ (solid line in (b)), while the dashed line uses $\xi_l = 1/\log[V]$. We have used a 1000 site linear chain and averaged over 100 different configuration of θ for numerical estimation of imbalance. In all the plots, we have set the lattice spacing, $a = 1$ and the hopping scale, $J = 1$ as the units of length and energy respectively.

the long time imbalance of the finite chain as,

$$\begin{aligned}
\langle I(\infty) \rangle &= \frac{1}{L}\left[\sum_{i=0,\pm 2,\ldots,\pm(L-1)} \sum_{j=0,\pm 2,\ldots,\pm(L-1)} e^{-2\frac{|i-j|\ a}{\xi_l}} - \sum_{i=0,\pm 2,\ldots,\pm(L-1)} \sum_{j=\pm 1,\pm 3,\ldots,\pm L} e^{-2\frac{|i-j|\ a}{\xi_l}} \right] \\
&= \left[2\left(\sum_{r=0,2,\ldots,(L-1)} e^{-2\frac{r\ a}{\xi_l}} - \sum_{r=1,3,\ldots,L} e^{-2\frac{r\ a}{\xi_l}} \right) - 1 \right] \\
&= \tanh\left(\frac{a}{\xi_l}\right) - \frac{2}{1+e^{-\frac{2\ a}{\xi_l}}} e^{-\frac{2(L+1)\ a}{\xi_l}}. \qquad (4.10)
\end{aligned}$$

In this equation, the second term gives the finite size correction to the long time imbalance, $\langle I(\infty) \rangle$. In the large system size limit, $L\ a/\xi_l >> 1$, the correction term exponentially decays to zero and we recover Eq. 4.9, relating the long time density imbalance and the localization length for the alternating pattern of initial density modulation.

We will now verify this analytical estimate of long time imbalance (Eq. 4.9) with the numerically calculated answer from Eq. 4.6 for different models of disordered and quasi-

periodic potentials on 1d lattice.

4.3.1 1d Aubry-Andre Model

We first consider the Aubry Andre (AA) model [125], with an incommensurate potential,

$$v(i) = 2V\cos[2\pi\alpha i + \theta], \tag{4.11}$$

imposed on a linear chain. Here α is a Diophantine number [132] and θ is the phase of the potential. This model is particularly interesting in the study of localization physics in one dimensional system as it exhibits a transition from delocalized phase to localized phase at $V/J = 1$, which can be shown from the self-duality property of the AA Hamiltonian [133, 125]. In the localized phase for $V/J < 1$, all the eigenstates of the Hamiltonian are localized with the same localization length, $\xi_l = a/\log(V/J)$.

We will verify our analytical answer of the long time imbalance, given in Eq. 4.9, for a linear chain initialized to $|10101..\rangle$ state, in case of the Aubry-Andre model with quasi-periodic potential. We choose, α to be the golden mean, i.e. $\alpha = (\sqrt{5}+1)/2$. "Disorder averaging" is achieved in this quasi-periodic model by averaging over the phase of the potential, θ. In the discussion of the localization physics, θ is an irrelevant parameter of the model and we choose it uniformly between $[0, 2\pi]$. The delocalization to localization phase transition in this model can be clearly seen Fig. 4.3(a), where we plot the infinite-time disorder averaged, $\langle|G_R^{\infty}(i,j)|^2\rangle = \langle\sum_n |\phi_n(i)\phi_n^*(j)|^2\rangle$ as a function of $|i-j|$ in a semi-log plot. The eigenfunctions, $\phi_n(i)$, are obtained by diagonalising AA Hamiltonian on a 1000-site linear chain. For $V/J = 0.6$, where the system is delocalized, $\langle|G_R^{\infty}|^2\rangle$ saturates to a finite value at large distances, whereas it shows an exponential decay for $V/J > 1$, with the decay length decreasing with increasing disorder strength. The slope extracted from the exponential decay of $\langle|G_R^{\infty}|^2\rangle$ gives a numerical estimate of the localization length, ξ_l, which is plotted as a function of the disorder strength, V in Fig. 4.3(b) (solid red line). This numerically obtained result for ξ_l closely matches with the analytical answer, $\xi_l = a/\log(V/J)$ [131], plotted by the dashed line in Fig. 4.3(b). In Fig. 4.3 (c), we plot the disorder-averaged long time imbalance as a function of V/J obtained using the numerical estimate from Eq. 4.6 (solid dots) . We also plot the analytic answer from

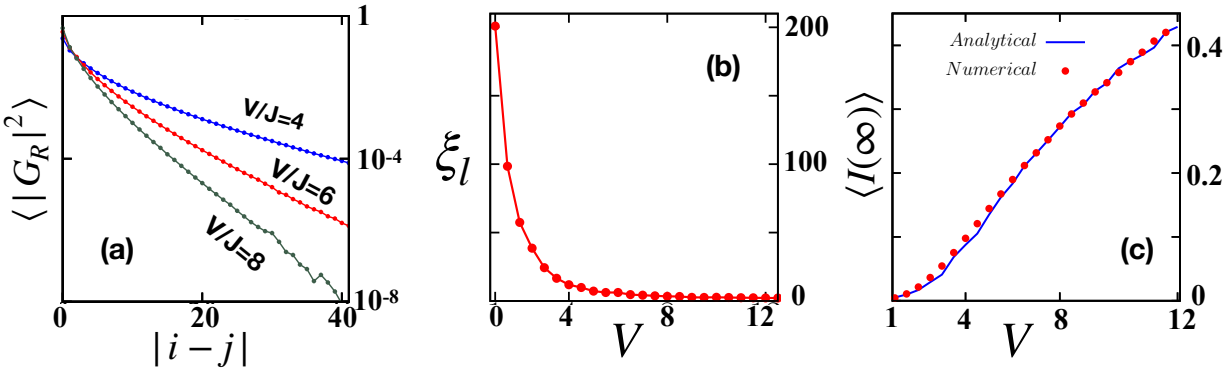

Figure 4.4: 1d Anderson model: (a) Exponential decay of long time disorder averaged Green's function, $\langle |G_R^{\infty}(i,j)|^2 \rangle$ with $|i-j|$ for the 1-d Anderson model for $V/J = 4, 6, 8$. This model exhibits localization for arbitrary small values of V. (b) The localization length, extracted from the exponential fit , as a function of V/J. (c) shows the agreement between analytically calculated imbalance (solid line) from Eq. 4.9 with the corresponding numerical answer from Eq. 4.6 for 1d Anderson model. We use a $N = 1000$ site linear chain and averaged over 100 disorder realizations. In all the plots, we have set the lattice spacing, $a = 1$ and the hopping scale, $J = 1$ as the units of length and energy respectively.

Eq. 4.9 with ξ_l obtained from (i) fitting $\langle |G_R^{\infty}|^2 \rangle$ (solid line) and (ii) the duality relation [131] $\xi_l = a\ log[V/J]$ (dashed line). The analytic answer matches the numerical estimate for $\xi_l/a > 1$. This verifies our theory relating the long time imbalance and the localization length in this non-interacting quasi-periodic system.

4.3.2 1d Anderson Model

We next consider the 1-d Anderson model [111] where potential, $v(i)$, at each site i is an independent random variable, chosen with the probability distribution, $P[v(i)] = \Theta[V^2/4 - v^2(i)]1/V$. In this model of random disorder potential on a linear chain, it is well established that all the eigenstates become localized in space in presence of infinitesimal disorder, V [113]. The localization length of these eigenstates depend on the energy and in the weak disorder limit, it takes the form, $\xi_l(E) = a(96 - 24E^2/J^2)/(V/J)^2$ [112, 134], where $E = 2\cos(k)$ is the energy of the unperturbed Bloch band. However, in our calculation, we bypass the complication arising out of the energy dependence of the localization length in this model by defining ξ_l from the exponential decay scale of $\langle |G_R^{\infty}(i,k)|^2 \rangle$ with distance, which includes contributions from all the eigenstates. In Fig.4.4(a), we have plotted $\langle |G_R^{\infty}(i,k)|^2 \rangle$ as a function of $|i-k|$ in a semi-log plot for three different disorder strength $V/J = 4, 6, 8$. Localization length, ξ_l, extracted from the slope of the exponential

decay of $\langle|G_R^{\infty}|^2\rangle$, is shown in Fig.4.4(b) as a function of V. These ξ_l for different V are used to calculate the analytical long time imbalance, $\langle I(\infty)\rangle = \tanh(a/\xi_l)$, shown by solid line in the Fig. 4.4 (c). We also plot the numerical result for long time imbalance obtained from Eq. 4.6 (solid dots) and find good quantitative match between these estimates. This establishes validity of our theory relating infinite time imbalance to the localization length in 1−d Anderson model.

4.4 Imbalance in Presence of Mobility Edges

In the previous section, we have provided an analytical relation between the long time imbalance and the localization length of a non-interacting one-dimensional system. We have verified our theory with examples of Anderson model with random potential and Aubry Andre model with quasi-periodic potential. In both the cases, eigenstates of the Hamiltonian are such that either all them are localized or all of them are delocalized at a given strength of the disorder (quasi-periodic) potential [114]. However, there are interesting examples of non-interacting systems where localized and delocalized eigenstates can coexist in the spectrum, separated by a single particle mobility edge. The idea of the presence of mobility edges in 3d Anderson model was theoretically established long ago by scaling theory of localization [114] and has been measured recently in ultra-cold atomic experiments [135]. On the other hand, while non-interacting one dimensional systems with uncorrelated random potential can not support a mobility edge in the spectrum [114], quasi-periodic systems exhibit single particle mobility edges [126, 127, 136, 137, 138] and lead to several interesting phenomena observed in recent experiments [139, 140]. These quasi-periodic potentials are presented in different forms of modified Aubry Andre model.

In this section, we consider a form of modified Aubry Andre model [126, 127] on a linear chain with the onsite quasi-periodic potential given by,

$$v(i) = 2V\frac{\cos[2\pi\alpha i + \theta]}{(1 - \nu\cos[2\pi\alpha i + \theta])}, \tag{4.12}$$

where $-1 < \nu < 1$. In this model, the limiting case, $\nu = 0$ corresponds to the usual Aubry Andre model discussed before. This model is particularly interesting in the study of localization physics in 1d systems as for intermediate strength of the disorder potential,

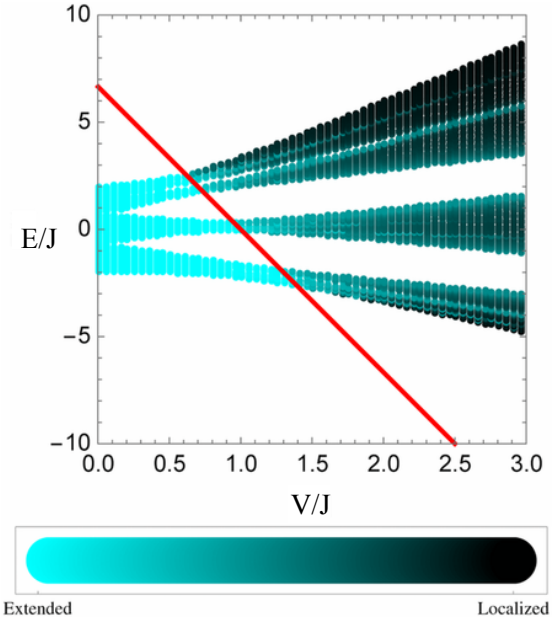

Figure 4.5: Spectrum of the modified Aubry Andre model given in Eq. 4.12: transition from delocalized eigenstates to localized eigenstates is shown in the energy, E/J vs potential strength, V/J plane. The color scheme denotes the inverse partition ratio (IPR) of the eigenstates. Black and cyan colors stand for IPR=1(fully localized) and IPR=1/system size (fully delocalized) respectively. The red line shows the position of the mobility edge, $E_c = 2(J - V)/\nu$, which is an energy threshold separating the localized and delocalized states in the spectrum. This shows that for large V/J, E_c goes below the lowest energy band and hence all the eigenstates are localized. On the other hand, for small V/J, E_c is above the highest energy band and hence all the eigenstates are delocalized. For intermediate values of V/J, localized and delocalized states coexist in the spectrum, separated by the mobility edge. For this, $\nu = 0.3$ and $J = 1$. This plot is taken from Ref. [127] with due permission.

V/J, it supports a mobility edge, $E_c = 2(J - V)/\nu$ [126] in the spectrum, shown in Fig. 4.5. At low V/J, all the eigenstates in the spectrum are delocalized, whereas at large V/J, all states are localized. In this model, the localization length of an eigenstate depends of its energy. Here, similar to the case of AA model, we choose, $\alpha = (\sqrt{5} + 1)/2$ and the phase, θ uniformly between 0 to 2π.

In Fig. 4.6 (a), we plot $\langle |G_R^{\infty}|^2 \rangle$ of the system as a function of distance for $V/J = 1.2$ and $\nu = 0.4$, where there is a mobility edge. The long distance behaviour of $\langle |G_R^{\infty}|^2 \rangle$ is dominated by delocalized states and saturates to a constant. In the same figure, we also plot the contribution to $\langle |G_R^{\infty}|^2 \rangle$ from states above the mobility edge, which clearly shows an exponential decay. This decay can be used to extract an "effective" localization length $\tilde{\xi}_l$ for the system. The infinite-time "disorder averaged" imbalance in this case is modified

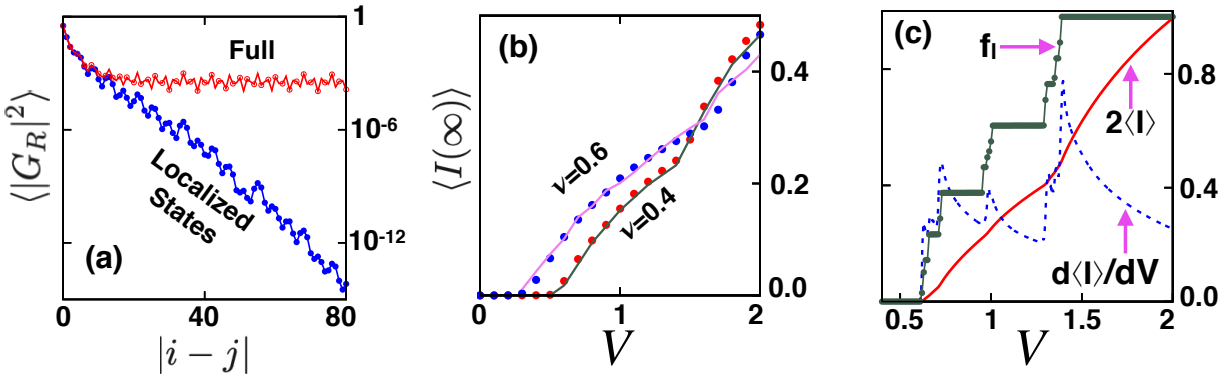

Figure 4.6: Modified Aubry Andre model: (a) $\langle |G_R^{\infty}|^2 \rangle$ in the modified Aubry Andre model with mobility edge as a function of distance ($V/J = 1.2$ and $\nu = 0.4$). The full Greens function (which saturates) and its projection onto the localized states (which decay exponentially) are both shown. (b) $\langle I(\infty) \rangle$ for the modified Aubry Andre model as a function of V/J for $\nu = 0.4, 0.6$ obtained from (i) Eq. 4.6 (solid dots) (ii) Eq. 4.13(solid lines). $\bar{\xi}_l$ is obtained from fits of $|G_R|^2$. (c) The fraction of localized states (f_l), the long time imbalance $\langle I \rangle$(multiplied by 2 to plot on same scale)and the derivative $d\langle I \rangle/dV$ as a function of V/J for the modified Aubry Andre model ($\nu = 0.4$). The values of V/J, where the mobility edge leaves or enters a band are marked by derivative discontinuities in f_l and $\langle I \rangle$. All data are averaged over 100 disorder configurations on 1000 site lattice.

as,

$$\langle I(\infty) \rangle = f_l \tanh\left(\frac{a}{\tilde{\xi}_l}\right), \tag{4.13}$$

where f_l is the fraction of localized states in the spectrum. In Fig. 4.6 (b), we plot $\langle I(\infty) \rangle$ as a function of V/J for $\nu = 0.4, 0.6$. The numerical answer (solid dots) from Eq. 4.6 and the analytical result (solid lines) from Eq. 4.13 track each other. The imbalance goes to 0 when all states are delocalized at low V/J. At large V/J, the curve approaches the $\nu = 0$ answer.

There is a clear non-analytic feature in the long time imbalance as a function of V/J, which coincides with the V/J where the mobility edge coincides with the band edge. A closer scrutiny shows that the system has multiple bands, as shown in Fig. 4.5. There is a sharp change in derivative of $\langle I(\infty) \rangle$ every time the mobility edge coincides with a band edge. This can be seen in Fig. 4.6 (c), where we plot f_l, $\langle I(\infty) \rangle$ and $d\langle I(\infty) \rangle/dV$ vs V/J in the same plot for $\nu = 0.3$. To understand this non-analyticity, we recall the definition of energy dependent localization length, $\xi_l(E)$, in terms of the density of states, $\rho(E)$, given by [141],

$$\xi_l(E) = \frac{1}{\int dE' \ \rho(E') \log|E - E'|}. \tag{4.14}$$

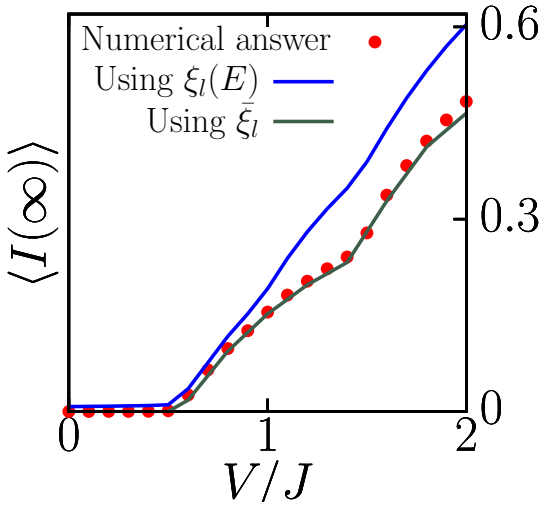

Figure 4.7: In this figure, long time imbalance as a function of V/J for modified Aubry Andre model obtained from three different calculations: (1) The red dots correspond to the numerical answer obtained from Eq. 4.6, (2) The green line is obtained from Eq. 4.13 using the effective localization length, $\bar{\xi}_l$, extracted from the decay of $\langle|G_R^{\infty}|^2\rangle$, projected onto the localized states. (3) The blue line is obtained by using the energy dependent localization length, $\xi_l(E_n) = 1/\sum_{m\neq n}\log|E_n - E_m|$ for each eigenstate, n, to calculate, $\langle I(\infty)\rangle = (1/N)\sum_n \tanh(a/\xi_l(E_n))$. Although this answer does not match with (1) and (2), the non-analytic features in $\langle I(\infty)\rangle$ are evident from all the curves.

We first consider the rightmost non-analytic feature in Fig. 4.6 (c), at $V_0 \sim 1.4J$. For $V > V_0$, the mobility edge is below the lowest band; all states are localized and contribute to I. As we approach V_0, the singular part of the imbalance, I_s, is governed by the scaling of, $\xi_l(E) \sim (E - E_c)^{-\beta}$, leading to $I_s \sim (V - V_0)^{\beta}$. On the other hand, for $V < V_0$, there is an additional effect as the fraction of localized states also decreases. If the Van Hove singularity in the density of states at the band edge E_b, $\rho(E) \sim (E - E_b)^{-\delta}$, the fraction of localized states changes as $\Delta f_l \sim |V - V_0|^{1-\delta}$, and hence $I_s \sim |V - V_0|^{\beta+1-\delta} \sim |V - V_0|^{2\beta}$. Here we have used the well known formula $\beta = 1 - \delta$ [142]. This leads to the cusp like behaviour of $d\langle I(\infty)\rangle/dV$ in Fig. 4.6 (c) when the mobility edge and band edge coincide.

At this point, it is worthwhile to note that, in our calculation of $\langle I(\infty)\rangle$ from Eq. 4.13, we have used the effective localization length, $\bar{\xi}_l$ which is the decay length of $\langle|G_R^{\infty}|^2\rangle$, projected onto the localized states (see Fig. 4.6 (a)). However, there is an alternative way of calculating localization length, $\xi_l(E_n)$ of each eigenstate, n, using $\xi_l(E_n) = 1/\sum_{m\neq n}\log|E_n - E_m|$, which is the discrete version of Eq. 4.14. Using this, one can calculate the long time imbalance, $\langle I(\infty)\rangle = (1/N)\sum_n \tanh(a/\xi_l(E_n))$ and the corresponding answer is plotted in Fig. 4.7 (blue line) as a function of V/J. Although, this result does

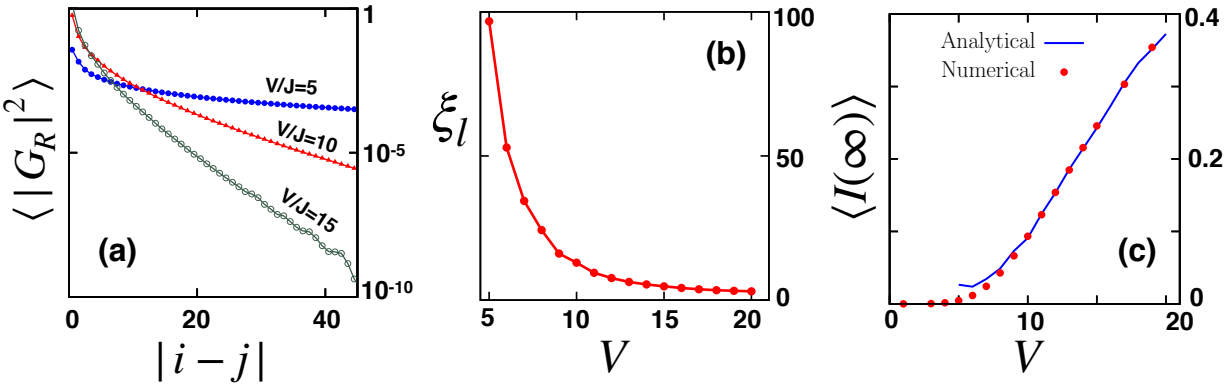

Figure 4.8: 2d Anderson model: (a) Exponential decay of long time disorder averaged Green's function, $\langle |G_R^{\infty}(i,j)|^2 \rangle$ with $|r_i - r_j|$ for the 2-d Anderson model for $V/J = 5, 10, 15$ (b) The localization length, extracted from the exponential fit , as a function of V/J. Note that at $V/J = 5$, the extracted localization length $\xi_l \sim 100$ and the system is effectively delocalized. (c) shows agreement between analytically calculated imbalance (solid line) for 2d Anderson model from Eq. 4.15 with the corresponding numerical answer(dots) from Eq. 4.6. In all the plots, we have set the lattice spacing, $a = 1$ and the hopping scale, $J = 1$ as the units of length and energy respectively. All the data are calculated for 100×100 lattice and averaged over 100 realizations.

not track the numerical answer of $\langle I(\infty) \rangle$ obtained from Eq. 4.6 as well as the analytical result calculated from Eq. 4.13 using the effective localization length, $\bar{\xi_l}$, the non-analytic features are evident from all the curves. This mismatch between the results obtained by using two alternate definitions of localization length can be understood in the following way: the formula connecting the long time imbalance to $\tanh(a/\xi_l)$, assumes translationally invariant Green's functions which are only true for disorder averaged $\langle |G_R^{\infty}|^2 \rangle$, but not for the individual eigenstates.

4.5 Imbalance in Disordered Square Lattice

In this section, we will consider 2d Anderson model, where the random potential, v_i, at each site on the square lattice is chosen from the box distribution, $[-V/2, V/2]$. By the scaling theory of localization, 2d random disorder model shows localization for any arbitrarily small strength of the disorder potential, V/J, where localization length, $\xi_l \sim a\ e^{J^2/V^2}$ in the weak disorder limit. In the localized system, the infinite-time disorder-averaged, $\langle |G_R^{\infty}(r)|^2 \rangle$, which is the key ingredient of our theory, decays exponentially with distance, r, on the square lattice, i.e $\langle |G_R^{\infty}(r)|^2 \rangle \sim e^{-2\sqrt{r_x^2 + r_y^2}/\xi_l}$. We will study the imbalance dynamics of this system, initialized to a density pattern consisting of alternating vertical chains of

1 and 0 particles respectively, as shown in Fig. 4.1(c). The choice of the initial density pattern is motivated by its relevance in recent cold-atomic experiments [63, 68]. The disorder averaged infinite time imbalance between the filled and the empty chains on the square lattice is related to the localization length, ξ_l, by,

$$\langle I(\infty)\rangle = \sum_{n_x,n_y=-\infty}^{\infty} (-1)^{n_x} e^{-\frac{2a}{\xi_l}\sqrt{n_x^2+n_y^2}}. \tag{4.15}$$

While this summation can not be done analytically to obtain closed form solution, we will calculate $\langle I(\infty)\rangle$ for a finite size $L \times L$ lattice by restricting the limits of the summation to $[-L, L]$.

In Fig. 4.8(a), we plot $\langle |G_R^{\infty}(i,j)|^2\rangle$ as a function of the distance, $|\vec{r}_i - \vec{r}_j|$ on the 2d lattice for $V/J = 5, 10, 15$, where the eigenfunctions are obtained by diagonalizing the Hamiltonian of the 100×100 lattice. Localization length, ξ_l is extracted from the exponential decay of $\langle |G_R^{\infty}(r)|^2\rangle$ and plotted in Fig. 4.8(b). This ξ_l is then used to obtain the analytical estimate of $\langle I(\infty)\rangle$ from Eq. 4.15, which is plotted in Fig. 4.8(c) as a function of V/J by the solid line. We also plot the numerical answer of $\langle I(\infty)\rangle$ (solid dots) from Eq. 4.6. The two approaches match till $V/J \sim 5$, where the localization length increases upto $\xi_l = 100a$. Since we are working with a 100×100 lattice, the system sees effective delocalization at $V/J \sim 5$ and the estimates for $V/J \leq 5$ are unreliable. The cold-atom experiments which are also restricted to similar system sizes, report effective delocalization at this length scale [143].

To estimate the finite size correction in the analytical result of $\langle I(\infty)\rangle$, obtained from Eq.4.15, we plot $\langle I(\infty)\rangle$ as function of a/ξ_l in Fig.4.9, for two different size of the square lattice, $L = 100$ and $L = 1000$. The graphs follow a straight line, showing that the imbalance scales with the inverse localization length. Numerically, we find the slope to be $\sqrt{32}/\pi^2$, i.e $\langle I(\infty)\rangle \sim (\sqrt{32}/\pi^2)(a/\xi_l)$ for $\xi_l \gg a$. For $L = 100$, we see a sharp upturn at $a/\xi_l \sim 0.1$, where the finite size effects start to play a role. Hence, for $L = 100$, reliable estimates of $\langle I(\infty)\rangle$ can be obtained for $V/J > 10$, which corresponds to $\xi_l < 10a$. For $L = 1000$, the curve continues with the same slope. Thus (a) finite size effects are easy to detect in the analytical estimate and (ii) the slope calculations from such finite size sums are reliable as long as we stay away from the upturn in the curve.

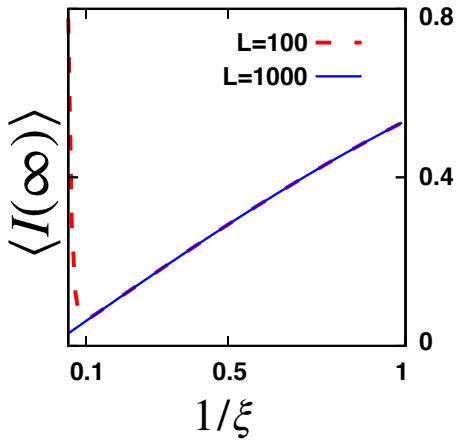

Figure 4.9: Numerical evaluation of the analytic formula given in Eq. 4.15 for long time imbalance in the 2d disordered lattice, as a function of the inverse localization length. The two plots are evaluating the formula in a lattice of size $N = 100\times100$ and $N = 1000\times1000$. Note $\langle I(\infty)\rangle$ linearly scales with ξ for large ξ as seen in both curves. The upturn in the $N = 100$ curve is due to finite size effects.

Our discussion on non-interacting disordered (quasi periodic) systems ends here. In the next section, we will study the effect of inter-particle interactions in the imbalance dynamics of a one dimensional system and provide new insights to the microscopic mechanism of memory retention in the long time limit.

4.6 Imbalance Dynamics in Interacting Bosonic Systems

In this section, we focus our attention on 1d Bose-Hubbard model with quasi-periodic potential and work with the Hamiltonian,

$$H = \sum_i \left[-Ja_i^\dagger a_{i+1} + v(i)a_i^\dagger a_i + Un_i(n_i-1)\right] \tag{4.16}$$

where $U > 0$ is the onsite Hubbard repulsion and $v(i) = 2V\cos(2\pi\alpha i + \theta)$ is the Aubry Andre potential with $\alpha = (\sqrt{5}-1)/2$ and the phase, θ uniformly chosen between 0 to 2π. The system is taken to be initialized to the same Fock state, $|101010...\rangle$, as shown Fig. 4.1(b). The effects of inter-particle interaction are incorporated in the physical correlation functions through the one-particle self-energies, having the retarded component, $\Sigma_R(i,t;j,t')$ and the Keldysh component, $\Sigma_K(i,t;j,t')$. The physical meaning of the self energies can be interpreted from the classical saddle point equation of motion for the boson

fields, $\phi_{cl}(i,t)$ (see Eq. 2.19),

$$[\mathbf{i}\partial_t - v(i)]\phi_{cl}(i,t) + J\phi_{i\pm1}(t) - \sum_j \int dt' \Sigma_R(i,t;j,t')\phi_{cl}(j,t') = \eta_i(t) \tag{4.17}$$

where the random noise η has correlators $\langle \eta_i(t)\eta_j(t')\rangle = -\mathbf{i}\Sigma_K(i,t;j,t')$. The imaginary part of Σ_R gives the dissipative effects induced by the inter-particle interaction in the dynamics and Σ_K is the noise correlator of the effective bath formed by the other particles in the system [49]. The interacting physical correlation functions are obtained from [55, 57],

$$\mathcal{G}_R(i,t;j,t') = G_{R0}(i,t;j,t') + \int_{t'}^{t} dt_1 \int_{t'}^{t_1} dt_2 G_{R0}(i,t;k,t_1)\Sigma_R(k,t_1;l,t_2)\mathcal{G}_R(l,t_2,j,t') \tag{4.18}$$

$$\begin{aligned}\mathcal{G}_K(i,t;j,t') &= -\mathbf{i}\,\mathcal{G}_R(i,t;k,0)[1+2n_k(0)]\mathcal{G}_R^*(j,t';k,0) \\ &\quad + \int_0^t dt_1 \int_0^{t'} dt_2 \mathcal{G}_R(i,t;k,t_1)\Sigma_K(k,t_1;l,t_2)\mathcal{G}_R^*(j,t';l,t_2).\end{aligned} \tag{4.19}$$

Here G_{R0} is the non-interacting retarded Green's function and summation over the repeated spatial indices is implied. At this point, we note that in the present calculation for interacting Bosonic systems, we have ignored connected many particle correlations in the initial Fock state and hence recover Wick's theorem for physical correlation functions (see section 3.6). This gives closed form Dyson equation, given in Eq. 4.18 and 4.19, in terms of one particle physical correlation functions, $\hat{\mathcal{G}}$ and the irreducible one-particle self-energies, $\hat{\Sigma} = \hat{\Sigma}(\mathcal{G})$. We work with a conserving approximation [129] by constructing skeleton expansion for self-energies. We keep all skeleton diagrams upto second order in U, shown in Fig. 4.10 to calculate the self-energies from,

$$\begin{aligned}\Sigma_R(i,t;j,t') &= 2\delta_{ij}\delta(t-t')(\mathbf{i}U)\mathcal{G}_K(i,t;i,t) - 2U^2[2\mathcal{G}_K(i,t;j,t')\mathcal{G}_K(j,t';i,t)\mathcal{G}_R(i,t;j,t') + \\ &\quad \mathcal{G}_K(i,t;j,t')\mathcal{G}_A(j,t';i,t)\mathcal{G}_K(i,t;j,t') + \mathcal{G}_R(i,t;j,t')\mathcal{G}_A(j,t';i,t)\mathcal{G}_R(i,t;j,t')], \\ \Sigma_K(i,t;j,t') &= -2U^2[2\mathcal{G}_K(i,t,j,t')\mathcal{G}_A(j,t',i,t)\mathcal{G}_R(i,t,j,t') + \\ &\quad \mathcal{G}_K(j,t';i,t)\mathcal{G}_R(i,t;j,t')\mathcal{G}_R(i,t;j,t') + \mathcal{G}_K(j,t';i,t)\mathcal{G}_K(i,t;j,t')\mathcal{G}_K(i,t;j,t')]\end{aligned} \tag{4.20}$$

We note that the approximation is non-perturbative in U, since the propagators used

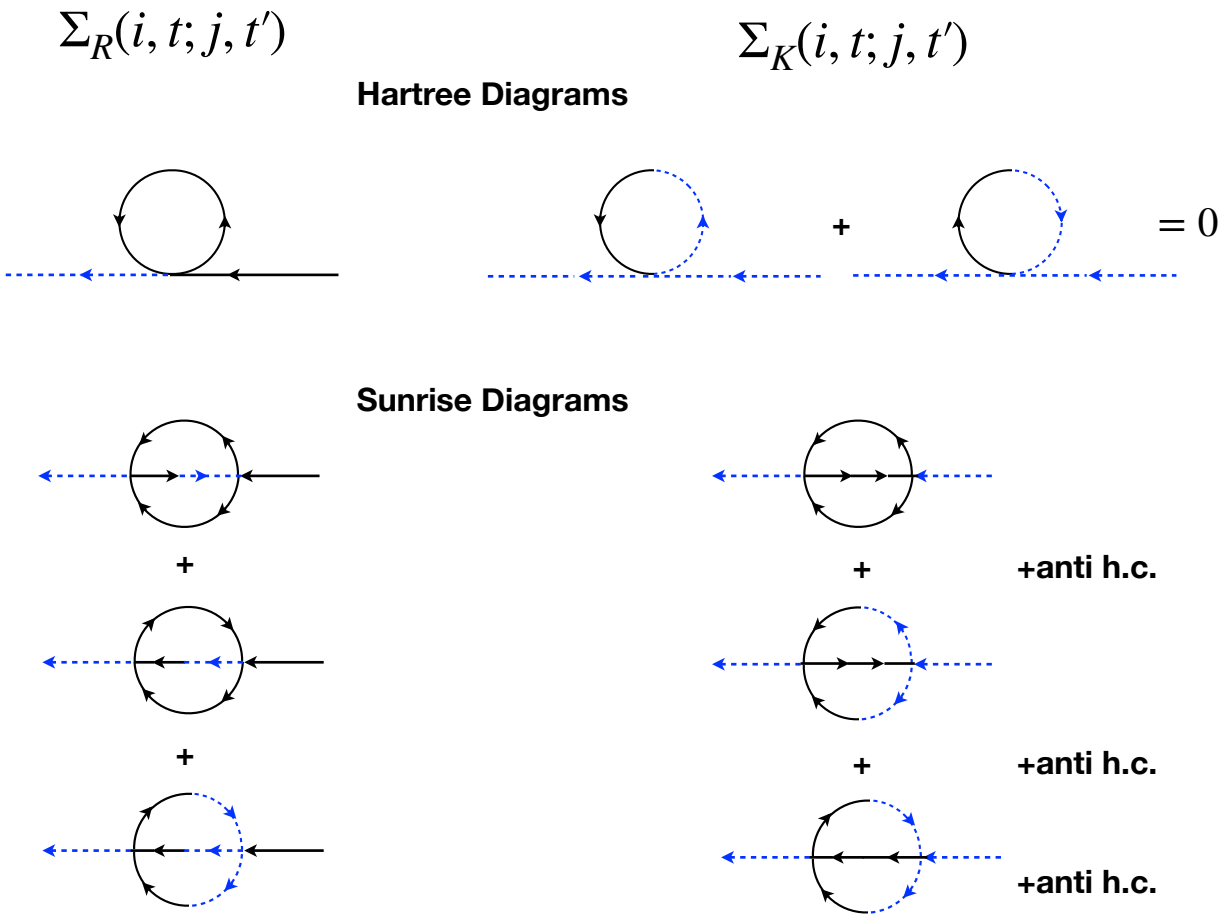

Figure 4.10: The Feynman diagrams used to evaluate self energies in the Bose Hubbard model with the Aubry Andre potential. The Green's functions are all interacting Green's functions, so that a conserving approximation is obtained. The self energies contain skeleton diagrams up to second order in U. This is the minimal approximation needed to include effect of dissipation and noise fluctuations in the dynamics to account for possible thermalization in the long time limit.

in the diagrams are the full interacting physical correlation functions, $\mathcal{G}$s , which are determined by solving Eq.4.18 and 4.19 self-consistently. The first order diagrams, shown in Fig. 4.10, lead to the self-consistent Hartree approximation. At this order, $\Sigma_K = 0$ and Σ_R is real. Thus there is no dissipation or noise in the dynamics of the system and the dynamics is controlled only by time dependent dephasing. The second order sunrise diagrams lead to both dissipation and noise. Hence, unlike Hartree Fock theory [123], our approximation keeps the minimal non-trivial diagrams which lead to dissipative and stochastic dynamics for this interacting Bosonic system. This is crucial to account for the possibility of thermalization in the system in the long time limit as well as to understand the microscopic mechanism of memory retention in the localized system, which

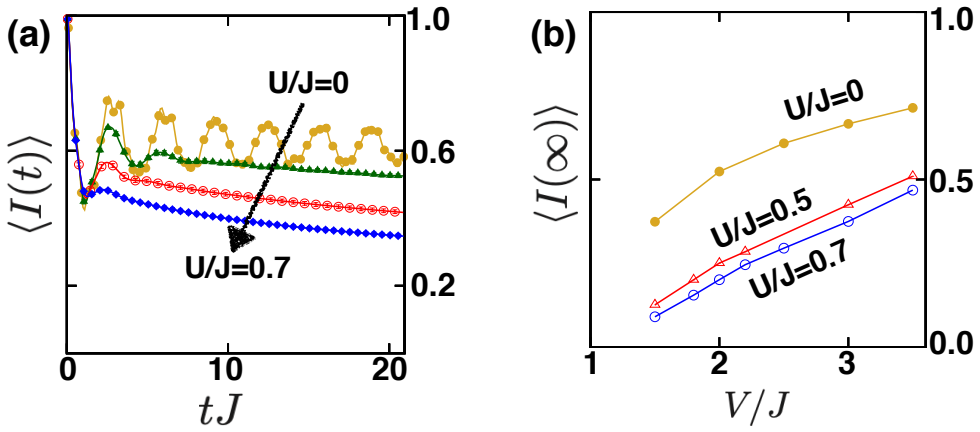

Figure 4.11: (a) $I(t)$ for Bosons in an interacting Aubry Andre Hubbard model with $V/J = 2.5$ and $U/J = 0.0,\ 0.3,\ 0.5,\ 0.7$. Even for finite U, the imbalance decays exponentially to a finite value. (b) The long time imbalance $\langle I(\infty)\rangle$ as function of V/J for different values of U/J. $\langle I(\infty)\rangle$ is obtained from the exponential fit, $\langle I(t)\rangle = \langle I(\infty)\rangle + \kappa e^{-\mu t}$. All data are for $L = 20$ sites and averaged over 50 configurations.

will be evident in the next section. We numerically solve these large number of integral equations by evolving them self-consistently with time, maintaining an error of $< 0.5\%$ in the number conservation. The resulting imbalance is plotted in Fig. 4.11(a) as a function of time for $V = 2.5J$ and different values of $U/J = 0.0, 0.3, 0.5, 0.7$ for a 20 site linear chain. It shows an exponential decay with time in the long time limit, which can be fitted to $\langle I(t)\rangle = \langle I(\infty)\rangle + \kappa e^{-\mu t}$. The long time imbalance $\langle I(\infty)\rangle$, obtained from this fit, is plotted for different V/J in Fig 4.11(b). The system can sustain a finite imbalance, although interaction reduces its value. We note that our calculation to study this imbalance dynamics of a finite size interacting system by solving the self-consistent Dyson equation up to long time will break down close the transition point because of the limitation of the system size. We would also like to point out that our calculation is likely to overestimate the effects of interaction, since we do not take into account screening of the bare interaction strength. Nevertheless, this non-equilibrium field theoretic approach to study imbalance dynamics in MBL systems renders important insights into the microscopic mechanism responsible for memory retention in the long time dynamics of these systems, which will be discussed in the next section.

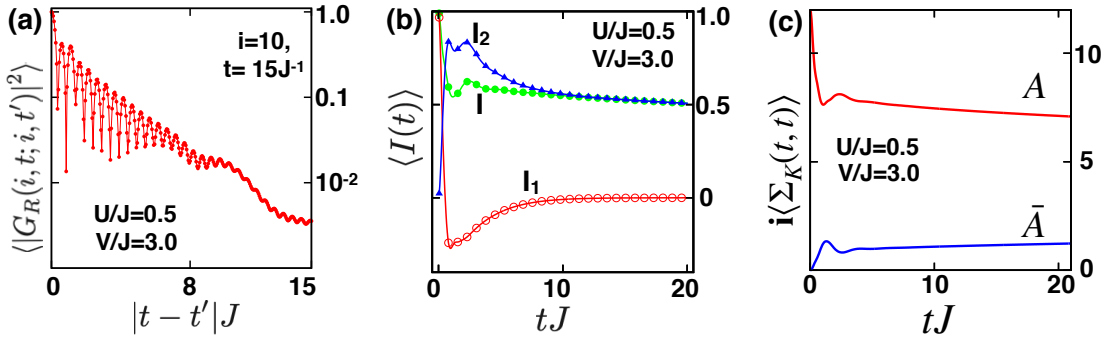

Figure 4.12: (a) The exponential decay of the spatially local disorder averaged $\langle |G_R(i,t;i,t')|^2\rangle$ with time, $t-t'$ due to dissipative process induced by the inter-particle interaction. (b) The contribution to imbalance due to (i) the direct decay of initial correlations I_1 and (ii) stochastic fluctuation due to effective bath I_2. The long time imbalance is dominated by I_2.(c) The space-time local part of $\mathbf{i}\Sigma_K$, averaged over A and $\bar{A}$ sites. The bath clearly distinguishes between A and $\bar{A}$ sites at long times. All data are for $L = 20$ sites and averaged over 50 configurations.

4.7 Microscopic Mechanism of Retaining Initial Memory

In this section, we will show that the microscopic mechanism that sustains the memory of the initial condition in the long time dynamics of a disordered system is very different for a non-interacting system than that of an interacting system. This is one of the key findings of this work.

In section 4.2, we have shown that for a non-interacting system, the memory of the initial density imbalance imprinted on the system is carried by the retarded Green's function, $G_R(i,t;k,0)$, in the long time dynamics through Eq. 4.6,

$$\langle I(t)\rangle = \frac{2}{N}\sum_{k\in A,i}\sigma_i\langle |G_R(i,t;k,0)|^2\rangle.$$

Here $\sigma_i = \pm$ for the filled and the empty subsystems, A and $\bar{A}$ respectively. In presence of inter-particle interaction, the dynamics includes effects of dissipation and noise and the local density, given in Eq. 4.3 is modified from the non-interacting answer (Eq. 4.4) as,

$$\begin{aligned} n_i(t) &= \frac{1}{2}\Bigg[\sum_k |\mathcal{G}_R(i,t;k,0)|^2\{1+2n_k(0)\} \\ &\quad +\mathbf{i}\sum_{k,l}\int_0^t dt_1\int_0^t dt_2 \mathcal{G}_R(i,t;k,t_1)\Sigma_K(k,t_1;l,t_2)\mathcal{G}_R^*(i,t;l,t_2) - 1\Bigg]. \quad (4.21) \end{aligned}$$

Here, the first term is a modification of the non-interacting answer (Eq. 4.4), with the initial density profile being propagated by the interacting $\mathcal{G}_R$. In the interacting system, as a particle propagates, it creates additional excitations in the system by scattering. Since $\mathcal{G}_R$ is the amplitude of propagation *without creating additional excitations*, $\langle|\mathcal{G}_R(i,t;k,0)|^2\rangle$ decays exponentially with time, as shown in Fig 4.12(a). This shows up as dissipation coming through the imaginary part of $\Sigma_R(i,t,j,t')$. This implies that the first term of Eq. 4.21, which directly contains the information of the initial distribution, goes to zero in the long time limit. However, the interaction induced excitations created in the medium act as a bath for the particle, and the stochastic fluctuations of this bath are represented by the second term. The contributions of these two terms to the density imbalance, I_1 and I_2, are plotted with time in Fig 4.12(b). As expected, I_1 decays to zero at long times and hence, the mechanism which was solely responsible for memory retention in the non-interacting system is unable to sustain initial memory in an interacting system at long time. The contribution coming from the second term in Eq. 4.21, i.e I_2 dominates the finite imbalance in the long time limit of the interacting Bosonic system.

Now, we analyze the second term of Eq. 4.21 in more details to understand the microscopic mechanism behind remembering the initial memory of density imbalance in the long time dynamics of the interacting system. The memory of the initial conditions now resides in the noise correlators of the interaction-induced athermal bath, which distinguishes between A and $\bar{A}$ sites, and sustains the finite imbalance. To see this, we realize that in this interacting system, since the self-energies are constructed using the interacting correlation functions in Eq. 4.20, they are also exponentially decaying in $|t-t'|$. Hence, the most dominant contribution of $\Sigma_K(i,t;j,t')$ in Eq. 4.21, is the space-time local piece of Σ_K. In this case, the local density, $n_i(t)$, at long time t can be approximated as,

$$n_i(t) \approx \frac{1}{2}\left[\mathbf{i}\sum_j \int_0^t dt_1 |\mathcal{G}_R(i,t;j,t_1)|^2 \Sigma_K(j,t_1;j,t_1) - 1\right]. \tag{4.22}$$

In Fig. 4.12(c), we plot the space-time local part of the disorder averaged Keldysh self-energy, $\mathbf{i}\langle\Sigma_K(i,t;i,t)\rangle$, which is the effective variance of the local noise fluctuations, averaged over A and $\bar{A}$ sites as a function of time. Here $\langle\Sigma_K^A\rangle$ and $\langle\Sigma_K^{\bar{A}}\rangle$ saturates to different values in the long time limit, which is the key to sustaining a finite imbalance.

To understand this, we note that in presence of strong interaction, as t_1 deviates from t, $\mathcal{G}_R(i,t;j,t_1)$ decays exponentially over a short timescale, say τ, which restricts the effective range of the time integration in Eq. 4.22. It is evident from Fig. 4.12(c) that in the long time limit, $\Sigma_K(i,t;i,t)$ is essentially time independent and hence within the timescale τ around t, it can be taken out of the integration in Eq. 4.22 to obtain the expression for long time imbalance as,

$$\langle I(t)\rangle = \frac{1}{N}\left\langle \sum_j \Sigma_K(j,t;j,t)\left[\sum_{i\in A}\int_{t-\tau}^{t} dt_1|\mathcal{G}_R(i,t;j,t_1)|^2 - \sum_{i\in\bar{A}}\int_{t-\tau}^{t} dt_1|\mathcal{G}_R(i,t;j,t_1)|^2\right]\right\rangle. \tag{4.23}$$

Now,we see from Fig. 4.13 that within the filled (or empty) subsystem, $\Sigma_K(j,t;j,t)$ becomes independent of j and hence we can write $\sum_{j\in A}\Sigma_K(j,t;j,t) = L\Sigma_K^A/2$. This leads to,

$$\begin{aligned}\langle I(t)\rangle = \frac{1}{2}\Bigg\langle\Bigg[&\Sigma_K^A\sum_{j\in A}\sum_{i\in A}\int_{t-\tau}^{t} dt_1|\mathcal{G}_R(i,t;j,t_1)|^2 + \Sigma_K^{\bar{A}}\sum_{j\in\bar{A}}\sum_{i\in A}\int_{t-\tau}^{t} dt_1|\mathcal{G}_R(i,t;j,t_1)|^2 \\ -\ &\Sigma_K^A\sum_{j\in A}\sum_{i\in\bar{A}}\int_{t-\tau}^{t} dt_1|\mathcal{G}_R(i,t;j,t_1)|^2 - \Sigma_K^{\bar{A}}\sum_{j\in\bar{A}}\sum_{i\in\bar{A}}\int_{t-\tau}^{t} dt_1|\mathcal{G}_R(i,t;j,t_1)|^2\Bigg]\Bigg\rangle.\end{aligned} \tag{4.24}$$

Now, if we approximate the spatial dependence of the disorder averaged interacting $\mathcal{G}_R(i,t;j,t')$ to be only a function of $|i-j|$, then the above expression immediately leads to the long time imbalance, $\langle I(t)\rangle$ being proportional to the difference in averaged noise correlations on filled and empty sub-system, i.e $\Sigma_K^A - \Sigma_K^{\bar{A}}$,

$$\langle I(t)\rangle = \frac{1}{2}\left\langle (\Sigma_K^A - \Sigma_K^{\bar{A}})\left[\sum_{j\in A}\sum_{i\in A}\int_{t-\tau}^{t} dt_1|\mathcal{G}_R(i,t;j,t_1)|^2 + \sum_{j\in\bar{A}}\sum_{i\in A}\int_{t-\tau}^{t} dt_1|\mathcal{G}_R(i,t;j,t_1)|^2\right]\right\rangle. \tag{4.25}$$

This concludes that for interacting bosonic systems, the dissipative processes lead to a decay of the direct memory of initial conditions. However, the excitations created in the process act as a bath, whose noise correlators retain information of the initial pattern.

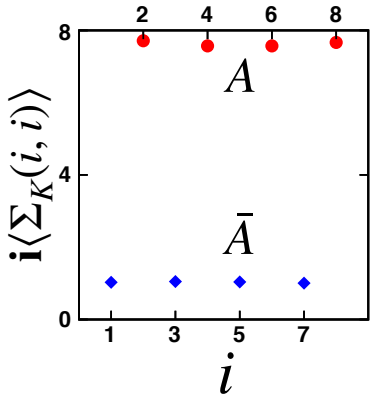

Figure 4.13: The disorder averaged space-time local piece of the Keldysh self energy (noise correlator), $\mathbf{i}\langle\Sigma_K(i,t;i,t)\rangle$, as a function of i at a long time instant, $tJ = 18$. Σ_K distinguishes between A and $\bar{A}$ sites, but does not depend on i within filled (A) or empty ($\bar{A}$) sub-system. This plot is for $L = 10$ site chain with Aubry-Andre potential at $U = 0.5J$ and $V = 3.5J$.

This sustains a finite imbalance at long times in strongly disordered interacting systems.

In the next section, we will extend this analysis to the case of an interacting Fermionic system.

4.8 Imbalance Dynamics in Interacting Fermionic Systems

In this section, we will study the imbalance dynamics in a one dimensional AA model for Fermions, interacting via nearest-neighbour interaction Hamiltonian,

$$H_{int} = U \sum_{i=1}^{L-1} n_i n_{i+1}. \tag{4.26}$$

The system is initialized to the same density pattern of alternating empty and filled sites, as shown in Fig. 4.1(b). In the Keldysh action, the inter-particle scattering term leads to four bare interaction vertices which are local in time but non-local in space, as shown in Fig. 4.14. In this case, the full interacting Keldysh action, S_{int}, takes the following form,

$$\begin{aligned} S_{int} &= -\frac{U}{2}\int dt \sum_{i=0}^{L-1}\Big[\\ &\quad \bar{\psi}_1(i,t)\bar{\psi}_1(i+1,t)\psi_1(i+1,t)\psi_2(i,t) + \bar{\psi}_1(i,t)\bar{\psi}_1(i+1,t)\psi_2(i+1,t)\psi_1(i,t) \\ &+ \bar{\psi}_2(i,t)\bar{\psi}_1(i+1,t)\psi_1(i+1,t)\psi_1(i,t) + \bar{\psi}_1(i,t)\bar{\psi}_2(i+1,t)\psi_1(i+1,t)\psi_1(i,t) \\ &+ \bar{\psi}_2(i,t)\bar{\psi}_2(i+1,t)\psi_2(i+1,t)\psi_1(i,t) + \bar{\psi}_2(i,t)\bar{\psi}_2(i+1,t)\psi_1(i+1,t)\psi_2(i,t) \end{aligned}$$

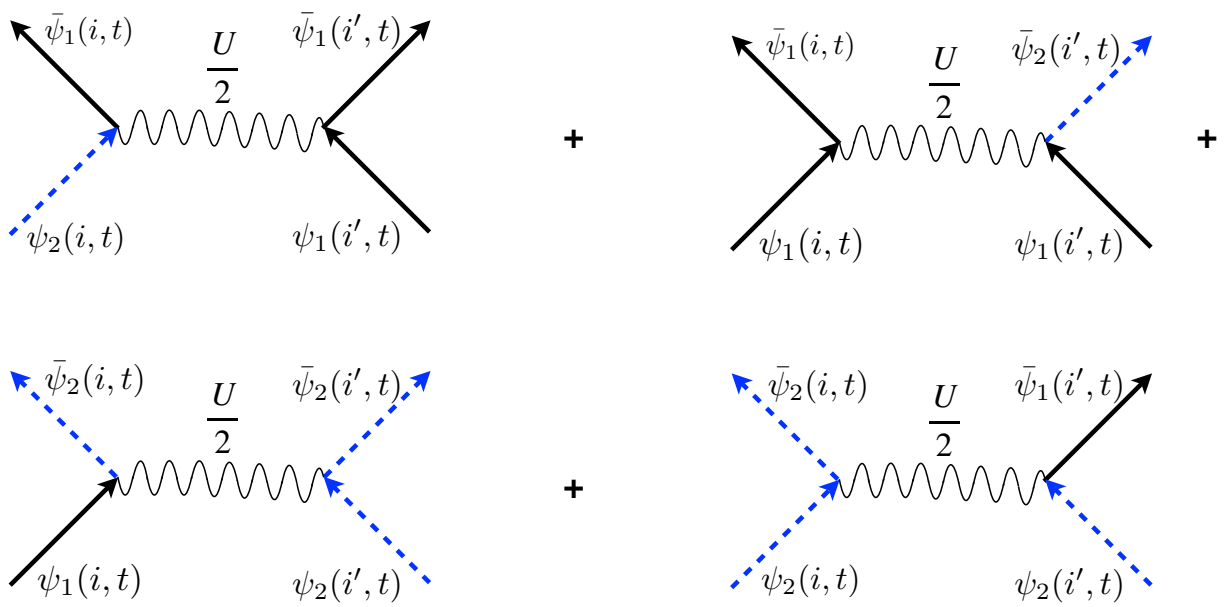

Figure 4.14: Spinless Fermions interacting via nearest-neighbour repulsive interaction of strength, U. This leads to four bare vertices in the interacting Keldysh action which are diagrammatically represented in the figure. Note that the interaction vertices are local in time. But since Fermions residing only on the nearest-neighbour sites repel each other, the interaction is non-local in space. The spatial non-locality is represented by the wiggly lines between the nearest neighbour sites, i and $i' = i + 1$. All the diagrams have their $i \leftrightarrow i'$ counterpart diagrams (not shown in the figure), leading to 8 terms in Eq. 4.27.

$$+ \quad \bar{\psi}_1(i,t)\bar{\psi}_2(i+1,t)\psi_2(i+1,t)\psi_2(i,t) + \bar{\psi}_2(i,t)\bar{\psi}_1(i+1,t)\psi_2(i+1,t)\psi_2(i,t)\Big] \tag{4.27}$$

[1] Similar to the case of Bosons, the effect on inter-particle scattering between the neighbouring Fermions is included in the dynamics through the self-energies, $\Sigma_R(i,t;j,t')$ and $\Sigma_K(i,t;j,t')$ in the Dyson equations given in Eq. 4.19 and 4.18.

However, there is a crucial difference in the structure of the Fermionic field theory compared to that of the Bosonic one, starting from a Fock state. To understand this, we recall the discussion on violation of Wick's theorem in non-interacting systems discussed in section 3.6. We showed that in the dynamics of a non-interacting many body system starting from an arbitrary $\hat{\rho}_0$, the multi-particle physical correlation functions can not be decomposed as product of only one particle physical correlation functions and the correction

[1]Note that there is an additional factor of 1/2 in the vertex factor, compared to that for Bosons. This is due to the nearest neighbour interaction for Fermions, which makes the number of vertices twice compared to Bosons.

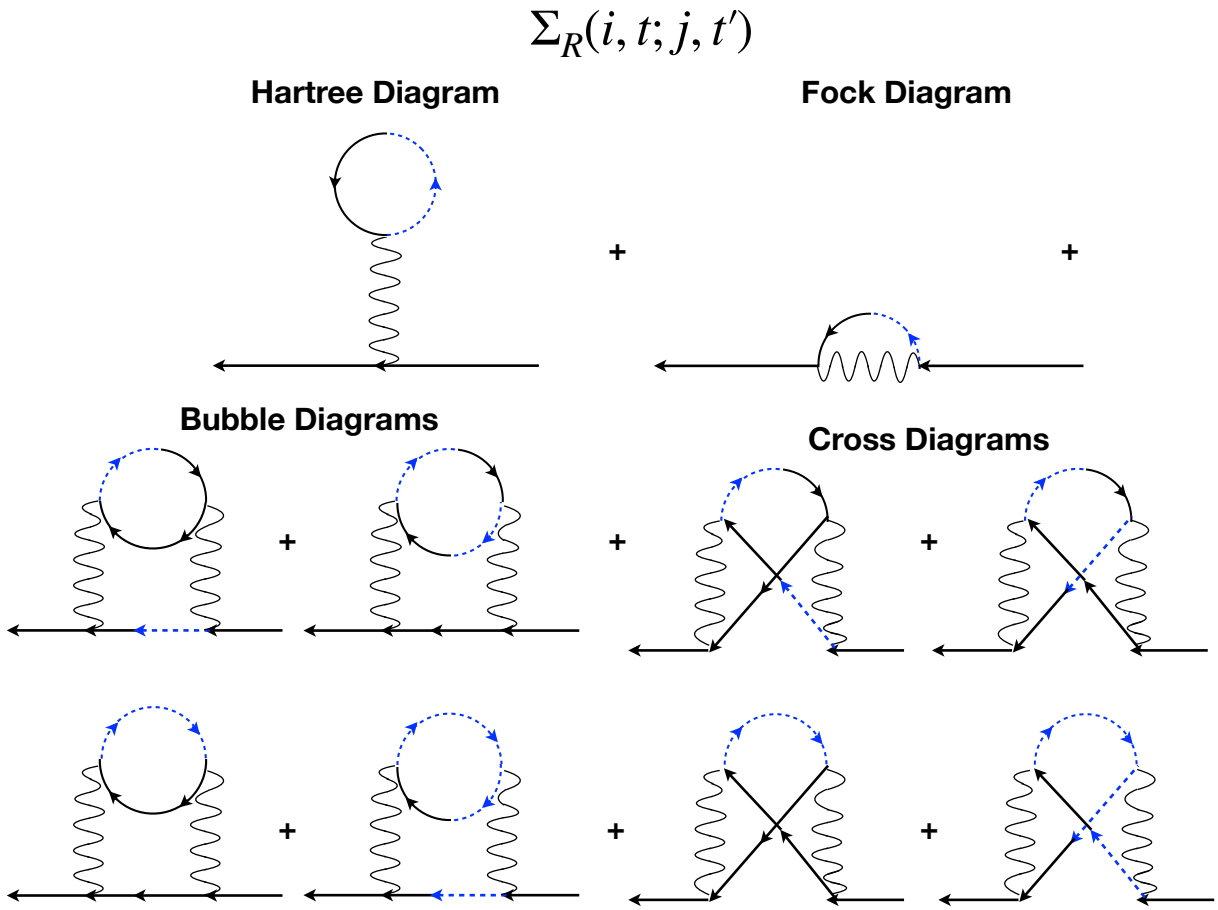

Figure 4.15: Skeleton diagrams for Σ_R(i,t;j,t') up to second order in U. ψ_1 and ψ_2 fields are represented by solid and dashed lines respectively.

terms are proportional to the multi-particle correlators calculated in $\hat{\rho}_0$. This absence of Wick's theorem in the non-interacting system is at the heart of all the complications arising in formulating a diagrammatic perturbation theory in an interacting system. However, for Fermionic system starting from a Fock state, we have a crucial advantage at this point, as Wick's theorem is valid by the construction of the theory. To see this, we recall the simple example of two particle physical correlation function, $\langle \phi^*_{cl}(\alpha,t)\phi^*_{cl}(\beta,t')\phi_{cl}(\gamma,t')\phi_{cl}(\delta,t)\rangle = \mathbf{i}^2\mathcal{G}^{(2)}_{\rho_0}(\alpha,t,\beta,t',\gamma,t'\delta,t)$ for non-interacting Fermions from Eq. 3.38,

$$\begin{aligned}\mathcal{G}^{(2)}_{\rho_0}(\alpha,t,\beta,t',\gamma,t',\delta,t) &= \sum_{x,y}[G_R(\alpha,t,x,0)G^*_R(\gamma,t',x,0)G_R(\beta,t',y,0)G^*_R(\delta,t,y,0)\\ &- G_R(\alpha,t,x,0)G^*_R(\delta,t,x,0)G_R(\beta,t',y,0)G^*_R(\gamma,t',y,0)]\\ &\times[\langle(1-2\hat{n}_x)(1-2\hat{n}_y)\rangle_0 - 2\delta_{x,y}\langle\hat{n}_x(\hat{n}_x+1)\rangle_0]\end{aligned}$$

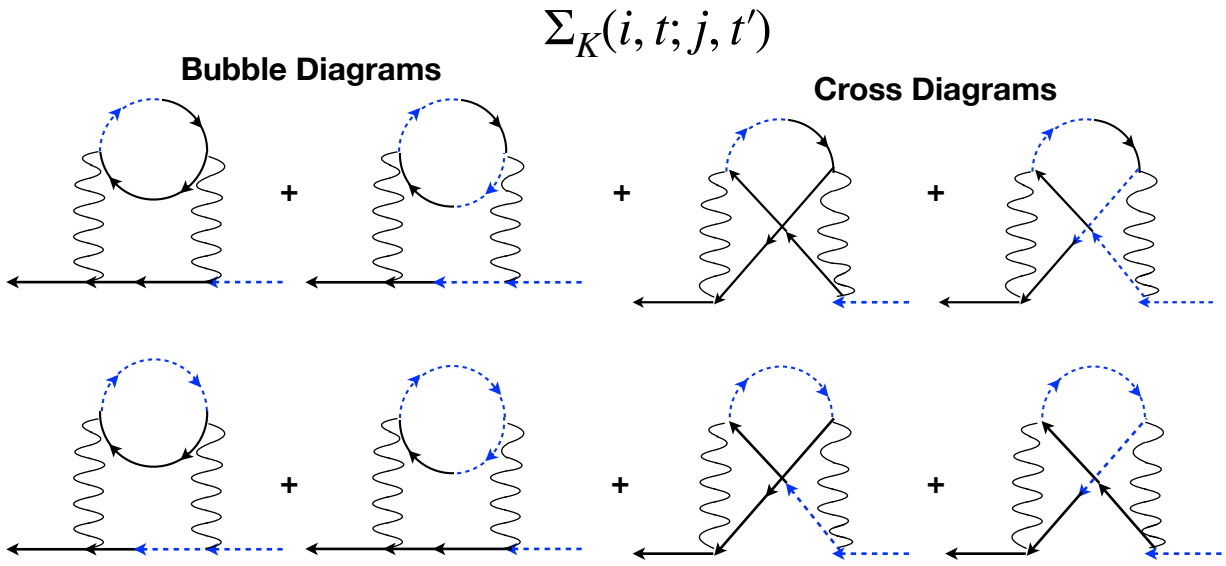

Figure 4.16: Skeleton diagrams for Σ_K(i,t;j,t') in second order in U. The contribution in Σ_K coming from the Hartree-Fock diagrams (first order in U) add up to zero. Hence, the diagrams shown in this figure are the minimal diagrams needed to generate Σ_K which is crucial to include effects of interaction induced noise correlations in the dynamics. ψ_1 and ψ_2 fields are represented by solid and dashed lines respectively.

If the initial state is a single Fock state, (a) $\langle(1-2\hat{n}_x)(1-2\hat{n}_y)\rangle_0 = \langle(1-2\hat{n}_x)\rangle_0\langle(1-2\hat{n}_y)\rangle_0$ and (b) the coefficient is zero for $x = y$. Hence,

$$\mathcal{G}^{(2)}_{\rho_0}(\alpha,t,\beta,t',\gamma,t'\delta,t) = \mathcal{G}_{K\rho_0}(\alpha,t,\gamma,t')\mathcal{G}_{K\rho_0}(\beta,t',\delta,t) - \mathcal{G}_{K\rho_0}(\alpha,t,\delta,t)\mathcal{G}_{K\rho_0}(\beta,t',\gamma,t'). \tag{4.28}$$

This argument can easily be generalized for higher order physical correlation functions and hence we recover Wick's theorem for non-interacting Fermions starting from a Fock state. Thus, in presence of inter-particle interaction in this system, we can construct a diagrammatic expansion of irreducible one-particle self-energies in terms of physical one particle correlation functions. This leads to a conserving approximation for $\mathcal{G}$s which need to be solved self-consistently from Eq. 4.19 and 4.18. In our calculation, we keep all skeleton diagrams for Σ_R and Σ_K upto second order in U, as shown in Fig. 4.15 and 4.16 (for details see Appendix B.1). We note that our approximation is non-perturbative in U, as the self-energy diagrams are calculated using full interacting propagator, $\mathcal{G}(i,t;j,t')$s. In Hartree-Fock (HF) approximation, which comprises of the first order diagrams in U, $\Sigma_K(i,t;j,t') = 0$ and hence the dynamics does not include effect of stochastic fluctuations coming from inter-particle scattering. Our approximation, keeping all diagrams upto second order in U,

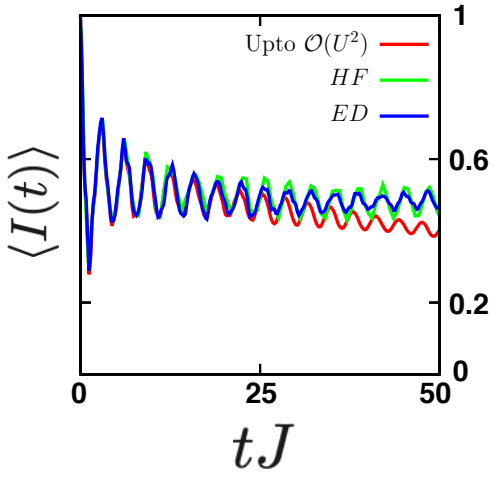

Figure 4.17: The density imbalance as a function of time for a spinless one dimensional Fermions having nearest neighbour repulsive interaction of strength $U/J = 0.9$. The strength of the onsite AA potential, $V/J = 2.0$. The blue curve shows the ED data obtained for $L = 16$ site linear chain. The red cure corresponds to the field theoretic answer obtained within self-consistent Hartree-Fock approximation. In this approximation, $\Sigma_K = 0$ and hence it does not include the effects of stochastic fluctuations in the dynamics. The green curve shows the field theoretic result obtained by solving the Dyson equations self-consistently, keeping all the skeleton diagrams upto second order in U, as shown in Fig. 4.15 and 4.16. This includes effects of both dissipation and noise induced by interaction in the dynamics. This answer overestimates the effect of dissipation at long times as compared to the exact answer shown in blue curve. The field theoretic answers are obtained for a $L = 20$ site system.

has non-zero Σ_R and Σ_K and thus includes effects of both dissipation and noise correlations induced by interaction in the dynamics. This is crucial to describe possible thermalization in the long time limit.

Solving the dynamics of the system, we obtain the time evolution of the density imbalance in the system. In Fig. 4.17, we plot $\langle I(t) \rangle$ as a function time for $U = 0.9$ and $V = 2.0$ using three different methods: (a) the blue line represents the exact answer obtained by diagonalizing (ED) the interacting AA Hamiltonian for spinless Fermions on a $L = 16$ site linear chain, (b) the green line shows the answer within self-consistent Hartree-Fock (HF) approximation for a 20 site linear chain, and (c) the red line corresponds the result obtained by self-consistently solving the Dyson equations keeping all diagrams up to second order in U, i.e Hartree, Fock, bubble and cross diagrams. The curve, (c), seems to overestimate the effect of dissipation at long times compared to the exact answer, shown in (a). This is possibly coming from the fact that we are using the bare interaction strength, U, as the

vertex factor in the skeleton diagrams. A more sophisticated approximation scheme that takes into account the effect of screening by renormalizing the bare vertex factor is needed to clarify this point. The results on interacting Fermionic systems presented in this thesis form the initial steps towards this direction and a more careful and detailed analysis is under investigation and will be part of future studies.

4.9 Discussions

In this chapter, we use a new formulation of Schwinger-Keldysh path integral formalism, which can include arbitrary initial conditions in the many body dynamics, to work out a theory of imbalance dynamics in disordered (quasi-periodic) linear and square lattice of bosons/fermions, both in presence and absence of inter-particle interaction. The system is initialized in a Fock state with a pattern of 1 and 0 particles on A and $\bar{A}$ subsystems respectively, similar to the experimental set-up used to detect MBL. We, for the first time, provide exact connection between experimentally measurable non-equilibrium observables and traditional ways of characterizing disordered systems in terms of localisation length. Our analytical results can be inverted to obtain localisation lengths from experimental data on long time density imbalance. We extend this analysis to the systems having mobility edges in the spectrum and explain why the imbalance as a function of disorder shows non-analytic behaviour when the mobility edge passes through a band edge. This work, to the best of our knowledge, is the first one in the literature which provides a comprehensive non-equilibrium field theoretical study of the imbalance dynamics of a disordered interacting Bosonic system, which includes the effects of both the dissipation and noise fluctuations coming from inter-particle interaction. This is the minimal approximation needed to account for possible thermalization of the system in the long time limit. Our work gives a profound understanding of the very different microscopic processes that are responsible for sustaining long time imbalance in both non-interacting and interacting disordered systems. In interacting Bosonic systems, our calculations show that long time imbalance is sustained at strong disorder by the noise correlations which remember the initial density pattern.

In the next chapter, we switch our focus to the non-equilibrium dynamics of a non-Markovian open quantum system and study the effect of having long range memory kernel in the dissipative stochastic dynamics.

Chapter 5

Dynamics of Many Body Non-Markovian Open Quantum System

5.1 Introduction

An interesting class of problems related to thermalization [72] and generation of entanglement [71] and entropy [69, 70] involves solving the dynamics of open quantum systems (OQS)[23], where a quantum system can exchange energy/particles with a large external reservoir/bath. It is also crucial to understand the dynamics of a open quantum system to design and control possible platforms for creating an architecture of quantum computing, like superconducting qubits [144, 145], spin-qubits [146], cavity QED [147], cavity optomechanics [148], quantum dot arrays coupled to cavities [149], nanowire junctions [150], ultracold atomic systems [151] etc. The phenomenal experimental advance over the past decade in implementing and controlling these platforms has reignited interest in the dynamics of OQS. Additionally, theoretical ideas of bath/dissipation engineering [152] to guide open quantum systems to novel steady states [153] and using these states as resources in quantum computing [154] also require a deep understanding of the behaviour of OQS.

The Born-Markov approximation is widely used to study the dynamics of open quantum systems coupled to external baths. It assumes that (i) coupling of the quantum system to the bath does not change the dynamics of the bath and (ii) the effective reduced dynamics of the system is local in time. This is often presented in the form of a time local (Markovian) quantum master equation (QME) [44], where the positive rates of transition from one configuration of the system to another depend only on the state of the system

at that time. Markovian dynamics has been studied using the well-known Redfield [155] and Lindblad [156, 157] master equations. The other related approach is that of stochastic Schrodinger equations [158, 159, 160], which are generalizations of familiar Langevin equations in classical systems.

However, going beyond the scope of the Born-Markov approximation and studying the effects of long-range memory kernels in the non-Markovian dynamics of OQS has been gaining a lot of prominence in recent years [81, 82]. Non-Markovian dynamics has been key to recent proposals for bath engineering [161], quantum metrology [162], and can be used as resources for quantum communication [163] and quantum memory [164]. Recent experiments have been successful in tuning the dynamics of an open quantum system from Markovian to non-Markovian by controlling the bath degrees of freedom [165]. Non-Markovian dynamics [166, 167, 168, 169, 170, 171, 172, 173, 174, 175, 176] has been traditionally treated using Nakajima-Zwanzig type master equation [48, 177] as well as effective time convolution-less master equation [178, 179, 180, 181]. In fact, different types of dynamical behaviour or properties of the equation of motion are clubbed under the rubric of non-Markovian dynamics with debates over essential definition of "non-Markovian"ness [182].

The applicability of Born-Markov approximation to study the dynamics of OQS is restricted to only a selected class of problems in the regime of weak system-bath coupling where the density of states in the bath is a smooth function of frequency. However, there is a large class of OQS which exhibits sharp features in the bath spectral function. Such non-analytic behaviour can arise from a variety of sources like band edges, Van-Hove singularities, Kohn anomalies [83] in phonon spectrum, phase transitions in the bath [183] and non-Fermi liquid [184, 185] nature of the bath. Recently, evidences of such non-Markovianness have been observed in experiments [186] in the form of non-exponential decay in fluorescence intensity of dissolved organic materials. In this chapter, we study the non-Markovian dynamics of open quantum systems induced by non-analyticites in the bath spectrum and provide exact analytic solutions for the reduced dynamics of the system at arbitrary system-bath coupling. We probe the system at two different regimes during its evolution: (a) we first work out the complete structure of the steady state dynamics of the OQS where the memory of the initial condition of the system is erased and the effects of non-Markovianness in the dynamics are manifested in multi-time observables.

This gives useful insights about the interplay between multiple time-scales relevant in the non-Markovian dynamics. (b) We then extend this study to probe transient dynamics of the non-Markovian OQS initialized to non-trivial density matrices. For this, we use the new extension of non-equilibrium field theory developed in chapter 3 which can include arbitrary athermal initial conditions.

A canonical model of OQS [187], consisting of a few bosons (fermions) coupled linearly to non-interacting bath of bosons (fermions), has been studied previously using QME [188, 189, 190, 191, 192] as well as non-equilibrium Green's function technique [193, 194, 195, 56, 196, 197, 198, 199, 200]. In this chapter, we use Schwinger-Keldysh field theory formalism [55] to study a system bosons(fermions) hopping on a 1d lattice where each site is connected to a non-interacting bosonic (fermionic) bath kept at fixed temperature and chemical potential. Integrating out the bath degrees of freedom, we obtain a description of the effective steady state dynamics of the OQS. We relate the self-energies induced by the bath to the dissipative and noise kernels in a stochastic Schrodinger equation through a saddle point approximation. We show that any non-analyticity in the bath spectral function leads to temporally long range dissipative and noise kernels with power law tails. The exponent of the power law is determined solely by the nature of the non-analyticity and is independent of other microscopic details. The power law tail in the kernels precludes the possibility of coarse graining to obtain a Markovian description for the dynamics of the system. We emphasize that, for bosonic baths kept at fixed chemical potentials, i.e when the bath, decoupled from the system has a conserved number/charge, the bath spectrum must be bounded from below. Hence its spectral function at least be non-analytic at the bottom of the band. Non-Markovian dynamics will be ubiquitous in such bosonic systems.

The Green's functions inherit these power law tails along with a short time exponential decay. The crossover from the exponential decay to the power law tail occurs at a time $\tau_0 \sim 1/\epsilon^2$, where ϵ is the scale of system bath coupling. Thus at very weak system bath coupling, the system dynamics appears Markovian for a very long time, and we call this regime "quasi-Markovian". With increase in system bath coupling, the power law tail dominates the dynamics and the non-Markovian behaviour is easier to detect in experiments. We study both the density and current profile in the system, as well as the unequal time observables like current-current correlators. While the steady state answers for equal time

correlators show important quantitative differences from a Markovian calculation, the unequal time correlators inherit the power law tails and can be used as a direct probe of these singularities in the bath spectrum. The nature of the non-analyticity controls the power law exponent while the location of the non-analyticity in the bath spectrum governs the cross-over timescale. We explicitly show this by analytically solving the dynamics in case of a semi-infinite 1-dimensional bath whose spectral function having square root derivative singularity at the band edges. We obtain the analytic expressions for the Green's function of a full 1d chain which provide the starting point for calculating the dynamics of the interacting many-body OQS. We consider the effect of the inter-particle interactions on the dynamics of OQS within self-consistent Hartree-Fock approximation. We find that, the power law tail survives, while the crossover scale increases with increasing interaction strength.

Having understood the structure of the non-Markovian dynamics in the steady state, we consider the transient dynamics of the many body OQS initialized to Fock states and work out the dynamics using the newly developed extension of SK field theory (chapter 3). We first study the dynamics of Bosons hopping on a linear chain where the system is initialized to a wedge shaped pattern of density. We study how the density and current patterns evolve with time as the system approaches its thermal state in the long time limit. At short times, the density pattern shows interesting see-saw type oscillations, leading to pilling of current around the central site on the chain. At long times, dissipative and stochastic effects from the external bath come into play and the density and current profiles settle in their steady patterns, governed by the bath. We also consider a 1d Fermionic system initialized in a density pattern where the left half of the chain is filled with one Fermion per site and the right half is empty, i.e the system has a domain wall at the center. We study the dynamics of the density and current patterns in the transient state of the system. It exhibits ballistic oscillation of the domain wall in the system before settling to the steady state profile.

We have organized the chapter into several sections: section 5.2 to section 5.7 deals with the steady state dynamics of the system while section 5.8 treats the transient dynamics of the system by the extending the new SK field theory formalism developed in chapter 3 to include effects of arbitrary initial conditions in the dynamics of many body OQS. In section 5.2, we discuss a model of non-interacting bosons linearly coupled to a bosonic

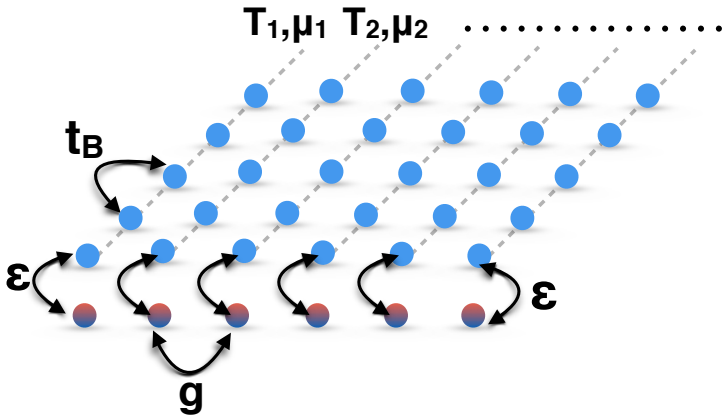

Figure 5.1: Schematic diagram of the open quantum system setup considered in this chapter. The red-blue circles denote the system sites, whereas the line of light blue circles denotes the semi-infinite bath. Note that the baths are not interconnected to each other and have their independent temperature T_l and chemical potential μ_l. The system sites couple to the first site of the respective bath with scale ϵ. Here g is the hopping in the system, while t_B is the hopping in the bath.

bath. We set up the Keldysh formalism and sketch the steps taken to calculate the Green's function and observables in the resulting OQS. In section 5.3, we connect the self energies induced by integrating out the bath variables with the dissipative and noise kernels in an equation of motion approach and discuss the power law kernels induced by the non-analyticities in the bath spectral function. In section 5.4, we solve the Dyson equation and find the analytic Green's function for the linear chain. We discuss the non-analytic structure of the Green's function in frequency space, and its behaviour in real time. In section 5.5, we consider equal time and unequal time observables and show how the unequal time correlators show the signature of the power law tails. In section 5.6, we generalize the results to the case of a fermionic system coupled to a fermionic bath and show that similar results hold in this case. In section 5.7, we consider the effect of inter-particle interactions in the system on the power law tail and the crossover time-scale. Finally, in section 5.8, we extend the new SK field theory formalism to include arbitrary athermal initial conditions in the dynamics of a many body OQS. We also work out some examples of the above formalism to compute the evolution of densities and currents in the many-body non-Markovian open quantum system staring from non-trivial initial states.

5.2 Bosonic system coupled to Bosonic Baths

We consider a system of 1-dimensional lattice of non-interacting bosons (representing arrays of oscillators) hopping between nearest neighbours with an amplitude g (representing coupling between successive oscillators). The fermionic version of this model, which can represent quantum dot arrays, will be taken up in section 5.6. Each site, l, of the lattice is coupled to an independent bosonic bath with a temperature T_l and a chemical potential μ_l. The setup is schematically shown in Fig. 5.1. We will be interested in the steady state response of the system to different profiles of μ_l and T_l.

We describe each bath by a semi-infinite 1 dimensional lattice of non-interacting bosons with nearest neighbour hopping t_B and assume each system site is coupled locally to the first site of the corresponding bath, as shown in Fig. 5.1. The system bath coupling , controlled by the scale ϵ , is linear in both the system and bath degrees of freedom . The total Hamiltonian of the system (H_s) , the baths (H_b) and system bath coupling (H_{sb}) are then given by,

$$\begin{aligned} H_s &= -g\sum_{l=1}^{N} a_l^\dagger a_{l+1} + h.c \;\; and \;\; H_{sb} = \epsilon \sum_{l=1}^{N} a_l^\dagger b_1^{(l)} + h.c \\ H_b &= -t_B \sum_{l=1}^{N}\sum_{s=1}^{\infty} b_s^{(l)\dagger} b_{s+1}^{(l)} + h.c. \end{aligned} \tag{5.1}$$

where $a_l^\dagger$ creates a boson at site l of the system, $b_s^{(l)\dagger}$ is the bosonic creation operator at site s of l^{th} bath. It is useful to rewrite the bath degrees of freedom in terms of the eigenoperators $B_\alpha^{(l)\dagger}$ which diagonalize the bath Hamiltonian.

$$H_b = \sum_{l,\alpha} \Omega_\alpha B_\alpha^{(l)\dagger} B_\alpha^{(l)} \;\; , \;\; H_{sb} = \epsilon \sum_{l,\alpha} \kappa_\alpha B_\alpha^{(l)\dagger} a_l + h.c \tag{5.2}$$

where Ω_α is the energy of the eigenmode α and κ_α is its amplitude on the first site of the bath.

We use Schwinger Keldysh functional integral [55] to study the effective non-unitary dynamics of the OQS in the steady state. The field theoretic technique yields exact results for arbitrary parameter values in non-interacting system, and is not restricted to weak system bath couplings. The Keldysh approach constructs a path integral representation of

the dynamics of the density matrix . It requires two copies of fields at each instant of time t, namely $\phi_+(t)$ and $\phi_-(t)$, corresponding to the forward and backward evolution inherent in $\rho(t) = \mathcal{U}(t,-\infty)\rho(-\infty)\mathcal{U}^\dagger(t,-\infty)$. Here $U(t)$ is the time evolution operator for the system as well as the baths and $\rho(-\infty)$ is the initial density matrix, which is factorizable into system and bath density matrices. It is customary to work with the symmetric or classical $\phi_{cl} = (\phi_+ + \phi_-)/\sqrt{2}$ and anti-symmetric or quantum $\phi_q = (\phi_+ - \phi_-)/\sqrt{2}$ fields. Using $\phi^{(l)}$ and $\chi_\alpha^{(l)}$ as the fields corresponding to a_l and $B_\alpha^{(l)}$, the steady state Keldysh action for the system S_s, baths S_b, and the system bath couplings S_{sb} is given by

$$S_s = \sum_{l,l'} \int d\omega \phi_l^\dagger(\omega) \begin{bmatrix} 0 & G_0^{-1A}(l,l',\omega) \\ G_0^{-1R}(l,l',\omega) & G_0^{-1K}(\omega)\ \delta_{l,l'} \end{bmatrix} \phi_{l'}(\omega)$$

$$S_b = \sum_{l,\alpha} \int d\omega\ \chi_{l\alpha}^\dagger(\omega) \begin{bmatrix} 0 & \omega - \Omega_\alpha - \mathbf{i}\eta \\ \omega - \Omega_\alpha + \mathbf{i}\eta & 2\mathbf{i}\eta\ F_l(\Omega_\alpha) \end{bmatrix} \chi_{l\alpha}(\omega)$$

$$S_{sb} = -\epsilon \sum_{l,\alpha} \int d\omega\ \kappa_\alpha \chi_{l\alpha}^\dagger(\omega) \hat{\sigma}_1 \phi_l(\omega) + h.c \tag{5.3}$$

where σ^1 is the Pauli matrix encoding the Keldysh rotation and $\phi_l^\dagger = [\phi_{cl}^{*(l)}\ ,\ \phi_q^{*(l)}]$, $\chi_{l\alpha}^\dagger = [\chi_{cl,\alpha}^{*(l)}\ ,\ \chi_{q,\alpha}^{*(l)}]$ and $G_0^{-1R/A}(l,l',\omega) = (\omega \pm \mathbf{i}\eta)\ \delta_{l,l'} + g\ \delta_{l,l'\pm1}$, and $\eta \to 0^+$ [201]. Here $F_l(\omega) = \coth\left(\frac{\omega-\mu_l}{2T_l}\right)$ is related to the distribution function in the l^{th} bath. We assume that all the baths remain in thermal equilibrium throughout the dynamic evolution of the system. The bath Green's functions given by

$$\begin{aligned} G_b^{R/A}(\alpha;\omega) &= \frac{1}{\omega - \Omega_\alpha \pm \mathbf{i}\eta} \\ G_b^K(\alpha,l;\omega) &= -2\pi\mathbf{i}\ \delta(\omega - \Omega_\alpha)\ \coth\left(\frac{\omega-\mu_l}{2T_l}\right) \end{aligned} \tag{5.4}$$

Since the action (5.3) is quadratic in $\chi_\alpha^{(l)}$, we can integrate out the bath degrees of freedom to obtain the effective dissipative action for the open quantum system which describes the

non-unitary dynamics of the system coupled to the bath,

$$S_{oqs} = \sum_{l,l'} \int d\omega \phi_l^\dagger(\omega) \begin{bmatrix} 0 & G_0^{-1A}(l,l',\omega) - \Sigma^A(w)\ \delta_{l,l'} \\ G_0^{-1R}(l,l',\omega) - \Sigma^R(w)\ \delta_{l,l'} & -\Sigma_l^K(\omega)\ \delta_{l,l'} \end{bmatrix} \phi_{l'}(\omega), \tag{5.5}$$

where $\hat{\Sigma}_l(\omega) = \sum_\alpha |\kappa_\alpha|^2\ \epsilon^2\ \hat{\sigma}_1 \hat{G}_b(\alpha, l; \omega)\hat{\sigma}_1$. Here, integrating out the bath induces a finite Keldysh component of the self-energy matrix, $\Sigma_l^K(\omega)$, which is purely imaginary. Thus, although we start from unitary description of the combined system, the effective dynamics of the OQS after tracing over bath degrees of freedom, governed by the action (5.5), is non-unitary. The summation over the bath eigenmodes makes the self-energy matrix a function only of the bath spectral function

$$J(\omega) = 2\pi \sum_\alpha |\kappa_\alpha|^2 \delta(\omega - \Omega_\alpha), \tag{5.6}$$

and the distribution function $F_l(\omega)$. All the results of this chapter will depend on properties of $J(\omega)$ and not on other microscopic details of the baths. In that sense, we can simply think of different kinds of baths being represented by different $J(\omega)$, and the results obtained here are applicable to a large class of systems . For our particular case, we will mainly focus on $1-$d semi-infinite bath given by the Hamiltonian (5.2) which is diagonalized in the quasi-momentum basis α with the eigen-energies, $\Omega_\alpha = -2t_B \cos(\alpha)$. Baths are assumed to have infinite number of degrees of freedom so that their energy spectrum is continuous and κ_α is proportional to the eigen-function of H_b at the first site of the bath, $\kappa_\alpha = \sqrt{2/\pi}\sin(\alpha)$. Using equation (5.6) we then get,

$$J(\omega) = \Theta(4t_B^2 - \omega^2)\frac{2}{t_B}\sqrt{1 - \frac{\omega^2}{4t_B^2}}, \tag{5.7}$$

which has a square root derivative singularity at the band edges $\omega = \pm 2t_B$ where $|2t_B| < |\mu_l|\ \forall\ l$, to avoid BEC forming in the baths. We discuss the cases of some other physically relevant $J(\omega)$ in section 5.3. Writing the components of self energy matrix explicitly, we

have

$$\begin{aligned}\Sigma^R(\omega) &= -\epsilon^2 \int \frac{d\omega'}{2\pi}\ \frac{J(\omega')}{\omega'-\omega-i\eta} \\ \Sigma^K_l(\omega) &= -\mathbf{i}\epsilon^2 J(\omega)\ \coth\left[\frac{\omega-\mu_l}{2T_l}\right]\end{aligned} \tag{5.8}$$

Inverting the kernel in the action (5.5) we obtain exact expressions for the 1-particle Green's function of the bosons. Using this, we calculate equal time observables (e.g. current, occupation number) as well as unequal time observables (e.g. current current correlation functions) in the steady state. Green's functions and current-current correlators in the steady state show power law tails indicative of non-Markovian dynamics of the system. In the next section, we work in real time domain and connect the Keldysh formalism with the widely used stochastic Schrodinger equation [158] formalism.

5.3 Power law Tail in Dissipative and Noise Kernels

The Keldysh field theory description obtained in the previous section can be connected to a stochastic Schrodinger equation with non-local memory kernels for dissipation and noise in the system given by the self-energies Σ^R and Σ^K_l. To see this, we write the effective Keldysh action for the OQS in real time,

$$S = \sum_{l,l'} \int dt\ dt' \phi^\dagger_l(t) \begin{bmatrix} 0 & G^{-1A}_{ll'}(t,t') \\ G^{-1R}_{ll'}(t,t') & -\Sigma^K_l(t,t')\delta_{l,l'} \end{bmatrix} \phi_{l'}(t') \tag{5.9}$$

where $G^{-1R}_{l,l'}(t,t') = \delta(t-t')\big(\mathbf{i}\partial_t\delta_{l,l'} + g\delta_{l,l'\pm1}\big) - \Sigma^R(t-t')\delta_{l,l'}$. The terms quadratic in ϕ_q are first converted into terms linear in ϕ_q (source terms) by a Hubbard Stratanovich transformation with an auxiliary field $\zeta_l(t)$. The Keldysh partition function is then given by $\mathcal{Z} = \int \mathcal{D}[\zeta^*\zeta]\ F(\zeta^*\zeta) \int \mathcal{D}[\phi^*\phi] e^{\mathbf{i}S(\phi^*,\phi,\zeta^*,\zeta)}$, where

$$\begin{aligned} S &= \int dt \int dt' \sum_{l,l'} [\phi^{*(l)}_q(t)\ G^{-1R}_{l,l'}(t,t')\phi^{(l)}_{cl}(t') + h.c] \\ &+ \int_{-\infty}^{\infty} dt\ \sum_l \Big[\phi^{*(l)}_q(t)\zeta_l(t) + \zeta^*_l(t)\phi^{(l)}_q(t)\Big] \quad \text{and} \\ F(\zeta^*\zeta) &= e^{\ \mathbf{i}\int_{-\infty}^{\infty}\int_{-\infty}^{\infty} dt\ dt'\ \zeta^*_l(t)[\Sigma^K_l(t,t')]^{-1}\zeta_l(t')} \end{aligned} \tag{5.10}$$

The equation of motion, obtained from classical saddle point condition $\frac{\partial \mathcal{S}}{\partial \phi_q}\Big|_{\phi_q=0} = 0$, is

$$\mathbf{i}\partial_t \phi_{cl}^{(l)}(t) - \int dt'\ \Sigma_l^R(t,t')\phi_{cl}^{(l)}(t') + g\phi_{cl}^{(l)\pm 1}(t) = \zeta_l(t), \tag{5.11}$$

where $\zeta_l(t)$ is a complex random field with a non-local but Gaussian distribution, $\langle \zeta_l^*(t)\zeta_{l'}(t')\rangle = -\mathbf{i}\delta_{l,l'}\Sigma_l^K(t,t')$. The imaginary part of the retarded self energy is thus the dissipative kernel, while the Keldysh self energy is the noise correlation kernel. The self energies in real time are related to the bath spectral function by

$$\begin{aligned} \Sigma^R(t-t') &= -\mathbf{i}\epsilon^2\Theta(t-t')\int \frac{d\omega}{2\pi} J(\omega)e^{-\mathbf{i}\omega(t-t')} \\ \Sigma_l^K(t-t') &= -\mathbf{i}\epsilon^2 \int \frac{d\omega}{2\pi} J(\omega)\coth\left[\frac{\omega-\mu_l}{2T_l}\right] e^{-\mathbf{i}\omega(t-t')} \end{aligned} \tag{5.12}$$

We note that for any $J(\omega)$ which is even in ω, the retarded self energy is purely imaginary and hence dissipative in nature. For the bath spectral function that we consider (eqn. 5.7),

$$\Sigma^R(t,t') = -\mathbf{i}\ \Theta(t-t')\frac{\epsilon^2}{t_B}\frac{\mathcal{J}_1(2t_B|t-t'|)}{|t-t'|}, \tag{5.13}$$

where $\mathcal{J}_1(x)$ is the Bessel function of first order. It is clear from the above exact expression, that $\Sigma^R(t-t') \sim -\mathbf{i}\epsilon^2[t_B(t-t')]^{-\frac{3}{2}}\cos[2t_B(t-t')-3\pi/4]$ for $|t-t'|\to\infty$ i.e the dissipative kernel decays slowly as a power law in the long time limit. Hence, there is no time scale in the system over which one can coarse grain to obtain an effective local description. The dynamics is thus essentially non-Markovian. Although a closed form expression for $\Sigma^K(t-t')$ cannot be obtained, it can be shown (see Appendix C.1) that at long times the envelop of $\Sigma^K \sim -\epsilon^2(2/\pi)^{1/2}\ |2t_B(t-t')|^{-3/2}\left(\coth\left[(2t_B-\mu)/2T\right] \mp \coth\left[(2t_B+\mu)/2T\right]\right)$ where the $-(+)$ sign corresponds to its real (imaginary) part. Hence it has the same $\sim |t-t'|^{-3/2}$ tail as Σ^R. In Fig. 5.2, we plot the imaginary part of the Keldysh self energy of a site coupled to a bath with temperature $T/t_B = 0.625$ and chemical potential $\mu/t_B = -2.25$ as a function of $|t-t'|$ on a log-log plot. The analytic envelop of Σ^K is plotted in the same figure with a solid line. It matches with the numerically obtained results remarkably well. Here, the chemical potential is kept below the band bottom to avoid the pathological case of non-interacting BEC in the bath. We note that in the limit $\mu \to -2t_B$, i.e a BEC transition is approached, the $\Sigma^K(\omega)$ has a square root divergence at

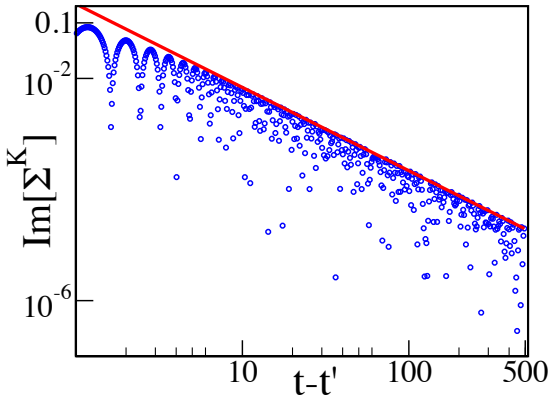

Figure 5.2: The imaginary part of the noise kernel (Keldysh self energy) $\Sigma_l^K(t-t')$ of a site l coupled to a bath with $T_l = 0.625t_B$ and $\mu_l = -2.25t_B$ as a function of $|t-t'|$ on a log-log plot. The system bath coupling in this case is $\epsilon = 0.3t_B$. Note that the absolute value of the self energy is plotted in this case. The solid line is the analytic answer for the envelop of the leading power law $\sim |t-t'|^{-3/2}$ decay of the kernel. We use $t_B = 2$ to set units of $t-t'$ and $\Sigma^K(t-t')$.

$\omega = \pm 2t_B$ and the power law tail will change to $|t-t'|^{-1/2}$.

The origin of the power law tail can be traced back to the fact that the bath spectral function $J(\omega)$ is non-analytic at $\omega = \pm 2t_B$. This is similar to Friedel oscillations [202] or RKKY interaction for impurities in a Fermi gas, where non-analyticity of the polarization function leads to power law decays in space. We will focus on a particular model of OQS with square root derivative singularity at the band edge of the density of states of the bath in most of the parts of this chapter, which will allow us to obtain analytic expressions for various quantities. However, the relation between power law tails and singularities is very robust, and we will work out the power law exponents for a different types of non-analytic spectral functions. For example, one can consider the arrangement where each lattice site is coupled to 1-dimensional bath, where the coupling is to a central site of the bath (infinite 1d bath) as opposed to the one end of the bath (semi-infinite 1d bath). In this case, the bath spectral function is, $J(\omega) = \Theta(4t_B^2 - \omega^2)(2/t_B)\left[1 - \omega^2/(4t_B^2)\right]^{-1/2}$. Using the same formalism, the analytical expression for $\Sigma^R(t,t') = -\mathbf{i}\ \Theta(t-t')\ 2\epsilon^2 \mathcal{J}_0(2t_B|t-t'|)$, which scales as $|t-t'|^{-1/2}$ for large $|t-t'|$. Another commonly used spectral function [48] is $J(\omega) = \Theta(\omega)\frac{\omega^x}{\omega_c^{x+1}}\ exp(-\frac{\omega}{\omega_c})$ which is a prototype of ohmic ($x = 1$), sub-ohmic ($x < 1$), super-ohmic ($x > 1$) baths respectively. In this case, we obtain closed form analytic solutions $\Sigma^R(t,t') = -\mathbf{i}\ \Theta(t-t')\ \epsilon^2\Gamma[1+x]/(2\pi)\left[1 + \mathbf{i}\ w_c(t-t')\right]^{-(x+1)} \sim |t-t'|^{-x-1}$ in the long time limit. Finally we consider the spectral density of a 2d square lattice which has

Physical model	Form of $J(\omega)$	$\Sigma^R(t-t')\ \sim$	Asymptotic limit
Semi-infinite 1-d bath	$\Theta(4t_B^2-\omega^2)\frac{2}{t_B}\sqrt{1-\frac{\omega^2}{4t_B^2}}$	$\frac{\mathcal{J}_1(2t_B\lvert t-t'\rvert)}{\lvert t-t'\rvert}$	$\lvert t-t'\rvert^{-\frac{3}{2}}$
Infinite 1-d bath	$\Theta(4t_B^2-\omega^2)\frac{2}{t_B}\frac{1}{\sqrt{1-\frac{\omega^2}{4t_B^2}}}$	$\mathcal{J}_0(2t_B\lvert t-t'\rvert)$	$\lvert t-t'\rvert^{-\frac{1}{2}}$
Ohmic,Sub and Super Ohmic bath	$\Theta(\omega)\frac{\omega^x}{\omega_c^{x+1}}\ exp(-\frac{\omega}{\omega_c})$	$\frac{\Gamma[1+x]}{[1-\mathbf{i}\ w_c(t-t')]^{x+1}}$	$\lvert t-t'\rvert^{-x-1}$
2-d square lattice bath	$\frac{1}{w_c}\log\left(\frac{\lvert w-w_0\rvert}{w_c}\right)$	$-\ e^{\mathbf{i}w_0(t-t')}\ \frac{sign(t-t')}{t-t'}$	$\lvert t-t'\rvert^{-1}$

Table 5.1: Leading power law decay in dissipative kernel ($\Sigma^R(t-t')$) at large $t-t'$ for different non-analytic bath spectral functions $J(\omega)$.

a logarithimic Van-Hove singularity (not coming from the band edge) of the form $J(\omega) \sim 1/w_c \log(|w-w_0|/w_c)$ as $\omega \to \omega_0$. In this case, we obtain $\Sigma^R(t,t') \sim e^{\mathbf{i}w_0(t-t')}\ sign(t-t')/(t-t')$ which decays as power law $\sim |t-t'|^{-1}$. This provides a clear exposition of how the power law exponent is related to the nature of non-analyticity in the bath spectral function. We summarize these results in Table (5.1) where the exact and asymptotic forms are tabulated. The non-Markovian dynamics can then be used to detect the presence and nature of these non-analyticities. If the bath spectral function has sharp but non-singular features, the kernel will be an approximate power law for a large intermediate time period, before showing exponential decay on the time scale at which the singularity is smoothed out.

In the next section, we obtain analytic expression for the Green's function of a linear chain, which we will later use to calculate correlation functions in the OQS.

5.4 Analytic Green's function for a linear chain

We consider bosons hopping on a 1D chain of N sites where each site is connected to an independent bath with its own temperature and chemical potential. We note that this arrangement is different from the standard transport setup [200] , where two reservoirs are connected to the two end sites of the chain. We revert back to eqn. [5.5] and solve the Dyson equation to obtain the exact retarded and Keldysh Green's functions of this model.

For the 1D chain, the retarded inverse propagator is a symmetric tridiagonal matrix:

$G^{-1R}_{ll'} = g[\mathcal{D}\ \delta_{l,l'} + \delta_{l,l'\pm1}]$, where $\mathcal{D}^R(\omega) = g^{-1}[\omega - \Sigma^R(\omega)]$ is independent of the site index. This can be inverted [203] to obtain

$$G^R_{i,j}(\omega) \quad = \quad (-1)^{i+j}\frac{M_{i-1}M_{N-j}}{gM_N} \quad for\ i<j \tag{5.14}$$

and $G^R_{i,j} = G^R_{j,i}$ for $i > j$, where

$$M_i = \frac{\sinh[(i+1)\lambda]}{\sinh[\lambda]} \quad with \quad \cosh[\lambda] = \mathcal{D}/2. \tag{5.15}$$

The Keldysh Green's function is then given by,

$$G^K_{i,j}(\omega) = -\mathbf{i}\epsilon^2 J(\omega)\sum_{l=1}^{N} G^R_{i,l}(\omega)\coth\left(\frac{\omega-\mu_l}{2T_l}\right)G^{*R}_{j,l}(\omega). \tag{5.16}$$

To obtain a clear insight about the structure of the Green's function, we first consider a simplified toy model consisting of 2-sites connected to two different baths [192]. In this two site model,

$$G^R_{\alpha,\alpha}(\omega) = \frac{\mathcal{D}}{g(\mathcal{D}^2-1)} \quad and \quad G^R_{\alpha,\bar{\alpha}}(\omega) = \frac{-1}{g(\mathcal{D}^2-1)}. \tag{5.17}$$

Here, the site indices, $\bar{\alpha} = 1$ for $\alpha = 2$ and $\bar{\alpha} = 2$ for $\alpha = 1$ for the two site system. For the bath spectral function given in eqn.(5.7),

$$\Sigma^R(\omega) = \frac{\epsilon^2\omega}{2t_B^2} - \mathbf{i}\,\frac{\epsilon^2}{t_B}\left[1-\frac{(\omega+\mathbf{i}\eta)^2}{4t_B^2}\right]^{1/2}. \tag{5.18}$$

In this case, the Green's functions $G^R(z)$ have isolated poles at z_0, where

$$z_0 = \frac{g}{1-\frac{\epsilon^2}{t_B^2}}\left[1-\frac{\epsilon^2}{2t_B^2}\right] - \mathbf{i}\frac{\epsilon^2}{t_B\left(1-\frac{\epsilon^2}{t_B^2}\right)}\left[1-\frac{g^2}{4t_B^2}-\frac{\epsilon^2}{t_B^2}\right]^{1/2}. \tag{5.19}$$

For $g^2/4+\epsilon^2 < t_B^2$, z_0 has a finite imaginary part leading to an exponential decay in $G^R(t,t')$ with a rate $\gamma \sim \epsilon^2/t_B$. For $g^2/4+\epsilon^2 > t_B^2$, the pole is on the real axis (outside the bandwidth), leading to an oscillation in the long time limit, similar to the behaviour found by Nori *et. al* in Ref. [48]. In this chapter we will focus on the regime

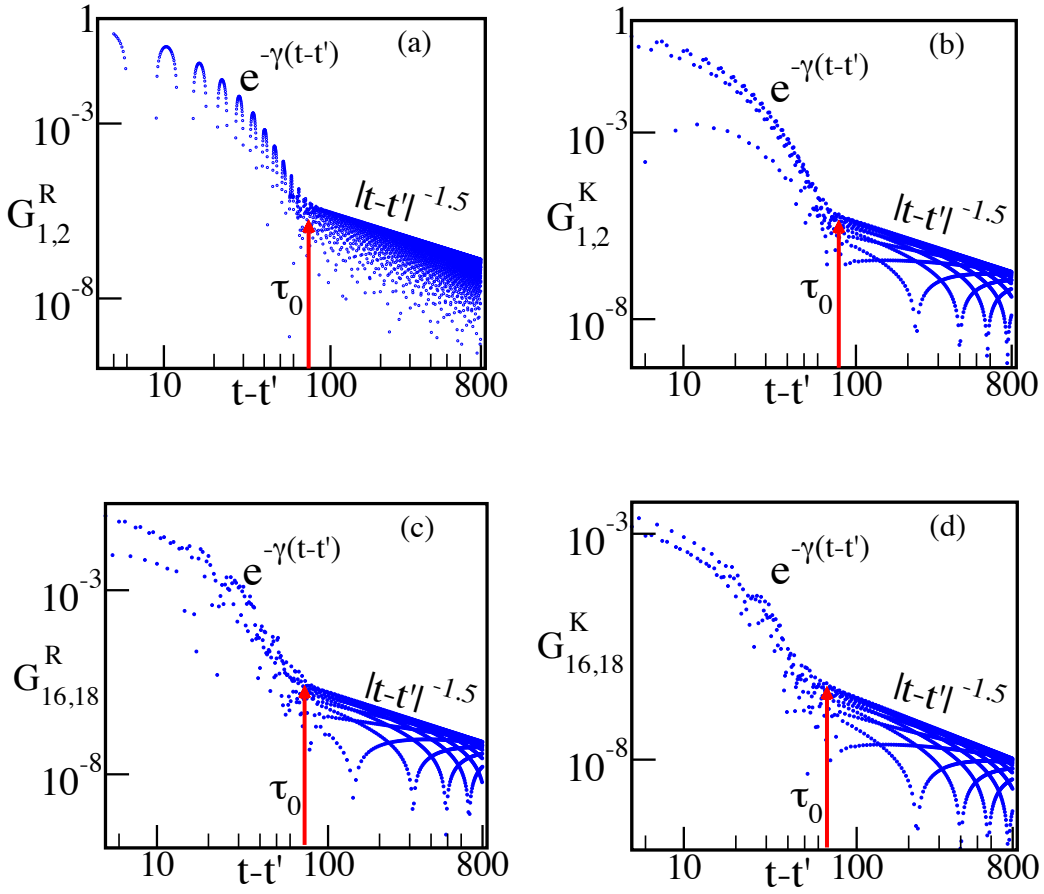

Figure 5.3: (a) and (b): Greens functions of a two-site system connected to two baths with $\mu_1 = -2.5t_B$ and $\mu_2 = -5t_B$, plotted as function of $t-t'$ for (a) $G^R_{1,2}$ and (b) $Re[G^K_{1,2}]$. (c) and (d): Green's functions for a $N = 50$ site chain, where each site is connected to an independent bath, plotted as a function of $t-t'$ in (c) $G^R_{16,18}$ and (d) $Re[G^K_{16,18}]$. The baths have a μ profile linearly varying with site number, with $\mu_1 = -2.5t_B$ and $\mu_{50} = -5t_B$. Note that absolute values are plotted in the log-log plot. All the Green's functions show an initial exponential decay, followed by a power law tail $\sim |t-t'|^{-3/2}$. The arrows mark the cross-over time scale between exponential decay and the non-Markovian power law tail, $\tau_0 = \gamma^{-1} \sim t_B/\epsilon^2$. All graphs are calculated for system hopping $g = 0.5t_B$, system bath coupling $\epsilon = 0.3t_B$ and uniform bath temperature $T = 0.625t_B$.

where the presence of the bath leads to damping in the system. Even in this case, there is an additional non-analyticity in $G^R(\omega)$ at $\omega = \pm 2t_B$, inherited from the non-analytic nature of $\Sigma^R(\omega)$. A careful analysis (see section C.1) shows that the nature of the leading non-analyticity of $G^R(\omega)$ is same as that of $\Sigma^R(\omega)$. This leads to a power law tail at long time with $G^R(t-t') \sim (t-t')^{-3/2}$. The Keldysh Green's function also inherits the same power law tail in long time, as can be easily seen from eqn.[5.16]. In Fig. 5.3 (a) and (b), we plot respectively the retarded Green's function $G^R_{12}(t-t')$ and the real part of the Keldysh Green's function $G^K_{12}(t-t')$ for the two site model as a function of time in a

log-log plot. The plots are obtained for a system with $\epsilon = 0.3t_B$ and $g = 0.5t_B$ connected to two independent baths of common temperature $T = 0.625t_B$ and chemical potential $\mu_1 = -2.5t_B$ and $\mu_2 = -5t_B$. At short times, the Green's functions are dominated by the exponential decay from the poles, while the long time behaviour is governed by the power law due to the non-analytic $J(\omega)$. The power law is clearly visible after the exponential part has decayed i.e beyond a time scale $\tau_0 = \gamma^{-1} \sim \frac{t_B}{\epsilon^2}$, which is marked in the figures with an arrow. τ_0 is large at weak system-bath coupling and we recover a quasi-Markovian dynamics for a long time, $t < \tau_0$ which finally crosses over to a non-Markovian regime for $t > \tau_0$. However, at strong system-bath coupling, τ_0 is very short and the dynamics is mostly governed by the non-Markovian power law decay in the memory kernels. Thus, it would be easier to detect observable consequences of non-Markovian dynamics at large ϵ. τ_0 has a very weak dependence on temperature and is essentially set by the system-bath coupling. We emphasise that , in spite of the presence of a scale τ_0 in the system dynamics, we can not coarse - grain over this scale and obtain a Markovian description, as we are then left with the power law decay of the Green's function.

The characteristic features shown by the two-site system is carried over to the solution for the N site system given in eqn.[5.14]. In this case, the poles are given by $\sinh[(N+1)\lambda] = 0$, where the location of the poles satisfies $z_0(1 - \epsilon^2/2t_B^2) + \mathbf{i}\epsilon^2/t_B\sqrt{1 - z_0^2/4t_B^2} = 2g\cos[m\pi/(N+1)]$, with $m = 1, 2, ...N$ [204]. The pole has a positive imaginary part $\gamma \sim \epsilon^2/t_B$ for $g^2\cos^2[\pi/(N+1)] + \epsilon^2 < t_B^2$. With this modification, a similar structure of an exponential decay followed by a power law tail is also obtained in this case. We consider a $N = 50$ site chain with $\epsilon = 0.3t_B$ and $g = 0.5t_B$, connected to independent baths with common temperature $T = 0.625t_B$ and a chemical potential profile which varies linearly with the site number of the system going from $\mu_1 = -2.5t_B$ and $\mu_{50} = -5t_B$. In Fig. 5.3 (c) and (d), we respectively plot the retarded Green's function $G^R_{i,j}(t-t')$ and the real part of the Keldysh Green's function $G^K_{i,j}(t-t')$ of the system as a function of time in a log-log plot. We have used $i = 16$ and $j = 18$ to avoid the boundary of the chain. These Green's functions also show a quasi-Markovian exponential decay followed by a non-Markovian $|t-t'|^{-\frac{3}{2}}$ decay, similar to those found in the two site system.

In the next section, we will construct experimentally accessible quantities that can clearly distinguish between the quasi-Markovian and non-Markovian dynamics and discuss

the observable consequences of long range memory kernels.

5.5 Observables in Steady state

In this section, we focus on experimental observables which can detect non-Markovian behaviour in these open quantum systems. We will divide these observables into two classes: (i) equal time observables like occupation numbers and currents and (ii) unequal time current-current correlators. While the first class of observables show interesting quantitative deviations from Markovian answers, especially in the limit of large system bath couplings, the unequal time correlators show qualitatively different behaviour indicating the presence of non-Markovian power law tails.

5.5.1 Equal Time Correlators

We will study two types of equal time correlators: (a) occupation number of sites or eigenmodes and (b) current through the system. We first consider the two site problem. In absence of any coupling to the bath, the system Hamiltonian can be diagonalized to obtain two states at $E = \mp g$ with mode operator $A^{\pm} = (1/\sqrt{2})(a_1 \pm a_2)$. The first observable we focus on is the occupation number of these modes, $n^{\pm}$. The change in occupation number of the modes due to coupling to baths,

$$\delta n^{\pm} = \frac{\mathbf{i}}{4} \sum_{\alpha} \int \frac{d\omega}{2\pi} \Big[G^K_{\alpha,\alpha}(\omega) \pm G^K_{\alpha,\bar{\alpha}}(\omega) \Big]. \tag{5.20}$$

We first consider the case where a system with $g = 0.5t_B$ is coupled to two baths kept at the same temperature and chemical potential. In Fig. 5.4(a) we plot the change in occupation of the ground state, δn^{+}, in solid (red and green) lines as a function of the system bath coupling ϵ for two different bath temperatures, $T = 0.5t_B$ and $T = 1.25t_B$. The common chemical potential of the baths is $\mu = -2.25t_B$. We have also plotted the distribution function obtained from Markovian description given in Ref [192], $n^{+}_{eq} = [e^{\frac{-g-\mu}{T}} - 1]^{-1}$, in dotted lines. The exact steady state distribution approaches the Markovian answer at small ϵ, but starts deviating as ϵ grows. This deviation increases with the temperature of the bath. However, the one particle Green's functions of the two site system do satisfy the fluctuation dissipation relation, $G^K_{\alpha,\alpha}(\omega) = 2\mathbf{i}\ Im\left[G^R_{\alpha,\alpha}(\omega)\right]\ \coth\left[(\omega-\mu)/2T\right]$, indicative

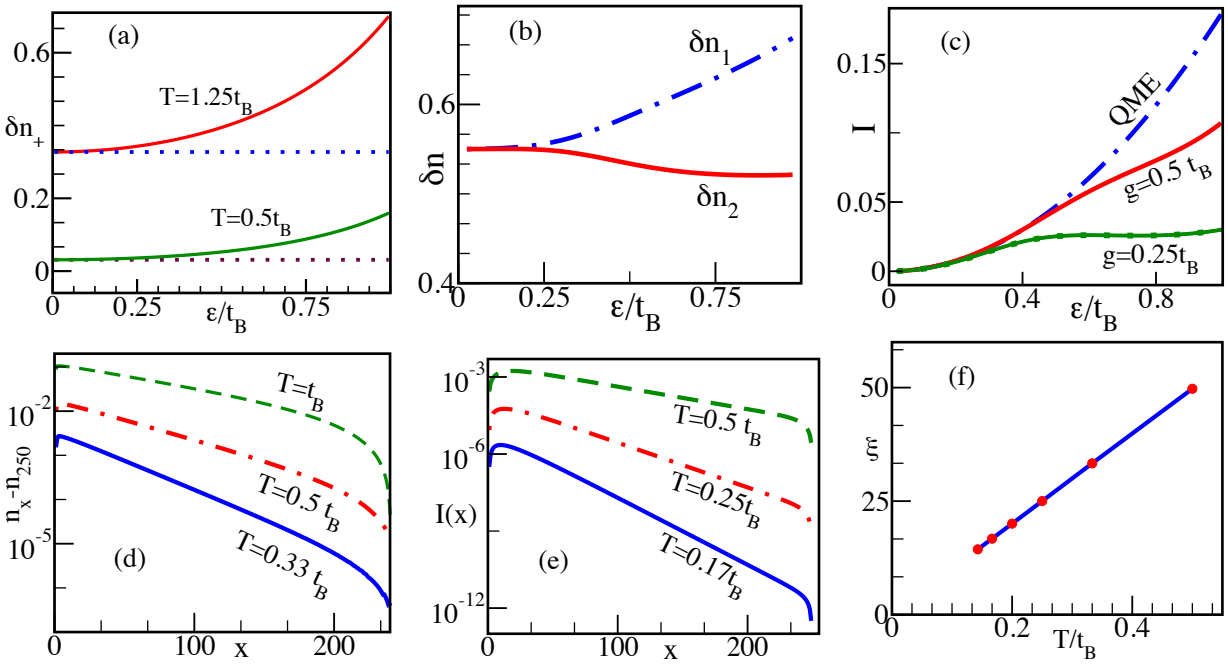

Figure 5.4: (a) Change in occupation of ground state (δn^+) of a two site system with $g = 0.5t_B$ as a function of system bath coupling ϵ (solid lines) for coupling to a bath with common $\mu = -2.25t_B$ and common temperature $T = 0.5t_B$ and $T = 1.25t_B$. Also plotted are the distribution functions obtained from Markovian master equation given in Ref.[[192]] (dotted line). The exact answer deviates from the markovian results as ϵ increases. The deviation increases with temperature. (b) Occupation number of the two sites and (c) current through a two site system with $g = 0.25t_B$, coupled to two baths with common temperature $T = t_B$ and chemical potentials $\mu_1 = -2.5t_B$ and $\mu_2 = -5.0t_B$, as a function of ϵ. In (c) the current is also plotted for a system with $g = 0.5t_B$. The steady state current deviates from the quantum master equation result given in Ref.[[192]] for $\epsilon > g$. (d) Number density profile (measured w.r.t density of N^{th} site) and (e) Current profile for a $N = 250$ site chain, where each site is connected to an independent bath. The baths have a μ profile linearly varying with site number, with $\mu_1 = -2.25t_B$ and $\mu_{250} = -5t_B$. In (d) the common temperature for the baths are $T = 0.33t_B, 0.5t_B, t_B$ while in (e) $T = 0.17t_B, 0.25t_B, 0.5t_B$. In both cases $\epsilon = 0.2t_B$ and $g = 0.5t_B$. Both density and current profiles show an exponential decay. The length scale of the decay ξ is plotted as a function of T in (f). The length scale increases linearly with T.

of thermalization of the system.

We now consider the steady state where the 2 baths coupled to the two sites are kept at same T, but different μ. In this case, a finite current flows through the system and it is simpler to analyze the system in the site basis. The change in the local occupation numbers, δn_1 and δn_2, is plotted with ϵ in Fig. 5.4(b) for $T = t_B$ and $g = 0.25t_B$, $\mu_1 = -2.5t_B$ and $\mu_2 = -5.0t_B$. As ϵ increases, the influx of particles to site 1 increases, but the probability of particles tunneling from site 1 to 2 saturates when $\epsilon \geq g$. The steady state number

density on site 1 then needs to increase to match the outflux with the influx, as seen in Fig. 5.4(b). The density at site 2 simultaneously shows a decrease with ϵ in the same regime, since the influx to site 2 has saturated. The number density at site 2 then needs to decrease to to maintain a steady current. Finally, the current, $I_l = \mathbf{i}\ g\langle a_l^\dagger a_{l+1} - a_{l+1}^\dagger a_l\rangle$, in the link between sites l and $l+1$ is given by,

$$I_l = g\int \frac{d\omega}{2\pi}\ Re[G^K_{l,l+1}(\omega)] \tag{5.21}$$

The current on the link between site 1 and 2 is plotted as a function of ϵ in Fig. 5.4(c) for two different values of $g = 0.5t_B$ and $0.25t_B$. The current matches with the Born-Markov answer obtained through the solution of Redfield equations [192] in the small ϵ limit and deviates from the master equation result for $\epsilon \geq g$. At small ϵ , the current in the system is constrained by exchange of particles between baths and sites of the system . Any particle that has reached site 1 can be thought to be delocalized to site 2 on a time scale g^{-1} with $g^{-1} << \epsilon^{-1}$ in the Markovian limit. For $\epsilon \geq g$, this is no longer true and steady state current is constrained by the hopping rate g and becomes almost independent of ϵ for $\epsilon >> g$. This leads to the saturating trends seen in Fig. 5.4(c). The increase of n_1 and decrease of n_2 in Fig. 5.4(b) is a consequence of this bottleneck between sites 1 and 2.

We now consider a linear chain of N sites where each site l is connected to an independent bath of temperature T_l and chemical potential μ_l. We focus on the situation where the baths have a fixed temperature $T_l = T$ and a chemical potential linearly varying with space i.e $\mu_l = \mu_1 + \nu(l-1)$. Specifically we look at a $N = 250$ site system with $g = 0.5t_B$, $\epsilon = 0.2t_B$, $\mu_1 = -2.25t_B$ and $\mu_{250} = -5t_B$. The density profile in the system shows an exponential decay with site number on top of a constant value, as seen in a semi-log plot in Fig. 5.4(d), where the local density is measured with respect to the density at the N^{th} site. We plot the density profile for three different temperatures, $T = 0.33t_B, 0.5t_B, t_B$. We find that the decay length scale increases with temperature. The current through the link between sites l and $l+1$, I_l, is plotted as function of l in Fig. 5.4(e). The current initially increases with distance from the boundary, then settles into an exponential decay over a large range of sites, as seen in the linear graph in the semi-log plot. We plot the current profile for three different temperatures, $T = 0.17t_B, 0.25t_B, 0.5t_B$. Once again we find a decay length scale increasing with temperature. In Fig. 5.4(f), we plot the decay length

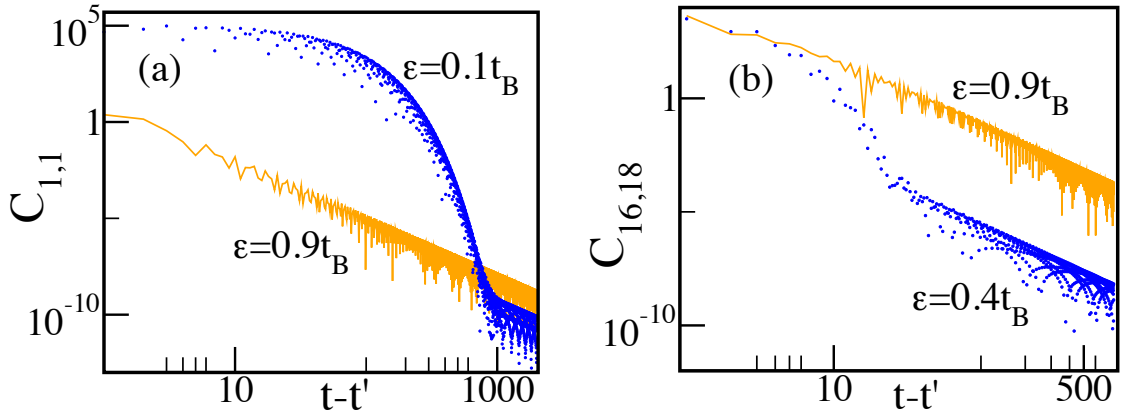

Figure 5.5: Unequal time current current correlator $C_{kl}(t-t')$ is plotted as a function of $|t-t'|$ for (a) $N=2$ site model and (b) for a $N=50$ site chain with $k=16,18$. Here each site is connected to a bath. The baths have common temperature $T=0.625t_B$ and linearly varying μ_l where $\mu_1=-2.5t_B$, $\mu_N=-5.0t_B$, $g=0.5t_B$. In (a) the blue dots corresponds to $\epsilon=0.1t_B$ while the orange line corresponds to $\epsilon=0.9t_B$. In (b) the blue dots corresponds to $\epsilon=0.4t_B$ while the orange line corresponds to $\epsilon=0.9t_B$. It shows a short time exponential decay followed by a non-Markovian power law tail $\sim|t-t'|^{-3}$ in the long time limit. The power law tail appears at shorter times as ϵ increases.

from the current profile, ξ, as a function of temperature and show that ξ is proportional to T. In the extreme classical limit, when $T\to\infty$, the system shows a constant current independent of the link number. The exponential decay and the variation of the decay length with temperature can be understood from the exact Green's function for the linear chain, as shown in Appendix C.2. We have checked that a similar exponential decay is also seen when the temperature of the baths vary linearly in space while the chemical potential is kept fixed.

5.5.2 Unequal Time Correlators

The density and current profiles in the open quantum system show important quantitative traits as a function of the system bath coupling. However they do not provide a smoking-gun signature of the underlying non-Markovian dynamics. This is provided by the unequal time density-density or current-current correlator, which shows a long time power law decay with an exponent that is twice the exponent of the power law tail in Σ and G. Here we compute the unequal time current-current correlator , which is given by,

$$C_{kl}(t-t') = \langle I_k(t) I_l(t') \rangle = g^2 [\quad G^{<}_{l+1,k}(t',t)\, G^{>}_{k+1,l}(t,t') + G^{<}_{l,k+1}(t',t)\, G^{>}_{k,l+1}(t,t') - (l \leftrightarrow l+1)] \tag{5.22}$$

where $G^{>(<)} = (G^K \pm (G^R - G^A))/2$. We note that we have considered here a current-current correlator symmetrized between the forward and backward contours; however, the qualitative statements we make are also true for a normal ordered correlator. We first focus on the 2 site system. In Fig 5.5(a), we plot $C_{1,1}(t-t')$, normalized by I_1^2, as a function of $t-t'$ on a log-log plot. We plot the correlator for two values of ϵ: a weak system bath coupling of $\epsilon = 0.1t_B$ (blue circles) and a strong system-bath coupling of $\epsilon = 0.9t_B$ (orange line). The graphs are obtained for a system with $g = 0.5t_B$, coupled to two baths with common $T_1 = 0.625t_B$ and chemical potentials $\mu_1 = -2.5t_B$ and $\mu_2 = -5.0t_B$. In the weak coupling limit ($\epsilon = 0.1t_B$), we see that $C_{1,1}(t-t')$ decreases exponentially in time before crossing over to a power law $C_{1,1}(t-t') \sim |t-t'|^{-3}$ at a very large time $\sim t_B/\epsilon^2$. However, by this time the correlator has decayed by orders of magnitude and the power law tail may be hard to observe experimentally. Thus, although the behaviour of the system is not Markovian in the long time limit, experiments may see an effectively Markovian dynamics. However, at large $\epsilon \sim 0.9t_B$, the initial exponential dynamics is extremely short lived and the power law tail in the autocorrelation function should be clearly visible in the experiments. This observable can hence be used to identify non-Markovian dynamics in the system and detect the nature of non-analyticity in the corresponding bath spectral function. Further, one can tune the system dynamics from "quasi" Markovian to non-Markovian by tuning the system-bath coupling in these OQS.

We now consider the current current correlations in a linear chain of $N = 50$ sites coupled to independent baths of fixed temperature and linearly varying chemical potential. We ignore the boundary regions (where the current is not exponentially decaying) and focus on the middle of the chain . In Fig. 5.5(b), we plot the current-current correlator $C_{ij}(t-t')$ as a function of $t-t'$ by fixing $i = 16$ and $j = 18$ for a system with $g = 0.5t_B$ coupled to baths with $\mu_1 = -2.5t_B$, $\mu_{50} = -5.0t_B$ and $T = 0.625t_B$. The current current

correlation function is normalized by $I_{16}I_{18}$ in this case. Once again, we plot $C_{i,j}(t-t')$ for two values of ϵ : (i) a moderate value of $\epsilon = 0.4t_B$ (blue dots) where an exponential decay is followed by a slow decrease $|t-t'|^{-3}$ and (ii) a large $\epsilon = 0.9t_B$ where the exponential decay is almost invisible and the power law decay dominates. This regime should be easily observed in experiments.

5.6 Fermionic system coupled to Fermionic baths

The formalism developed in the previous sections for treating a bosonic open quantum system with non-Markovian dynamics can be easily modified to treat a system of fermions interacting with fermionic baths. The key features, which make it exactly solvable, are non-interacting Hamiltonians for the system and bath and a linear system-bath coupling. As long as these conditions are met, minor changes in the formalism allow us to treat the fermionic system with similar power law tails obtained for self-energies, Green's function and unequal time correlators.

For fermions, the Keldysh field theory is set up in terms of doubled Grassmann fields $\psi_\pm$ and their conjugates $\psi^*_\pm$. The only difference from the bosonic theory is that it is more convenient to work in terms of $\psi_{1(2)} = [\psi_+ \pm \psi_-]/\sqrt{2}$ and $\psi^*_{1(2)} = [\psi^*_+ \mp \psi^*_-]/\sqrt{2}$, which take care of anti-commutation relations between fermionic fields in a natural way. We consider a fermionic chain, where each site is coupled to an independent fermionic bath with its own temperature and chemical potential. The Hamiltonian of the system is given by equations (5.1,5.2), with $a^\dagger_l$ and $B^{(l)\dagger}_\alpha$ now representing fermionic creation operators. The Keldysh action for the system is given by,

$$S_s = \sum_{l,l'} \int d\omega \psi^\dagger_l(\omega) \begin{bmatrix} G_0^{-1R}(l,l',\omega) & G_0^{-1K}(\omega)\ \delta_{l,l'} \\ 0 & G_0^{-1A}(l,l',\omega) \end{bmatrix} \psi_{l'}(\omega)$$

$$S_b = \sum_{l,\alpha} \int d\omega\ \xi^{\dagger(l)}_\alpha(\omega) \begin{bmatrix} \omega - \Omega_\alpha + \mathbf{i}\eta & 2\mathbf{i}\eta\ F_l(\Omega_\alpha) \\ 0 & \omega - \Omega_\alpha - \mathbf{i}\eta \end{bmatrix} \xi^{(l)}_\alpha(\omega)$$

$$S_{sb} = -\epsilon \sum_{l,\alpha} \int d\omega\ \kappa_\alpha \xi^{\dagger(l)}_\alpha(\omega)\psi_l(\omega) + h.c. \tag{5.23}$$

where $\psi^\dagger_l = \left[\psi^{*(l)}_1, \psi^{*(l)}_2\right]$ are the system fields and $\xi^{\dagger(l)}_\alpha = \left[\xi^{*(l)}_{1,\alpha}, \xi^{*(l)}_{2,\alpha}\right]$ are the fields for bath

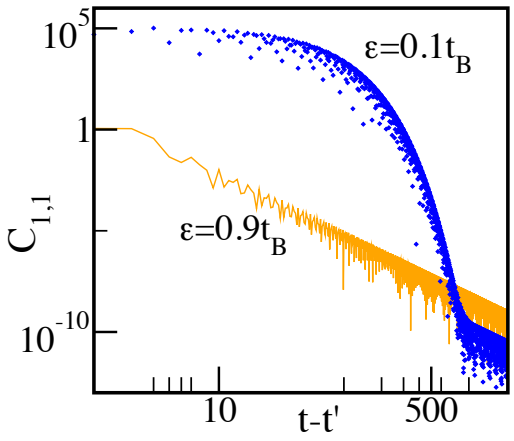

Figure 5.6: The current current correlator $C_{11}(t-t')$ (normalized by I_1^2) is plotted for a two site fermionic system with $g = 0.5t_B$, coupled linearly to two fermionic baths of same temperature $T = 0.625t_B$ and chemical potentials $\mu_1 = -2.5t_B$ and $\mu_2 = -5.0t_B$. It shows a short time exponential decay followed by a non-Markovian power law tail $\sim |t-t'|^{-3}$ in the long time limit. Power law kernel appears at shorter times as ϵ increases.

degrees of freedom in eigenbasis. The main difference from the bosonic case is the equilibrium distribution function of the fermionic baths $F_l(\Omega_\alpha) = \tanh\left(\frac{\Omega_\alpha - \mu_l}{2T_l}\right)$. Integrating out the bath degrees of freedom, we obtain the action for the reduced dynamics of the system,

$$S_{oqs} = \sum_{l,l'} \int d\omega \psi_l^\dagger(\omega) \begin{bmatrix} G_0^{-1R}(l,l',\omega) - \Sigma^R(\omega)\ \delta_{l,l'} & -\Sigma_l^K(\omega)\ \delta_{l,l'} \\ 0 & G_0^{-1A}(l,l',\omega) - \Sigma^A(\omega)\ \delta_{l,l'} \end{bmatrix} \psi_{l'}(\omega) \tag{5.24}$$

where $\Sigma^R(\omega)$ is given by equation [5.8], just as in case of bosons, while the Keldysh self energy $\Sigma_l^K(\omega)$ is given by,

$$\Sigma_l^K(\omega) = -\mathbf{i}\epsilon^2 J(\omega)\ \tanh\left(\frac{\omega - \mu_l}{2T_l}\right) \tag{5.25}$$

The Keldysh self energy function for the fermionic case can thus be obtained from the bosonic case by replacing $\coth\left(\frac{\omega-\mu_l}{2T_l}\right)$ by $\tanh\left(\frac{\omega-\mu_l}{2T_l}\right)$, as one would expect due to different statistics of particles. With this replacement, all the expression for the Green's functions and observables, obtained in section 5.3 , 5.4 and 5.5 for bosonic system, can be used for the fermionic system as well. We note that, unlike the bosonic case, there is no reason to place the bath chemical potentials below the band bottom for the fermionic baths. The self-

energies in real time show similar power law behaviour $\Sigma^R(t-t') \sim \Sigma_l^K(t-t') \sim |t-t'|^{-\frac{3}{2}}$ for large time, with the power law originating from the non-analyticities in the bath spectral function given by equation [5.7]. However, it is harder in this case to give an interpretation to self-energies, since fermions do not have a classical limit and it is impossible to talk about a "classical saddle point" for non-interacting fermionic action. We note that the mere presence of the singularity in the bath spectral function is enough to generate the power law tail, the singularity does not need to be either close to the spectral gap of the system or to the chemical potential of the bath. The Green's functions then inherit this power law along with an exponential decay, which also gets reflected in the long time behaviour of density-density auto-correlation function and current-current correlation function, similar to the bosonic system considered earlier. Working with the 2-site fermionic system, we plot $C_{1,1}(t-t') = \langle I_1(t) I_1(t') \rangle$, normalized by I_1^2, as a function of $t-t'$ on a log-log plot in Fig. 5.6 for a system with $g = 0.5t_B$ coupled to baths with $\mu_1 = -2.5t_B$, $\mu_2 = -5.0t_B$ and $T = 0.625t_B$. The current-current correlator clearly shows an exponential decay followed by a power law tail $\sim |t-t'|^{-3}$, as seen in the bosonic system. Once again the power law dominates the dynamics and leads to large values of the correlators for long $t-t'$ at strong system bath coupling.

We have obtained exact solutions for Green's functions of 1D non-interacting bosonic and fermionic chains coupled to independent baths and demonstrated non-Markovian behaviour in both systems. An obvious question is how the interaction among system degrees of freedom, which is inadvertently present in any realistic system, affects the description we have obtained here. In the next section, we try to answer this question by focusing on the bosonic system and making mean field approximation to the underlying interaction terms.

5.7 Effect of Interaction

We consider the case of an interacting chain of bosons coupled linearly to independent non-interacting bosonic baths. In addition to the hopping g, the system bosons are interacting with each other with a local repulsion U and nearest neighbour repulsion V, i.e. We add

to the Hamiltonian given by equation [5.1], a term

$$H_{int} = U \sum_i \hat{n}_i(\hat{n}_i - 1) + V \sum_i \hat{n}_i \hat{n}_{i+1}, \tag{5.26}$$

where $\hat{n}_i = a_i^\dagger a_i$ is the density at site i. The bath degrees of freedom can be integrated out as before to obtain the quadratic dissipative action S_{oqs} (eqn.[5.5]). This action and its associated Green's functions can then be used as a free theory around which we consider the effects of interactions. The Keldysh action corresponding to the inter-particle interaction is given by [95],

$$\begin{aligned} S_{int} &= -\frac{U}{2} \sum_l \int dt \phi_{cl}^{*(l)}(t)\phi_{cl}^{(l)}(t)\phi_{cl}^{*(l)}(t)\phi_q^{(l)}(t) \\ &- \frac{V}{2} \sum_l \int dt \phi_{cl}^{*(l)}(t)\phi_{cl}^{(l)}(t)\phi_{cl}^{*(l\pm1)}(t)\phi_q^{(l\pm1)}(t) + h.c + cl \leftrightarrow q. \end{aligned} \tag{5.27}$$

We consider the effect of this interaction on the Green's functions within mean field theory. This is equivalent to considering the one-loop corrections to the self energy, shown in Fig. 5.7 (a) and (b) for the Keldysh and retarded self-energies. Note that the Keldysh self energy correction vanishes because $G^R(t,t) + G^A(t,t) = 0$ [55]. The corrections to self-energy, Σ^R induced by the interaction term are given by, $\Sigma^I_{ii} = U n_{i,i} + (V/2) n_{i\pm1,i\pm1} - U$, and $\Sigma^I_{i,i+1} = (V/2)(n_{i,i+1})$, where $n_{ij} = \mathbf{i} \int (d\omega/2\pi)\ G^K_{i,j}(\omega)$. The retarded self-energy due to inter-particle interaction change the retarded Green's functions obtained from $(G^{-1R}_{l,l'} - \Sigma^I_{l,l'})^{-1}$ where G^{-1R} already includes self-energies induced by the bath. These retarded Green's functions in turn change G^K through $G^K = G^R \Sigma^K G^A$ where Σ^K is the Keldysh self-energy induced by the bath (the interaction contribution to it is zero, as shown above). The Keldysh Green's function used in calculating the retarded self-energy shown in Fig. 5.7 (b) is this renormalized G^K, obtained self-consistently. Hence, this completes a self-consistency loop. The mean field approximation is then equivalent to resummation of particular set of loop diagrams. From an equation of motion perspective, this is also equivalent to solving stochastic Gross-Pitaevskii equation [205].

A key question we want to answer is how does the interaction affect the non-Markovian dynamics? We have seen earlier that the Green's functions and unequal time observables

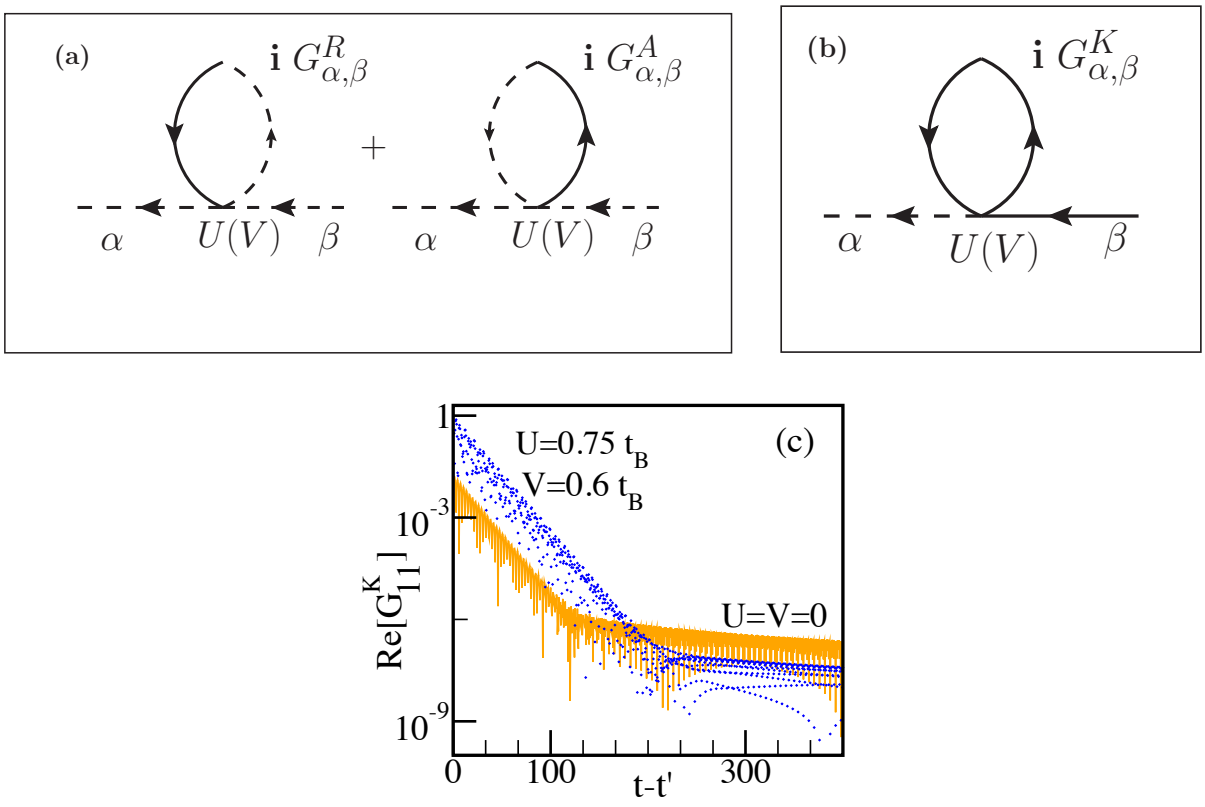

Figure 5.7: (a) and (b): Feynman diagrams corresponding to (a) Keldysh and (b) Retarded self energy due to interparticle interactions in a two site bosonic system coupled to external bath in the mean field approximation. The correction to Keldysh self energy vanishes. The loop propagator in (b) is the self consistent Keldysh Green's function. (c) The real part of the local Keldysh Green's function $G^K_{11}(t,t')$ for a two site bosonic system coupled to two baths plotted as a function of $t-t'$ in a semi-log plot. In both cases the bath temperature $T = 0.625t_B$ and chemical potentials $\mu_1 = -2.5t_B$ and $\mu_2 = -5.0t_B$. The systems have a hopping $g = 0.5t_B$ and system-bath coupling $\epsilon = 0.2t_B$. The orange line is for a non-interacting system, while the blue circles are for an interacting system with $U = 0.75t_B$ and $V = 0.6t_B$. The interaction increases the crossover scale, but does not eliminate the power law tail.

for non-interacting systems show a pattern of exponential decay at short times, which crosses over to power law tail with exponent fixed by the nature of the non-analyticity in the bath spectral function. We can then ask if the power law tail survives in the interacting system, and, if it survives, whether the crossover time scale increases or decreases with the interaction strength.

In order to gain analytic insight into the problem, we once again consider the case of a chain with 2-sites. In this case, $\Sigma^I_{11} = Un_{11} + (V/2)n_{22} - U$, $\Sigma^I_{22} = Un_{22} + (V/2)n_{11} - U$

and $\Sigma^I_{12} = (V/2)n_{12}$. The retarded Green's function is then given by

$$G^R(\omega) = \frac{1}{Q(\omega)} \begin{bmatrix} \omega - \Sigma^R - \Sigma^I_{22} & -g + \Sigma^I_{12} \\ -g + \Sigma^{*I}_{12} & \omega - \Sigma^R - \Sigma^I_{11} \end{bmatrix} \tag{5.28}$$

where $Q(\omega) = [\omega - \Sigma^R - \Sigma^I_{11}][\omega - \Sigma^R - \Sigma^I_{22}] - |\Sigma^I_{12} - g|^2$. Considering the denominator of the equation [5.28], we find that the poles of the Green's function are shifted from z_0 in the non-interacting case to $z_\pm$, where $z_\pm$ is obtained from z_0 (given in eqn.[5.19]) by replacing g with $c_\pm = a \pm \sqrt{b^2 + |\tilde{g}|^2}$. Here $a(b) = (\Sigma^I_{11} \pm \Sigma^I_{22})/2$, and $\tilde{g} = -g + \Sigma^I_{12}$. The interaction induced self-energy splits the single pole of the non-interacting case into two. Using the fact that $a = (U + V/2)(n_1 + n_2) + V/2$, where $n_{1(2)}$ are the densities at site 1(2), one can show that $a > 0$, and hence $c_+ > g$, for small Σ_{12}. We have checked that Σ^I_{12} is not large enough to change this argument for a wide range of U and V (see Appendix C.3 for details). Comparing z_+ and z_0, we then see that z_+ has a smaller imaginary part compared to z_0. This leads to an exponential decay slower than the non-interacting case. The power law tail survives (in fact it can be shown to survive to all orders in perturbation theory), but the crossover scale is further pushed out because of the slower exponential decay. In Fig. 5.7(c), we plot the real part of the Keldysh Green's function $G^K_{1,1}$ of the two site system with the same non-interacting parameters $g = 0.5t_B$, $\epsilon = 0.2t_B$, bath temperature $T = 0.625t_B$, $\mu_1 = -2.5t_B$, $\mu_2 = -5.0t_B$ for two cases in a semi log plot : (i) the non-interacting case plotted with orange lines and (ii) the interacting system plotted with blue circles for $U = 0.75t_B$ and $V = 0.6t_B$. We clearly see that crossover to the power law tail is pushed out to larger values of $|t - t'|$ for the interacting case. In Appendix C.3, we have shown how the crossover timescale changes with U and V for a range of interaction strengths.

The fact that the exponential decay is slowed down in presence of the interaction seems odd, given our expectation of faster decay due to scattering events. This is due to the fact that the mean field theory misses processes leading to redistribution of energy, which contributes at two loops or higher order. The one-loop corrections lead to the dressing of the 1 particle Green's function (to form quasi particles) without leading to additional energy relaxations. Thus, although the mean field theory is non-perturbative in interaction strength, we expect that at larger interaction strengths, additional process may increase

the rate of exponential decay of the Green's function, thus pulling back the timescale for crossover from "quasi" Markovian to non-Markovian dynamics in the system.

So far in this chapter, we have studied the steady state dynamics of the non-Markovian OQS. In the next section, we turn our attention to the transient dynamics of the OQS and develop an extension of the Keldysh field theory formalism discussed in chapter 3 to include arbitrary athermal initial conditions in the open quantum dynamics.

5.8 Dynamics Starting from Arbitrary Initial Conditions

The initial preparation protocol of an OQS crucially governs its subsequent dynamics while the dissipation and stochastic fluctuations coming from the bath try to erase the initial memory in the long time dynamics leading to thermalization of the system. Hence, to study the effects of non-trivial initial conditions in the transient dynamics of the OQS, we need to develop a non-equilibrium field-theoretic formalism for an open quantum system which can include arbitrary initial conditions explicitly. In this section, we extend the new non-equilibrium field theory formalism formalism, developed in chapter 3, to study the transient dynamics of many particle open quantum systems starting from arbitrary athermal initial conditions. We will then work out examples of a Bosonic and a Fermionic non-Markovian OQS undergoing non-unitary dynamics starting from different non-trivial initial density matrices.

Continuing our discussions on non-interacting OQS, we assume that both H_s and H_b are non-interacting Hamiltonians, whereas the system bath coupling H_{sb} is linear in both the bath and system degrees of freedom, so that the combined system can be represented by a Gaussian theory. We will assume that the system bath coupling H_{sb} is turned on through an infinitely rapid quench at $t = 0$ which breaks the time-translation invariance of the full problem. At $t = 0$, the density matrix of the combined system, $\hat{\rho}_0 = \hat{\rho}_{0S} \otimes \hat{\rho}^l_{0B}$, where $\hat{\rho}_{0S}$ is an arbitrary density matrix of the system, which will be encoded by using an initial bilinear source $\hat{u}$, similar to one discussed in chapter 3. Here $\hat{\rho}^l_{0B}$ is a thermal density matrix for the l^{th} bath with temperature T_l and chemical potential μ_l.

We will also assume that while the coupling to the baths changes the system dynamics for $t > 0$, the baths themselves are not affected by the presence of the system. The bath Green's functions are then time-translation invariant and are given by the thermal Green's

functions. These can be evaluated either by using standard infinitesimal regularization [55] or by using an initial source field for the baths and setting them to their thermal value.

For $t > 0$, we trace out the bath degrees of freedom and study the effective action of the system. Since the bath is non-interacting and the couplings are linear, this produces only quadratic terms in the effective action of the OQS, which can be written in the form of retarded and Keldysh self energies, Σ^R and Σ^K respectively. Since the bath Green's functions are time translation invariant, it is easy to see that the self energies have the following structure,

$$\Sigma^{R/K}(t,t') = \Theta(t)\Theta(t')\int \frac{d\omega}{2\pi}\Sigma^{R/K}(\omega)e^{\mathbf{i}\omega t}$$

where $\Sigma^{R/K}(\omega)$ are given by Eq. 5.8. The Dyson equation for the retarded Green's function can be solved to get

$$\begin{aligned} G^R(t,t') &= G_O^R(t-t') && \text{for } t,t^{'} > 0 \\ &= G_O^R(t)G_0^R(-t') && \text{for } t > 0,\ t^{'} < 0 \\ &= G_0^R(t-t') && \text{for } t,t^{'} < 0 \end{aligned}$$

where G_0 is the Green's function for the closed system decoupled from the bath (see Eq. 5.3) [48] and

$$G_O^R(t-t') = \mathbf{i}\int \frac{d\omega}{\pi}e^{\mathbf{i}\omega t}\mathrm{Im}[G_0^{-1R}(\omega) - \Sigma^R(\omega)]^{-1}. \tag{5.29}$$

We note that the retarded Green's function of the OQS is still independent of the source $\hat{u}$ and hence represents the physical retarded Green's function, which is independent of $\hat{\rho}_{0S}$. In this case, $G_O^R(\alpha,t;\gamma,t') = G_O^R(\alpha,\gamma,t-t')$. Note that we have suppressed the quantum number indices for brevity in Eq. 5.29. The information of $\hat{\rho}_{0S}$ is carried by the physical Keldysh correlation function,

$$\begin{aligned} \mathcal{G}^K_{O\rho_0}(\alpha,t;\beta,t') &= -\mathbf{i}\sum_{\gamma\delta} G_O^R(\alpha,t;\gamma,0)[\delta_{\gamma\delta} + 2\zeta\langle a_\gamma^\dagger a_\delta\rangle_0]G_O^A(\delta,0;\beta,t') \\ &+ \int_0^t dt_1\int_0^{t'} dt_2 \sum_\gamma G_O^R(\alpha,\gamma,t-t_1)\Sigma_\gamma^K(t_1-t_2)G_O^A(\delta,\beta,t_2-t') \end{aligned} \tag{5.30}$$

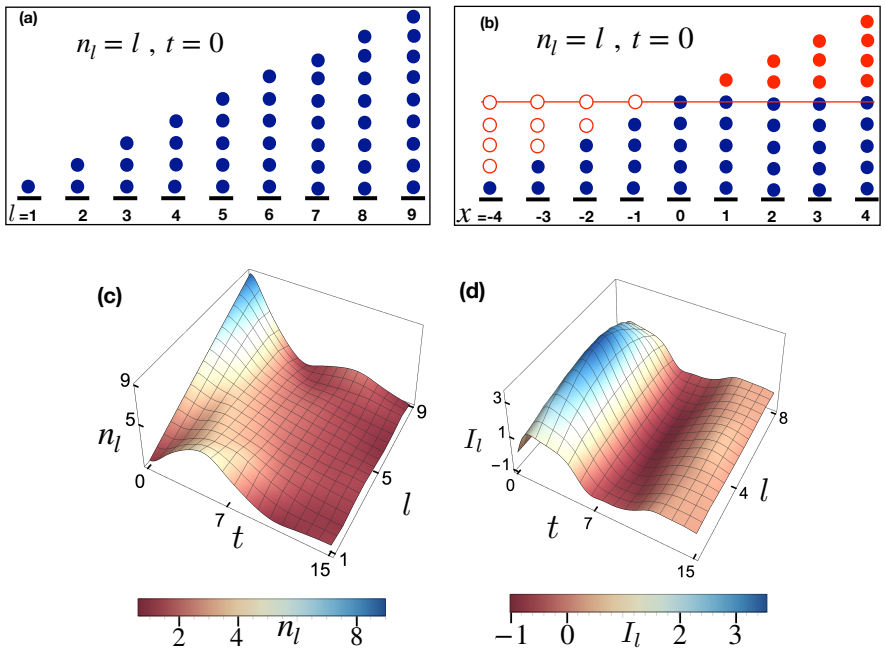

Figure 5.8: Evolution of a linear chain of Bosons, starting from a Fock state. Each site l is connected to a bath with temperature $T = g$ and chemical potential μ_l, where $\mu_l = \mu_1 + \nu(l-1)$ with $\mu_1 = -4.05g$ and $\nu = 0.75g$. Here g is the tunneling amplitude in the linear chain. (a) The initial Fock state in a $N = 9$ site system where the l^{th} site is occupied by l particles. Each circle represents a particle. (b) The same Fock state with the origin shifted to the central site and local densities defined in terms of their deviations from the occupation of the central site, i.e 5. The filled red circles indicate positive deviations while empty red circles indicate negative deviations. In terms of the deviations, the initial profile is anti-symmetric under reflection about the central site. (c) Color-plot of density, $n_l(t)$ and (d) current, $I_l(t)$ in the system as a function of site (link) number and time in under-damped regime with system bath coupling $\epsilon = 0.35g$. The density profile executes a see-saw motion keeping the density of the central site almost constant at short times. The current shows a maximum at the center at short times. At long times, system settles to a density profile decreasing from left to right, governed by the chemical potential gradient in the baths. We use $g = 1$ to set the unit of time, t and l is measured in units of lattice spacing.

where we have reinstated the quantum number of the modes and $\zeta = \pm$ for Bosons (Fermions). $\langle a^\dagger_\gamma a_\delta \rangle_0$ represents the initial correlator calculated in $\hat{\rho}_{0S}$. We note that the first term carries information about initial condition and is not a function of $(t - t')$. This, along with integration limits in the second term break the time translation invariance of the physical observables.

We now illustrate the potency of this formalism by studying the dynamics of current and density profiles in Fermionic/ Bosonic OQS initialized to specific $\hat{\rho}_{0S}$. We consider the microscopic model of a non-Markovian OQS given in Eq. 5.1 where the effects of the

external bath are included through the bath spectral function, given in Eq. 5.7. The motivation for choosing this model is two-fold: (i) to show that our formalism can easily treat non-Markovian dynamics of OQS and (ii) this is an ideal case to study the effects of the initial condition, since the system retains memories over long timescales.

In this case [49], $\Sigma^R(\omega)$ is obtained from Eq. 5.18 while $G^R_O(\alpha, \beta, \omega)$ is given in Eq. 5.14. From these analytical solutions, we obtain the retarded Green's functions in time domain by performing the integral in Eq. 5.29. Finally, the physical Keldysh Green's functions are obtained by plugging $G^R_O(\alpha, \beta, t-t')$ and $\Sigma^K_\alpha(t-t')$ back in eqn. 5.30.

The inherent non-Markovianness of the model is manifested as power law kernels, $\sim (t-t')^{-3/2}$ in $\Sigma^R(t-t')$ and $\Sigma^K_\alpha(t-t')$. This leads to an initial exponential decay in $G^R_O(\alpha, \beta, t-t')$, followed by a long time power law tail $\sim (t-t')^{-3/2}$, appearing at a time scale $\sim t_B/\epsilon^2$, which have been explored in great details in previous sections.

We now apply this formalism to study the transient quantum transport in the non-Markovian OQS. We first consider a linear chain of Bosons of $N = 9$ sites. The system is initialized in a Fock state where the first site has 1 particle, the second site has 2 particles etc,. the l^{th} site has l particles, as shown in Fig. 5.8 (a). This creates a positive density gradient from left to right in the initial state. We couple each site to a bath, with the chemical potential $\mu_l = \mu_1 + \nu(l-1)$, keeping the temperature same for all baths. The chemical potential is set up in such a way that in the steady state, the system will have a positive density gradient from right to left, thus ensuring a non-trivial dynamics in this OQS. We choose the system bath coupling strength to be in the under-damped regime, i.e. $\epsilon/g = 0.35 < 1$, so that we can study the interesting transient quantum dynamics of the OQS. The other parameters are chosen to be $t_B = 2g, T_l = g, \mu_1 = -4.05g$ and $\nu = 0.75g$.

The time-dependent density at site l and the current on the link between the sites l and $l+1$ sites are given by,

$$n_l(t) = \zeta \frac{1}{2}[\mathbf{i}\mathcal{G}^K_{O\rho_0}(l,t,l,t) - 1] \ , \ I_l(t) = g \ Re[\mathcal{G}^K_{O\rho_0}(l,t,l+1,t)], \tag{5.31}$$

with $\zeta = \pm$ for Bosons (Fermions). The change in the density profile with time is plotted in Fig. 5.8(c), while the change in current profile along the links of the system is plotted in Fig. 5.8(d). At short times, we find that the density at the central site, $\bar{n}$ does not change with time, while the profile executes a see-saw type motion with the central site as a

fulcrum, i.e. the local density deviation from $\bar{n}$ increases in magnitude with distance from the central site and is antisymmetric under reflection through this point. To understand the short time quantum dynamics of the system, it is enough to consider the dynamics of a closed system with an odd $(2N+1)$ number of sites (we will comment on the case of even number of sites later). This description will be valid up to a time scale $\sim t_B/\epsilon^2$, when the effect of the bath starts to become prominent. In this case, it is useful to set the origin at the central site, and denote the new co-ordinates by x $(-N \leq x \leq N)$, so that the Hamiltonian has a reflection symmetry about the origin $(x \to -x)$. Further we consider the deviation of the density from $\bar{n}$, $\delta n_x(t)$. The initial profile $\delta n_x(0)$ is antisymmetric under reflection. This is shown in Fig. 5.8(c) in terms of open (negative $\delta n_x(0)$) and filled (positive $\delta n_x(0)$) red circles. Probability conservation of the closed system implies that $\sum_y |G_0^R(x,t;y,0)|^2 = 1$. Using this we get,

$$\delta n_x(t) = \sum_y |G_0^R(x,t;y,0)|^2 \delta n_y(0) \tag{5.32}$$

Here the retarded Green's function G^R does not depend on the initial conditions and exhibits the reflection symmetry of the Hamiltonian, i.e. $G_0^R(x,t;y,0) = G_0^R(-x,t;-y,0)$, while $\delta n_{-y}(0) = -\delta n_y(0)$. It is then easy to see that $\delta n_x(t)$ is antisymmetric under reflection, and hence $\delta n_x(t)$ is 0 for the central site $(x = 0)$. This leads to a piling up of current in the middle at shown in figure 5.8(d). The maximum of the current at the center can be understood from the continuity equation $\partial n/\partial t \sim \nabla.\vec{j}$.We can get further insight for a large system, where the boundaries can be neglected. In this case, $|G_0^R(x,t,y,0)|^2$ is a function of $|x-y|$, and using the anti-symmetry of the initial profile, it can be shown that $\delta n_x(t) \sim x$, i.e it increases in magnitude linearly with the distance from the central site. In presence of a series of baths with a chemical potential gradient, the reflection symmetry is broken, and at long times $\sim t_B/\epsilon^2$, the system gradually settles down to a steady state behaviour. Note that for a system with an even number of sites, the reflection symmetry is about the center of a link. Sites at the two ends of this central link will have a small but non-zero change in density with mutually opposite signs at short times.

We next consider spinless Fermions hopping on a 1D lattice of $N = 20$ sites. We first consider an initial Fock state, where the left half of the lattice (sites 1 to 10) is occupied

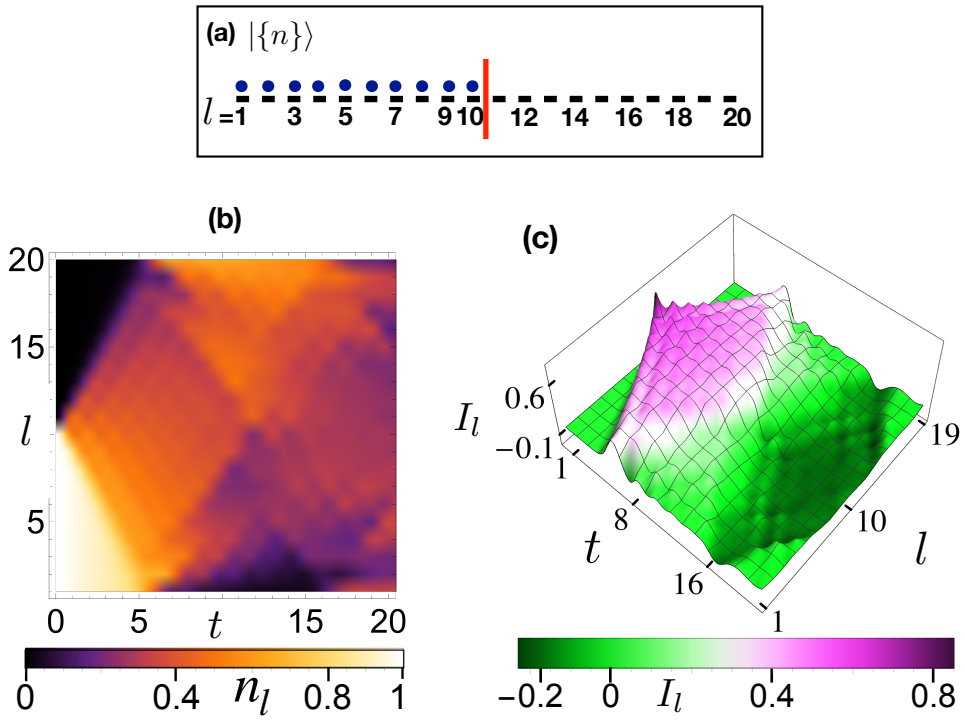

Figure 5.9: Dynamics of a Fermionic OQS starting from arbitrary initial condition. A 20 site linear chain of spin-less Fermions with nearest neighbour tunneling amplitude g is coupled at each site to the baths at temperature $T_l = g$ and the chemical potential $\mu_l = -4.05g$ through a coupling $\epsilon = 0.2g$. (a) The initial state $|\{n\}\rangle$, with left half occupied, the right half empty and a domain wall at the center. Color plot of (b) for density and (c) for current as a function of site (link) number and time for a system starting with $|\{n\}\rangle\langle\{n\}|$. The diamonds are defined by ballistic motion of domain walls and their reflection from the edges. We use $g = 1$ to set the unit of time, t and l is measured in units of lattice spacing.

by particles, while the right half of the system is empty, creating a domain wall in the middle of the lattice, as shown in Fig 5.9 (a). The Fermionic bath parameters are fixed to $T_l = g$ and $\mu_l = -4.05g$ and $\epsilon = 0.2g$, i.e there is no inhomogeneity in the bath parameters. At short times, the effect of the bath can be ignored and the quantum dynamics can be understood by considering the domain wall as a free particle. This particle splits coherently and moves in either direction ballistically with a timescale $\sim g^{-1}$. The effect is seen both in the changes in the density profile (Fig. 5.9 (b)) and in the current profile (Fig. 5.9 (c)), which shows a sudden jump at a site when the particle first passes through that site, creating the initial wedge shaped profiles. The particle is coherently reflected back at the boundary and rephases at a single point [206], creating the diamond shape in the profile. Since the system is underdamped, this cycle is repeated with associated sign change in the

current profile, as seen in Fig. 5.9 (c). Beyond the time scale $\sim t_B/\epsilon^2$, the presence of the bath governs the dynamics; here the current goes to zero and the density profile attains its steady uniform value dictated by the chemical potential in the bath at long times, but the approach to the steady state is governed by the power law of the non-Markovian bath.

5.9 Conclusions

We have used a Schwinger Keldysh field theory to describe the dynamics of a bosonic (fermionic) system coupled linearly to a non-interacting bosonic (fermionic) bath. Integrating out the bath degrees of freedom we obtain the effective dissipative action for the open quantum system. We identify the retarded and Keldysh self energies induced by the bath with the dissipative and noise kernel in a non-local stochastic Schrodinger equation. We show that the presence of non-analyticities in the bath spectral function leads to power law tails in these kernels for both bosonic and fermionic system. The exponent of the power law is governed solely by the nature of the non-analyticity and is independent of the location of the non-analyticity. This leads to retarded and Keldysh Green's functions showing an exponential decay followed by a power law tail with the same exponent as the kernels. The crossover timescale is set by the system bath coupling and decreases quadratically with increasing system bath couplings. It is independent of the temperature and chemical potential of the baths. Thus the non-Markovian dynamics, characterized by the power law tails, are easier to observe in systems with stronger system bath couplings. We note that for bosonic baths with chemical potentials, the spectrum must be bounded from below, ensuring at least one point of non-analyticity, and hence non-Markovian dynamics will be ubiquitous in such systems. The power law tails in the Green's functions lead to corresponding power laws in unequal time correlators like the current-current correlator, which can be measured by noise spectroscopy.

As a concrete example, we consider a linear chain of bosons (fermions) hopping between nearest neighbours, where each site is coupled to an independent bath of non-interacting bosons (fermions). The bath consists of another 1-dimensional lattice of bosons (fermions) with nearest neighbour hopping. We consider a linear coupling between the system and the bath, where the system is coupled to an edge site of the bath. This leads to a bath spectral function which has square root derivative singularities at the band edge of the

bath, leading to a $(t-t')^{-3/2}$ power law in the dissipative and noise kernels. We obtain analytic expressions for the self energies and hence for the exact Green's functions of the open quantum system of 1-d chain, and verify the existence of the power law tails. We use a two site model, with simpler expressions for Green's functions to illustrate the main features, before showing that the features are retained in the exact Green's functions for the full 1-d chain.

We focus our attention on two classes of observables in the open quantum system: equal time correlators like density and current, and unequal time correlators like current-current correlation functions. We first consider a two site system coupled to two baths of same temperature and chemical potential and show that the steady state mode occupation numbers deviate from the thermal equilibrium answers with increasing strength of system bath couplings which cannot be explained by a simple dressing of the system spectrum. For the same system, if the two baths are kept at different chemical potentials, as the system-bath coupling becomes larger than the hopping within the system, both local densities and current through the system deviate from the answers provided by the quantum master equation approach. The densities show a pileup on one site compared to the other, while the current saturates for $\epsilon > g$. We then consider the 1-d chain, with sites coupled to independent baths at the same temperature, but with a chemical potential profile. For a linear variation of μ with space, we find an exponential decay of the current with distance. The density also shows an exponential variation in space on the top of a constant value. The length scale obtained from the decay of the current increases with temperature, with a spatially independent current obtained in the limit of infinite temperature. This behaviour of the current is understood analytically from the exact Green's function obtained for the chain.

We next focus our attention on the unequal time current-current correlators and show that they follow a pattern similar to the Green's functions: a short time exponential decay, followed by a power law tail $\sim (t-t')^{-3}$. This occurs both in the two site system and in the linear chain, and is common to both bosonic and fermionic systems. The timescale for the crossover from exponential to power law decay decreases while the value of the correlator in the power law regime increases with system-bath coupling. These power law tails can then be used to detect non-analyticities in the bath spectral functions, and hence possible

phase transitions in the baths.

We also consider the effect of interactions on the above picture. The power law tails survive to all orders in perturbation theory in the interaction strength. Within a mean field theory for the bosonic two site system, which is equivalent to solving a stochastic Gross Pitaevski equations, we find that the exponential decay slows down and the crossover timescale for observing the power law tails is pushed to larger values. We understand this analytically in terms of the structure of the Green's functions in the system. Increasing interaction strength, should, in principle lead to a larger scattering rate and hence to faster decays, but such two loop processes redistributing energy is not captured within the mean field theory. This needs to be further investigated, although our prediction of a larger crossover timescale should hold in the weakly interacting system.

We finally study the transient quantum transport in the non-Markovian OQS by formulating a new extension of the SK field theory formalism which can include arbitrary initial conditions in the dynamics.

In the first five chapters of the thesis, we have focused to study dynamics of quantum many body systems by using the conventional approach of calculating physical correlation functions of the system. In the next chapter, we turn our attention to a different approach to study quantum systems, namely the *phase space representation of quantum dynamics*. This involves calculating information theoretic measures like Wigner functions and entanglement entropy of the time-evolving density matrix. We construct a new non-equilibrium field theoretic formalism to calculate these quantities in a generic closed/ open quantum system and study their evolution starting from arbitrary athermal initial conditions, both in presence or absence of inter-particle interaction.

Chapter 6

Wigner Function and Entanglement Entropy for Bosons

6.1 Introduction

The Wigner quasiprobability distribution (WQD) is the closest approximation to a "phase-space distribution function" for quantum systems [87, 207, 41], which provides tomographic information about the density matrix of the system. The quantum nature of the system manifests itself throught the fact that the WQD is not positive definite for generic density matrices [208, 209]. Ground states, coherent states and thermal states have positive WQD and are classified as "classical" states, while non-classical states like Fock states have negative values of the WQD. Such states cannot be efficiently sampled using classical Monte Carlo algorithms [89] and can be used as a resource in quantum computing algorithms [90, 210, 211].

Phase space construction of quantum systems in the form of WQD leads to impotant information theoretic quantities like entanglement entropy [42] of a sub-system with the rest of the degrees of freedom. The reduced density matrix of a many-body system is obtained from the full density matrix by tracing out a set of degrees of freedom. The Renyi entanglement entropy of the reduced density matrix is an indicator of quantum separability between the traced out and remaining degrees of freedom in the state of the system [42]. It plays the role of an "inverse participation ratio"; i.e it looks at whether the support of the density matrix is delocalized over all Fock states in the remaining Hilbert space or is finite only over a small cluster of states. It has been used to study quantum

phase transitions [84, 85, 212] and many-body localization transition [43, 86, 213, 214, 215] in interacting disordered systems. Wigner quasiprobability distribution and Renyi entanglement entropy are not mere theoretic constructions since the Wigner function has been recently measured in different single mode quantum systems [216, 217, 91, 218, 219, 220], while the Renyi entropy has been measured in ultracold atomic expetiments [92].

It was shown by K. E. Cahill and R. J. Glauber in Ref. [41] that the Renyi entropy of a density matrix can be written as an integral of the square of its Wigner function. Since then, there have been stream of efforts in calculating WQD [221] and entanglement entropy [222] of (interacting) quantum systems under various approximation. However, in case of (closed) Bosnic systems, the most direct approach of calculating them by diagonalizing the Hamiltonian immediately runs into difficulty as the dimension of the local Hilbert space of Bosons is infinity and hence the diagonalization can not be performed exactly, even for a single mode system. This requires truncation of the Bosonic Hilbert space and severely restricts the calculation to a few mode Bosonic system [223]. The problem of infinitely large Hilbert space in a Bosonic system can be dealt with field theoretic techniques for Bosons which are naturally suited to this case. For a non-interacting system in ground state, the entanglement entropy, defined as, $S^n = Tr[\hat{\rho}^n]$, has been calculated using the replica method of equilibrium field theory [224, 225, 94]. A field theory construction of S^n involves n copies of the path integral corresponding to the matrix element of each powers of $\hat{\rho}^n$ where the consecutive copies of the functional integrals are glued by the appropriate boundary conditions. Implementation of these boundary conditions in this complicated manifold makes this technique hard to apply beyond simple systems.

In this chapter, we develop a new method, based on Schwinger Keldysh field theory, to calculate the Wigner quasi-probability distribution and hence Renyi entanglement entropy for a generic (interacting) open or closed many body Bosonic system undergoing arbitrary non-equilibrium dynamics. The key result of this work is to show that the Wigner characteristic function (WCF), i.e. the characteristic function corresponding to the WQD, is the Schwinger-Keldysh (SK) partition function of the system in the presence of "quantum" sources turned on only at the time of measurement. This relation holds for a generic interacting many-body Bosonic system (open or closed) undergoing arbitrary non-equilibrium dynamics. For a subsystem, the sources need to be turned on only for degrees of freedom

residing in the subsystem. For non-interacting systems (closed or open), we find an analytic expression for the exact time-dependent WCF and WQD in terms of single-particle Green's functions. For interacting systems, we find the WCF in terms of a series involving connected n-particle correlators of the classical fields in the theory. Our formalism can calculate the WCF of a reduced density matrix, and provides a new method to calculate the evolution of Renyi entanglement entropy in many body systems. Note that our formalism is quite different from earlier attempts to calculate WQDs [88, 221, 226, 227, 228] within path integral approaches. Our calculation of Renyi entropy does not require the boundary conditions between the replica fields in a field theory defined on complicated manifolds [224, 229, 94, 225, 230, 231, 232, 233, 84].

We use these results in an extended SK field theory [57] to study the evolution of WQD and Renyi entropy in open quantum systems of one and two bosonic modes, coupled to one or more thermal baths, when the system is initialized to particular Fock states. The negative patches in the WQD, signifying quantum character, vanishes with time as the system thermalizes. We find that the Renyi entropy shows non-monotonic behaviour with time, both within Markovian and non-Markovian dynamics. In a two mode system, where the dynamics is governed by the competition between the incoherent system-bath coupling and the coherent quantum tunneling, we find that the Renyi entropy is anti-correlated with negativity of the Wigner function. We also study the effect of interactions in the system on the evolution of the entanglement entropy and find that repulsive interactions lead to lowering of entropy in the long time limit.

6.2 Wigner Characteristics and Keldysh Partition Function

For a many body bosonic system, the WQD W, and the WCF χ_W of the density matrix $\hat{\rho}(t)$, are defined by [41],

$$\begin{aligned} W(\{\alpha_j\},t) &= \int \prod_j \frac{d^2\beta_j}{\pi^N} \chi_W(\{\beta_j\},t) e^{\sum_j \beta_j^* \alpha_j - \beta_j \alpha_j^*}, \\ \chi_W(\{\beta_j\},t) &= Tr\left[\hat{\rho}(t) e^{\sum_j \beta_j a_j^\dagger - \beta_j^* a_j}\right], \end{aligned} \tag{6.1}$$

where $a_j^\dagger$ is the creation operator for the j^{th} mode. The reduced density matrix of A modes $\hat{\rho}_A(t) = Tr_B \hat{\rho}(t)$ is obtained by tracing over the rest of the modes (B). The reduced

WCF, χ_W^A, of $\hat{\rho}_A(t)$ can be obtained from Eq. 6.1 by restricting β_j s to the set A. The second Renyi entropy, $S^{(2)} = -\log Tr\left[\hat{\rho}_A^2(t)\right]$ can then be calculated from χ_W^A as,

$$S^{(2)} = -\log\left[\int \prod_{i\in A} \frac{d^2\beta_i}{\pi^N} |\chi_W^A(\{\beta_i\}, t)|^2\right]. \tag{6.2}$$

In this section, we will develop a new formulation of calculating the WCF of a Bosonic system by relating it with the Keldysh partition function in presence of a particular combination of the linear sources in the two-contour Keldysh action.

In SK field theoretic approach, the partition function, Z, encodes the time evolution of the many body density matrix, $\hat{\rho}(t) = U(t,0)\hat{\rho}_0 U^\dagger(t,0)$. Z is expressed as a path integral over two copies of fields for each mode, $\phi_+(j,t)$ and $\phi_-(j,t)$, corresponding to the forward and backward evolution along the closed Keldysh contour shown in Fig. 6.1. The partition function in presence of the sources, $J_+(j,t)$ and $J_-(j,t)$ coupled linearly to the fields in the action can be expressed as,

$$Z\left[J_+, J_-\right] = \int D[\phi_+]D[\phi_-] e^{\mathbf{i}[\mathcal{A}_+ - \mathcal{A}_-] + \mathbf{i}\sum_j \int\ dt\ \left[J_+(j,t)\phi_+^*(j,t) + h.c. - J_-(j,t)\phi_-^*(j,t) - h.c.\right]}. \tag{6.3}$$

Here $D[\phi] = \prod_n d\phi^*(t_n)d\phi(t_n)/\pi$ and $\mathcal{A}_\pm$ encodes the evolution of $\hat{\rho}(t)$ along the $\pm$ branches. For a closed non-interacting system evolving with the Hamiltonian, $H_s = \sum_{i,j} h_{ij} a_i^\dagger a_j + h.c.$, $\mathcal{A}_\pm = \sum_{j,j'} \int\ dt \int\ dt' [\phi_\pm^*(j,t)(i\partial_t - h_{ij})\phi_\pm(j't')]$, whereas for an OQS coupled linearly to an external bath, $\mathcal{A}$ will be modified by the corresponding bath induced self-energies. We note that the information about the initial density matrix of the system is incorporated as a boundary term in the action $\mathcal{A}$ (see Eq. 2.4) [95, 49].

To calculate the expectation value, $\langle\mathcal{O}\rangle$ of any observable, $\mathcal{O}$, the standard technique in Keldysh field theory is to additively decompose the operator into $\mathcal{O} = (\mathcal{O}_+ + \mathcal{O}_-)/2$ and write down the path integral for $\langle\mathcal{O}_+\rangle$ and $\langle\mathcal{O}_-\rangle$ by inserting the operator only on the forward branch of the Keldysh contour for $\langle\mathcal{O}_+\rangle$ and on the backward branch for $\langle\mathcal{O}_-\rangle$. Taking derivatives of $Z\left[J_+, J_-\right]$ w.r.t the sources J_+ and J_- accordingly gives the corresponding contributions, $\langle\mathcal{O}_+\rangle$ and $\langle\mathcal{O}_-\rangle$, from $+$ and $-$ branches respectively. Finally the average of these two contributions yields the quantum mechanical average of the physical observable in the density matrix $\hat{\rho}(t)$.

In this section, in order to calculate WCF, $\chi_W(\{\beta_j\}, t) = Tr\left[\hat{\rho}(t)D\right]$, we introduce

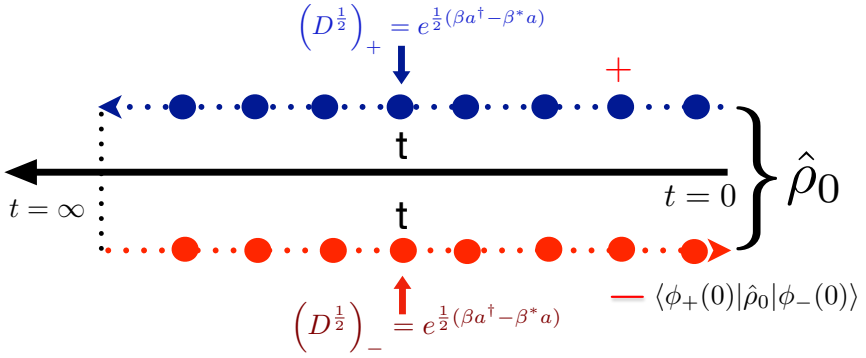

Figure 6.1: Two contour ($\pm$) evolution of the density matrix, $\hat{\rho}(t)$ in SK field theory. For calculating $\chi_W(\beta_j, t)$, the displacement operator, $D(\{\beta_j\})$ is decomposed into $D \to D^{1/2}D^{1/2}$ with each $D^{1/2}$ placed on the $+$ and $-$ contour at time t. $\chi_W(\beta_j, t)$ is the resultant path integral; i.e. $\chi_W(\beta_j, t) = Z[J_{cl} = 0, J_q(j, t') = -\mathbf{i}\beta_j/\sqrt{2}\delta(t - t')]$.

a different technique to calculate the expectation value of the displacement operator, $D(\{\beta_j\}) = e^{\sum_j \beta_j a_j^\dagger - \beta_j^* a_j}$, where the creation and annihilation operator already appear in the exponent. Instead of the additive decomposition of the operator as stated above, we perform a multiplicative decomposition of the displacement operator, $D \to D_+^{1/2} \times D_-^{1/2}$, and insert $D^{1/2}$ symmetrically on both the branches within a single two-contour evolution (see Fig. 6.1) represented by the path integral,

$$\chi_W = Tr\left[U^\dagger(t,0)\; e^{\frac{1}{2}\sum_j \beta_j a_j^\dagger - \beta_j^* a_j}\; U^\dagger(\infty,t)U(\infty,t)\; e^{\frac{1}{2}\sum_j \beta_j a_j^\dagger - \beta_j^* a_j}\; U(t,0)\hat{\rho}_0\right] \tag{6.4}$$

This is the key new ingredient in this work. Comparing equation 6.4 with 6.3, we observe that the insertion of the operators, $D_\pm^{1/2} = e^{\frac{1}{2}\sum_j \beta_j a_j^\dagger - \beta_j^* a_j}$, correspond to turning on a set of sources,

$$J_\pm(j, t') = \mp\mathbf{i}(\beta_j/2)\delta(t - t'), \tag{6.5}$$

coupled linearly to the fields, and evaluating the SK partition function in presence of these sources. Hence, at any instant of time t, $\chi_W(\{\beta_j\}, t)$ is equal to the Keldysh partition function $Z[J_+, J_-]$ if the linear source fields J_+, J_- are identified with the delta-function sources turned on only at the instant t, i.e.

$$\chi_W = Z[J_\pm(j, t') = \mp\mathbf{i}(\beta_j/2)\delta(t - t')] \tag{6.6}$$

This identification becomes further simplified if we work in the rotated cl/q basis, where

$J_{cl}(j,t') = [J_+(j,t') + J_-(j,t')]/\sqrt{2}$ and $J_q(j,t') = [J_+(j,t') - J_-(j,t')]/\sqrt{2}$, and hence,

$$\chi_W(\{\beta_j\},t) = Z\left[J_{cl}=0, J_q(j,t') = -\mathbf{i}\frac{1}{\sqrt{2}}\beta_j\delta(t-t')\right]. \tag{6.7}$$

This is the main result of this work. Here it is important to note that $D^{1/2}$ is not a normal-ordered operator, but in the path integral equation 6.4, the commutation relations between $a_i, a_j^\dagger$, in the expansion $e^{\frac{1}{2}\sum_j \beta_j a_j^\dagger - \beta_j^* a_j}$ are exactly captured by the commutation relations of the operator valued fields $\phi_\pm, \phi_\pm^*$ at equal times. We would also like to point out that the choice of placing $D^{1/2}$ symmetrically on both the branches and hence setting $J_\pm(j,t') = \mp i(\beta_j/2)\delta(t-t')$ is not a unique choice. But it is the most convenient choice of the sources as it leads to $J_{cl}(j,t) = 0$ for all time and $J_q(j,t) = \mathbf{i}\beta_j\delta(t-t')/\sqrt{2}$ couples only to $\phi_{cl}(j,t)$. Within this choice, $\chi_W(\{\beta_j\},t)$ (and also $W(\{\alpha_j\},t)$, $S^{(2)}(t)$) for a generic many body (interacting) system (closed/open) can be completely formulated in terms of only the classical correlation functions at equal time which will be discussed in the next section.

A complex Laplace transform converts $\chi_W(\beta_j)$ to the WQD $W(\alpha_j)$ as shown in Eq. 6.1, and the integration over $\vec{\beta}$ variables forces $\phi_{cl}(j,t) = \sqrt{2}\alpha_j$. $W(\{\alpha_j\},t)$ is thus the partition function summed over field configurations with the boundary condition $\phi_{cl}(j,t) = \sqrt{2}\alpha_j$. Note that the absence of a classical source implies an unconstrained functional integration over the quantum fields. The result derived above applies to generic non-equilibrium dynamics of interacting bosons, since we have not used any assumption about the form of the Keldysh action in deriving Eq. 6.7.

We note that, in this formalism, integrating out a mode without turning on a source is equivalent to tracing over that degree of freedom, while integrating out a mode after turning on a quantum source is equivalent to calculating the WCF. Hence it is straightforward to see that the WCF of the reduced density matrix, χ_W^A, can be obtained by restricting the quantum sources β_j to be turned on only for the modes in A, which are not traced over. This simplification for the reduced WCF, together with Eq. 6.2 allows us to study the evolution of Renyi entropy without considering field theories with complicated boundary conditions [94].

We now use this new formulation of calculating Wigner characteristics functions from Keldysh partition functions to work out the dynamics of WQD and Renyi entropy in a

generic non-interacting/ interacting Bosonic quantum system. Our formalism relates them to the correlation functions in cases of both closed and open quantum system, starting from thermal/ non-thermal $\hat{\rho}_0$, which will be discussed in the subsequent sections. This technique posses significant advantages over the existing methods of calculating WQD and Renyi entropy for Bosonic systems, as (a) it can deal with the dynamics of a system starting from arbitrary non-trivial initial conditions and (b) this non-equilibrium field theoretic technique is easily applicable to many body systems.

6.3 Dynamics Starting from Thermal $\hat{\rho}_0$

In this section, we first focus our attention on non-interacting quantum systems starting from thermal initial density matrix,

$$\hat{\rho}_0 = e^{-\frac{\sum_\nu (\omega_\nu - \mu) a_\nu^\dagger a_\nu}{2T}}.$$

In this case, the path integral expansion of the equation 6.7 can be expressed as,

$$\chi_W(\beta_j, t) = \int D[\phi_{cl}] D[\phi_q] \;\times \; e^{\left[\mathbf{i}\int_0^\infty dt_1 \int_0^\infty dt_2 \sum_{j,j'} \phi^\dagger(j,t_1)\hat{G}^{-1}(j,t_1;j',t_2)\phi(j',t_2) + \mathbf{i}\sum_j \int_0^\infty dt_1 J^\dagger(j,t_1)\phi(j,t_1) + h.c\right]}\Bigg|_{J_{cl}=0, J_q(j,t_1) = -\mathbf{i}\frac{1}{\sqrt{2}}\beta_j \delta(t-t_1)} \tag{6.8}$$

where $\phi^\dagger(j,t) = [\phi_{cl}^*(j,t), \phi_q^*(j,t)]$ and $J^\dagger(j,t) = [J_{cl}^*(j,t), J_q^*(j,t)]$. $\hat{G}^{-1}$ is the inverse Green's function of the standard SK field theory which posses the 2×2 structure in the (cl, q) basis. Here, the Gaussian integration over the fields, ϕ_{cl} and ϕ_q, can then be performed exactly to obtain,

$$\chi_W(\beta_j, t) \;\; = \;\; e^{-\frac{1}{2}\beta_i^* \beta_j \Lambda_{ij}(t)},$$

where $\Lambda_{ij}(t)$ is the one particle Keldysh correlator at equal times, i.e

$$\Lambda_{ij}(t) = \langle \phi_{cl}(i,t) \phi_{cl}^*(j,t) \rangle = \mathbf{i} G_K(i,t;j,t). \tag{6.9}$$

Using this, the WQD and $S^{(2)}$ can be obtained from Eq. 6.1 and are given by,

$$\begin{aligned} W(\alpha_j, t) &= \frac{e^{-\frac{1}{2}\alpha_i^* \alpha_j \Lambda_{ij}^{-1}(t)}}{Det[\hat{\Lambda}/2]} \\ S^{(2)} &= Tr\ log\Lambda_{ij}(t) \end{aligned} \tag{6.10}$$

In this case, the WCF and WQD are both gaussian, while the Renyi entropy matches with earlier results obtained from the equilibrium field theory for a system in ground state using the replica trick [224].

Now, if we consider the system to be a closed quantum system, governed by the Hamiltonian $H_s = \sum_{i,j} h_{ij} a_i^\dagger a_j + h.c.$, the thermal form of Λ_{ij} is obtained from Eq. 3.17, by setting $(2n_\nu + 1) = \coth\left(\frac{\omega_\nu - \mu}{2T}\right)$, i.e

$$\Lambda_{ij} = \sum_\nu \coth\left(\frac{\omega_\nu - \mu}{2T}\right) G^R_{i\nu}(t) G^{*R}_{j\nu}(t). \tag{6.11}$$

where $G^R_{i\nu}(t) = G_R(i, t; \nu, 0)$ and $G_R(i, t; j, t')$ is obtained by inverting, $G_R^{-1}(j, j', t - t') = \delta(t - t')[i\partial_t \delta_{j,j'} - h_{jj'}]$.

We will next extend the above formalism for an open quantum system. We consider a generic OQS model where a non-interacting system of Bosons (H_s) is linearly coupled to a non-interacting Bosonic bath (H_b) via the particle exchange Hamiltonian H_{sb} given by Eq. 5.2. The system bath coupling is turned on at $t = 0$. After tracing out the bath degrees of freedom, the reduced dynamics of the system includes the effect of the bath in the form of the retarded and Keldysh self-energies, $\Sigma^R(t - t')$ and $\Sigma^K_i(t - t')$, given in Eq. 5.12, in the effective action of the system [49]. In this case, Λ_{ij} is modified by the bath induced self-energies (see Eq. 5.30) as,

$$\begin{aligned} \Lambda_{ij} &= \sum_\nu \coth\left(\frac{\omega_\nu - \mu}{2T}\right) G^R_{i\nu}(t) G^{R*}_{j\nu}(t) \\ &+ \mathbf{i} \int_0^t dt_1 \int_0^t dt_2 \sum_m G^R_{im}(t - t_1) \Sigma^K_m(t_1 - t_2) G^A_{mj}(t_2 - t), \end{aligned} \tag{6.12}$$

where, the retarded Green's function of the OQS, $G^R_{i\nu}(t)$, dressed by Σ^R, is obtained from Eq. 5.29.

For an interacting closed system, we use the fact that the logarithm of a partition

function is the generator of connected correlators to write,

$$\chi_W(\beta_j,t) = e^{\sum_n (-1)^n \frac{1}{2^n n!^2} \Lambda^{i_1..i_n}_{j_1..j_n}(t)\beta^*_{i_1}..\beta^*_{i_n}\beta_{j_1}..\beta_{j_1}}, \tag{6.13}$$

where $\Lambda^{i_1..i_n}_{j_1..j_n}(t) = \langle \phi_{cl}(i_1,t)..\phi_{cl}(i_n,t)\phi^*_{cl}(j_1,t)..\phi^*_{cl}(j_n,t)\rangle_C$ is the connected n particle equal time correlator of the classical fields for $n \neq 1$ and $\Lambda^i_j = \Lambda_{ij}$. This exact relation between χ (and hence $S^{(2)}$) and the standard correlation functions is the starting point for making different approximations for entanglement entropy of interacting systems.

We will next extend this new formulation of calculating WCF and hence WQD and $S^{(2)}$ from SK field theory in the dynamics of a system starting from arbitrary athermal $\hat{\rho}_0$.

6.4 Dynamics Starting from Arbitrary Athermal $\hat{\rho}_0$

In this section, we focus on the case where the system is initialized in Fock states where the dynamics can be treated within a recent extension of SK theory [57], developed in chapter 3. We consider a many body system starting from an initial density matrix, $\hat{\rho}_0 = |\{n\}\rangle\langle\{n\}|$ where $|\{n\}\rangle = \prod_\nu |n_\nu\rangle$ is a configuration in the Fock space. The partition function in presence of the sources including the boundary term can be written as,

$$Z_\rho[J_+,J_-] = \int D[\phi_+]D[\phi_-]e^{\mathbf{i}[\mathcal{A}_+-\mathcal{A}_-]+\mathbf{i}\sum_j \int dt \left[J_+(j,t)\phi^*_+(j,t)+h.c.-J_-(j,t)\phi^*_-(j,t)-h.c.\right]} \times \langle\phi_+(0)|\hat{\rho}_0|\phi_-(0)\rangle \tag{6.14}$$

As we discussed in chapter 3, in the extended SK field theory, the matrix element of $\hat{\rho}_0$ can be written as a term in the action where a source u_ν, turned on only at $t=0$, is coupled to the bi-linears of the initial fields $\phi_+(\nu,0)\phi_-(\nu,0)$. At this point, we would like to note the difference between the quadratic source u_ν, turned on only at the initial time $t=0$, and the linear sources, $J_\pm(j,t') = \mp i(\beta_j/2)\delta(t-t')$, turned on only at the time measurement t of WQD. Here, the role of the quadratic source, $\vec{u}$ is to incorporate the initial non-thermal density matrix, whereas the linear sources $J_\pm(j,t)$ are turned on to measure $\chi_W(\{\beta_j\},t)$ at time t.

The physical partition function, $Z_\rho[J_+(j,t),J_-(j,t)]$ corresponding to the initial density matrix, $\hat{\rho}_0$ is computed in a two step process: first we will calculate the partition function $Z[J_+(j,t),J_-(j,t),\vec{u}]$ in presence of the initial source $\vec{u}$ and then by taking its appropriate

number of derivative w.r.t $\{u_\nu\}$, dictated by $\hat{\rho}_0$, we will get Z_ρ given by equation 6.14. The calculation of WCF, which is related to Z_ρ via Eq. 6.6 or 6.7, also follows the two step process stated above for the partition function: first we will calculate an intermediate quantity, $\chi_W(\beta_j, t, \vec{u})$ that is the partition function in presence of both the linear quantum sources β_j, turned on at time of measurement t, and the initial bilinear sources u_ν turned on at $t = 0$, i.e

$$\chi_W(\beta_j, t, \vec{u}) = Z[J_\pm(j, t') = \mp i(\beta_j/2)\delta(t-t'), \vec{u}] = Z\left[J_{cl} = 0, J_q(j, t') = -\mathbf{i}\frac{1}{\sqrt{2}}\beta_j\delta(t - t'), \vec{u}\right]. \tag{6.15}$$

The physical WCF corresponding to the particular initial state is then obtained from,

$$\chi_W(\{\beta_j\}, t) = \prod_\nu \frac{1}{n_\nu!}\left(\frac{\partial}{\partial u_\nu}\right)^{n_\nu} \chi_W(\beta_j, t, \vec{u})\Big|_{u=0}. \tag{6.16}$$

We will now illustrate the detailed procedure of calculating $\chi_W(\beta_j, t, \vec{u})$ and hence $\chi_W(\{\beta_j\}, t)$ for a generic quantum many body system (closed/open), starting from arbitrary $\hat{\rho}_0$, both in absence and in presence of inter-particle interaction within the scope of the new SK field theory formalism developed in chapter 3 [49].

6.4.1 Non-interacting System

We first consider a non-interacting system of bosons where $\chi_W(\beta_j, t, \vec{u})$ can be calculated from the path integral expansion of $Z[J, \vec{u}]$, similar to Eq. 6.8. The cost we need to pay to include arbitrary initial conditions in the dynamics is that the inverse Green's functions, $\hat{G}^{-1}$ now depend explicitly on the initial sources, $\vec{u}$ as discussed in section 3.4 in great details. The Gaussian integrations over the ϕ_{cl} and ϕ_q fields can be done exactly to obtain,

$$\begin{aligned}\chi_W(\beta_j, t, \vec{u}) &= \prod_\kappa \left(\frac{1}{1-u_\kappa}\right) exp\left[-\frac{1}{2}\beta_i^*\beta_j\ \mathbf{i}G_K(i, t; j, t; \vec{u})\right] \\ &= e^{-\frac{1}{2}\beta_i^*\beta_j\Lambda^0_{ij}(t)} \prod_\nu \frac{e^{-\beta_i^*\beta_j\Lambda^\nu_{ij}(t)\frac{u_\nu}{1-u_\nu}}}{1-u_\nu}\ ,\end{aligned} \tag{6.17}$$

where $\Lambda^0_{ij}(t) = \langle\phi_{cl}(i, t)\phi^*_{cl}(j, t)\rangle_0 = \mathbf{i}G_K(i, t; j, t; \vec{u} = 0)$ is the equal time classical correlator in a system that starts from the vacuum state with 0 particles, and $\Lambda^\nu_{ij}(t) = G^R_{i\nu}(t)G^{R*}_{j\nu}(t)$. After taking $\vec{u}$ derivatives [234], we obtain the closed form analytical expression for the

physical WCF as

$$\chi_W(\beta_j, t) = e^{-\frac{1}{2}\beta_i^*\beta_j\Lambda_{ij}^0(t)} \prod_\nu L_{n_\nu}\left[\beta_i^*\beta_j\Lambda_{ij}^\nu(t)\right] \tag{6.18}$$

where $L_n(x)$ is the Laguerre polynomial of order n.

We note that our formalism can treat open and closed quantum systems on equal footing, although detailed expression for Λ will change. For a closed system,

$$\Lambda_{ij}^0(t) = \sum_\nu G_{i\nu}^R(t)G_{j\nu}^{R*}(t) = \delta_{ij}, \tag{6.19}$$

obtained from orthonormality relations of the eigenfunctions, while for an OQS,

$$\Lambda_{ij}^0(t) = \sum_\nu G_{i\nu}^R(t)G_{j\nu}^{R*}(t) + \mathbf{i}\int_0^t dt_1 \int_0^t dt_2 \sum_m G_{im}^R(t-t_1)\Sigma_m^K(,t_1-t_2)G_{mj}^A(t_2-t) \tag{6.20}$$

.

Using this formulation, we now study the evolution of WQD and Renyi entropy in the transient dynamics of a OQS which is initialized in Fock states (with negative WQD and zero entropy) and evolve to a thermal state (with positive definite WDQ and non-zero entropy) due to coupling to thermal baths. Our analytical results provide useful insights in their dynamics.

Evolution of WQD and $S^{(2)}$ in OQS:

In this section, for the sake of concreteness, we consider a specific model of open quantum system where each site of the system is coupled to the first site of a semi-infinite bath of non-interacting Bosons hopping along the $1D$ chain with the tunneling strength t_B. The microscopic form of H_b and H_{sb} are given in Eq. 5.1. In this model, the bath spectral function, given in Eq. 5.7, shows a square root derivative singularity at the two band edges $\omega = \pm 2t_B$. This non-analyticity in $\mathcal{J}(\omega)$ renders the reduced dynamics of the system to be non-Markovian which has been explored in great details in chapter 5 [49].

We first consider a OQS consisting of single mode harmonic oscillator, governed by $H_s = \omega_0 a^\dagger a$, linearly coupled to the bath with strength, ϵ. The system is initialized in the number state $\rho_0 = |n\rangle\langle n|$. In this case, $\Lambda^0(t)$ changes from 1 at $t = 0$ to a finite value determined by the bath parameters, while $\Lambda(t) = |G^R|^2$ decays from 1 to 0 at long

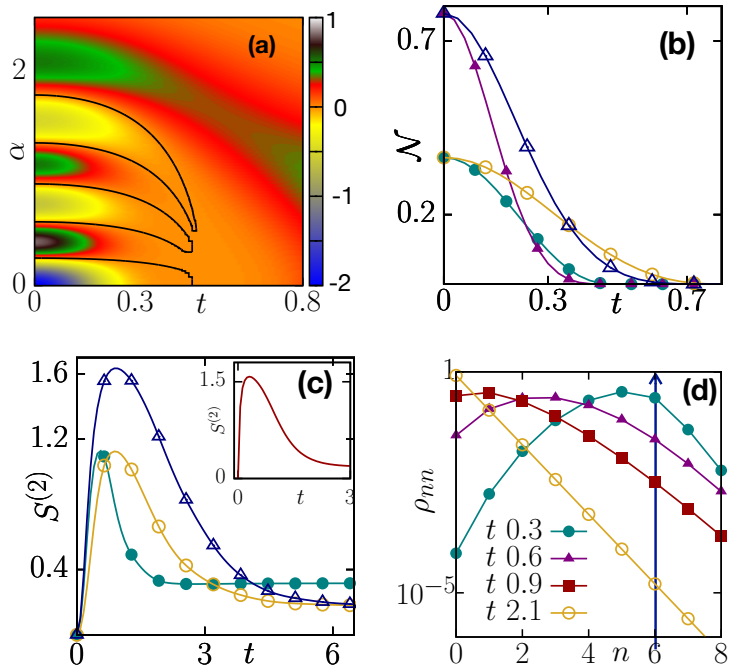

Figure 6.2: (a)- (d) Evolution of a single mode non-interacting system coupled to a bath ($T = 1$, $\mu = -4.05$) starting from a Fock state: (a) The WQD, $W(\alpha, t)$ is shown in the $|\alpha| - t$ plane as a density plot. The system starts from the state $|n = 5\rangle$. The negative patches present at the initial time, indicating a non-classical state, shrinks and vanishes as the system thermalizes to a classical state. (b) Negativity, $\mathcal{N}$ of WQD is plotted with t for two different initial conditions $|n = 6\rangle$ (triangles) and $|n = 2\rangle$ (circles). In each case the open symbols correspond to a system bath coupling $\epsilon = 1$, and the closed symbols are for $\epsilon = 1.5$. Increasing ϵ makes the decay of $\mathcal{N}$ faster in both cases. For same ϵ, the negativity for $n = 6$ starts at higher value but decays faster than that for $n = 2$. (c) Renyi entropy, $S^{(2)}(t)$ vs t for $\epsilon = 1$ for $n = 6$(open triangles) and $\epsilon = 1, n = 2$ (open circles), and $\epsilon = 1.5, n = 2$ (closed circles). Inset shows evolution of $S^{(2)}$ for Markovian dynamics. $S^{(2)}$ varies non-monotonically with t with a peak location at $\sim t_B/\epsilon^2$ and a long time value independent of initial conditions in all cases. (d) $\hat{\rho}_{nn}(t)$ vs n at different times for $\epsilon = 1.5$ starting from $n = 6$. The distribution of ρ_{nn} broadens initially, leading to increasing $S^{(2)}$. Later, ρ_{nn} for larger n falls off to attain its thermal form, leading to shrinking of the distribution and negative $dS^{(2)}/dt$. $t_B = 2$ sets the unit of energy for all plots.

times. The decay is exponential at short times upto $t \sim t_B/\epsilon^2$, and have a $t^{-3/2}$ power law tail for the spectral density we use. However, most interesting features discussed here are insensitive to the non-Markovian nature of the dynamics.

Using the new SK field theory formulation, we obtain closed form analytical solution of WQD, $W(|\alpha|, t)$, given by,

$$W(\alpha, t) = \frac{2(\tilde{\Lambda} - \Lambda)^n}{(\Lambda^0)^{n+1}} e^{-\frac{2|\alpha|^2}{\Lambda^0}} L_n \left[\frac{2|\alpha|^2}{\Lambda^0} \frac{2\Lambda}{\Lambda - \tilde{\Lambda}} \right], \tag{6.21}$$

where $\tilde{\Lambda}(t) = \Lambda^0(t) - \Lambda(t)$. $W(\alpha, 0) = 2e^{-2|\alpha^2|} L_n(4|\alpha^2|)$ has n zero crossings in $|\alpha|$ resulting in alternating positive and negative patches. Here, $\Lambda(t)$ controls the decay of the initial distribution function, whereas $\tilde{\Lambda}(t)$ is the stochastic contribution from the bath. Since $L_n(x) > 0$ for $x < 0$, all the negative patches in W disappear simultaneously when $\tilde{\Lambda}(t) > \Lambda(t)$ turns negative, i.e. when the stochastic contribution from the bath overwhelms the remnants of the initial quantum state. We consider a system with $\omega_0 = -1$ and a bath with $T = 1$ and $\mu = -4.05$ where bath hopping scale, $t_B = 2$ sets the units. Fig. 6.2(a) shows a density plot of $W(\alpha, t)$ in the $|\alpha| - t$ plane for a system starting in the $n = 5$ state. The 3 negative patches shrink in size with time until they simultaneously disappear around $t = 0.45$. In the long time limit, the system thermalizes and a gaussian WQD is recovered.

A quantitative measure of the "non-classicality" is the negativity,

$$\mathcal{N}(t) = \int d^2\alpha \left(|W(\alpha, t)| - W(\alpha, t) \right) / (4\pi), \tag{6.22}$$

which measures the area in the complex α plane over which the WQD is negative. In Fig 6.2(b) $\mathcal{N}$ is plotted as a function of t for two different initial conditions, $n = 2$ and $n = 6$, at two different system-bath coupling strength $\epsilon = 1, 1.5$. The system has more non-classicality for higher n as the number of negative patches increase, but the negativity also decays faster in this case. With increasing ϵ, the negativity falls off faster.

We use Eq.s 6.2 and 6.18 to calculate the Renyi entropy,

$$S^{(2)} = -log \left[\frac{(-1)^n \ {}^{2n}C_n \ [\tilde{\Lambda}]^{2n}}{[\Lambda^0]^{2n+1}} {}_2F_1 \left[-n, -n, -2n, \frac{-\Lambda^0[\Lambda - \tilde{\Lambda}]}{[\tilde{\Lambda}]^2} \right] \right] \tag{6.23}$$

where ${}_2F_1$ is the hypergeometric function. Fig 6.2(c), shows $S^{(2)}(t)$ after tracing out the bath degrees of freedom, for two different initial conditions, $n = 2$ and $n = 6$ at $\epsilon = 1$. In both cases, we see a non-monotonic time dependence of $S^{(2)}$, with a peak at a timescale $\sim t_B/\epsilon^2$, and a fixed long time limit indicating the erasure of initial state memories. Increasing ϵ to 1.5 leads to a faster decay to a different equilibrium.

The non-monotonicity of $S^{(2)}$ with time is a generic feature of both Markovian and non-Markovian dynamics. To see this, we consider a Markovian bath model, with the generic form of the time-local dissipation and noise kernel governing the dynamics that are

given by,

$$\Sigma_R^B(t-t') = \mathbf{i}\gamma\delta(t-t') \ , \ \Sigma_K^B(t-t') = \mathbf{i}m_q\delta(t-t')$$

These lead to exponentially decaying Green's functions,

$$\begin{aligned} G^R(t-t') &= -\mathbf{i}\Theta(t-t')e^{-\gamma(t-t')-\mathbf{i}\omega_0(t-t')} \\ \Lambda^0(t) &= (1+m_q)G^R(t)G^A(t') - m_q e^{-\gamma|t-t'|-\mathbf{i}\omega_0(t-t')} \end{aligned} \tag{6.24}$$

where m_q is related to the steady state density in the system and hence dictated by the temperature and the chemical potential of the bath. Here, $\gamma > 0$ gives the dissipation in the Markovian dynamics. $S^{(2)}$ in case of the single mode OQS starting from the Fock state, for this Markovian bath model is plotted as a function of t in inset of Fig 6.2(c), which also exhibits the non-monotonic feature with time.

To gain insight into the non-monotonicity of $S^{(2)}$, we construct the instantaneous reduced density matrix $\hat{\rho}_s(t)$ which is diagonal in the number basis. We constructed the matrix elements, $\rho_{nn}(t)$ from WCF through the following equation [41],

$$\begin{aligned} \chi_W(|\beta|,t) &= \sum_n \rho_{nn}(t) \ \langle n|e^{\beta \ a^\dagger - \beta^* \ a}|n\rangle \\ \rho_{nn}(t) &= \frac{1}{\pi}\int d^2\beta \ \chi_W(|\beta|,t) \ \langle n|e^{\beta \ a^\dagger - \beta^* \ a}|n\rangle \end{aligned} \tag{6.25}$$

where $\langle n|e^{\beta \ a^\dagger - \beta^* \ a}|n\rangle$ is obtained to be,

$$\langle n|e^{\beta \ a^\dagger - \beta^* \ a}|n\rangle = e^{-\frac{1}{2}|\beta|^2} \ L_n[|\beta|^2] \tag{6.26}$$

This leads to the closed form analytic answer for the matrix elements, $\rho_{nn}(t)$, from a system starting from a Fock state $|N\rangle\langle N|$, given as,

$$\rho_{nn}(t) = {}^{N+n}C_n \frac{2\left(\Lambda_0+1-2\Lambda\right)^N \ \left(\Lambda_0-1\right)^n}{\left(\Lambda_0+1\right)^{N+n+1}} \ {}_2F_1\left[-n,-N,-N-n,\frac{\left(\Lambda_0+1\right)\left(\Lambda_0-1-2\Lambda\right)}{\left(\Lambda_0-1\right)\left(\Lambda_0+1-2\Lambda\right)}\right]. \tag{6.27}$$

In Fig 6.2(d), we plot the time evolution of the matrix elements , ρ_{nn} for a system starting at $n = 6$. At $t = 0$, $\rho_{nn} = \delta_{n,6}$ and hence $S^{(2)} = 0$. As time evolves,the distribution of ρ_{nn}

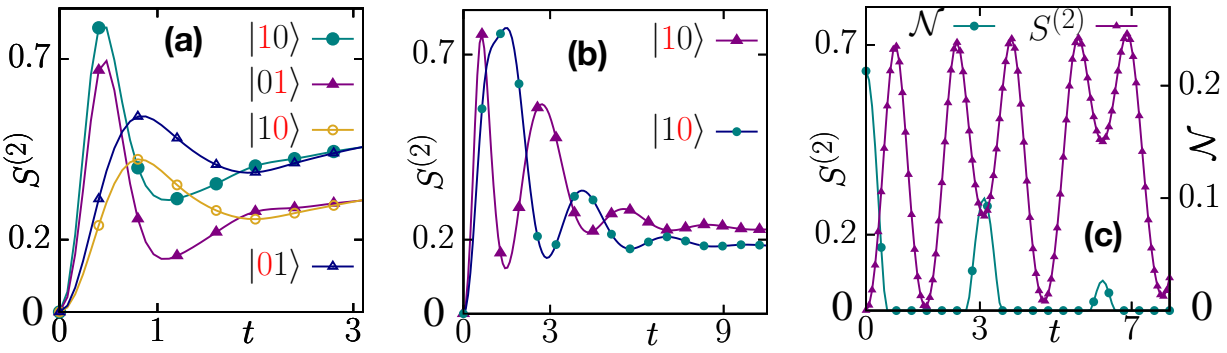

Figure 6.3: (a) $S^{(2)}$ vs t in a 2−mode system coupled to two baths ($T_L = T_R = 1$, $\mu_L = -4.05, \mu_R = -10.05, \omega_0 = -1.5$) for $\epsilon = 1.5 > g = 1$ (overdamped) and (b) $\epsilon = 0.8 < g = 1.0$ (under-damped) for different initial states, marked in the graph. The bath and the site index shown in black is traced out to obtain $S^{(2)}$. (c) $\mathcal{N}$ and $S^{(2)}$ for a system with $\epsilon = 0.2$. The negativity shows a peak at alternate dips of $S^{(2)}$, where the density matrix comes close to $n = 1$ Fock state. $t_B = 2$ sets the units for all plots.

broadens due to stochastic exchange with bath, giving rise to an increase of $S^{(2)}$ with t. At later times, the entropy decreases as the distribution narrows down to reach an exponential form.

While the single mode system illustrates the effect of incoherent coupling to the bath, a more interesting dynamics occurs in a two mode system, where the coherent intermode coupling competes with the incoherent coupling to the bath. We consider a system of two sites (left (L) and right (R)) with the Hamiltonian $H_s = \omega_0(a_L^\dagger a_L + a_R^\dagger a_R) - g(a_L^\dagger a_R + h.c)$, where g is the coherent tunneling matrix element. The two sites are linearly coupled to two baths with the same temperature T, but different chemical potentials μ_L and μ_R. This leads to a steady state with a finite current flowing through the system in the long time limit. We study the evolution of $S^{(2)}$ in the dynamics of the OQS when the system starts from $|10\rangle$ and $|01\rangle$. The subsystem for calculating $S^{(2)}$ is obtained by tracing out the bath and one site of the system. We see that at short times, the behaviour of $S^{(2)}$ depends on whether the site with the initial particle is traced out or not. For example, in Fig 6.3 (a), the curves for the system starting from $|10\rangle$ with R traced out (closed circles) and $|01\rangle$ with L traced out (closed triangles) follow each other at short times. Similarly, curves for system starting at $|10\rangle$ with L traced out (open circles) and $|01\rangle$ with R traced out (open triangles) follow each other at short times. At large times, this initial memory is erased and $S^{(2)}$ simply depends on whether L or R is traced over. This is because the chemical

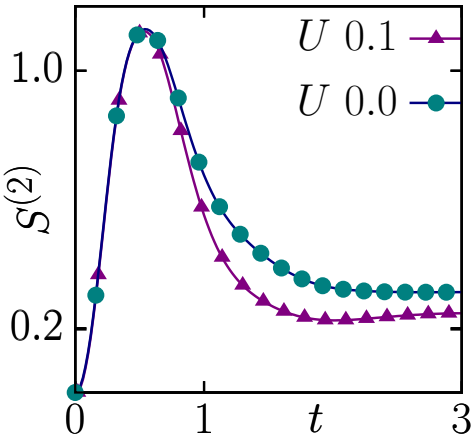

Figure 6.4: (e) $S^{(2)}$ vs t in a single mode OQS in presence of repulsive interaction, $U = 0.1$ starting from $n = 2$ with $\epsilon = 1.5$. Repulsive interaction leads to faster decay of $S^{(2)}$ compared to the non-interacting one, leading to a steady state with lower entropy. The parameters which are not specified here are taken to be same as Figure 6.2.

potentials in the baths break the $L - R$ symmetry of the problem. Fig. 6.3(c) plots the evolution of $S^{(2)}$ and the negativity of the Wigner function of the reduced ρ for the left site in the under-damped limit. The system comes close to a Fock state at the minima of the entropy oscillations. When the corresponding state is $|0\rangle$, the negativity is zero, since the ground state has positive definite Wigner function, while the negativity shows a pronounced peak at alternate $S^{(2)}$ minima, when the system comes very close to $|1\rangle$.

6.4.2 Interacting System

In this section, we will extend the SK field theory formalism to calculate WCF and hence $S^{(2)}$ in presence of interparticle interaction in the system. Here, we will restrict the calculation to the case of a single mode OQS starting from the Fock state, $\rho_0 = |n\rangle\langle n|$, where an interaction term, $H_{int} = Ua^\dagger a^\dagger aa$ (also called Kerr non-linearity) is added to the Hamiltonian of the system, i.e

$$H_s = \omega_0 a^\dagger a + Ua^\dagger a^\dagger aa. \tag{6.28}$$

The bath is still assumed to be non-interacting and hence a linear system-bath coupling leads to an effective dynamics of the system with an added interaction term in the action,

$$\mathcal{A}_{int} = -U \int dt \Big[\phi^*_{cl}(t)\phi_{cl}(t)\Big(\phi^*_{cl}(t)\phi_q(t) + h.c\Big) + \phi^*_q(t)\phi_q(t)\Big(\phi^*_q(t)\phi_{cl}(t) + h.c\Big)\Big] \quad (6.29)$$

In order to incorporate the effects of the non-trivial initial conditions in the dynamics, we will extend the definition of one particle Green's function, $G_K(t,t,u)$ to introduce the connected m-particle Green's function of the classical fields at equal time t as,

$$\Lambda^{(m)}(t,u) = \mathbf{i}^m G^{(m)}_K(t,t,u) = (-1)^m \left. \frac{\partial^{2m} \log\ Z[J_{cl}, J_q, u]}{\partial J_q(t)..\partial J_q(t)\partial J^*_q(t)...\partial J^*_q(t)} \right|_{J_{cl/q}=0} \quad (6.30)$$

Using the fact that logarithm of partition function, $Z[J_{cl}, J_q, u]$ is the generator of the connected correlator and the relation between WCF and the partition function (Eq. 6.7), we write the WCF in presence of the initial source, u for an interacting system as,

$$\chi_W(\beta_j, t, u) = e^{\sum_{m=1}^{\infty} \frac{(-1)^m}{2^m\ m!m!} \Lambda^{(m)}(t,u)\ |\beta|^{2m}} \quad (6.31)$$

We will approximate the series in the exponent by truncating it at the order $m = 2$, i.e. keeping upto $2-$ particle connected Green's function in the exponent. This approximation leads to analytical solution for Renyi entanglement entropy given by,

$$\begin{aligned} S^{(2)} &= -\log\left[2\int_0^\infty d|\beta|\ |\beta|\ e^{-\Lambda^{(2)}(t,0)|\beta|^2 + \frac{1}{4}\Lambda^{(4)}(t,0)|\beta|^4}\right]\ \mathcal{M}\left(|\beta|^2\right) \\ &= -\log\left[\sum_p a_p \frac{2^{\frac{p+1}{2}}\Gamma(p+1)}{[-\Lambda^{(2)}(t,0)]^{\frac{p+1}{2}}}\ \mathcal{H}_{p+1}\left(\frac{\Lambda(t,0)}{\sqrt{-2\Lambda^{(2)}(t,0)}}\right)\right] \end{aligned} \quad (6.32)$$

where $\mathcal{H}$ is the Hermite polynomial and $\mathcal{M}\left(|\beta|^2\right) = \sum_p a_p |\beta|^{2p}$ is a polynomial in $|\beta|^2$, which is brought down by the n^{th} order derivative w.r.t. u in $\chi_W(\beta, t)$ given by equation 6.16.

We evaluate the effects of the interaction on the one and two particle Green's function in perturbation theory upto $\mathcal{O}(U^2)$ by evaluating the Feynman diagrams shown in Fig. 6.5 and Fig. 6.6. We calculate the time dependent Renyi entropy of this system after integrating out the bath. The time evolution of $S^{(2)}$ for interacting and non-interacting

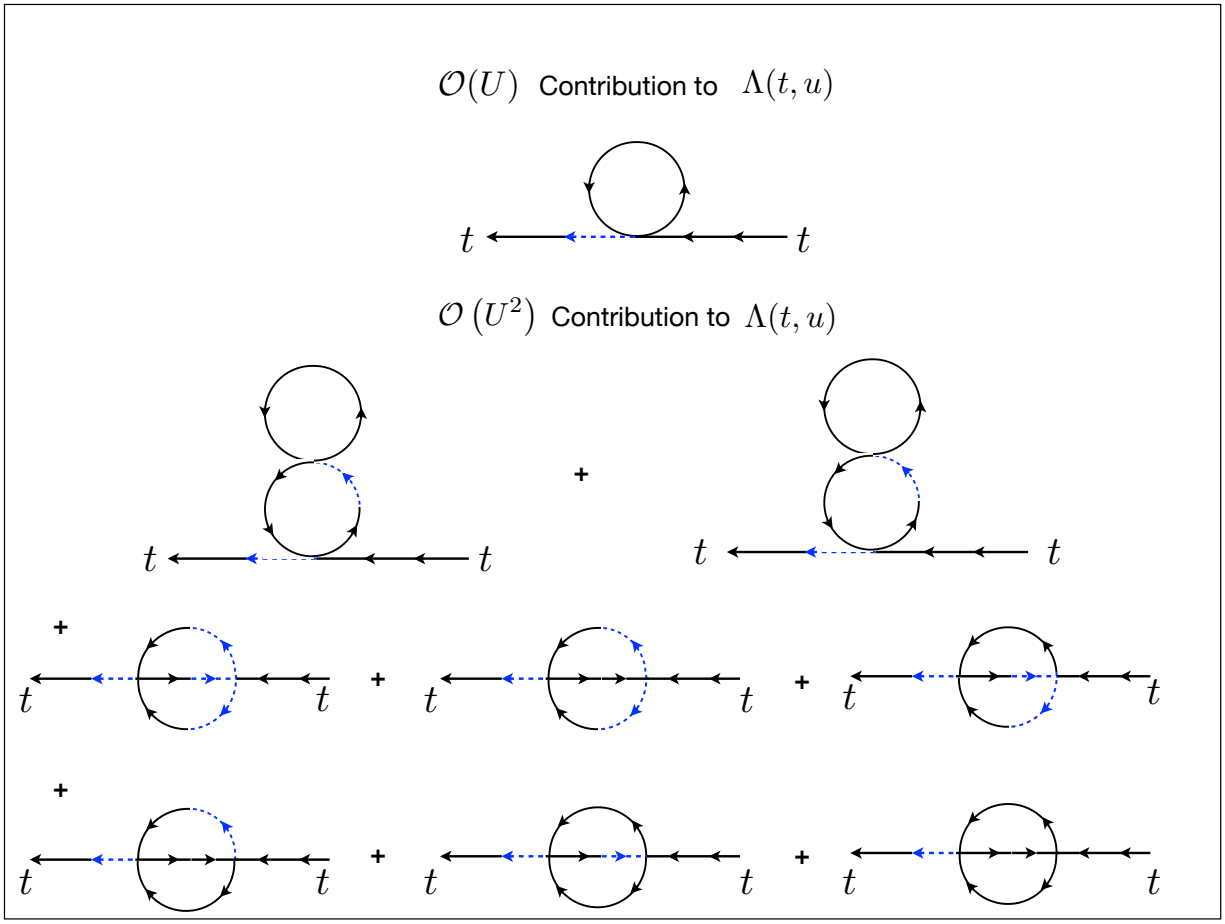

Figure 6.5: Feynman Diagrams for $\Lambda(t,u)$ upto $\mathcal{O}(U^2)$. The diagrams are evaluated in perturbation theory where all the lines represent non-interacting Green's functions for the OQS in presence of the initial source, i.e. $G_{R/A}(t-t')$ and $G_K(t,t',u)$. We note that all the external lines in the diagrams start from and end at the time of measurement t.

systems are plotted together in Fig. 6.4. The repulsive interaction reduces the long time value of the entanglement entropy and leads to a faster decay of $S^{(2)}$ from its peak value. In the regime of U used in our calculation, we obtain $\Lambda^{(2)}(t,0) < 0$, which regulates the integral in equation 6.32.

Our analysis thus provides promising directions in constructing a controlled diagrammatic expansion to calculate Renyi entropy in an interacting system from non-equilibrium field theory approach. In order to extend this analysis beyond perturbation theory and include the effects of higher order connected Green's functions in the dynamics, we need to deal with the regulation of the series in the exponent in Eq. 6.32 carefully. Currently, this is a topic under investigation and will be part of future studies.

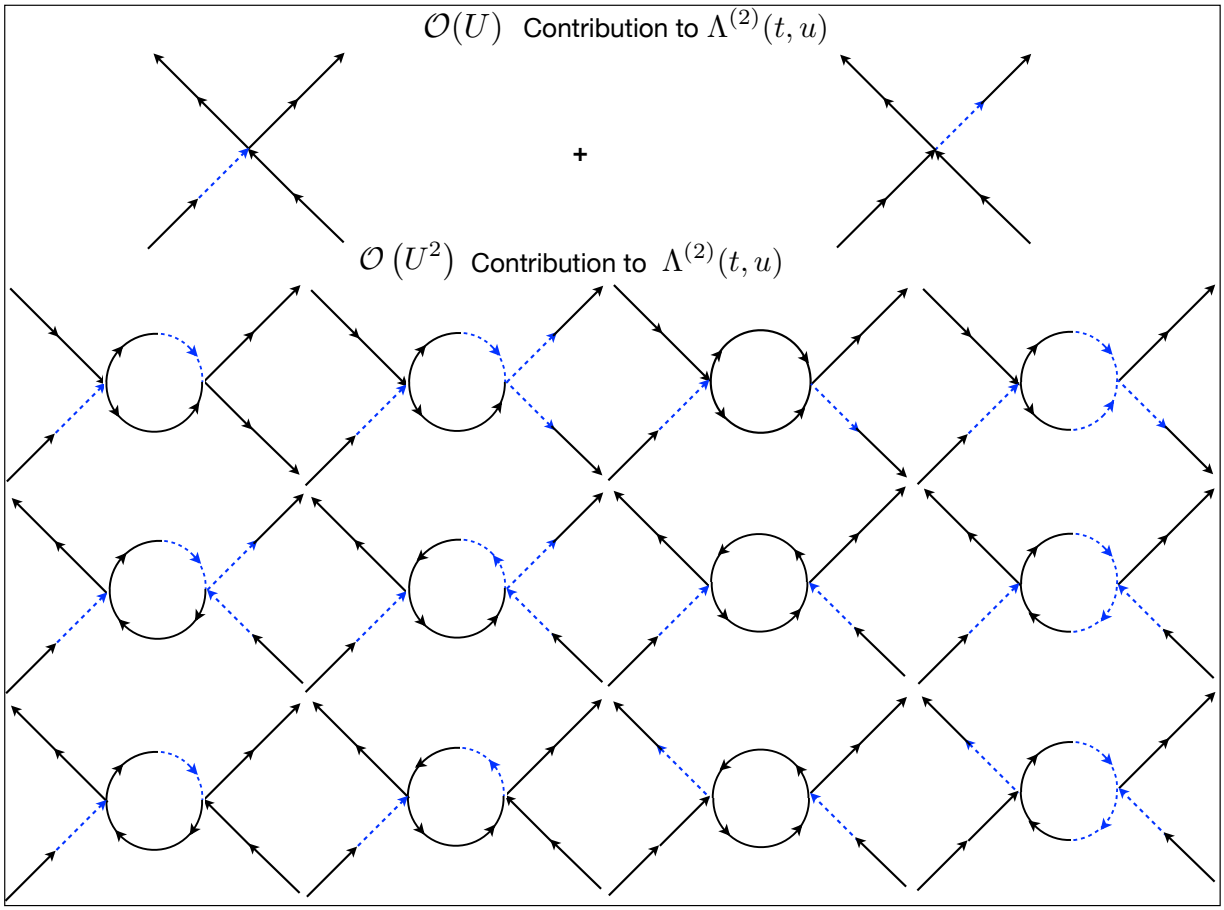

Figure 6.6: Feynman Diagrams for $\Lambda^{(2)}(t,u)$ upto $\mathcal{O}(U^2)$. In addition to the 2nd order diagrams for $\Lambda^{(2)}$ shown in (b), there are additional diagrams (not shown in the figure) which can be obtained from the first order diagrams for $\Lambda^{(2)}$ by adding first order corrections to any one of the Green's functions. The diagrams are evaluated in perturbation theory where all the lines represent non-interacting Green's functions for the OQS in presence of the initial source, i.e. $G_{R/A}(t-t')$ and $G_K(t,t',u)$. We note that all the external lines in the diagrams start from and end at the time of measurement t.

6.5 Discussion

In this chapter, we have provided a new non-equilibrium field theoretic way of calculating the evolution of the Wigner function and entanglement entropy of a many body interacting bosonic system (open or closed) undergoing non-equilibrium dynamics starting from arbitrary initial conditions. Thermal equilibrium forms a special case of our approach. Our method works equally well for the full density matrix of the system as well as a reduced density matrix of a subsystem. Hence it can be used to calculate the Renyi entropy of a subsystem without the use of replica methods and associated complicated boundary conditions. Our work substantially expands the class of systems for which Wigner function

and Renyi entropy can be calculated from field theoretic approaches, and provides a much simpler pathway to calculate entanglement entropy in these systems. The formalism can be used to study entanglement entropy in many other contexts including quantum phase transitions and many body localization transitions.

The key result of this work is to identify the characteristic function of the Wigner quasiprobability distribution (the Wigner characteristic function) as the Keldysh partition function of the system with a quantum source function turned on only at the time of measurement. For a subsystem, the sources need to be turned on only for degrees of freedom residing in the subsystem. We use this technique to provide exact analytical expressions for the time evolution of Winger function and Renyi entanglement entropy of a Bosonic system undergoing non-equilibrium dynamics starting from arbitrary initial conditions in terms of single-particle Green's functions for non-interacting system and connected multi-particle Green's functions for an interacting system. We applied this new formalism to study the evolution of Winger function and Renyi entanglement entropy in transient dynamics of an non-interacting/ interacting open quantum system (OQS). We make definite predictions of anti-correlation between negativity of Wigner function and Renyi entropy for a 2 mode open quantum system, which can be tested by experiments.

To our knowledge this is the first work which cleanly relates the Wigner function (rather its characteristic function) to a field theoretic quantity (i.e. the partition function in presence of certain sources), thus providing a way to calculate this quantity in Bosonic systems, where the size of the Hilbert space precludes more direct methods of calculation. Our formalism is equally applicable to equilibrium as well as non-equilibrium systems, to Markovian and non-Markovian dynamics for open quantum systems. This is also the starting point of making different approximations for interacting systems. In this way, our work opens up a new direction, where this formulation can be applied to large number of specific systems with their associated approximations to understand evolution of quantum many body systems in great details.

Another important aspect of our formalism is that this is not restricted only to the systems starting from Gaussian initial state, rather it allows us to study evolution of Wigner function and entanglement entropy of a system starting from arbitrary initial density matrix. Hence, most of the interesting and physically relevant situations, where

the system starts from a nom-thermal initial state and either approach towards a thermal state or does not, can now be studied within the scope of this new formalism.

Chapter 7

Conclusion

In this chapter, we summarize the main results of the thesis.

- Non-equilibrium field theory is a powerful technique to study quantum dynamics of a many body system. However, the current formulation of this field theoretic approach has a drawback that it can only efficiently deal with systems starting from thermal initial conditions. In this thesis, we have formulated a new extension of Schwinger-Keldysh field theoretic description of dynamics of a quantum many-body (bosonic or fermionic) system starting from an arbitrary athermal initial density matrix. This extends the scope of applicability of the non-equilibrium field theory formalism to a broad class of systems where the initial conditions of the system crucially govern the subsequent dynamics and need to be tracked explicitly during the evolution. This comprehensive action based formalism, developed in chapter 3, is valid for a generic (interacting) many body system (open/closed) starting from arbitrary initial density matrix. We have shown that in a quantum many body system, starting from arbitrary athermal initial condition, physical correlation functions do not satisfy Wick's theorem. We have quantified the violation of Wick's theorem in terms of multi-particle correlators calculated in the density matrix.

- In chapter 4, we applied this formalism to work out the imbalance dynamics of a strongly disordered (quasi-periodic) non-interacting and interacting (many body localized) systems, both in 1 and 2 dimensions. We have established a new way of extracting localization length from long-time imbalance in the system, which has been measured in experiments to detect MBL. Our analysis reveals useful insights

regarding the microscopic mechanism responsible for retention of the initial memory in the long time dynamics, both in non-interacting and interacting systems.

- In chapter 5, we have studied non-Markovian dynamics of a many body open quantum system induced by a vast set of non-analyticites in the bath spectral function. We probed the dissipative stochastic dynamics both in the steady state as well as in the transient phase within the recent extension of SK field theory formulated by us. We have also provided a detailed connection between, (a) the cross-over time-scale from the short time "quasi-Markovian" exponential decay to long time power law decay and the location of the non-analyticity, and (b) the exponent of the power law to the nature of the non-analyticity in the bath spectrum. We have discussed the effects of inter-particle interaction on these long-range memory kernels governing the dynamics.

- In chapter 6, we have derived a new way of calculating Winger quasi-probability distribution and Renyi entanglement in a generic quantum many body (open/closed) system from SK field theory. This new technique completely bypasses the complicated boundary conditions among the replica fields used in earlier methods using ground state free field theory. We have provided exact analytical results of non-interacting many body OQS and extended it to the presence of Kerr non-linearity under suitable approximation.

The works presented in the thesis thus opens up a wide window to study a large class of problems related to the dynamics of many body open quantum systems and disordered systems, some of which we are pursuing currently.

- As a direct consequence of the violation of Wick's theorem in dynamics starting arbitrary athermal initial conditions, formulating a diagrammatic perturbation theory for the physical correlation functions in an interacting system is a hard task. This leads to cumbersome derivative expansion of the intermediate Green's functions w.r.t the initial sources, introduced in chapter 3. In our current results on interacting systems, presented in the thesis, we have bypassed this problem by neglecting the two-particle and higher order initial correlators. This recovers Wick's theorem. However, how to include effects of multi-particle initial correlations in the dynamics of an interacting

system in an action based formalism, is an interesting and unresolved question which needs to be explored in great details. We are addressing some of the related questions in ongoing projects which will presented in future studies.

- In chapter 6, we have proposed a new non-equilibrium field theoretic approach of calculating Wigner characteristics, Wigner quasi-probability distribution and Renyi entropy for a generic Bosonic system. It would be interesting to generalize this formulation for Fermionic systems expressed in terms of Grassmann fields. Some progresses have been made in this direction using non-trivial extension of the formalism presented in chapter 6. This is currently under investigation and will be presented in future works.

Appendix A

Technical Details of Chapter 3

A.1 Calculation of $\mathcal{N}(u)$ and $\hat{G}(u)$ for the Diagonal Initial Density Matrix

An important step in the formalism we have developed for a quantum many body system starting from $\hat{\rho}_0 = \sum_{\{n\}} c_{\{n\}} |\{n\}\rangle\langle\{n\}|$ is to invert the kernel $\hat{G}^{-1}(\alpha, t, \beta, t', \vec{u})$ in the inverse Green's function analytically and obtain the closed form expression for the $\vec{u}$ dependent normalization, $\mathcal{N}(u) = Det[-\mathbf{i}\hat{G}^{-1}(u)]^{-\zeta}$ and also the Green's function, $\hat{G}(u)$ with the initial source $\vec{u}$, as they serve as the building blocks for the further steps of the many body formalism. In this appendix, we will work out the structure of calculating $\mathcal{N}(u)$ and $\hat{G}(u)$ from $\hat{G}^{-1}(\alpha, t, \beta, t', \vec{u})$ for a many body Bosonic system.

To construct these objects, it is useful to isolate the $\vec{u}$ dependent part in the action from the from part independent of the initial condition to write,

$$\hat{G}^{-1}(u_\alpha) = \hat{G}^{-1}(0) - \hat{\Delta}(u_\alpha) \tag{1.1}$$

where $\hat{G}^{-1}(0) = \hat{G}^{-1}(\alpha, t; \beta, t')|_{\vec{u}=0}$ is the two component inverse Green's function when the system starts in the vacuum state, and is obtained by setting $u_\alpha = 0$. It is evident from the text below equation 3.14, that the $\vec{u}$ dependent part Δ is finite only for the $+-$ component, i.e.

$$\Delta_{++} = \Delta_{--} = \Delta_{-+} = 0 \ , \ \Delta_{+-}(\alpha, t; \beta, t', \vec{u}) = \mathbf{i}\delta_{\alpha\beta}\delta_t\delta_{t'}u_\alpha. \tag{1.2}$$

Now, we will write,

$$Det[-\mathbf{i}\hat{G}^{-1}(\vec{u})] = e^{Tr[\log\{-\mathbf{i}\hat{G}^{-1}(\vec{u})\}]}$$

which leads to,

$$\begin{aligned} Tr[\log\{-\mathbf{i}\hat{G}^{-1}(\vec{u})\}] &= Tr[\log\{-\mathbf{i}\hat{G}^{-1}(0)\}] + Tr[\log\{1-\hat{G}(0)\hat{\Delta}(\vec{u})\}] \\ &= Tr[\log\{-\mathbf{i}\hat{G}^{-1}(0)\}] - Tr\left[\hat{G}(0)\hat{\Delta}(\vec{u}) + \frac{1}{2}\hat{G}(0)\hat{\Delta}(\vec{u})\hat{G}(0)\hat{\Delta}(\vec{u}) + ..\right] \end{aligned} \tag{1.3}$$

where,

$$Tr\left[\hat{G}(0)\hat{\Delta}(\vec{u})\right] = Tr\left[\hat{G}_{-+}(0)\hat{\Delta}_{+-}(\vec{u})\right] = \mathbf{i}\sum_{\alpha} G_{-+}(\alpha,0;\beta,0;0)u_\alpha = \sum_{\alpha} u_\alpha. \tag{1.4}$$

Here the vacuum Green's functions $\hat{G}(0) = \hat{G}^v$are given by

$$\begin{aligned} G^v_{-+}(\alpha,t;\beta,t') &= -\mathbf{i}\sum_a \psi^*_a(\beta)\psi_a(\alpha)e^{-iE_a(t-t')}\ ,\ G^v_{+-}(\alpha,t;\beta,t') = 0, \\ G^v_{++}(\alpha,t;\beta,t') &= \Theta(t-t')G^v_{-+}(\alpha,t;\beta,t')\ ,\ and\ G^v_{--}(\alpha,t;\beta,t') = \Theta(t'-t)G^v_{-+}(\alpha,t;\beta,t'), \end{aligned} \tag{1.5}$$

where E_a are the eigenvalues and $\psi_a(\alpha)$ are the corresponding eigenvectors of the Hamiltonian of the multimode system. Using the orthogonality property of eigenmodes we get, $\mathbf{i}G_{-+}(\alpha,0;\beta,0;0) = \delta_{\alpha,\beta}$ at the initial time $t = t' = 0$, Similarly,

$$Tr\left[\hat{G}(0)\hat{\Delta}(\vec{u})\hat{G}(0)\hat{\Delta}(\vec{u})\right] = \frac{1}{2}Tr\left[\hat{G}_{-+}(\alpha,0;\beta,0;0)\mathbf{i}u_\beta\hat{G}_{-+}(\beta,0;\gamma,0;0)\mathbf{i}u_\gamma\right] = \frac{1}{2}\sum_\alpha u^2_\alpha. \tag{1.6}$$

Using similar argument for all terms in the expansion (equation 1.3) and adding them up, we obtain,

$$\begin{aligned} Tr[\log\{-\mathbf{i}\hat{G}^{-1}(\vec{u})\}] &= Tr[\log\{-\mathbf{i}\hat{G}^{-1}(0)\}] + \sum_\alpha \log(1-u_\alpha) \\ Det[-\mathbf{i}G^{-1}] &= Det[-\mathbf{i}G^{-1}(0)]\prod_\alpha 1-u_\alpha \end{aligned} \tag{1.7}$$

which is quoted in equation 3.15.

Now, we will show how to invert the kernel $\hat{G}^{-1}(u)$ to obtain closed form answer for $\hat{G}(u)$. We have,

$$\hat{G}(\vec{u}) = \left[\hat{G}^{-1}(0) - \hat{\Delta}(u_\alpha)\right]^{-1} = \hat{G}(0)\left[1 - \hat{G}(0)\hat{\Delta}(u_\alpha)\right]^{-1}$$
$$= \hat{G}(0) + \hat{G}(0)\hat{\Delta}(u_\alpha)\hat{G}(0) + \hat{G}(0)\hat{\Delta}(u_\alpha)\hat{G}(0)\hat{\Delta}(u_\alpha)\hat{G}(0) + ...$$

We will show here the structure of the above sum for one of the components, say $G_{++}(\alpha, t; \beta, t'; \vec{u})$. The expansion of $\hat{G}_{++}(\vec{u})$ can be written as,

$$\begin{aligned}
G_{++}(\alpha, t; \beta, t'; \vec{u}) &= G^v_{++}(\alpha, t; \beta, t') + \mathbf{i}\sum_\gamma G^v_{++}(\alpha, t; \gamma, 0)u_\gamma G^v_{-+}(\gamma, 0; \beta, t') \\
&+ \mathbf{i}^2\sum_{\gamma,\kappa} G^v_{++}(\alpha, t; \gamma, 0)u_\gamma G^v_{-+}(\gamma, 0; \kappa, 0)u_\kappa G^v_{-+}(\kappa, 0; \beta, t') + .. \\
&= G^v_{++}(\alpha, t; \beta, t') + \mathbf{i}\sum_\gamma G^v_{++}(\alpha, t; \gamma, 0)u_\gamma G^v_{-+}(\gamma, 0; \beta, t') \\
&+ \mathbf{i}\sum_\gamma G^v_{++}(\alpha, t; \gamma, 0)u^2_\gamma G^v_{-+}(\gamma, 0; \beta, t') \\
&= G^v_{++}(\alpha, t; \beta, t') + \mathbf{i}\sum_\gamma \frac{u_\gamma}{1-u_\gamma} G^v_{++}(\alpha, t; \gamma, 0)G^v_{-+}(\gamma, 0; \beta, t') \quad (1.8)
\end{aligned}$$

Similar arguments will apply to the other components as well which will lead to equation for $G_{\mu\nu}(\alpha, t; \beta, t'; \vec{u})$.

Appendix B

Technical Details of Chapter 4

B.1 Skeleton Expansion for Self-energies in Interacting Fermionic System

In section 4.8, we have worked out the imbalance dynamics in an interacting Fermionic system where the particles are interacting via nearest-neighbour interaction. We have obtained the self-energies by the skeleton expansion of Σ_R and Σ_K, evaluating all the diagrams shown in Fig. 4.15 and Fig. 4.16. In this appendix, we will write down the explicit expressions of the self-energies, for the convenience of the readers. The retarded self-energy is given by,

$$\begin{aligned}
\Sigma_R(i,t;j,t') &= \delta_{i,j}\delta(t-t')(-\mathbf{i}U)\left[\mathcal{G}_K(i-1,t;i-1,t)+\mathcal{G}_K(i+1,t;i+1,t)\right] \\
&+ \delta(t-t')(\mathbf{i}U)\left[\delta_{i,i+1}\mathcal{G}_K(i,t;i+1,t)+\delta_{i,i-1}\mathcal{G}_K(i,t;i-1,t)\right] \\
&+ U^2\sum_{\bar{i}\bar{j}}\Big[G_R(\bar{i},t;\bar{j},t')G_K(i,t;j,t')G_K(\bar{j},t';\bar{i},t) \\
&+ G_K(\bar{i},t;\bar{j},t')G_R(i,t;j,t')G_K(\bar{j},t';\bar{i},t) \\
&+ G_R(\bar{i},t;\bar{j},t')G_R(i,t;j,t')G_A(\bar{j},t';\bar{i},t) \\
&+ G_K(\bar{i},t;\bar{j},t')G_K(i,t;j,t')G_A(\bar{j},t';\bar{i},t) \\
&- G_K(\bar{i},t;j,t')G_R(i,t;\bar{j},t')G_K(\bar{j},t';\bar{i},t) \\
&- G_R(\bar{i},t;j,t')G_K(i,t;\bar{j},t')G_K(\bar{j},t';\bar{i},t) \\
&- G_R(\bar{i},t;j,t')G_R(i,t;\bar{j},t')G_A(\bar{j},t';\bar{i},t) \\
&- G_K(\bar{i},t;j,t')G_K(i,t;\bar{j},t')G_A(\bar{j},t';\bar{i},t)\Big]
\end{aligned} \tag{2.1}$$

where $\bar{i}$ and $\bar{j}$ are the nearest-neighbour sites of i and j respectively. The Keldysh self-energy is given by,

$$\begin{aligned}
\Sigma_K(i,t;j,t') &= U^2 \sum_{\bar{i}\bar{j}} \Big[G_R(\bar{i},t;\bar{j},t') G_R(i,t;j,t') G_K(\bar{j},t';\bar{i},t) \\
&+ G_K(\bar{i},t;\bar{j},t') \mathcal{G}_K(i,t;j,t') \mathcal{G}_K(\bar{j},t';\bar{i},t) \\
&+ G_R(\bar{i},t;\bar{j},t') \mathcal{G}_K(i,t;j,t') G_A(\bar{j},t';\bar{i},t) \\
&+ \mathcal{G}_K(\bar{i},t;\bar{j},t') G_R(i,t;j,t') G_A(\bar{j},t';\bar{i},t) \\
&- G_R(\bar{i},t;j,t') G_R(i,t;\bar{j},t') \mathcal{G}_K(\bar{j},t';\bar{i},t) \\
&- \mathcal{G}_K(\bar{i},t;j,t') \mathcal{G}_K(i,t;\bar{j},t') \mathcal{G}_K(\bar{j},t';\bar{i},t) \\
&- \mathcal{G}_K(\bar{i},t;j,t') G_R(i,t;\bar{j},t') G_A(\bar{j},t';\bar{i},t) \\
&- G_R(\bar{i},t;j,t') \mathcal{G}_K(i,t;\bar{j},t') G_A(\bar{j},t';\bar{i},t) \Big]
\end{aligned} \tag{2.2}$$

Appendix C

Technical Details of Chapter 5

C.1 Power Law Tails and Non-analytic Bath Spectral Functions

In section (5.3) and (5.4), we have claimed that the non-analyticity of the bath spectral function leads to power law tails in self energies and Greens' functions using Keldysh formalism. We have also claimed that the exponent of the power law depends solely on the nature of the non-analyticity and is independent of its location. In chapter 5, we had shown this with an exact expression for retarded self-energy for the spectral function of semi-infinite bath having $J(\omega) = \Theta(4t_B^2 - \omega^2)(2/t_B)\left(1 - \omega^2/(4t_B^2)\right)^{1/2}$. In this appendix , we make the connection between non-analyticites of $J(\omega)$ and power law tails clearer by showing the relation between the non-analyticity and the exponent of the power law for $\Sigma^K(t-t')$ and $G^{R/K}(t-t')$ for the semi-infinite bath, where the Fourier transform cannot be obtained in a closed form. To do this, we will first focus on non-analyticity in $\Sigma^K(\omega)$ for $J(\omega) = \Theta(4t_B^2 - \omega^2)\frac{2}{t_B}\sqrt{1 - \frac{\omega^2}{4t_B^2}}$ and show how this is connected to power law exponent . This connection will help up in understanding the nature of power law for any non-analytic spectral function , if we know its leading order non-analytic piece. We will then use this argument to show that $\Sigma^K(\omega), G^R(\omega), G^K(\omega)$ all have the same leading singularity and hence the same power law tail appears in their long time profile. The Keldysh self energy is given by,

$$\Sigma_l^K(t-t') = -\mathbf{i}\epsilon^2 \int \frac{d\omega}{2\pi} J(\omega) \coth\left[\frac{\omega - \mu_l}{2T_l}\right] e^{-\mathbf{i}\omega(t-t')} \tag{3.1}$$

We note that the chemical potential, $\mu_l < -2t_B$ and hence $\coth\left[\frac{\omega-\mu_l}{2T_l}\right]$ is a smooth function in the integration range and $J(\omega)$ and hence $\Sigma^K(\omega)$ is non-analytic only at $\omega = \pm 2t_B$.

Expanding $w = \pm 2t_B(1-\delta)$ we get $J(\omega) \sim \delta^{\frac{1}{2}}$ for $\delta \to 0^+$ and hence the integrand $\mathcal{I}(\omega) = \frac{1}{2\pi} J(\omega) \coth\left[\frac{\omega-\mu_l}{2T_l}\right]$ can be expanded as $\mathcal{I}(\pm 2t_B(1-\delta)) = \sum_{n=0}^{\infty} C_n^{\pm}\ \delta^{n+\frac{1}{2}}$ where $C_0^{\pm} = \frac{\sqrt{2}}{\pi\ t_B} \coth\left[\frac{\pm 2t_B-\mu_l}{2T_l}\right]$. Considering the combination of the non-analytic piece , we get,

$$\begin{aligned}
\Sigma^K(t-t') &= -\mathbf{i}\epsilon^2\ 2t_B \sum_{n=0}^{\infty}\Big[\int_0^1 d\delta\ C_n^+\ \delta^{n+\frac{1}{2}}\ e^{-\mathbf{i}(1-\delta)\tau} + \int_0^1 d\delta\ C_n^-\ \delta^{n+\frac{1}{2}}\ e^{\mathbf{i}(1-\delta)\tau}\Big] \\
&= -\mathbf{i}\epsilon^2\ \frac{2t_B}{\tau^{\frac{3}{2}}}\Big[e^{-\mathbf{i}\tau}\int_0^{\tau} dz\ \sum_{n=0}^{\infty}\frac{C_n^+}{\tau^n}\ z^{n+\frac{1}{2}}e^{\mathbf{i}\ z} + e^{i\tau}\int_0^{\tau} dz\ \sum_{n=0}^{\infty}\frac{C_n^-}{\tau^n}\ z^{n+\frac{1}{2}}e^{-\mathbf{i}\ z}\Big]
\end{aligned} \tag{3.2}$$

where $\tau = 2t_B\ (t-t')$,$z = \delta\ \tau$ and the subscript l is dropped here for notational convenience. These integrations can be performed in the form of incomplete Gamma function $\Gamma(\alpha, z)$,

$$\int_0^{\tau} dz\ z^{n+\frac{1}{2}}e^{\mathbf{i}\ z} = -(-\mathbf{i})^{-n-\frac{3}{2}}\Big[\Gamma(n+\frac{3}{2}, -\mathbf{i}\tau) - \Gamma(n+\frac{3}{2}, 0)\Big] \tag{3.3}$$

which has its asymptotic form,

$$\Gamma(n+\frac{3}{2}, -\mathbf{i}\tau) = e^{\mathbf{i}\tau}(-\mathbf{i}\tau)^{n+\frac{1}{2}}\left[1 + \frac{\mathbf{i}}{\tau}\Big(n+\frac{1}{2}\Big) + \mathcal{O}\Big(\frac{1}{\tau^2}\Big)\right]$$

Using this and substituting the values of $C_0^{\pm}$, we obtain $\Sigma^K(t-t')$ which is given by equation (3.4). It is thus clear that the leading order power law tail in $\Sigma^K(t-t')$ goes as $|t-t'|^{-\frac{3}{2}}$.

$$\begin{aligned}
\Sigma^K(t-t') &\sim -\mathbf{i}\epsilon^2\ t_B\ \sqrt{\frac{\pi}{|2t_B(t-t')|^3}}\Big((-\mathbf{i})^{-\frac{3}{2}}e^{-\mathbf{i}2t_B(t-t')}\ C_0^+ + (\mathbf{i})^{-\frac{3}{2}}e^{\mathbf{i}2t_B(t-t')}\ C_0^-\Big) \\
&+ \mathcal{O}\Big(\frac{1}{\tau^2}\Big) \\
&\sim -\mathbf{i}\epsilon^2\ \sqrt{\frac{2}{\pi\ |2t_B(t-t')|^3}}\Big(e^{-\mathbf{i}\left[2t_B(t-t')-\frac{3\pi}{4}\right]}\coth\left[\frac{2t_B-\mu}{2T}\right] \\
&+ e^{\mathbf{i}\left[2t_B(t-t')-\frac{3\pi}{4}\right]}\coth\left[\frac{-2t_B-\mu}{2T}\right]\Big) + \mathcal{O}\Big(\frac{1}{\tau^2}\Big)
\end{aligned} \tag{3.4}$$

The leading order answer for $Im[\Sigma^K(t-t')]$ is then ,

$$\begin{aligned} Im[\Sigma^K(t-t')] &\sim -\epsilon^2 \sqrt{\frac{2}{\pi\ |2t_B(t-t')|^3}} \Bigg(\coth\left[\frac{2t_B-\mu}{2T}\right] \\ &+ \coth\left[\frac{-2t_B-\mu}{2T}\right] \Bigg) \cos\left[2t_B(t-t') - \frac{3\pi}{4}\right] \end{aligned} \tag{3.5}$$

The expression , without the oscillation , is plotted in Fig. [1] as a solid line and matches with the numerically obtained plot very well.

Having shown the connection between the non-analyticity and power law tails, we now show that for the 2-site model , $G^R_{1,2}$ also has a $|t-t'|^{-\frac{3}{2}}$ tail . Similar considerations will apply for other $G^R_{i,j}$ and $G^K_{i,j}$, both in the 2 site model and in the chain. Writing $\mathcal{D} = \mathcal{D}^{'} + \mathbf{i}\mathcal{D}^{''}$ the retarded Greens' function $G^R_{1,2}$ is given by,

$$\begin{aligned} Re\left[G^R_{1,2}\right] &= -\frac{1}{g}\ \frac{\mathcal{D}^{'2} - \mathcal{D}^{''2} - 1}{(\mathcal{D}^{'2} - \mathcal{D}^{''2} - 1)^2 + 4\mathcal{D}^{'2}\mathcal{D}^{''2}} \\ Im\left[G^R_{1,2}\right] &= -\frac{1}{g}\ \frac{-2\mathcal{D}^{'}\mathcal{D}^{''}}{(\mathcal{D}^{'2} - \mathcal{D}^{''2} - 1)^2 + 4\mathcal{D}^{'2}\mathcal{D}^{''2}} \end{aligned} \tag{3.6}$$

where

$$\begin{aligned} &\mathcal{D}^{'} \\ = &\frac{1}{g}\left[w\left(1 - \frac{\epsilon^2}{2t_B^2}\right) + \frac{\epsilon^2}{t_B} sign(\omega)\Theta\big(|\omega| - 2t_B\big)\sqrt{\frac{\omega^2}{4t_B^2} - 1}\right] \\ &\mathcal{D}^{''} = \frac{1}{g}\frac{\epsilon^2}{t_B}\Theta\big(4t_B^2 - \omega^2\big)\sqrt{1 - \frac{\omega^2}{4t_B^2}} \end{aligned} \tag{3.7}$$

We note that $\mathcal{D}^{''} \sim \delta^{\frac{1}{2}}$ for $\omega = \pm 2t_B(1-\delta)$ while $\mathcal{D}^{'} \sim \left(1 + C_0\ \delta^{\frac{1}{2}}\right)$ for $\omega = \pm 2t_B(1+\delta)$ and one needs to consider all these non-analytic pieces to calculate the power law tail. For Fourier transform of $Im[G^R_{1,2}]$, the integration goes from $-2t_B < \omega < 2t_B$ and since $\mathcal{D}^{'}$ is smooth in this region, only non-analyticity of $\mathcal{D}^{''}$ leads to power law. One can then follow an argument similar to that of $\Sigma^K(t-t')$ and show that leading $\delta^{\frac{1}{2}}$ non-analyticity implies a power law $\sim |t-t'|^{-\frac{3}{2}}$. For $Re[G^R_{1,2}]$, the argument is more complicated. The integral is broken into three ranges, (a) from $-\infty$ to $-2t_B$, (b) from $2t_B$ to ∞ and (c) from $-2t_B$ to $2t_B$. Note that in the regions (a) and (b) the integrand can be expanded

near $\omega = \pm 2t_B(1+\delta)$ as $\sum_{n=0}^{\infty} C_n^{\pm}\ \delta^{\frac{n}{2}}$ coming from $\mathcal{D}'^2$ while the same in the region (c) goes as $\sum_{n=0}^{\infty} C_n^{\pm}\ \delta^n$ near $\omega = \pm 2t_B(1-\delta)$. Then all the three integral in the ranges (a) , (b) and (c) have $\mathcal{O}\left(\tau^{-1}\right)$ coefficients which add up to zero and only integrals (a) and (b) contribute to obtain a finite $\mathcal{O}\left(\tau^{-\frac{3}{2}}\right)$ coefficient. Thus Fourier transform of $Re[G^R_{1,2}]$ also scales as $|t-t'|^{-\frac{3}{2}}$ for $|t-t'| \to \infty$. We note that similar arguments can also be applied in analysis of G^K to show its $|t-t'|^{-\frac{3}{2}}$ decay in the long time limit.

C.2 Exponential Decay of Current in a Linear Chain

In section 5.4, we have derived the retarded and the Keldysh Greens' function for a linear chain, where each site is coupled to an independent bath with its own temperature and chemical potential. In section section 5.5 , we found that when the baths have a common temperature but chemical potential of the bath varies linearly with lattice site no., the current in the links of the system show an exponential decay in space, away from the edges of the chain. In this appendix we use the analytic forms of the Greens' function in section 5.4 and consider their low temperature form to explain the exponential decay of current. We will also show that the decay length is proportional to the temperature of the baths. To illustrate this, we use eqns. 5.14 and 5.16 to write,

$$\begin{aligned} G^K_{l,l+1} \;=\; \mathbf{i}\frac{\epsilon^2\ J(w)}{g^2\ |M_N|^2}\Bigg(& M_{N-l}\ M^*_{N-l-1}\ \sum_{j=1}^{l} |M_{j-1}|^2 \coth\left[\frac{w-\mu_j}{2T}\right] \\ & + M_{l-1}\ M^*_l\ \sum_{j=l+1}^{N} |M_{N-j}|^2 \coth\left[\frac{w-\mu_j}{2T}\right]\Bigg) \end{aligned} \tag{3.8}$$

where M_l is now written in a form different from eqn 5.15 to facilitate the derivation. We now write,

$$M_l = \frac{y^{l+1} - \frac{1}{y^{l+1}}}{2\sqrt{\frac{D^2}{4}-1}} \qquad with \qquad y = \frac{\mathcal{D}}{2} + \sqrt{\frac{\mathcal{D}^2}{4}-1} \tag{3.9}$$

where $\mathcal{D}$ is given by eqn (3.7) of Appendix C.1. One can easily check that this definition of M_l is equivalent to that in equation 5.15.

We now consider the low temperature limit , where $(\omega - \mu_j) >> T$,$\forall\ \omega$ and $\forall\ j$. In this case, $\coth\left[\frac{w-\mu_j}{2T}\right] \sim\ 1+2\ e^{-(\omega-\mu_j)/T} = 1+2e^{-(\omega-\mu_1+\nu)/T}e^{\nu\ j/T}$ where $\mu_l = \mu_1 + \nu\ (l-1)$ with $\nu = \frac{d\mu}{dx}$ setting the slope of linear variation of μ . Now the first term in the expansion

of coth must sum up to zero , since this has no information about the variation of μ across the chain and current must be zero if all $\mu_j = \mu$. We then focus on the second term. Writing $y = re^{\mathbf{i}\theta}$, we then get for this term,

$$\begin{aligned}
\sum_{j=1}^{l} |M_{j-1}|^2 \coth\left[\frac{w-\mu_j}{2T}\right] &= 2\ e^{-(\omega-\mu_1+\nu)/T}\ \sum_{j=1}^{l}\left[r^{2j} + r^{-2j} - 2\ \cos(2j\ \theta)\right]\ e^{\nu\ j/T} \\
\sum_{j=1}^{l} |M_{N-j}|^2 \coth\left[\frac{w-\mu_j}{2T}\right] &= 2\ e^{-(\omega-\mu_1+\nu)/T}\ \sum_{j=1}^{l}\Big[r^{2(N-j+1)} + r^{-2(N-j+1)} \\
&- 2\ \cos\big(2(N-j+1)\ \theta\big)\Big]\ e^{\nu\ j/T}
\end{aligned}$$

Now, we can have either $r > 1$ or $r < 1$. We will first focus on the case $r > 1$ and later show that similar argument works for $r < 1$. Here, we are interested in the region of the chain far away from its boundary so that $r^N >> r^l$. The first series can then be summed (GP) to obtain terms like, $\left[\left(r^2e^{\nu/T}\right)^l - 1\right] r^2e^{\nu/T}/\left(r^2e^{\nu/T} - 1\right) + r \leftrightarrow e^{\pm\mathbf{i}\theta}$. One can then multiply with appropriate factors using equation (3.8) to obtain $G^K_{l,l+1}$ whose leading order terms fall off exponentially $\sim e^{\nu\ l/T}$ where the other terms are suppressed by factor of r^{2N} coming from $|M_N|^2$. This shows that $\xi = T\ /\ \nu$ and explains the linear scaling of ξ with T seen in Fig 3(f). One can similarly work out the other terms and the conclusion obtained above remains robust. If $r < 1$, one can neglect r^i in favour of r^{-i} , but the final conclusion $I \sim e^{\nu\ l/T}$ works out. Note that $\nu < 0$ in our case, and hence this indicates a decay of current in space. A similar argument can be made for the density profile, except the term with 1 in the expansion of coth does not sum to zero. So $n(x) \sim n_0 + n_1e^{\nu\ l/T}$, i.e the variation around the constant value decays exponentially.

C.3 Effect of Interaction on Non-Markovian Dynamics

In section 5.7 , we had shown that, within mean field theory , the exponential decay in the temporal profile of the Greens' functions of the interacting system is slower than that of the non-interacting system, and hence the time scale for cross-over from the "quasi-Markovian" to non-Markovian dynamics increases. We argued this based on the fact that imaginary part of the one of the poles of the Greens' function, which controls the decay rate, decreases with interaction. In Fig [C.1] , we plot the differences in imaginary part of the pole between non-interacting and interacting systems as a function of U and V .

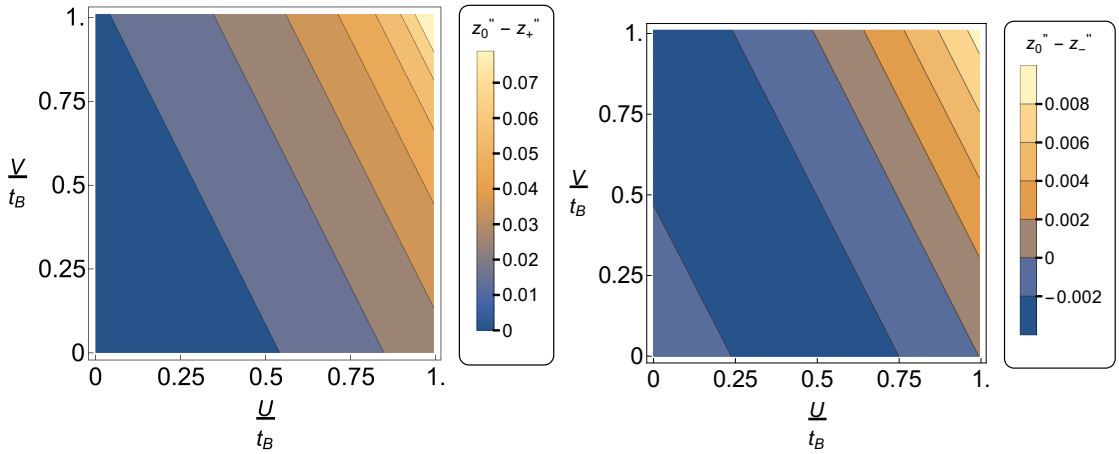

Figure C.1: The difference between the imaginary part of the pole for the non-interacting case (z_0'') and those of the interacting case ($z_\pm''$) is plotted as a function of the interaction strength U/t_B and V/t_B for the 2-site model connected to two independent baths of same temperature $T = 0.625t_B$ but different chemical potential $\mu_1 = -2.5t_B$ and $\mu_2 = -5.0t_B$ where we use $g = 0.5t_B$, $\epsilon = 0.2t_B$. It shows that in the entire parameter space of the interaction strength , one of the two poles (z_+) of the interacting model always has smaller imaginary part than the non-interacting one. Hence the cross-over timescale from the exponential decay to power law tail in Greens' function and consequently in unequal time obsevables always shifts to larger $t - t'$ values as depicted in Fig. 6(c).

We have considered a 2-site system with $g = 0.5t_B$, $\epsilon = 0.2t_B$, coupled to two baths with common temperature $T = 0.625t_B$, $\mu_1 = -2.5t_B$ and $\mu_2 = -5.0t_B$. We find that the difference > 0 for all U and V for one of the poles , i.e, the non-interacting Greens' function decay faster. For the other pole , the difference is negative for small vales of U and V and becomes positive for larger values of U and V . We note that the long time decay (before power law tail) is governed by the smallest decay rate , and hence the cross-over time scale increases for all U and V .

Bibliography

[1] Martin Bojowald. Essay: Initial conditions for a universe. General Relativity and Gravitation, 35(11):1877–1883, Nov 2003.

[2] T. G. Tiecke, J. D. Thompson, N. P. de Leon, L. R. Liu, V. Vuletić, and M. D. Lukin. Nanophotonic quantum phase switch with a single atom. Nature, 508:241 EP –, 04 2014.

[3] F. Fleming Crim. Chemical reaction dynamics. Proceedings of the National Academy of Sciences, 105(35):12647–12648, 2008.

[4] William Graham Hoover. Time Reversibility, Computer Simulation, and Chaos, volume 13. 1999.

[5] Stephen M. Barnett, Almut Beige, Artur Ekert, Barry M. Garraway, Christoph H. Keitel, Viv Kendon, Manfred Lein, Gerard J. Milburn, Hctor M. Moya-Cessa, Mio Murao, Jiannis K. Pachos, G. Massimo Palma, Emmanuel Paspalakis, Simon J.D. Phoenix, Benard Piraux, Martin B. Plenio, Barry C. Sanders, Jason Twamley, A. Vidiella-Barranco, and M.S. Kim. Journeys from quantum optics to quantum technology. Progress in Quantum Electronics, 54:19 – 45, 2017. Special issue in honor of the 70th birthday of Professor Sir Peter Knight FRS.

[6] Niklas Mann, M. Reza Bakhtiari, Axel Pelster, and Michael Thorwart. Nonequilibrium quantum phase transition in a hybrid atom-optomechanical system. Phys. Rev. Lett., 120:063605, Feb 2018.

[7] D. Leibfried, R. Blatt, C. Monroe, and D. Wineland. Quantum dynamics of single trapped ions. Rev. Mod. Phys., 75:281–324, Mar 2003.

[8] D. Jaksch, C. Bruder, J. I. Cirac, C. W. Gardiner, and P. Zoller. Cold bosonic atoms in optical lattices. Phys. Rev. Lett., 81:3108–3111, Oct 1998.

[9] A. Assion, M. Geisler, J. Helbing, V. Seyfried, and T. Baumert. Femtosecond pump-probe photoelectron spectroscopy: Mapping of vibrational wave-packet motion. Phys. Rev. A, 54:R4605–R4608, Dec 1996.

[10] Tim Langen, Remi Geiger, and Jrg Schmiedmayer. Ultracold atoms out of equilibrium. Annual Review of Condensed Matter Physics, 6(1):201–217, 2015.

[11] Michael A. Nielsen and Isaac L. Chuang. Quantum Computation and Quantum Information: 10th Anniversary Edition. Cambridge University Press, 2010.

[12] Zhizhou Yu, Gao-Min Tang, and Jian Wang. Full-counting statistics of transient energy current in mesoscopic systems. Phys. Rev. B, 93:195419, May 2016.

[13] Petri Myöhänen, Adrian Stan, Gianluca Stefanucci, and Robert van Leeuwen. Kadanoff-baym approach to quantum transport through interacting nanoscale systems: From the transient to the steady-state regime. Phys. Rev. B, 80:115107, Sep 2009.

[14] Jinshuang Jin, Matisse Wei-Yuan Tu, Wei-Min Zhang, and YiJing Yan. Non-equilibrium quantum theory for nanodevices based on the feynmanvernon influence functional. New Journal of Physics, 12(8):083013, 2010.

[15] Chenyi Zhou, Xiaobin Chen, and Hong Guo. Theory of quantum transport in disordered systems driven by voltage pulse. Phys. Rev. B, 94:075426, Aug 2016.

[16] P. Myhnen, A. Stan, G. Stefanucci, and R. van Leeuwen. A many-body approach to quantum transport dynamics: Initial correlations and memory effects. EPL (Europhysics Letters), 84(6):67001, 2008.

[17] Joseph Maciejko, Jian Wang, and Hong Guo. Time-dependent quantum transport far from equilibrium: An exact nonlinear response theory. Phys. Rev. B, 74:085324, Aug 2006.

[18] Pei-Yun Yang and Wei-Min Zhang. Master equation approach to transient quantum transport in nanostructures. Frontiers of Physics, 12(4):127204, Nov 2016.

[19] Daniel Karlsson, Robert van Leeuwen, Enrico Perfetto, and Gianluca Stefanucci. The generalized kadanoff-baym ansatz with initial correlations. Phys. Rev. B, 98:115148, Sep 2018.

[20] Massimiliano Esposito, Upendra Harbola, and Shaul Mukamel. Nonequilibrium fluctuations, fluctuation theorems, and counting statistics in quantum systems. Rev. Mod. Phys., 81:1665–1702, Dec 2009.

[21] Gao-Min Tang and Jian Wang. Full-counting statistics of charge and spin transport in the transient regime: A nonequilibrium green's function approach. Phys. Rev. B, 90:195422, Nov 2014.

[22] Gao-Min Tang, Fuming Xu, and Jian Wang. Waiting time distribution of quantum electronic transport in the transient regime. Phys. Rev. B, 89:205310, May 2014.

[23] Heinz-Peter Breuer and Francesco Petruccione. The theory of open quantum systems. Oxford University Press on Demand, 2002.

[24] Mark Srednicki. Chaos and quantum thermalization. Phys. Rev. E, 50:888–901, Aug 1994.

[25] J. M. Deutsch. Quantum statistical mechanics in a closed system. Phys. Rev. A, 43:2046–2049, Feb 1991.

[26] Luca D'Alessio, Yariv Kafri, Anatoli Polkovnikov, and Marcos Rigol. From quantum chaos and eigenstate thermalization to statistical mechanics and thermodynamics. Advances in Physics, 65(3):239–362, 2016.

[27] Marcos Rigol. Breakdown of thermalization in finite one-dimensional systems. Phys. Rev. Lett., 103:100403, Sep 2009.

[28] Tim Langen, Sebastian Erne, Remi Geiger, Bernhard Rauer, Thomas Schweigler, Maximilian Kuhnert, Wolfgang Rohringer, Igor E. Mazets, Thomas Gasenzer, and Jörg Schmiedmayer. Experimental observation of a generalized gibbs ensemble. Science, 348(6231):207–211, 2015.

[29] Rahul Nandkishore and David A. Huse. Many-body localization and thermalization in quantum statistical mechanics. Annual Review of Condensed Matter Physics, 6(1):15–38, 2015.

[30] Michael Schreiber, Sean S. Hodgman, Pranjal Bordia, Henrik P. Lüschen, Mark H. Fischer, Ronen Vosk, Ehud Altman, Ulrich Schneider, and Immanuel Bloch. Observation of many-body localization of interacting fermions in a quasirandom optical lattice. Science, 349(6250):842–845, 2015.

[31] Jae-yoon Choi, Sebastian Hild, Johannes Zeiher, Peter Schauß, Antonio Rubio-Abadal, Tarik Yefsah, Vedika Khemani, David A. Huse, Immanuel Bloch, and Christian Gross. Exploring the many-body localization transition in two dimensions. Science, 352(6293):1547–1552, 2016.

[32] C. J. Turner, A. A. Michailidis, D. A. Abanin, M. Serbyn, and Z. Papić. Weak ergodicity breaking from quantum many-body scars. Nature Physics, 14(7):745–749, 2018.

[33] Hannes Bernien, Sylvain Schwartz, Alexander Keesling, Harry Levine, Ahmed Omran, Hannes Pichler, Soonwon Choi, Alexander S. Zibrov, Manuel Endres, Markus Greiner, Vladan Vuletić, and Mikhail D. Lukin. Probing many-body dynamics on a 51-atom quantum simulator. Nature, 551:579 EP –, 11 2017.

[34] D.M. Basko, I.L. Aleiner, and B.L. Altshuler. Metalinsulator transition in a weakly interacting many-electron system with localized single-particle states. Annals of Physics, 321(5):1126 – 1205, 2006.

[35] Ralf Labouvie, Bodhaditya Santra, Simon Heun, and Herwig Ott. Bistability in a driven-dissipative superfluid. Phys. Rev. Lett., 116:235302, Jun 2016.

[36] Leticia F. Cugliandolo, Thierry Giamarchi, and Pierre Le Doussal. Dynamic compressibility and aging in wigner crystals and quantum glasses. Phys. Rev. Lett., 96:217203, Jun 2006.

[37] Malcolm P. Kennett, Claudio Chamon, and Jinwu Ye. Aging dynamics of quantum spin glasses of rotors. Phys. Rev. B, 64:224408, Nov 2001.

[38] Jad C. Halimeh, Matthias Punk, and Francesco Piazza. Aging dynamics in quenched noisy long-range quantum ising models. Phys. Rev. B, 98:045111, Jul 2018.

[39] Alexander Altland and Ben D Simons. Condensed matter field theory. Cambridge University Press, 2010.

[40] Arijeet Pal and David A. Huse. Many-body localization phase transition. Phys. Rev. B, 82:174411, Nov 2010.

[41] K. E. Cahill and R. J. Glauber. Density operators and quasiprobability distributions. Phys. Rev., 177:1882–1902, Jan 1969.

[42] J. Eisert, M. Cramer, and M. B. Plenio. Colloquium: Area laws for the entanglement entropy. Rev. Mod. Phys., 82:277–306, Feb 2010.

[43] Maksym Serbyn, Z. Papić, and Dmitry A. Abanin. Universal slow growth of entanglement in interacting strongly disordered systems. Phys. Rev. Lett., 110:260601, Jun 2013.

[44] G. S. Agarwal. Master equations in phase-space formulation of quantum optics. Phys. Rev., 178:2025–2035, Feb 1969.

[45] Sadao Nakajima. On quantum theory of transport phenomenasteady diffusion. Progress of Theoretical Physics, 20(6):948–959, 1958.

[46] R. Zwanzig. Ensemble method in the theory of irreversibility. The Journal of Chemical Physics, 33:1338, 1960.

[47] Inés de Vega and Daniel Alonso. Dynamics of non-markovian open quantum systems. Rev. Mod. Phys., 89:015001, Jan 2017.

[48] Wei-Min Zhang, Ping-Yuan Lo, Heng-Na Xiong, Matisse Wei-Yuan Tu, and Franco Nori. General non-markovian dynamics of open quantum systems. Phys. Rev. Lett., 109:170402, Oct 2012.

[49] Ahana Chakraborty and Rajdeep Sensarma. Power-law tails and non-markovian dynamics in open quantum systems: An exact solution from keldysh field theory. Phys. Rev. B, 97:104306, Mar 2018.

[50] Ulrich Schollwck. The density-matrix renormalization group in the age of matrix product states. Annals of Physics, 326(1):96 – 192, 2011. January 2011 Special Issue.

[51] J. Eisert. Entanglement and tensor network states. In Autumn School on Correlated Electrons: Emergent Phenomena in Correlated Matter , 2013.

[52] G. Evenbly and G. Vidal. Tensor network renormalization. Phys. Rev. Lett., 115:180405, Oct 2015.

[53] E.M. Stoudenmire and Steven R. White. Studying two-dimensional systems with the density matrix renormalization group. Annual Review of Condensed Matter Physics, 3(1):111–128, 2012.

[54] Tao Xiang, Jizhong Lou, and Zhaobin Su. Two-dimensional algorithm of the density-matrix renormalization group. Phys. Rev. B, 64:104414, Aug 2001.

[55] Alex Kamenev. Field theory of non-equilibrium systems. Cambridge University Press, 2011.

[56] Antti-Pekka Jauho, Ned S. Wingreen, and Yigal Meir. Time-dependent transport in interacting and noninteracting resonant-tunneling systems. Phys. Rev. B, 50:5528–5544, Aug 1994.

[57] Ahana Chakraborty, Pranay Gorantla, and Rajdeep Sensarma. Nonequilibrium field theory for dynamics starting from arbitrary athermal initial conditions. Phys. Rev. B, 99:054306, Feb 2019.

[58] D.M. Basko, I.L. Aleiner, and B.L. Altshuler. Metal–insulator transition in a weakly interacting many-electron system with localized single-particle states. Annals of Physics, 321(5):1126 – 1205, 2006.

[59] I. V. Gornyi, A. D. Mirlin, and D. G. Polyakov. Interacting electrons in disordered wires: Anderson localization and low-t transport. Phys. Rev. Lett., 95:206603, Nov 2005.

[60] Dmitry A. Abanin and Zlatko Papi. Recent progress in many-body localization. Annalen der Physik, 529(7):1700169.

[61] Rahul Nandkishore and David A. Huse. Many-body localization and thermalization in quantum statistical mechanics. Annual Review of Condensed Matter Physics, 6(1):15–38, 2015.

[62] Fabien Alet and Nicolas Laflorencie. Many-body localization: An introduction and selected topics. Comptes Rendus Physique, 19(6):498 – 525, 2018. Quantum simulation / Simulation quantique.

[63] Pranjal Bordia, Henrik P. Lüschen, Sean S. Hodgman, Michael Schreiber, Immanuel Bloch, and Ulrich Schneider. Coupling identical one-dimensional many-body localized systems. Phys. Rev. Lett., 116:140401, Apr 2016.

[64] Henrik P. Lüschen, Pranjal Bordia, Sean S. Hodgman, Michael Schreiber, Saubhik Sarkar, Andrew J. Daley, Mark H. Fischer, Ehud Altman, Immanuel Bloch, and Ulrich Schneider. Signatures of many-body localization in a controlled open quantum system. Phys. Rev. X, 7:011034, Mar 2017.

[65] Henrik P. Lüschen, Sebastian Scherg, Thomas Kohlert, Michael Schreiber, Pranjal Bordia, Xiao Li, S. Das Sarma, and Immanuel Bloch. Single-particle mobility edge in a one-dimensional quasiperiodic optical lattice. Phys. Rev. Lett., 120:160404, Apr 2018.

[66] U. Schollwöck. The density-matrix renormalization group. Rev. Mod. Phys., 77:259–315, Apr 2005.

[67] Ahana Chakraborty, Pranay Gorantla, and Rajdeep Sensarma. Memories of initial states and density imbalance in dynamics of interacting disordered systems. arXiv: 1906.02205.

[68] Pranjal Bordia, Henrik Lüschen, Sebastian Scherg, Sarang Gopalakrishnan, Michael Knap, Ulrich Schneider, and Immanuel Bloch. Probing slow relaxation and many-body localization in two-dimensional quasiperiodic systems. Phys. Rev. X, 7:041047, Nov 2017.

[69] Fabio Benatti and Roberto Floreanini. Irreversible quantum dynamics, volume 622. Springer Science & Business Media, 2003.

[70] T. B. Batalhão, A. M. Souza, R. S. Sarthour, I. S. Oliveira, M. Paternostro, E. Lutz, and R. M. Serra. Irreversibility and the arrow of time in a quenched quantum system. Phys. Rev. Lett., 115:190601, Nov 2015.

[71] Takashi Imamura, Akinori Nishino, and Naomichi Hatano. Entanglement generation through an open quantum dot: Exact two-electron scattering state in the anderson model. Phys. Rev. B, 80:245323, Dec 2009.

[72] Mark Srednicki. The approach to thermal equilibrium in quantized chaotic systems. Journal of Physics A: Mathematical and General, 32(7):1163, 1999.

[73] J. J. Hope, G. M. Moy, M. J. Collett, and C. M. Savage. Steady-state quantum statistics of a non-markovian atom laser. Phys. Rev. A, 61:023603, Jan 2000.

[74] H. P. Breuer, D. Faller, B. Kappler, and F. Petruccione. Non-markovian spectral broadening in interacting continuous-wave atom lasers. EPL (Europhysics Letters), 54(1):14, 2001.

[75] Dieter Jaksch and Peter Zoller. The cold atom hubbard toolbox. Annals of physics, 315(1):52–79, 2005.

[76] A. Recati, P. O. Fedichev, W. Zwerger, J. von Delft, and P. Zoller. Atomic quantum dots coupled to a reservoir of a superfluid bose-einstein condensate. Phys. Rev. Lett., 94:040404, Feb 2005.

[77] Philipp Treutlein, David Hunger, Stephan Camerer, Theodor W. Hänsch, and Jakob Reichel. Bose-einstein condensate coupled to a nanomechanical resonator on an atom chip. Phys. Rev. Lett., 99:140403, Oct 2007.

[78] David Hunger, Stephan Camerer, Theodor W. Hänsch, Daniel König, Jörg P. Kotthaus, Jakob Reichel, and Philipp Treutlein. Resonant coupling of a bose-einstein condensate to a micromechanical oscillator. Phys. Rev. Lett., 104:143002, Apr 2010.

[79] Sajeev John and Tran Quang. Spontaneous emission near the edge of a photonic band gap. Phys. Rev. A, 50:1764–1769, Aug 1994.

[80] Yoshinori Tanaka, Jeremy Upham, Takushi Nagashima, Tomoaki Sugiya, Takashi Asano, and Susumu Noda. Dynamic control of the q factor in a photonic crystal nanocavity. Nat Mater, 6(11):862–865, 11 2007.

[81] Heinz-Peter Breuer, Elsi-Mari Laine, Jyrki Piilo, and Bassano Vacchini. Colloquium. Rev. Mod. Phys., 88:021002, Apr 2016.

[82] Inés de Vega and Daniel Alonso. Dynamics of non-markovian open quantum systems. Reviews of Modern Physics, 89(1):015001, 2017.

[83] W. Kohn. Image of the fermi surface in the vibration spectrum of a metal. Phys. Rev. Lett., 2:393–394, May 1959.

[84] G. Vidal, J. I. Latorre, E. Rico, and A. Kitaev. Entanglement in quantum critical phenomena. Phys. Rev. Lett., 90:227902, Jun 2003.

[85] Román Orús. Universal geometric entanglement close to quantum phase transitions. Phys. Rev. Lett., 100:130502, Apr 2008.

[86] J. Smith, A. Lee, P. Richerme, B. Neyenhuis, P. W. Hess, P. Hauke, M. Heyl, D. A. Huse, and C. Monroe. Many-body localization in a quantum simulator with programmable random disorder. Nature Physics, 12:907 EP –, 06 2016.

[87] E. Wigner. On the quantum correction for thermodynamic equilibrium. Phys. Rev., 40:749–759, Jun 1932.

[88] Anatoli Polkovnikov. Quantum corrections to the dynamics of interacting bosons: Beyond the truncated wigner approximation. Phys. Rev. A, 68:053604, Nov 2003.

[89] L. Shifren and D. K. Ferry. Wigner function quantum monte carlo. Physica B: Condensed Matter, 314(1-4):72–75, 3 2002.

[90] A. Mari and J. Eisert. Positive wigner functions render classical simulation of quantum computation efficient. Phys. Rev. Lett., 109:230503, Dec 2012.

[91] T. J. Dunn, I. A. Walmsley, and S. Mukamel. Experimental determination of the quantum-mechanical state of a molecular vibrational mode using fluorescence tomography. Phys. Rev. Lett., 74:884–887, Feb 1995.

[92] Rajibul Islam, Ruichao Ma, Philipp M. Preiss, M. Eric Tai, Alexander Lukin, Matthew Rispoli, and Markus Greiner. Measuring entanglement entropy in a quantum many-body system. Nature, 528:77 EP –, 12 2015.

[93] Ahana Chakraborty and Rajdeep Sensarma. Evolution of wigner function and entanglement entropy for bosons from non-equilibrium field theory. arXiv:1810.10545.

[94] Pasquale Calabrese and John Cardy. Entanglement entropy and conformal field theory. Journal of Physics A: Mathematical and Theoretical, 42(50):504005, 2009.

[95] Alex Kamenev and Alex Levchenko. Keldysh technique and non-linear σ-model: basic principles and applications. Advances in Physics, 58(3):197–319, 2009.

[96] J. W. Negele and H. Orland. Quantum Many Body Systems. Oxford University Press on Demand, 2002.

[97] Gordon Kadanoff, Leo P./Baym. Quantum Statistical Mechanics. Frontiers in Physics Series by W.A. Benjamin, Inc., 1962.

[98] Camille Aron, Giulio Biroli, and Leticia F. Cugliandolo. (Non) equilibrium dynamics: a (broken) symmetry of the Keldysh generating functional. SciPost Phys., 4:008, 2018.

[99] O. V. KONSTANTINOV and V. I. PEREL. A diagram technique for evaluating transport quantities. JETP, 12:142, January 1961.

[100] L. M. Sieberer, S. D. Huber, E. Altman, and S. Diehl. Nonequilibrium functional renormalization for driven-dissipative bose-einstein condensation. Phys. Rev. B, 89:134310, Apr 2014.

[101] Sangita De Sarkar, Rajdeep Sensarma, and K Sengupta. A perturbative renormalization group approach to driven quantum systems. Journal of Physics: Condensed Matter, 26(32):325602, 2014.

[102] Gordon Baym and Leo P. Kadanoff. Conservation laws and correlation functions. Phys. Rev., 124:287–299, Oct 1961.

[103] D. Semkat, D. Kremp, and M. Bonitz. Kadanoff-baym equations with initial correlations. Phys. Rev. E, 59:1557–1562, Feb 1999.

[104] D. Semkat, D. Kremp, and M. Bonitz. Kadanoffbaym equations and non-markovian boltzmann equation in generalized t-matrix approximation. Journal of Mathematical Physics, 41(11):7458–7467, 2000.

[105] Pei-Yun Yang, Chuan-Yu Lin, and Wei-Min Zhang. Transient current-current correlations and noise spectra. Phys. Rev. B, 89:115411, Mar 2014.

[106] Pei-Yun Yang, Chuan-Yu Lin, and Wei-Min Zhang. Master equation approach to transient quantum transport in nanostructures incorporating initial correlations. Phys. Rev. B, 92:165403, Oct 2015.

[107] R. van Leeuwen and G. Stefanucci. Wick theorem for general initial states. Phys. Rev. B, 85:115119, Mar 2012.

[108] Mathias Wagner. Expansions of nonequilibrium green's functions. Phys. Rev. B, 44:6104–6117, Sep 1991.

[109] Robert van Leeuwen and Gianluca Stefanucci. Equilibrium and nonequilibrium many-body perturbation theory: a unified framework based on the martin-schwinger hierarchy. Journal of Physics: Conference Series, 427(1):012001, 2013.

[110] Anatoli Polkovnikov, Krishnendu Sengupta, Alessandro Silva, and Mukund Vengalattore. Colloquium: Nonequilibrium dynamics of closed interacting quantum systems. Rev. Mod. Phys., 83:863–883, Aug 2011.

[111] P. W. Anderson. Absence of diffusion in certain random lattices. Phys. Rev., 109:1492–1505, Mar 1958.

[112] R Balian, R Maynard, and G Toulouse. Ill-Condensed Matter. co-published with North-Holland Publishing Co., 1984.

[113] E. Abrahams, P. W. Anderson, D. C. Licciardello, and T. V. Ramakrishnan. Scaling theory of localization: Absence of quantum diffusion in two dimensions. Phys. Rev. Lett., 42:673–676, Mar 1979.

[114] Patrick A. Lee and T. V. Ramakrishnan. Disordered electronic systems. Rev. Mod. Phys., 57:287–337, Apr 1985.

[115] John Z. Imbrie. Diagonalization and many-body localization for a disordered quantum spin chain. Phys. Rev. Lett., 117:027201, Jul 2016.

[116] Jonas A. Kjäll, Jens H. Bardarson, and Frank Pollmann. Many-body localization in a disordered quantum ising chain. Phys. Rev. Lett., 113:107204, Sep 2014.

[117] Henrik P. Lüschen, Pranjal Bordia, Sean S. Hodgman, Michael Schreiber, Saubhik Sarkar, Andrew J. Daley, Mark H. Fischer, Ehud Altman, Immanuel Bloch, and Ulrich Schneider. Signatures of many-body localization in a controlled open quantum system. Phys. Rev. X, 7:011034, Mar 2017.

[118] Michael Schreiber, Sean S. Hodgman, Pranjal Bordia, Henrik P. Lüschen, Mark H. Fischer, Ronen Vosk, Ehud Altman, Ulrich Schneider, and Immanuel Bloch. Observation of many-body localization of interacting fermions in a quasirandom optical lattice. Science, 349(6250):842–845, 2015.

[119] Thomas Kohlert, Sebastian Scherg, Xiao Li, Henrik P. Lüschen, Sankar Das Sarma, Immanuel Bloch, and Monika Aidelsburger. Observation of many-body localization in a one-dimensional system with a single-particle mobility edge. Phys. Rev. Lett., 122:170403, May 2019.

[120] Rubem Mondaini and Marcos Rigol. Many-body localization and thermalization in disordered hubbard chains. Phys. Rev. A, 92:041601, Oct 2015.

[121] Piotr Sierant, Dominique Delande, and Jakub Zakrzewski. Many-body localization due to random interactions. Phys. Rev. A, 95:021601, Feb 2017.

[122] Piotr Sierant and Jakub Zakrzewski. Many-body localization of bosons in optical lattices. New Journal of Physics, 20(4):043032, apr 2018.

[123] Simon A. Weidinger, Sarang Gopalakrishnan, and Michael Knap. Self-consistent hartree-fock approach to many-body localization. Phys. Rev. B, 98:224205, Dec 2018.

[124] Mi Yan, Hoi-Yin Hui, Marcos Rigol, and V. W. Scarola. Equilibration dynamics of strongly interacting bosons in 2d lattices with disorder. Phys. Rev. Lett., 119:073002, Aug 2017.

[125] S. Aubry and G. André. Analyticity breaking and anderson localization in incommensurate lattices. Ann. Israel Phys. Soc., 3(18), 1980.

[126] Sriram Ganeshan, J. H. Pixley, and S. Das Sarma. Nearest neighbor tight binding models with an exact mobility edge in one dimension. Phys. Rev. Lett., 114:146601, Apr 2015.

[127] Dong-Ling Deng, Sriram Ganeshan, Xiaopeng Li, Ranjan Modak, Subroto Mukerjee, and J. H. Pixley. Many-body localization in incommensurate models with a mobility edge. Annalen der Physik, 529(7), 7 2017.

[128] Xingbo Wei, Chen Cheng, Gao Xianlong, and Rubem Mondaini. Investigating many-body mobility edges in isolated quantum systems. Phys. Rev. B, 99:165137, Apr 2019.

[129] Gordon Baym and Leo P. Kadanoff. Conservation laws and correlation functions. Phys. Rev., 124:287–299, Oct 1961.

[130] D. J. Thouless. Lectures on Localization, pages 17–41. Springer US, Boston, MA, 1983.

[131] S. Aubry and G. André. Analyticity breaking and anderson localization in incommensurate lattices. Ann. Israel Phys. Soc., 3(18), 1980.

[132] Christian Aulbach, André Wobst, Gert-Ludwig Ingold, Peter Hnggi, and Imre Varga. Phase-space visualization of a metal–insulator transition. New Journal of Physics, 6:70–70, jul 2004.

[133] Svetlana Ya. Jitomirskaya. Metal-insulator transition for the almost mathieu operator. Annals of Mathematics, 150(3):1159–1175, 1999.

[134] R. A Rmer and H Schulz-Baldes. Weak-disorder expansion for localization lengths of quasi-1d systems. Europhysics Letters (EPL), 68(2):247–253, oct 2004.

[135] G. Semeghini, M. Landini, P. Castilho, S. Roy, G. Spagnolli, A. Trenkwalder, M. Fattori, M. Inguscio, and G. Modugno. Measurement of the mobility edge for 3d anderson localization. Nature Physics, 11:554 EP –, 06 2015.

[136] Xiao Li, Xiaopeng Li, and S. Das Sarma. Mobility edges in one-dimensional bichromatic incommensurate potentials. Phys. Rev. B, 96:085119, Aug 2017.

[137] S. Das Sarma, Song He, and X. C. Xie. Localization, mobility edges, and metal-insulator transition in a class of one-dimensional slowly varying deterministic potentials. Phys. Rev. B, 41:5544–5565, Mar 1990.

[138] J. Biddle and S. Das Sarma. Predicted mobility edges in one-dimensional incommensurate optical lattices: An exactly solvable model of anderson localization. Phys. Rev. Lett., 104:070601, Feb 2010.

[139] Thomas Kohlert, Sebastian Scherg, Xiao Li, Henrik P. Lüschen, Sankar Das Sarma, Immanuel Bloch, and Monika Aidelsburger. Observation of many-body localization in a one-dimensional system with a single-particle mobility edge. Phys. Rev. Lett., 122:170403, May 2019.

[140] Henrik P. Lüschen, Sebastian Scherg, Thomas Kohlert, Michael Schreiber, Pranjal Bordia, Xiao Li, S. Das Sarma, and Immanuel Bloch. Single-particle mobility edge in a one-dimensional quasiperiodic optical lattice. Phys. Rev. Lett., 120:160404, Apr 2018.

[141] D J Thouless. A relation between the density of states and range of localization for one dimensional random systems. Journal of Physics C: Solid State Physics, 5(1):77–81, jan 1972.

[142] S. Das Sarma, Song He, and X. C. Xie. Localization, mobility edges, and metal-insulator transition in a class of one-dimensional slowly varying deterministic potentials. Phys. Rev. B, 41:5544–5565, Mar 1990.

[143] Jae-yoon Choi, Sebastian Hild, Johannes Zeiher, Peter Schauß, Antonio Rubio-Abadal, Tarik Yefsah, Vedika Khemani, David A. Huse, Immanuel Bloch, and Chris-

tian Gross. Exploring the many-body localization transition in two dimensions. Science, 352(6293):1547–1552, 2016.

[144] Yuriy Makhlin, Gerd Schön, and Alexander Shnirman. Quantum-state engineering with josephson-junction devices. Rev. Mod. Phys., 73:357–400, May 2001.

[145] John Clarke and Frank K. Wilhelm. Superconducting quantum bits. Nature, 453(7198):1031–1042, 06 2008.

[146] R. Hanson, L. P. Kouwenhoven, J. R. Petta, S. Tarucha, and L. M. K. Vandersypen. Spins in few-electron quantum dots. Rev. Mod. Phys., 79:1217–1265, Oct 2007.

[147] Herbert Walther et al. Cavity quantum electrodynamics. Rep. Prog. Phys., 69:1325, April 2006.

[148] Markus Aspelmeyer, Tobias J. Kippenberg, and Florian Marquardt. Cavity optomechanics. Rev. Mod. Phys., 86:1391–1452, Dec 2014.

[149] M. M. Desjardins, J. J. Viennot, M. C. Dartiailh, L. E. Bruhat, M. R. Delbecq, M. Lee, M. S. Choi, A. Cottet, and T. Kontos. Observation of the frozen charge of a kondo resonance. Nature, 545(7652):71–74, 05 2017.

[150] V. Mourik, K. Zuo, S. M. Frolov, S. R. Plissard, E. P. A. M. Bakkers, and L. P. Kouwenhoven. Signatures of majorana fermions in hybrid superconductor-semiconductor nanowire devices. Science, 336(6084):1003–1007, 2012.

[151] Kathy-Anne Brickman Soderberg, Nathan Gemelke, and Cheng Chin. Ultracold molecules: vehicles to scalable quantum information processing. New Journal of Physics, 11(5):055022, 2009.

[152] J. F. Poyatos, J. I. Cirac, and P. Zoller. Quantum reservoir engineering with laser cooled trapped ions. Phys. Rev. Lett., 77:4728–4731, Dec 1996.

[153] S. Diehl, A.Micheli, A.Kantian, B. Kraus, H. P. Buchler, and P. Zoller. Quantum states and phases in driven open quantum systems with cold atoms. Nature Physics, 4(11):878, 2008.

[154] Frank Verstraete, Michael M. Wolf, and J. Ignacio Cirac. Quantum computation, quantum state engineering, and quantum phase transitions driven by dissipation. Nature Physics, 5:633, 2009.

[155] A. G. Redfield. Master equations in phase-space formulation of quantum optics. Adv. Magn. Reson., 1:1, 1965.

[156] Vittorio Gorini, Andrzej Kossakowski, and E. C. G. Sudarshan. Completely positive dynamical semigroups of nlevel systems. Journal of Mathematical Physics, 17(5):821–825, 1976.

[157] G. Lindblad. On the generators of quantum dynamical semigroups. Communications in Mathematical Physics, 48(2):119–130, Jun 1976.

[158] J.-T. Hsiang and B.L. Hu. Nonequilibrium steady state in open quantum systems: Influence action, stochastic equation and power balance. Annals of Physics, 362:139 – 169, 2015.

[159] Walter T. Strunz. Stochastic path integrals and open quantum systems. Phys. Rev. A, 54:2664–2674, Oct 1996.

[160] Luc Bouten, Madalin Guta, and Hans Maassen. Stochastic schrdinger equations. Journal of Physics A: Mathematical and General, 37(9):3189, 2004.

[161] Shi-Bei Xue, Re-Bing Wu, Wei-Min Zhang, Jing Zhang, Chun-Wen Li, and Tzyh-Jong Tarn. Decoherence suppression via non-markovian coherent feedback control. Phys. Rev. A, 86:052304, Nov 2012.

[162] Alex W. Chin, Susana F. Huelga, and Martin B. Plenio. Quantum metrology in non-markovian environments. Phys. Rev. Lett., 109:233601, Dec 2012.

[163] Elsi-Mari Laine, Heinz-Peter Breuer, and Jyrki Piilo. Nonlocal memory effects allow perfect teleportation with mixed states. 4:4620 EP –, 04 2014.

[164] B. Bylicka, D. Chruściński, and S. Maniscalco. Non-markovianity and reservoir memory of quantum channels: a quantum information theory perspective. 4:5720 EP –, 07 2014.

[165] Bi-Heng Liu, Li Li, Yun-Feng Huang, Chuan-Feng Li, Guang-Can Guo, Elsi-Mari Laine, Heinz-Peter Breuer, and Jyrki Piilo. Experimental control of the transition from markovian to non-markovian dynamics of open quantum systems. Nat Phys, 7(12):931–934, 12 2011.

[166] Walter T. Strunz, Lajos Diósi, and Nicolas Gisin. Open system dynamics with non-markovian quantum trajectories. Phys. Rev. Lett., 82:1801–1805, Mar 1999.

[167] Ángel Rivas, Susana F. Huelga, and Martin B. Plenio. Entanglement and non-markovianity of quantum evolutions. Phys. Rev. Lett., 105:050403, Jul 2010.

[168] Ruggero Vasile, Paolo Giorda, Stefano Olivares, Matteo G. A. Paris, and Sabrina Maniscalco. Nonclassical correlations in non-markovian continuous-variable systems. Phys. Rev. A, 82:012313, Jul 2010.

[169] Vitalii Semin and Francesco Petruccione. Nonequilibrium-thermodynamics approach to open quantum systems. Phys. Rev. A, 90:052112, Nov 2014.

[170] L. Mazzola, S. Maniscalco, J. Piilo, K.-A. Suominen, and B. M. Garraway. Pseudo-modes as an effective description of memory: Non-markovian dynamics of two-state systems in structured reservoirs. Phys. Rev. A, 80:012104, Jul 2009.

[171] Marko Žnidarič, Carlos Pineda, and Ignacio García-Mata. Non-markovian behavior of small and large complex quantum systems. Phys. Rev. Lett., 107:080404, Aug 2011.

[172] S. Garmon, T. Petrosky, L. Simine, and D. Segal. Amplification of non-markovian decay due to bound state absorption into continuum. Fortschritte der Physik, 61(2-3):261–275, 2013.

[173] Bassano Vacchini. Non-markovian dynamics for bipartite systems. Phys. Rev. A, 78:022112, Aug 2008.

[174] Ulrich Weiss. Quantum dissipative systems, volume 13. World scientific, 2012.

[175] Dmitry V. Chichinadze, Pedro Ribeiro, Yulia E. Shchadilova, and Alexey N. Rubtsov. Transient phases and dynamical transitions in the post-quench evolution of the generalized bose-anderson model. Phys. Rev. B, 94:054301, Aug 2016.

[176] Heng-Na Xiong, Ping-Yuan Lo, Wei-Min Zhang, Da Hsuan Feng, and Franco Nori. Non-markovian complexity in the quantum-to-classical transition. 5:13353 EP –, 08 2015.

[177] Heinz-Peter Breuer. Non-markovian quantum dynamics and the method of correlated projection super-operators. Theoretical Foundations of Quantum Information Processing and Communication, 787:125–139, 2010.

[178] Andrea Smirne and Bassano Vacchini. Nakajima-zwanzig versus time-convolutionless master equation for the non-markovian dynamics of a two-level system. Phys. Rev. A, 82:022110, Aug 2010.

[179] Bassano Vacchini and Heinz-Peter Breuer. Exact master equations for the non-markovian decay of a qubit. Phys. Rev. A, 81:042103, Apr 2010.

[180] A. Gonzalez-Tudela, F. J. Rodríguez, L. Quiroga, and C. Tejedor. Dissipative dynamics of a solid-state qubit coupled to surface plasmons: From non-markov to markov regimes. Phys. Rev. B, 82:115334, Sep 2010.

[181] H. Z. Shen, M. Qin, Xiao-Ming Xiu, and X. X. Yi. Exact non-markovian master equation for a driven damped two-level system. Phys. Rev. A, 89:062113, Jun 2014.

[182] Dariusz Chruściński and Sabrina Maniscalco. Degree of non-markovianity of quantum evolution. Phys. Rev. Lett., 112:120404, Mar 2014.

[183] Subir Sachdev. Quantum phase transitions. Wiley Online Library, 2007.

[184] S. Kambe, H. Sakai, Y. Tokunaga, G. Lapertot, T. D. Matsuda, G. Knebel, J. Flouquet, and R. E. Walstedt. Degenerate fermi and non-fermi liquids near a quantum critical phase transition. Nat Phys, 10(11):840–844, 11 2014.

[185] T. Senthil, Matthias Vojta, and Subir Sachdev. Weak magnetism and non-fermi liquids near heavy-fermion critical points. Phys. Rev. B, 69:035111, Jan 2004.

[186] C. Rothe, S. I. Hintschich, and A. P. Monkman. Violation of the exponential-decay law at long times. Phys. Rev. Lett., 96:163601, Apr 2006.

[187] Richard Phillips Feynman and Frank Lee Vernon. The theory of a general quantum system interacting with a linear dissipative system. Annals of physics, 24:118–173, 1963.

[188] R. A. Pepino, J. Cooper, D. Meiser, D. Z. Anderson, and M. J. Holland. Open quantum systems approach to atomtronics. Phys. Rev. A, 82:013640, Jul 2010.

[189] Angel Rivas, A Douglas K Plato, Susana F Huelga, and Martin B Plenio. Markovian master equations: a critical study. New Journal of Physics, 12(11):113032, 2010.

[190] Jader P. Santos and Gabriel T. Landi. Microscopic theory of a nonequilibrium open bosonic chain. Phys. Rev. E, 94:062143, Dec 2016.

[191] L. Ferialdi. Exact closed master equation for gaussian non-markovian dynamics. Phys. Rev. Lett., 116:120402, Mar 2016.

[192] Archak Purkayastha, Abhishek Dhar, and Manas Kulkarni. Out-of-equilibrium open quantum systems: A comparison of approximate quantum master equation approaches with exact results. Phys. Rev. A, 93:062114, Jun 2016.

[193] Jian-Sheng Wang, Bijay Kumar Agarwalla, Huanan Li, and Juzar Thingna. Nonequilibrium green's function method for quantum thermal transport. Frontiers of Physics, 9(6):673–697, Dec 2014.

[194] C Caroli, R Combescot, P Nozieres, and D Saint-James. Direct calculation of the tunneling current. Journal of Physics C: Solid State Physics, 4(8):916, 1971.

[195] Yigal Meir and Ned S. Wingreen. Landauer formula for the current through an interacting electron region. Phys. Rev. Lett., 68:2512–2515, Apr 1992.

[196] Abhishek Dhar and Diptiman Sen. Nonequilibrium green's function formalism and the problem of bound states. Phys. Rev. B, 73:085119, Feb 2006.

[197] Bijay Kumar Agarwalla, Manas Kulkarni, Shaul Mukamel, and Dvira Segal. Tunable photonic cavity coupled to a voltage-biased double quantum dot system: Diagrammatic nonequilibrium green's function approach. Phys. Rev. B, 94:035434, Jul 2016.

[198] Dong E. Liu, Alex Levchenko, and Roman M. Lutchyn. Keldysh approach to periodically driven systems with a fermionic bath: Nonequilibrium steady state, proximity effect, and dissipation. Phys. Rev. B, 95:115303, Mar 2017.

[199] L. E. Bruhat, J. J. Viennot, M. C. Dartiailh, M. M. Desjardins, T. Kontos, and A. Cottet. Cavity photons as a probe for charge relaxation resistance and photon emission in a quantum dot coupled to normal and superconducting continua. Phys. Rev. X, 6:021014, May 2016.

[200] Abhishek Dhar, Keiji Saito, and Peter Hänggi. Nonequilibrium density-matrix description of steady-state quantum transport. Phys. Rev. E, 85:011126, Jan 2012.

[201] Here, G_0^{-1K} is a purely regulatory term governing intial condition of the system and can be neglected for steady state dynamics when the system is coupled to bath.

[202] Gerald D Mahan. Many-particle physics. Springer Science & Business Media, 2013.

[203] GY Hu and Robert F O'Connell. Analytical inversion of symmetric tridiagonal matrices. Journal of Physics A: Mathematical and General, 29(7):1511, 1996.

[204] $m = 0$ corresponds to $\lambda = 0$ and in this case $\sinh[(N+1)\lambda]/\sinh\lambda \to (N+1)$. Hence $m = 0$ does not correspond to a pole of the Greens' function.

[205] C W Gardiner, J R Anglin, and T I A Fudge. The stochastic gross-pitaevskii equation. Journal of Physics B: Atomic, Molecular and Optical Physics, 35(6):1555, 2002.

[206] Philipp M. Preiss, Ruichao Ma, M. Eric Tai, Alexander Lukin, Matthew Rispoli, Philip Zupancic, Yoav Lahini, Rajibul Islam, and Markus Greiner. Strongly correlated quantum walks in optical lattices. Science, 347(6227):1229–1233, 2015.

[207] M. Hillery, R.F. O'Connel, M.O. Scully, and E. P. Wigner. Distribution functions in physics: Fundamentals. Phys. Rep., 106:121, 1984.

[208] Anatole Kenfack and Karol yczkowski. Negativity of the wigner function as an indicator of non-classicality. Journal of Optics B: Quantum and Semiclassical Optics, 6(10):396, 2004.

[209] F. Siyouri, M. El Baz, and Y. Hassouni. The negativity of wigner function as a measure of quantum correlations. Quantum Information Processing, 15(10):4237–4252, Oct 2016.

[210] Mark Howard, Joel Wallman, Victor Veitch, and Joseph Emerson. Contextuality supplies the 'magic'for quantum computation. Nature, 510:351 EP –, 06 2014.

[211] Nicolas Delfosse, Philippe Allard Guerin, Jacob Bian, and Robert Raussendorf. Wigner function negativity and contextuality in quantum computation on rebits. Phys. Rev. X, 5:021003, Apr 2015.

[212] Huan-Qiang Zhou, Thomas Barthel, John Ove Fjærestad, and Ulrich Schollwöck. Entanglement and boundary critical phenomena. Phys. Rev. A, 74:050305, Nov 2006.

[213] Jens H. Bardarson, Frank Pollmann, and Joel E. Moore. Unbounded growth of entanglement in models of many-body localization. Phys. Rev. Lett., 109:017202, Jul 2012.

[214] David A. Huse, Rahul Nandkishore, and Vadim Oganesyan. Phenomenology of fully many-body-localized systems. Phys. Rev. B, 90:174202, Nov 2014.

[215] Rahul Nandkishore and David A. Huse. Many-body localization and thermalization in quantum statistical mechanics. Annual Review of Condensed Matter Physics, 6(1):15–38, 2015.

[216] D. T. Smithey, M. Beck, M. G. Raymer, and A. Faridani. Measurement of the wigner distribution and the density matrix of a light mode using optical homodyne tomography: Application to squeezed states and the vacuum. Phys. Rev. Lett., 70:1244–1247, Mar 1993.

[217] P. Bertet, A. Auffeves, P. Maioli, S. Osnaghi, T. Meunier, M. Brune, J. M. Raimond, and S. Haroche. Direct measurement of the wigner function of a one-photon fock state in a cavity. Phys. Rev. Lett., 89:200402, Oct 2002.

[218] D. Leibfried, D. M. Meekhof, B. E. King, C. Monroe, W. M. Itano, and D. J. Wineland. Experimental determination of the motional quantum state of a trapped atom. Phys. Rev. Lett., 77:4281–4285, Nov 1996.

[219] Yali Tian, Zhihui Wang, Pengfei Zhang, Gang Li, Jie Li, and Tiancai Zhang. Measurement of complete and continuous wigner functions for discrete atomic systems. Phys. Rev. A, 97:013840, Jan 2018.

[220] Todd Tilma, Mark J. Everitt, John H. Samson, William J. Munro, and Kae Nemoto. Wigner functions for arbitrary quantum systems. Phys. Rev. Lett., 117:180401, Oct 2016.

[221] Anatoli Polkovnikov. Phase space representation of quantum dynamics. Annals of Physics, 325(8):1790 – 1852, 2010.

[222] Luigi Amico, Rosario Fazio, Andreas Osterloh, and Vlatko Vedral. Entanglement in many-body systems. Rev. Mod. Phys., 80:517–576, May 2008.

[223] Lucas Hackl, Eugenio Bianchi, Ranjan Modak, and Marcos Rigol. Entanglement production in bosonic systems: Linear and logarithmic growth. Phys. Rev. A, 97:032321, Mar 2018.

[224] H Casini and M Huerta. Entanglement entropy in free quantum field theory. Journal of Physics A: Mathematical and Theoretical, 42(50):504007, 2009.

[225] Pasquale Calabrese, John Cardy, and Erik Tonni. Entanglement negativity in extended systems: a field theoretical approach. Journal of Statistical Mechanics: Theory and Experiment, 2013(02):P02008, 2013.

[226] J H Samson. Phase-space path-integral calculation of the wigner function. Journal of Physics A: Mathematical and General, 36(42):10637, 2003.

[227] Dries Sels, Fons Brosens, and Wim Magnus. Wigner distribution functions for complex dynamical systems: A path integral approach. Physica A: Statistical Mechanics and its Applications, 392(2):326 – 335, 2013.

[228] Patrick P. Hofer. Quasi-probability distributions for observables in dynamic systems. Quantum, 1:32, October 2017.

[229] Ingo Peschel and Viktor Eisler. Reduced density matrices and entanglement entropy in free lattice models. Journal of Physics A: Mathematical and Theoretical, 42(50):504003, 2009.

[230] Pasquale Calabrese, John Cardy, and Benjamin Doyon. Entanglement entropy in extended quantum systems. Journal of Physics A: Mathematical and Theoretical, 42(50):500301, 2009.

[231] Igor R. Klebanov, Silviu S. Pufu, Subir Sachdev, and Benjamin R. Safdi. Rényi entropies for free field theories. Journal of High Energy Physics, 2012(4):74, Apr 2012.

[232] Luca Bombelli, Rabinder K. Koul, Joohan Lee, and Rafael D. Sorkin. Quantum source of entropy for black holes. Phys. Rev. D, 34:373–383, Jul 1986.

[233] Mark Srednicki. Entropy and area. Phys. Rev. Lett., 71:666–669, Aug 1993.

[234] Table of integrals, series, and products (eighth edition). pages 1 – 24. Academic Press, Boston, eighth edition edition, 2014.